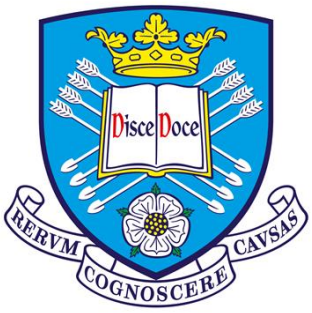

The University Of Sheffield.

Development of an immune competent human skin equivalent model of atopic dermatitis for pre-clinical drug testing

Inmaculada Barragan Vazquez

A thesis submitted in partial fulfilment of the requirements for the degree of Doctor of Philosophy

The University of Sheffield
Faculty of Medicine, Dentistry and Health
School of Clinical Dentistry

October 2022

Acknowledgements

First of all, I would like to express my sincere gratitude to my supervisors Professor Craig Murdoch, Dr Helen Colley and Dr Simon Danby for the guidance, time and continued support throughout my PhD. I cannot thank you enough for always encouraging me to work independently and bring new ideas to the project. Thank you for your patience, motivation, and immense knowledge. Thank you for supporting me with industry visits and opportunities to present at conferences. Although it has been stressful at times, you have made this whole experience fun and I have learnt so much from you.

I would also like to thank The University of Sheffield and Almirall S.A. for funding me and this project, and for the opportunity to visit the Almirall S.A. facilities.

Next, I would like to thank the Dental School, both staff and students, and for such wonderful atmosphere in the department. Thank you to the technicians Brenka, Jason, Matt, Kirsty and Emilia for all your help through these years. I would also like to thank my fellow students in particular Sara, Luna and Klaudia, thanks for being a friend, for the laughs and your support, you made this adventure full of unforgettable moments. Thank you, Amy, for all the help and the scientific support, and for the nice talks between experiments.

Lastly, I would like to thank my friends, the old ones and the new ones from all over the world I made in these years; and to Gabriele, thanks for always being there for me, for your patience, and for always supporting me. I would like to end by thanking my parents and brother, mamá, papá, Placi, thanks for your always unquestionable support, believing in me, and your hard work for making me accomplish my dreams. I hope that this makes you proud.

Abstract

Atopic dermatitis (AD) is a common inflammatory skin disorder that is frequently present in infancy, although it can occur at any age. The main signs of AD are IgE-mediated sensitisation to allergens, chronic skin inflammation and disruption of the epidermal-barrier culminating in dry skin. Innate and adaptive immune systems are involved in the development of AD; therefore, the immunopathogenesis of AD is a complex process involving keratinocytes, dendritic cells (DCs) and T_H2 cells in an escalating cycle of inflammation. There is no complete cure for AD and most treatments focus solely on symptom relief. Furthermore, murine experimental models that replicate aspects of AD can show markedly different responses to drug treatments. Therefore, new pre-clinical models are required to support drug development and testing. This study developed an immunocompetent human skin equivalent (IC-HSE) containing primary T_H2 cells that could be used to develop new drugs.

Purified peripheral blood human monocytes were differentiated into monocyte-derived DCs (Mo-DC), and purified naïve CD4+ T cells were polarised into T_H2 cells, both cell types were characterised using specific gene and cell surface markers. In response to the allergens 2,4-dinitrochlorobenzene and Derp1 from house dust mite, inflammatory marker expression by Mo-DC was variable, while skin keratinocytes were largely unresponsive. Human skin equivalents (HSE) were successfully generated using TERT-immortalised keratinocytes and fibroblasts into either human reconstituted epidermal (RHE)-only HSE or full-thickness HSE that contained a fibroblast populated dermis and epidermis. Both these HSE displayed structural and marker expression profiles similar to that of human epidermis and full-thickness skin. To generate immunocompetent-HSE (IC-HSE), T_H2 cells were embedded into a type I collagen gel. On top of this was placed a full-thickness HSE and the construct cultured at air-to-liquid interface for 10-16 days. The morphology of the IC-HSE showed marked deviation from the histology of that of non-immune cell-containing control HSE with loss of keratinisation, evidence of epidermal damage at 14 days and total destruction of the epidermis at 16 days, suggesting a role of T_H2 cells is this tissue damage. Moreover, IC-HSE made with T_H2 cells from severe AD patients displayed more epidermal damage than those from healthy control subjects, although their overall histological and marker expression profile morphology of IC-HSE was much different to those of patient biopsies.

In conclusion, T_H2 cell-containing IC-HSE were successfully developed, although further research is required to optimise the culture of these models for use in pre-clinical experiments to advance the AD drug delivery pipeline.

Table of contents

List of figures

List of tables

Abbreviations

2D	Two-dimensional
3D	Three-dimensional
AD	Atopic dermatitis
ALI	Air-to-liquid interface
AMP	Antimicrobial peptides
ANOVA	Analysis of variance
APC	Antigen-presenting cells
APC	Allophycocyanin
B2M	β-2-Microglobulin
BSA	Bovine serum albumin
$CaCl_2$	Calcium chloride
cDCs	Conventional dendritic cells
CO_2	Carbon dioxide
Cytotoxic T cells	Tc
DAB	3,3'-diaminobenzidine tetrahydrochloride
DCs	Dendritic cells
Der f	*Dermatophagoides pteronyssinus*
Der p	*Dermatophagoides pteronyssinus*
dH_2O	Distilled water
dLNs	Draining lymph nodes
DMEM	Dulbecco´s Modified Eagle Medium
DMSO	Dimethylsulfoxide
DNA	Deoxyribonucleic acid
DNCB	2,4-Dinitrochlorobenzene
dNTP	Deoxynucleoside triphosphate
DRG	Dorsal root ganglia
E.coli	*Escherichia coli*
ECM	Extracellular matrix
EDTA	Ethylenediaminetetraacetic acid
EGF	Epidermal growth factor
EoS	Eosinophils
Eur m	*Euroglyphus maynei*
FACS	Flow cytometry
FBS	Foetal bovine serum
FcεR1	High-affinity IgE receptor
FITC	Fluorescein isothiocyanate

FLG	Filaggrin
GAPDH	Glyceraldehyde 3-phosphate dehydrogenase
GM-CSF	Granulocyte-macrophage colony-stimulating factor
H&E	Haematoxylin and eosin
H_2O_2	Hydrogen peroxide
HBSS	Hank´s balanced salt solution
HDM	House dust mite
HEPES	4-(2-hydroxyethyl)-1-piperazineethanesulfonic acid
HSE	Human skin equivalents
IDA	Industrial denatured alcohol
IDEC	Inflammatory dendritic epidermal cells
IFN	Type I interferon
IgE	Immunoglobulin E
IL31RA	IL-31 receptor A
ILC	Innate lymphoid cells
ILC2	Innate lymphoid cells-group 2
JAKi	JAK inhibitors
KD	Knockdown
KGF	Keratinocyte growth factor
KLK	Kallikrein serin proteases
K-sfm	Keratinocyte serum-free medium
LCs	Langerhans cells
LDH	Lactate dehydrogenase
LPS	Lipopolysaccharide
LS	Large size
MC	Mast cells
M-CSF	Macrophage colony-stimulating factor
MDM	Monocyte-derived macrophages
MFI	Median fluorescence intensity
MHC	Major histocompatibility complex
Mo-DC	Monocyte-derived dendritic cells
Mo-LC	Monocyte-derived Langerhans cells
$NaHCO_3$	Sodium bicarbonate
NaN_3	Sodium azide
NaOH	Sodium hydroxide
NHS	National Health Service
NICE	National Institute for Health and Care Excellence

NK	Natural killer cells
^{o}C	Degree Celsius
OSMRβ	Oncostatin M receptor β
PBMCs	Peripheral blood mononuclear cells
PBS	Phosphate-buffered saline
pDCs	Plasmacytoid dendritic cells
PE	Phycoerythrin
PI	Propidium iodide
PRRs	Pattern recognition receptors
RHE	Reconstructed human epidermal
RNA	Ribonucleic acid
ROS	Reactive oxygen species
RPMI	Roswell Park Memorial Institute Medium
S. aureus	*Staphylococcus aureus*
siRNA	Small interfering RNA
SIRPα	Signal regulatory protein alpha
TBS	Tris-buffered saline
TCIs	Topical calcineurin inhibitors
TCR	T cell receptor
TCS	Topical corticosteroids
TEER	Transepithelial electrical resistance
TEWL	Transepidermal water loss
Tfh	Follicular helper T cell
TGF-β1	Transforming growth factor
T_H	T-helper
TLRs	Toll-like receptors
TMB	Tetramethylbenzidine
TNF	Tumour necrosis factor
Tregs	Regulatory T cells
TRKs	Tropomyosin receptor kinases
TSLP	Thymic stromal lymphopoietin
TT	Triiodothyronine
UBC	Ubiquitin C
UK	United Kingdom
USA	United States of America
UV	Ultraviolet
WHO	World health organisation

Chapter 1 – Introduction

1.1 Anatomy and physiology of the Skin

1.1.1 Skin function

The skin is the largest and one of the heaviest organs (around 16% of total body weight) that covers the body's total external surface, extending to approximately 1.5 - 2 m^2 in adults (Dąbrowska et al., 2018). It serves as a first-order physical barrier against the external environment, protecting against pathogens, allergens, environmental chemicals and ultraviolet (UV) light (Lopez-Ojeda et al., 2021). It also protects the body from water loss, plays a key role in thermoregulation, and it is involved in the functioning of the nervous system (Dąbrowska et al., 2018). The outermost skin layer, the epidermis, bears most of the responsibility for the protective characteristics. In addition, the skin microbiome, which is composed of commensal microorganisms such as fungi, bacteria and viruses, colonises the skin early after birth, aids epidermal maturation as well as providing an extra layer of defence for the host against pathogenic organisms (Nguyen & Soulika, 2019; Shang et al., 2018).

Maintenance of the epidermal skin barrier is very important, and its condition depends on not only its physical properties, such as epidermis hydration, transepidermal water loss (TEWL), sebum produced (Boer et al., 2016), skin surface pH and temperature, but also exposure to substances that may alter lipid composition of stratum corneum (e.g., cleaning substances or solvents among others) (Jansen van Rensburg et al., 2019). Several factors can influence these properties and function such as skin type, ethnicity, gender, age, lifestyle and body-mass index. Caucasians and African-Americans for example, usually exhibit drier skin, compared to those of Chinese origin, which is due to the low amount of stratum corneum moisturizing factors, eating habits and sun exposure (Dąbrowska et al., 2018).

1.1.2 Structure of the skin

The skin is divided into three main layers: epidermis (outer layer), dermis (middle layer), and hypodermis (subcutaneous tissue that provides support) (Figure 1.1). These layers work in concert, contributing to the strength and flexibility of the skin (Wickett & Visscher, 2006). Each skin layer is composed of different cell types that are involved with specific functions (Kolarsick et al., 2011; Lai-Cheong & McGrath, 2017).

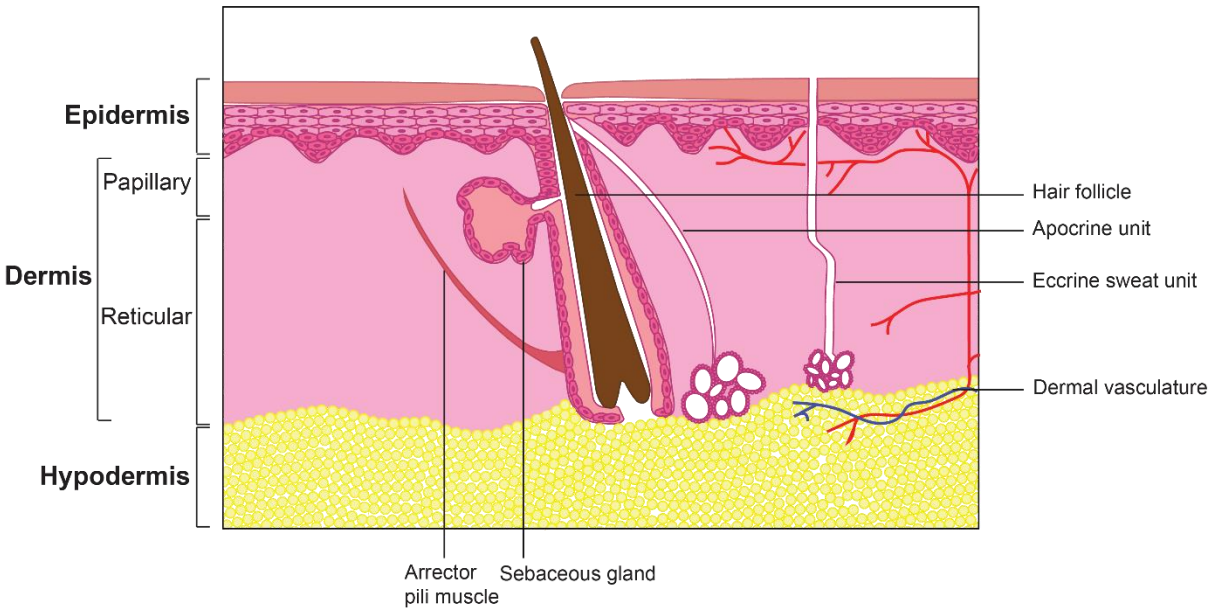

Figure 1.1 Schematic diagram showing the skin structure, its different layers and their components. The epidermis is formed of five layers: stratum basale, stratum spinosum, stratum granulosum, stratum lucidum, and stratum corneum. The dermis consists of the papillary and reticular dermis. the hypodermis is an adipose-rich layer that connects the dermis to the underlying tissues and organs.

1.1.2.1 Epidermis

The epidermis (Figure 1.2) is a stratified, squamous epithelium layer, that is constantly restoring taking 40-56 days to be completely regenerated in humans, although this is shorter in some skin disorders such as psoriasis, and produces derivative structures, such as nails and sweat glands (Benhadou et al., 2019; Kolarsick et al., 2011). The epidermis contains different cell types (keratinocytes, melanocytes, Langerhans cells and Merkel cells) and is composed of five layers, or "strata", depending on the state of the keratinocyte differentiation: stratum basale, stratum spinosum, stratum granulosum, stratum lucidum and stratum corneum (Koster, 2009; Lai-Cheong & McGrath, 2017). This generates the epidermal barrier at the level of the stratum corneum.

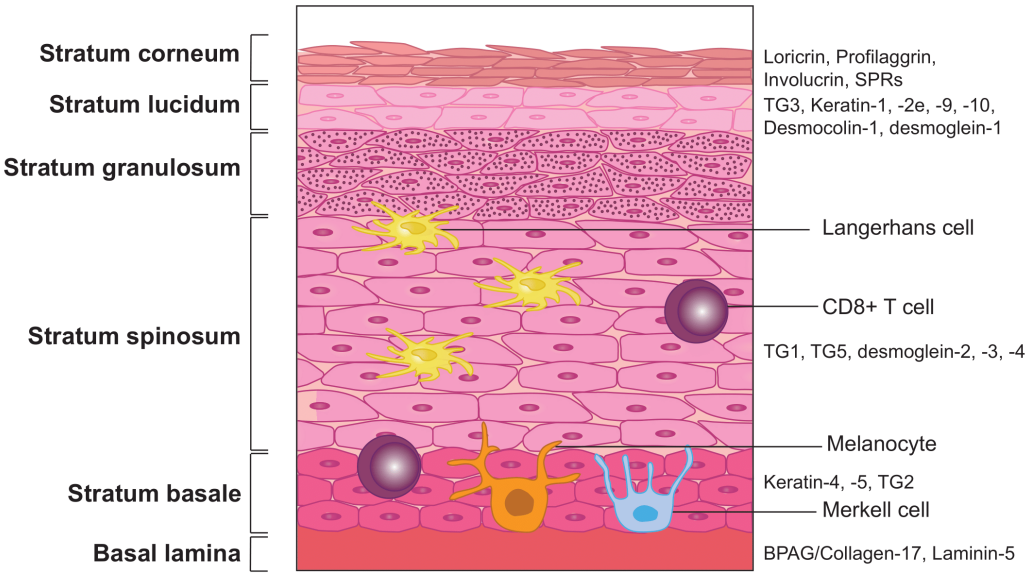

Figure 1.2 Schematic diagram illustrating the different layers and cells contained in the epidermis. The epidermis consists of five layers: stratum basale, stratum spinosum, stratum granulosum, stratum lucidum, and stratum corneum. It also includes specialist cells such as immune cells (Langerhans cells, infiltrating T cells) along with melanocytes and Merkell cells in the stratum basale.

1.1.2.1.1 CELL TYPES IN THE EPIDERMIS

Keratinocytes are the most abundant cell type in the epidermis, constituting 95% of the total cell number, while melanocytes, Langerhans cells (LCs) and Merkel cells make up the remaining 5% (Lai-Cheong & McGrath, 2017). Stratified, squamous keratinocytes are also found as the main cell type in the epithelium of the oral mucosa, oesophagus, tonsils, vagina, cornea and conjunctival epithelium.

The main role of epidermal keratinocytes is the maintenance of the physical barrier of the skin by developing into the stratum corneum. This is accomplished by the migration of keratinocytes along the different layers of the epidermis (stratum basale, stratum spinosum and stratum granulosum) until becoming corneocytes in the stratum corneum (Kabashima et al., 2019). Keratinocytes are eventually lost to the environment as they are shed from the skin surface by desquamation (Simpson et al., 2011). Keratinocytes also regulate calcium absorption by activation of cholesterol precursors (Khammissa et al., 2018) and are an important component of the innate immune system. They express different pattern recognition receptors (PRRs), including Toll-like receptors (TLRs) among others, and secrete cytokines, such as thymic stromal lymphopoietin (TSLP), tumour necrosis factor (TNF), and IL-33, during inflammation processes. These cytokines are important to activate skin-resident immune cells and to recruit other immune cells to the skin (Kabashima et al., 2019; Piipponen et al., 2020).

Melanoblasts are a precursor of melanocytes that derive from the neural crest, proliferate and migrate to the epidermis in the embryonic stage (Hirobe, 2014). Melanocytes are neuroectodermal dendritic cells that are located in the basal layer of the skin and in the hair of mammals, but also in the nervous system and in the inner ear (Cichorek et al., 2013). They produce pigment granules named melanosomes that contain melanin, a complex biopolymer that are usually located around the nucleus in keratinocytes, forming the melanosome microparasol over the keratinocytes nuclei and protecting against DNA damage (Hurbain et al., 2018). Each melanocyte joins around 30-40 keratinocytes to form the epidermal-melanin unit, allowing the transport of melanin into the surrounding basal keratinocytes by melanosomes that give colour to the skin. There are two main types of melanin present in human skin and hair follicles, eumelanin (brown/black melanin) and pheomelanin (yellow/red melanin), with eumelanin being the most frequently present in melanosomes in the skin. Functionally, melanin absorbs UV light thereby preventing keratinocyte DNA damage (Lai-Cheong & McGrath, 2017; Lambert et al., 2019; Wickett & Visscher, 2006).

LCs were first described by Paul Langerhans in 1868 who observed these cells in the epidermis, predominantly in the stratum spinosum, and over a century later they were classified as dendritic cells (DCs). LCs are also present in mucosal oral and vaginal epithelium (Deckers et al., 2018). LCs serve as antigen-presenting cells and appear to be derived from the adult foetal liver progenitor cells similar to tissue-resident macrophages, suggesting that LCs may be from a macrophage lineage (M. Otsuka et al., 2018) and not dendritic cells. Their precursors occupy the epidermis during ontogenesis, expressing immune molecules such as Langerin (CD207), major histocompatibility complex (MHC) class II and CD45 (Romani et al., 2003). LCs also contain cytoplasmic organelles, named Birbeck granules that are specific to these types of cells, aiding their identification (Thornton et al., 2020). During unstimulated conditions, LCs promote activation and proliferation of skin-resident regulatory T cells (Tregs), maintaining the epidermis in a quiescent state. However, upon penetration of microbial components into the epidermis, LCs, together with the epidermal keratinocytes take part in rapid innate antimicrobial responses. LCs migrate to the local lymph nodes where they present antigens to naïve T cells to initiate an adaptive immune response. LCs functions can be altered by cytokine signals from cells in the epidermis, such as keratinocytes, modifying the type of adaptive immune responses generated. Therefore, LCs are important in linking innate and adaptive immune processes as part of the immune barrier of the epidermis, indicating a key role in skin immunity (Clayton et al., 2017; Deckers et al., 2018; Lai-Cheong & McGrath, 2017).

LCs can be derived *in vitro* from CD14+ cells purified from peripheral blood by treatment with granulocyte macrophage colony-stimulating factor (GM-CSF), IL-4 and transforming growth factor (TGF-β1) (Y. Otsuka et al., 2018). These cells express CD207, which binds to carbohydrate moieties

found on microorganisms, and different TLRs that, when activated, induce secretion of IL-15, a cytokine that drives CD8+ T cell proliferation. LCs can present antigen to CD8+ T cells, but also to naïve CD4+ T cells polarising them towards a T-helper 2 (T_H2) immune response by secreting IL-4, IL-5, and IL-13 (Mizumoto & Takashima, 2004; Yanofsky et al., 2013) (see section 1.3.3).

Merkel cells are post-mitotic cells situated in the basal layer of the epidermis. Their origin is still uncertain, it is not clear yet whether Merkel cells differentiate from epidermal keratinocyte-like cells or if their precursors are migrated stem cells of neural crest origin. These cells express mechanoreceptors that transfer sensory information from the skin to sensory nerves. Merkel cells that are not associated to nerves are involved in endocrine and paracrine secretion processes. Furthermore, Merkel cells can also interact with LC, participating in the neuroimmunological system of the skin, although little is known about this function (Abraham & Mathew, 2019; Lai-Cheong & McGrath, 2017).

1.1.2.1.2 STRUCTURE OF THE EPIDERMIS

The epidermis is constituted of five layers: stratum basale, stratum spinosum, stratum granulosum, stratum lucidum and stratum corneum.

The stratum basale, also called basal layer or stratum germinativum, is the inmost layer of the epidermis and it is separated from the dermis by the basal lamina (basement membrane). The basal layer contains melanocytes, Merkel cells, and cuboidal-shaped stem cells (basal keratinocytes) that are attached to the basement membrane by hemidesmosomes (Kolarsick et al., 2011). Hemidesmosomes are specialized integrin-based epithelial junctional structures that bind laminin in the matrix and keratins within the cytoplasm, components very important for the structure of this stratum (Walko et al., 2015). Basal keratinocytes multiply by uneven mitosis to two daughter cells one of which stays in the basal layer, whilst the other progresses to terminal differentiation, which concludes in the stratum corneum (Lai-Cheong & McGrath, 2017).

Basal cells that leave the stratum basale next enter the stratum spinosum, also known as the prickle cell layer (Simpson et al., 2011), which is formed by 8 to 10 layers of keratinocytes. This layer also contains numerous LCs. Keratinocytes in this layer undergo a series of modifications in gene expression, chromatin-modifying markers, and cytoplasmic organization to become spinous cells. Keratinocytes synthetize keratin and secrete a water-repelling glycolipid that helps to avoid water loss from the body. The spinous keratinocytes vary in structure, shape and properties that are determined by their location. Suprabasal spinous cells resemble a polyhedron in shape and have a rounded

nucleus, while upperbasal spinous cells are larger and contain lamellar granules, which are membrane-bound organelles that contain glycolipids, phospholipids, and glycoproteins, among others. Lamellar granules transport precursors of stratum corneum lipids into the intercellular space. The keratinocytes in this layer adhere to each other by desmosomes that support mechanical coupling between cells of the epidermis to avoid physical stress (Kolarsick et al., 2011).

Keratinocytes of the stratum spinosum are driven into the stratum granulosum due to the production of new keratinocytes from the basal layer pushing the cells apically to the skin surface. The stratum granulosum or granular layer is the most superficial layer of the epidermis that contains nucleated, viable cells. It is formed by flattened cells that are involved in the synthesis and modification of proteins that are part of the keratinization process (Wickett & Visscher, 2006). These cells are noticeably squamous, produce keratins and contain functional tight junctions and keratohyalin granules in their cytoplasm that are important in the formation of the stratum corneum barrier. These granules contain proteins high in histidine and cysteine, such as profilaggrin, the precursor of filaggrin, which is essential for the formation of the cornified envelope (Lai-Cheong & McGrath, 2017; Sandilands et al., 2009).

The stratum lucidum is a thin layer only present in thick skin (palms, soles and digits). It is formed by non-viable keratinocytes that are flattened and filled with eleidin, a transformation protein derived from keratohyalin that is rich in lipids, giving a transparent appearance to these cells, and providing a barrier to water (Farley et al., 2012).

The stratum corneum or cornified layer is the most external layer of the epidermis and it serves as the primary barrier for the skin against the environment. It is a dry and dead layer that prevents microbial entry and the dehydration of underlying tissues, protecting against erosion of the underlying epithelial layers. It consists of 25-30 layers of non-viable, anuclear corneocytes, that are flattened keratinocytes in the final phase of differentiation (Farley et al., 2012; Murphrey et al., 2021). Lamellar bodies are also present between the corneocytes (Celebi Sözener et al., 2020). The plasma membranes of differentiating keratinocytes are replaced every 4 weeks by the cornified lipid envelopes, promoting the cells to become flat and to connect to each other with corneodesmosomes to form the stratum corneum (Murphrey et al., 2021). Corneocytes contain keratin (a family of proteins named intermediate filaments that constitute the cytoskeleton of nucleated cells and are the principal structural proteins of skin, nail and hair) within a filaggrin matrix surrounded by insoluble lipids, inducing the change of shape in the keratinocytes. Keratins K5 and K14 are the principal structural products in proliferating basal keratinocytes, while K1 and K10 are expressed during the process of cornification; and together with filaggrin, they constitute 80-90% of the proteins of the epidermis in

mammals. To reinforce the cornified envelope, other lipids such as ceramides, and structural proteins such as involucrin, loricrin or small proline-rich proteins, are synthesized and crosslinked by transglutaminase-1 (Candi et al., 2005; Lai-Cheong & McGrath, 2017).

The formation of the skin barrier is an important and complex process that requires a large number of proteins, lipids and enzymes. Consequently, impairment of the skin barrier function can cause skin disorders such as atopic dermatitis, psoriasis or ichthyosis.

1.1.2.2 Dermis

The dermis is usually <2 mm thick, but it can be thicker in some parts of the body such as the back in adults (Hirobe, 2014; Wong et al., 2016). It is the mesenchymal component of the skin and provides the skin with most of its mechanical strength. The dermis is composed of two layers of connective tissue that contains elastin and collagenous fibres, produced by fibroblasts, that are surrounded in an amorphous glycosaminoglycan ground substance (Brown & Krishnamurthy, 2022).

The dermis is divided into two layers: the superficial papillary dermis and the deeper reticular dermis, divided by the rete subpapillare. The superficial papillary dermis is the thinner layer that lies closer to the epidermis and it is organized into cords in the upper part, termed dermal papillae that are formed by nerve endings and microvascular vessels involved in supplying sensory perception, nourishment and oxygen supply, respectively. Compared to the reticular dermis, the papillary dermis contains significantly more proteoglycans and a higher density of cells such as leukocytes (macrophages) and mast cells (MC) as well as loose connective tissue, while the reticular dermis contains a high alignment of collagen fibres and denser connective tissue, enabling movement to the skin and resulting in a much thicker layer (about 80% of the dermis) (Nafisi & Maibach, 2018; Rippa et al., 2019).

Many cell types are found within the connective tissue of the dermis, such as macrophages, adipocytes, MC, Schwann cells or stem cells, however, fibroblasts are the main cell type in the dermis. Fibroblasts originate mainly from primary mesenchymal cells; but they may also derive from epithelia, endothelial cells or fibrocytes (precursor cells in the blood) (McAnulty, 2007). Fibroblasts are a heterogeneous and dynamic cell lineage that varies across human tissues. In the dermis, for example, different subpopulations of fibroblasts are present in the two dermal layers, expressing different numbers of collagen fibres and ratios of type I and type III collagen (Nilforoushzadeh et al., 2017; Sorrell & Caplan, 2004; Tracy et al., 2016). Their main function is to secrete components of the extracellular matrix (ECM) such as collagen I, but they are also involved in other processes, such as

maintenance of skin homeostasis, skin morphogenesis and interaction with other resident cells (e.g., inflammatory cells) (McAnulty, 2007; Rippa et al., 2019; Sriram et al., 2015).

1.1.2.3 Hypodermis

The hypodermis or subcutaneous tissue is the adipose-rich layer below the dermis that connects the skin to the fibrous tissue of the bones and muscles. It is principally constituted by connective and adipose tissue, which is responsible of fat storage and provides insulation for the integument. It protects deeper tissue and organs, whilst serving as a support to the dermis and epidermis. It helps to protect against internal body heat loss and has important biomechanical properties to allow unconstrained movement (Ahn & Kaptchuk, 2011).

1.2 Immune system

The skin acts as physical barrier against infection as well as an active immunological interface, serving as an organ of protection (Nagao, 2019). However, inflammation in the skin occurs in response to disease. Examples of this are post-wound infection, tumour immunity, allergic or autoimmune responses that occur in disorders such as atopic dermatitis, lupus, psoriasis or vitiligo, among others (Kumar et al., 2018; Richmond & Harris, 2014). Therefore, interaction of various immune cell types plays a crucial role for correct functioning of the skin.

The dermal immune system consists of cells and proteins that protect the skin from foreign antigens, such as microorganisms, viruses and toxins. Antimicrobial peptides (AMPs) and lipids are also important in skin defence as they disrupt bacterial membranes. AMPs such as defensins or cathelicidins, produced by keratinocytes, fibroblasts or dendritic cells, are peptides expressed after cell activation when inflammation occurs. Lipids such as phospholipids, glucosylceramides and sphingomyelin are intermediate molecules that have antimicrobial activity against foreign microorganisms (Nguyen & Soulika, 2019).

There are two lines of defence against pathogens: innate immunity and adaptive immunity. The innate immune response is the first line of defence and is a non-specific, inherent defence mechanism that is not antigen or lymphocyte-dependent. It possesses no immunologic memory, so is not able to specifically recognise and respond to the same pathogen upon the next exposure. Also, the innate immune response occurs immediately after pathogen intrusion, or within hours. Adaptive immunity is an antigen and lymphocyte-dependent specific defence mechanism that occurs after the first exposure to an antigen therefore takes longer to set the response (4-7 days) than innate immunity. It

has immunological memory to pathogens, so that it can act faster and more efficiently upon subsequent exposure to a specific pathogen (Marshall et al., 2018; Yatim & Lakkis, 2015).

The immune barrier includes cells from non-haematopoietic origin (keratinocytes, fibroblasts, and endothelial cells), innate immune tissue resident cells (DCs, LCs, macrophages and MC), and adaptive immune cells (T cells). In addition, other immune cells such as neutrophils, eosinophils (EoS), natural killer cells, monocytes and B cells can be recruited from the bloodstream (Figure 1.3) (Eyerich et al., 2018; Richmond & Harris, 2014).

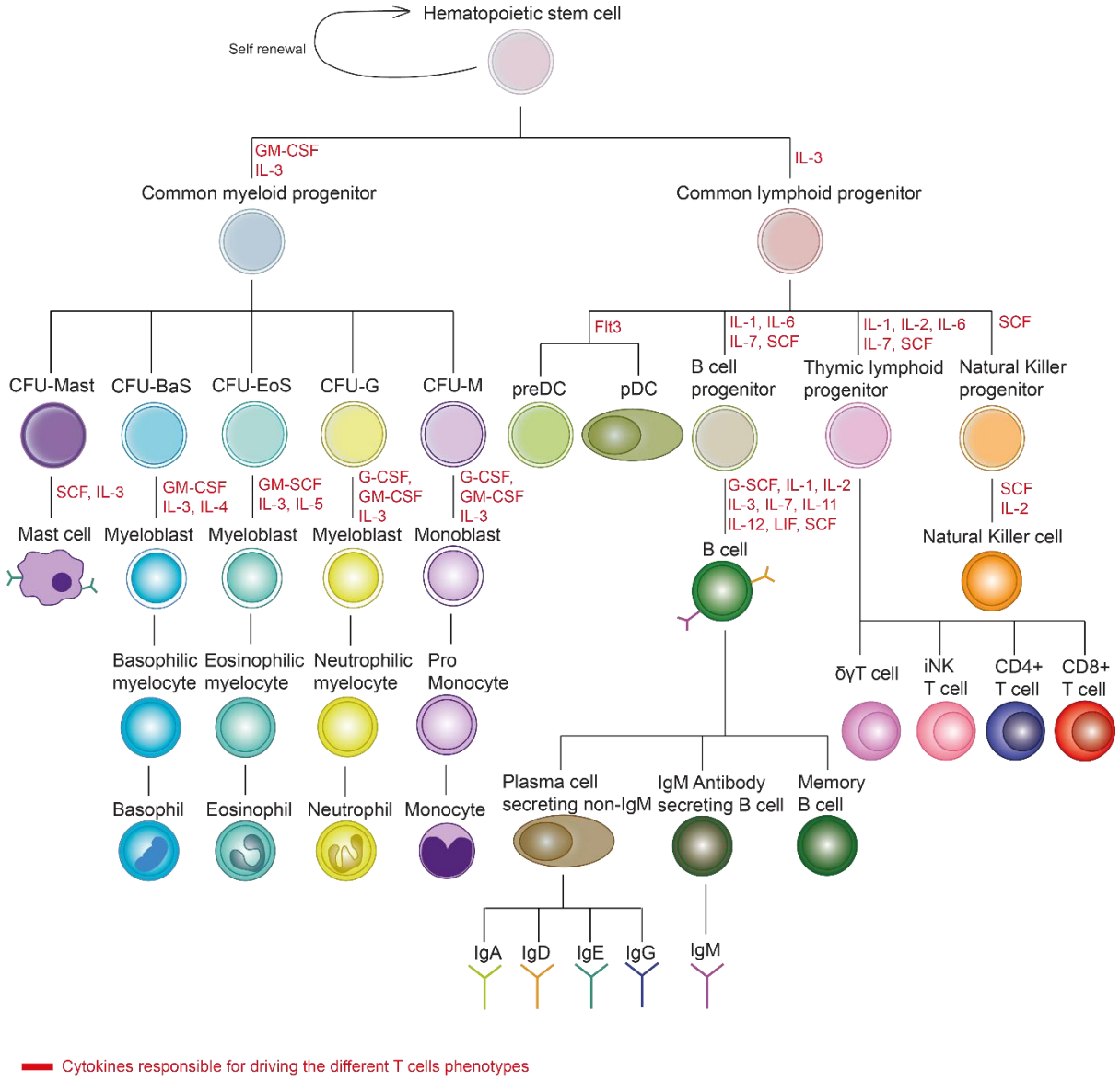

Figure 1.3 Immune cells lineage.

Common myeloid and lymphoid progenitors derive from hematopoietic stem cells. Mast cells, basophils, eosinophils, neutrophils and monocytes derive from different colony forming units (CFU) that originate from common myeloid progenitors, while pre-dendritic cells (DC), plasmacytoid DC (pDC) B cells, T cells and Natural Killer cells derive from lymphoid progenitors.
Cytokines required for cells differentiation are shown in red.

1.2.1 Dendritic cells

Dendritic cells are a heterogeneous population of leukocytes that are derived from the bone marrow and can be found in the circulation and peripheral tissue (mainly in skin, mucosa and lymphoid tissue) (Toebak et al., 2009; Yanofsky et al., 2013). DCs act as a link between the innate and adaptive immunity and are crucial to trigger the immune response. DCs are specialized antigen-presenting cells (APCs) that capture unknown or non-self-antigens when these penetrate the skin. DCs then migrate to the draining lymph nodes (dLNs) and mature, presenting antigens to naïve T cells that differentiate into effector T cells (T_H1, T_H2 or T_H17 cells) during sensitization, and producing cytokines that lead to antigen-specific immune responses (Haniffa et al., 2015; Honda et al., 2019; Patente et al., 2019). In addition, they induce tolerance and regulate immune homeostasis.

Dendritic cells can be subdivided in conventional DCs (cDCs) and plasmacytoid DCs (pDCs), and there are different subsets of these depending on the expression of surface markers and genetic profile. Furthermore, each subtype has different functions during immune responses.

cDCs correspond to the two subsets of myeloid DC classified as cDC1 and cDC2. Human cDC1s are cross-presenting DCs, triggering cytotoxic T cell immune responses (Macri et al., 2018) and are usually present in skin, blood, tonsil and lymph nodes among others. They correspond to the CD141+ or blood DC antigen 3 (BDCA3+) (Macri et al., 2018) and express high levels of HLA-DR, moderate CD11 expression, are negative for the lineage specific markers of CD19, CD14, CD16 and CD3, and do not express CD207 (Balan et al., 2019). cDC2s are usually present in skin, intestine, blood, lung and lymph nodes among others, and present antigen to CD4+ T cells. cDC2s express high levels of HLA-DR, CD11c, CD1c and signal regulatory protein alpha (SIRPα) (Balan et al., 2019).

pDCs are usually found in human blood and tonsil, produce large quantities of type I interferon (IFN) and participate in antiviral immunity. They express CD123, BDCA2 and BDCA4, among others.

Dendritic cells can originate from monocyte precursors during infection. These monocyte-derived dendritic cells (Mo-DC), often named “inflammatory Mo-DC”, express high level of HLA-DR and CD11c and are present in tissues after inflammation and can migrate to the draining lymph node. Mo-DCs are frequently involved in atopic dermatitis, psoriasis and rheumatoid arthritis, as they participate in innate immune responses and T cell activation (Balan et al., 2019; Marzaioli et al., 2020).

DCs can be differentiated *in vitro* from CD14+ blood monocytes by culture with GM-CSF and IL-4 (Kushwah & Hu, 2011). Mo-DC stimulate naïve CD4+ T cells towards a T_H2 phenotype, can present antigen to CD8+ T cells and produce cytokines IL-1, IL-6, TNFα, IL-12 and IL-23. Mo-DCs express CD1c, which is also expressed by monocytes and in CD14+ HLA-DR+ DCs (DCs present in non-lymphoid tissue

such as skin), CD1a, CD206, high-affinity immunoglobulin E receptor (FcεR1) and SIRPα. Other DCs present in blood and skin express markers such as CD80, CD86 and CD40 (Collin et al., 2013; Patente et al., 2019).

1.2.2 T cells

T cells are derived from lymphoid progenitors in the bone marrow and migrate to the thymus where they mature and develop their specific T cell markers before being exported to the periphery. They are present in every organ and tissue, but they mainly reside in lymphoid tissues, mucosal areas, skin and human peripheral blood (Clark, 2010; Farber et al., 2014). T cells are involved in homeostasis, memory and immune response, but also in inflammation and autoimmunity (Kumar et al., 2018).

T cells can be classified in four main types: helper T cells, which 'help' other immune cells; cytotoxic T cells that kill virally-infected or tumour cells (Andersen et al., 2006; Chaffey, 2003), regulatory T cells that participate in developing tolerance to offensive antigens and memory T cells, involved in recall protective response and maintenance of long-term immunity (Kumar et al., 2018).

1.2.2.1 Antigen presentation

Naïve cytotoxic or helper T cells recognise antigens by the T cell receptor (TCR) expressed on its cell surface (Chaffey, 2003) but only when the antigen is presented by an APC (e.g. DCs) (Figure 1.3.). The molecules on the APC that present the antigen to T cells are called MHC and can be sub-divided in MHC class I, where the antigen is presented by nucleated cells to cytotoxic CD8+ T cells; and MHC class II, where APC present antigens to CD4+ T cells, leading to the differentiation of these cells. The TCR-MHC binding complex requires co-receptors due to its instability: CD4 co-receptor is expressed by helper T cells and CD8 co-receptor by cytotoxic T cells (Wieczorek et al., 2017). The majority of T cells express either CD4 or CD8, although some cells can express both. Therefore, most T cells are described as CD4+ or CD8+, but some can also be defined as invariant natural killer T cells and mucosal-associated invariant T cells (Krovi & Gapin, 2018; Xiao & Cai, 2017). For T cell activation to occur, two signals must be produced by the APC. The first signal is generated by the TCR-CD3 complex, which changes the bound antigen peptide-MHC protein complex into intracellular signals. The second signal is produced by co-stimulatory proteins, mainly CD80 (B7.1) and CD86 (B7.2), recognised by the T cell co-receptor CD28, present on the cell surface (Figure 1.4). Expression of these B7 proteins is regulated by the activation state of the APC; therefore, activated DCs induce the expression of CD40L and CD28 on T cells. If both signals do not take place, cells can undergo apoptosis (Chen & Flies, 2013; Tai et al.,

2018). Therefore, CD80 and CD86 are important markers for APCs such as dendritic cells, while CD4+, CD8+, and CD40L, among others, are key markers for T cells.

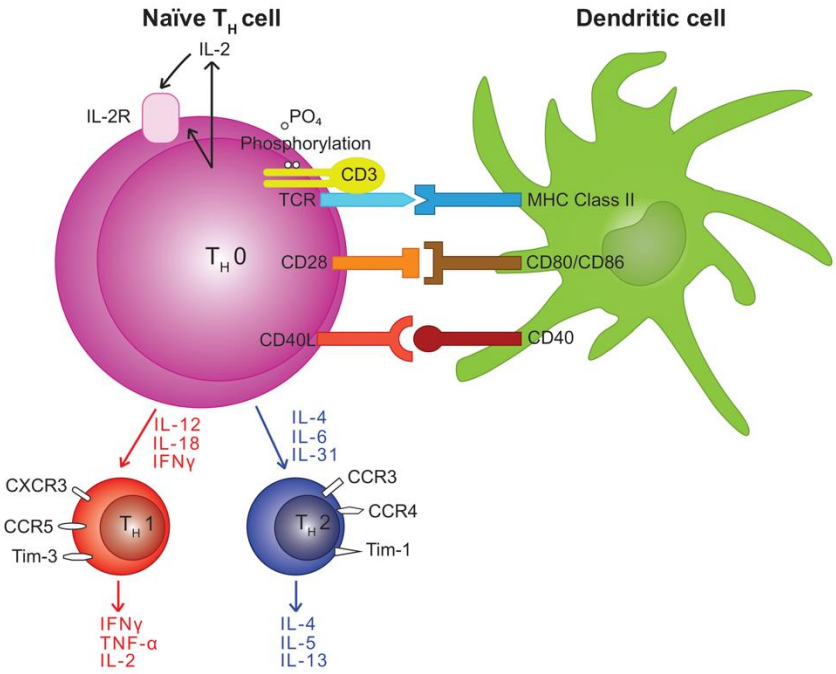

Figure 1.4 Antigen-presentation by DCs to T cells, and formation of T_H1 and T_H2 phenotypes. Naïve helper T cells (T_H0) recognise antigens by the T cell receptor (TCR) when the antigen has been presented by major histocompatibility complex (MHC) molecules present on the surface of an antigen presenting cell (APC), in this case a dendritic cell (DC). For the activation of T_H0 cells, two signals are required, the first signal is produced by MHC-peptide complexes that bind to TCR-CD3 complex; and the second signal is provided by CD80/CD86 molecules binding to CD28 on the T_H0 surface. In addition, CD40/CD40L interaction amplifies immune and inflammatory response. T_H0 cells also secrete IL-2 inducing T cell proliferation and differentiation into effector T cells. Once T_H0 have been activated by the APC, they can be polarised into T_H1 or T_H2 by different factors (IL-12, IL-18 and IFNγ stimulate T_H1 phenotype, while IL-4, IL-6 and IL-31 stimulates T_H0 towards a T_H2 phenotype), presenting different chemokines on their surface and secreting interleukins.

In addition, T cells are induced to secrete IL-2 that acts in an autocrine manner (Figure 1.4). This cytokine induces T cell proliferation and differentiation into effector T cells that then migrate around the body to remove pathogens. Effector T cells usually have a short life-span, although some can survive as memory T cells (Kumar et al., 2018; Tai et al., 2018).

1.2.2.2 Helper T cell

When a helper T cell is activated to become an effector cell, it can be further differentiated into specific subtypes depending on the presence of cytokines in the microenvironment: T-helper 1 (T_H1), T-helper

2 (T_H2), T-helper 17 (T_H17), T-helper 22 (T_H22), T-helper 9 (T_H9) or follicular helper T cell (Tfh) (Nguyen & Soulika, 2019). These subsets are phenotypically distinguished from each other by specific cell surface markers (Figure 1.5).

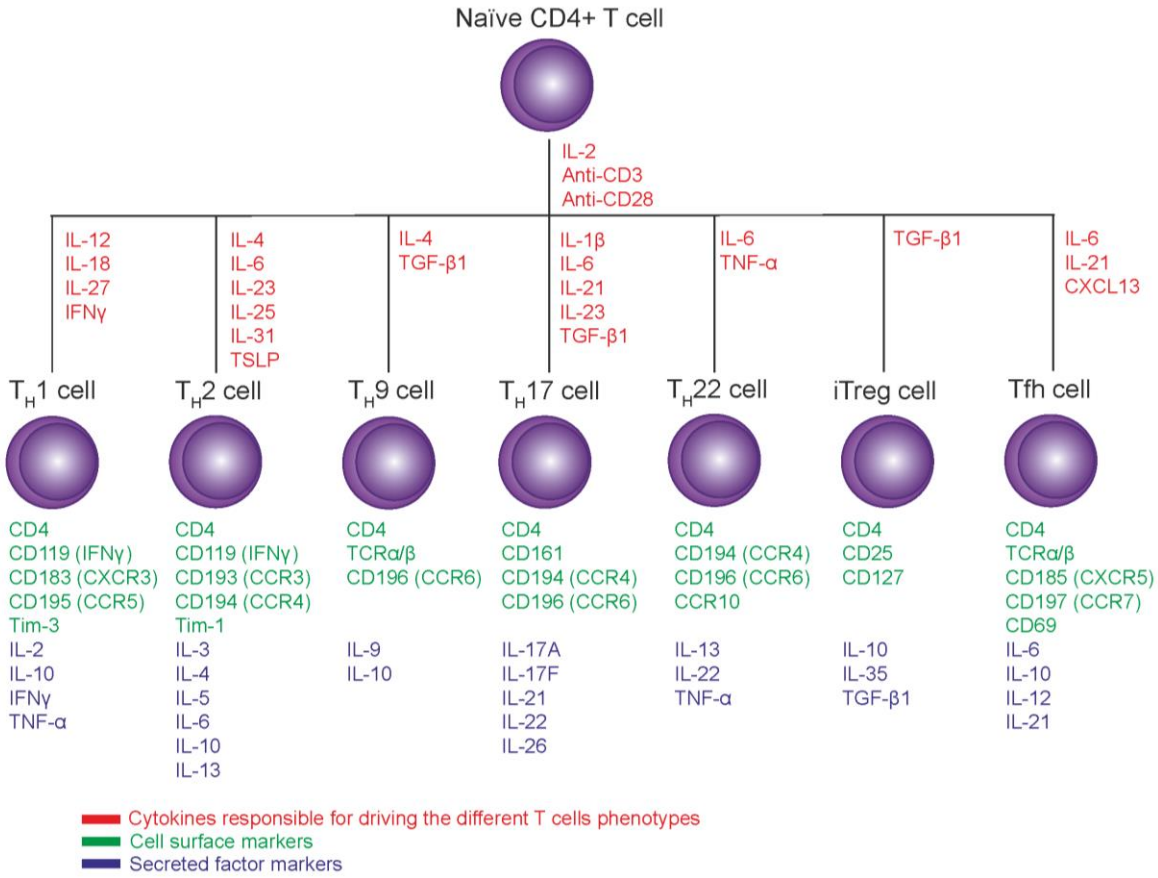

Figure 1.5 Helper T cells subtypes. Naïve CD4+ T cells can be differentiated into different T cell subtypes, shown in the image.
Cytokines required for helper T cells polarisation are shown in red; surface markers are shown in green; and secreted cytokines are shown in blue.

T_H1 cells are mainly involved in the elimination of intracellular pathogens but also in chronic and autoimmune diseases such as psoriasis, multiple sclerosis, autoimmune type 1 diabetes or oral lichen planus (Hirahara & Nakayama, 2016; Xie et al., 2012). Various cytokines are involved in T_H1 differentiation, although IL-12 and IFNγ are the principal cytokines required for differentiation. IL-12 is mainly produced by APCs such as DCs, activated monocytes or macrophages and is considered an early pro-inflammatory cytokine in response to infection (Luckheeram et al., 2012; Tugues et al., 2015). IL-12 stimulates STAT4 signalling inducing natural killer cells (NK) to secrete IFNγ, which then activates the STAT1 pathway (Glimcher & Murphy, 2000). IFNγ production is regulated by the transcription factor T-bet that represses T_H2 differentiation, as it inhibits IL-4 and reduces GATA3

function. In addition, T-bet avoids T_H17 development by interacting with the Rorc promoter (Luckheeram et al., 2012).

T_H1 cells secrete various cytokines such as IL-2, IL-10, IFNγ and TNFα. IL-2 is a growth factor secreted during the primary response of T_H cells, it activates other factors involved in cell proliferation, and defects in its ligand or receptor (IL-2R) can lead autoimmunity (Hwang et al., 2005). IL-10, also secreted by T_H2 cells, is an anti-inflammatory cytokine that can repress some NK and T cells functions as it inhibits pro-inflammatory cytokine production by APCs (Couper et al., 2008; Trinchieri, 2007). IFNγ is involved in T_H1 differentiation, but can also regulate CD8 T cytotoxic cell functions, as well as participate in the pro-inflammatory processes (Bhat et al., 2017). TNFα is a potent pro-inflammatory cytokine involved in antiviral T cell response, and development of cancer and autoimmunity (Mehta et al., 2018; Suresh et al., 2005). By secreting IFNγ and TNFα, macrophages are activated to destroy the pathogens. Cell surface markers specific of T_H1 differentiation are CD94 (Meyers et al., 2002); CD183 (CXCR3), which is a chemokine receptor involved in T cell function (Groom & Luster, 2011); CD119 (IFNγR1); CD4, CD195 (CCR5) (Lynch et al., 2003), and Tim-3, a molecule expressed on the T_H1 cell surface that reduces IFNγ secretion (Hastings et al., 2009).

T_H2 cells are involved with elimination of extracellular pathogens but also in allergic inflammation (hypersensitivity) disorders (Nakayama et al., 2017) such as asthma or atopic dermatitis. To polarize CD4+ T cells into T_H2 cells, IL-4 and IL-2 cytokines are required. IL-4 induces STAT6 signalling, which stimulates GATA3 (GATA-binding protein) and STAT5. GATA3 is involved in T_H2 cytokine production, inhibition of T_H1 differentiation and proliferation of T_H2 cells by Gfi-1 recruitment. T_H2 differentiation also involves other cytokines such as IL-6, IL-25 and TSLP. IL-6, secreted by APCs, and IL-4 promotes T_H2 differentiation whilst inhibiting T_H1 polarization (Luckheeram et al., 2012). IL-25 is structurally associated to IL-17 and induces IL-4, IL-5, and IL-13 gene expression (Fort et al., 2001), whereas TSLP stimulates DCs to polarize naïve T cells into T_H2 cells (Jang et al., 2013).

T_H2 cells secrete interleukins: IL-3, IL-4, IL-5, IL-6, IL-10 and IL-12 that are important in allergic inflammation (Hirahara & Nakayama, 2016). These cells can stimulate plasma cells to produce immunoglobulin E (IgE) and some subtypes of IgG that bind to basophils or MC (Marshall et al., 2018). Key surface markers for T_H2 differentiation include CD119 (also expressed by T_H1 cells) along with CD193 (CCR3) and CD194 (CCR4) (Yamamoto et al., 2000), and T cell immunoglobulin mucin-1 (Tim-1), a transmembrane protein whose function is to regulate T_H2 immune responses (Curtiss et al., 2012).

Other helper T cells include T_H9 and T_H17 cells, involved in autoimmune diseases (J. Li et al., 2017; Waite & Skokos, 2012) where TGF-β is required for both T_H9 and T_H17 cell polarization. TGF-β redirects

T_H2 towards T_H9 differentiation, while for T_H17 differentiation additional cytokines such as IL-6, IL-21 and IL-23 are required (Luckheeram et al., 2012). T_H17 cells secrete IL-17, IL-26 and TNFα that are involved in activation of NFκB and STAT1 signalling, inducing inflammation that stimulates T_H1 and T_H22 cell recruitment in psoriasis. Furthermore, T_H17 and T_H22 cells have been also shown in AD skin lesions, although AD has a strong T_H2 component (see section 1.3.3) (Guttman-Yassky & Krueger, 2017).

1.2.2.3 Cytotoxic T cells

Cytotoxic T cells (Tc) are activated after antigen presentation and can then be divided in naïve, effector, memory or effector/memory CD8+ T cells. Each of these Tc cell types is involved in different functions and is associated with diverse phenotypic characteristics. Naïve T cells circulate through the peripheral blood and lymphatic tissues; effector Tc cells express high levels of perforin (required for effective cell killing), and low levels of IL-2 and IFNγ; effector/memory Tc cells produce medium levels of perforin, therefore they have a limited cytotoxic activity but have high cytokines expression levels; and memory Tc cells can produce perforin and can be either CD4+ or virus-specific CD8+ depending on the type of antigen that they are presented to (Andersen et al., 2006; Ito & Seishima, 2010; Tungland, 2018).

1.2.2.4 Regulatory T cells

Treg are sub-divided in two types: iTreg cells that develop in the peripheral lymphoid organs and natural Treg derived from the thymus. These cells negatively regulate the immune response, preventing autoimmune diseases. Treg are also involved in immunologic tolerance to self and foreign antigen and they play an important role in the homeostasis of the immune system. They arise from naïve CD4+CD25- cells and express FOXP3. These cells secrete TGF-β as the main cytokine effector that has been shown to suppress IgE production (Dasgupta & Saxena, 2012; Luckheeram et al., 2012; Vignali et al., 2008).

1.2.2.5 Memory T cells

Memory T cells express CD45RO and chemokine receptor CCR7 as cell markers and function to provide life-long protection against pathogens. Their frequency changes throughout life. At birth, all T cells in peripheral blood are naïve, and memory T cells develop over time due to antigen exposure. During childhood, memory T cells are about 35% of circulating T cells, which also corresponds to the highest

susceptibility to pathogens. In adults, memory T cells remain stable and are maintained through cell turnover. In elderly individuals memory T cells become immunosenescent (Farber et al., 2014; Rudolph et al., 2018).

1.2.3 Other leukocytes involved in the immune response

1.2.3.1 Neutrophils

Neutrophils are the first line of host defence against invading microorganisms, including bacteria, fungi and protozoa. Neutrophils are the most abundant white blood cell in the circulation, constituting about 60% of all circulating leukocytes (Rosales, 2020). Neutrophiles are polymorphonuclear and granular leukocytes that are generated daily from the bone marrow during haematopoiesis, and during an infection neutrophil production is increased 10-fold (Liew & Kubes, 2019). Mature neutrophils leave the circulation and migrate to sites of tissue inflammation or infection. Their activation requires two steps: firstly, they are partially activated on their transit through the vascular endothelium; and secondly, they enter the inflammatory tissue where they become fully activated due to pro-inflammatory stimuli. Neutrophils participate in inflammatory responses producing cytokines and other inflammatory factors, but they can also interact with macrophages, DCs, and T cells, contributing to the immune response (Mayadas et al., 2014; Mortaz et al., 2018; Wright et al., 2010). In addition, neutrophils, as first line of defence against pathogens, are involved in antimicrobial functions such as the production of reactive oxygen species (ROS), phagocytosis, degranulation, and formation of neutrophil extracellular traps (Papayannopoulos, 2018).

Eosinophils and basophils are also blood granulocytes that are involved in allergic inflammation. They constitute about 15% and 0.1-1% of circulating leukocytes, respectively. Basophils participate in allergic diseases such as asthma or hay fever, as primary effector cells, while EoS are present during host defence, tissue remodelling and anti-inflammatory processes, among others (Nadif et al., 2013).

1.2.3.2 Monocytes

Monocytes are non-dividing cells that constitute about 10% of circulating peripheral leukocytes in humans. These cells derive from the bone marrow from a common myeloid progenitor shared with other cell types such as granulocytes and erythrocytes (Guilliams et al., 2018). Human monocytes can be divided into three main types based on the surface protein levels of the pattern recognition receptor CD14, which is a co-receptor for TLR4 and mediates lipopolysaccharide (LPS) signalling, and the Fc gamma III receptor CD16: classical (CD14+CD16-), non-classical (CD14dimCD16+), and

intermediate (CD14+CD16+). Classical monocytes are involved in ROS production and defence against fungal infections, and can be differentiated into monocyte-derived macrophages (MDM) and Mo-DC. Non-classical monocytes play an important role in wound healing, while intermediate monocytes participate in the rapid defence against pathogens (Kapellos et al., 2019).

Monocytes can phagocytose and present antigens as well as secrete chemokines. In response to inflammation or infection, monocytes are recruited into tissues where they quickly differentiate into mainly macrophages but also less frequently DCs (Jakubzick et al., 2017). In vitro, monocytes cultured for 7 days differentiate into macrophages, while they will differentiate into Mo-DC by addition of cytokines such as GM-CSF and IL-4. Monocytes are therefore important cells of the innate immunity and they participate in the regulation of the initiation, development, and resolution of inflammatory diseases. They are also involved in immunoregulatory and tissue-repairing processes (Ma et al., 2019).

1.2.3.3 Macrophages

Macrophages are mononuclear cells present within tissues with the ability of phagocytose pathogens and maintain tissue homeostasis (Yunna et al., 2020). Tissue macrophage progenitors are derived from the embryonic yolk sac and foetal liver during primitive haematopoiesis, while MDM are generated in the bone marrow by definitive haematopoiesis. Tissue macrophages self-renewal by cell division while MDM are terminally differentiated from peripheral blood monocytes (Viola et al., 2019).

Macrophages participate in innate immune response by secreting pro-inflammatory and antimicrobial mediators, and can also eliminate damaged host cells. They present antigens to T cells and serve as effectors for cell-mediated immunity. They are involved in the pathogenesis of infectious diseases, chronic inflammatory diseases and some cancers (Hirayama et al., 2017).

Macrophages are plastic cells that can be activated in different ways depending on changes in their local microenvironment, affecting their phenotypes. Macrophage polarization is a complex process where cytokines, chemokines and signalling molecules are involved. Two main phenotypes have been described: M1, classically activated macrophages; and M2, alternatively activated macrophages. Usually, inflammatory cytokines secreted by T_H1 lymphocytes, such as TNFα and IFNγ, along with LPS, induce an M1 phenotype, while IL-4, IL-10, IL-13 and TGF-β induce an M2 phenotype (Hirayama et al., 2017; Kumar et al., 2018; F. Zhang et al., 2016). M1 macrophages are activated by the interaction with pathogens and present their antigens to T cells to initiate the adaptive responses, therefore, M1 macrophages are involved in pro-inflammatory responses, secreting pro-inflammatory factors such as IL-6, IL-12 and TNFα. M2 macrophages are induced by innate and adaptive immune cells, such as T_H2

cells or MC and contribute to anti-inflammatory processes in wound healing, cancer progression, metastasis, and allergic reactions among others (Yunna et al., 2020). Macrophages can be phenotyped using aerobic (oxidative phosphorylation; M2) or anaerobic profiling (glycolysis, M1) (Viola et al., 2019).

1.2.3.4 Mast cells

Mast cells participate in innate immunity and are effectors of allergy that are normally present in its early and acute phases. Their origin has not been clear for several decades. It was thought that they are derived from mesenchymal cells but, lymphocytes, multipotent progenitors, and myeloid cells have also been proposed as mast cell precursors. Basophils have a similar morphology to MC and so have also been suggested as precursors. However, in a study carried out in 1977, researchers showed that MC derive from the bone marrow (Amin, 2012; da Silva et al., 2014).

MC are usually present at the interface between the host and the external environment, at easily accessible places for pathogens, such as skin or mucosa, and in the connective tissue. MC mature in the peripheral tissues after being transported from the bone marrow through the bloodstream (da Silva et al., 2014; Nguyen & Soulika, 2019). MC are usually involved in inflammation and allergy, where allergens stimulate MC activation by crosslinking IgE bound to the FcεRI, inducing the allergic cascade. MC, upon challenge with stimuli, secrete large quantities of histamine, cytokines, chemokines, lipid-derived mediators and growth factors (Mukai et al., 2018; Olivera et al., 2018). However, Fc receptors and alternative pathways (Redegeld et al., 2018) such as interaction with pathogens by PRRs also induces MC activation (Olivera et al., 2018).

1.3 Atopic Dermatitis

Atopic Dermatitis (AD), commonly known as eczema, is a chronic inflammatory, non-contagious, and common skin disorder that is frequently associated with other atopic diseases such as allergic rhinitis and asthma (the so-called “atopic march”) (Bieber, 2008). Atopy refers to the genetic tendency to produce IgE antibodies in response to common allergens such as pollen or house dust mites (HDM). Dermatitis comes from the Greek “*derma*” for skin, and “*itis*”, which means inflammation (Thomsen, 2014).

1.3.1 Epidemiology

According to the World Health Organisation (WHO) Global Burden of Diseases data, approximately 230 million people worldwide are affected by AD (Torres et al., 2019). AD is usually present in infancy or early childhood and affects up to 20% of children, although it can occur at any age (8% of adults affected in United Kingdom) (Cork et al., 2020). Despite the majority of cases of AD being resolved during childhood, 20-50% of adult patients continue to suffer from the condition (Fishbein et al., 2020). In addition, 50-75% of all children with early-onset AD develop allergic symptoms, while those patients with late-onset AD are usually less sensitized (Thomsen, 2014). Incidence levels vary worldwide and the severity and morbidity alters with age, gender, socioeconomic status, ethnicity and geographical location (Hadi et al., 2021). In industrialized countries, prevalence of AD has increased 2- to 3- fold over the last decade. Incidence is also rising in low-income countries (Nutten, 2015; Thomsen, 2014). Little is known about why the incidence is increasing, however, some studies suggest that this is due to genetic, social and/or environmental factors (Torres et al., 2019). Specifically in the United Kingdom (UK), urban areas such as London have a higher risk of developing AD compared to rural areas. People living in cities are likely to have increased exposure to risk factors such pollution, allergens and microbial exposures which may explain this trend (Cork et al., 2020). AD therefore has significant implications for health causing a large healthcare cost in the world. Indeed, a recent study in the United States of America (USA) calculated that the average lifetime cost for routine care was nearly $300,000 for patients with moderate and severe AD, while a European-based study estimated an average cost of £800 per annum per affected person, not taking into account extra everyday expenses or job disruption (Cork et al., 2020).

1.3.2 Diagnostic and clinical features

There is no specific diagnostic test or biomarker for AD diagnosis. Current diagnosis focuses on clinical manifestations, pruritus, personal and family history of atopy, and how the disease evolves. Diagnosis is normally simple in infants and young children, however it is more complicated in adults (Fishbein et al., 2020; Kapur et al., 2018; E. J. Yang et al., 2018). Increased levels of IgE in serum is the most typical feature, however, this is not evident in all AD patients (Torres et al., 2019). To support the diagnosis, several criteria have been proposed, but the criteria proposed by Hanifin and Rajka (Hanifin & Rajka, 1980) (Table 1.1) is the most used (Wollenberg et al., 2018).

Table 1.1 Diagnostic criteria for AD (Hanifin & Rajka, 1980)**.**

Must have 3 or more basic features:
Pruritus
Typical morphology and distribution: - Flexural lichenification or linearity in adults - Facial and extensor involvement in infants and children
Chronic or chronically-relapsing dermatitis
Personal or family history of atopy (asthma, allergic rhinitis, atopic dermatitis)
Plus 3 or more minor features:
Xerosis
Ichthyosis/palmar hyperlinearity/keratosis pilaris
Immediate (type I) skin test reactivity
Elevated serum IgE
Early age of onset
Tendency toward cutaneous infections/impaired cell-mediated immunity
Tendency toward non-specific hand or foot dermatitis
Nipple eczema
Cheilitis
Recurrent conjunctivitis
Dennie-Morgan infraorbital fold
Keratoconus
Anterior subcapsular cataracts
Orbital darkening
Facial pallor/facial erythema
Pityriasis alba
Anterior neck folds
Itch when sweating
Intolerance to wool and lipid solvents
Perifollicular accentuation
Food intolerance
Course influenced by environmental/emotional factors
White dermographism/delayed blanch

The UK's National Health Service (NHS) follows the guidelines set by the National Institute for Health and Care Excellence (NICE), which covers the diagnosis and management of AD in children and adults (Cork et al., 2020). Some clinicians face challenges classifying patients with AD. However, atopy (that should involve not only the presence of IgE but also the cytokine profile induced by the T helper cells response), pruritus, eczema and altered vascular reactivity are the four symptoms that seem to be universally accepted (Beltrani, 2002).

Many patients with AD present with dry skin (xerosis) due to the low tissue water content and trans-epidermal water loss. Skin colour is usually pale, as the tension in the dermal capillaries increases; and patients' hair is dry and fragile (Thomsen, 2014). However, clinical manifestations differ with age (Figure 1.6). In infancy, the first eczematous lesions appear on the cheeks and scalp, causing crusted erosions after scratching. During childhood, lesions include flexures, the nape, and the dorsal aspects of the limbs, while in adolescence and adulthood lichenified (thick skin) plaques involve the flexures, and head and neck (Bell & Brown, 2017; Bieber, 2008). Therefore, the main signs of AD are a chronic form of skin inflammation, a disruption of epidermal-barrier function that ends in dry skin, and IgE-mediated sensitization to food and seasonal allergens (Bieber, 2008; Cork et al., 2006; Guttman-Yassky & Krueger, 2017).

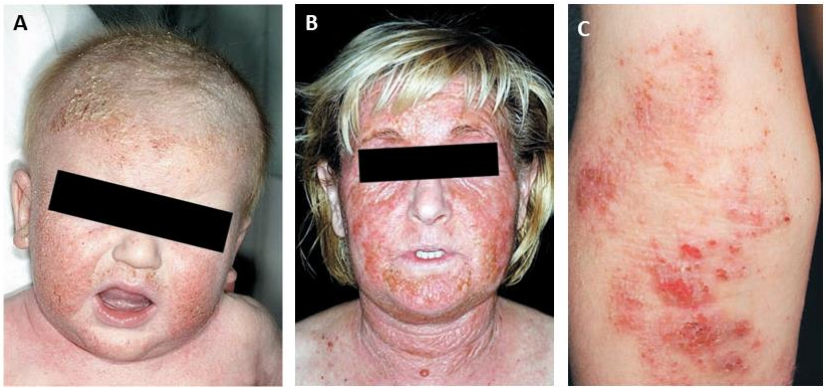

Figure 1.6 Clinical manifestations of atopic dermatitis.
Image shows initial lesions involving the cheek and scalp in an infant (A); head and neck manifestations in an adult (B); and chronic, lichenified flexural lesions in an adult (C). Image reproduced with permission from (Bieber, 2008), Copyright Massachusetts Medical Society.

1.3.3 AD pathogenesis

1.3.3.1 Genetics of AD

Families with members already affected by atopic dermatitis are at higher risk of developing the condition, and AD can arise from gene-gene and gene-environment interactions (Boguniewicz &

Leung, 2011; Thomsen, 2014). Previous studies have shown a concordance rate of approximately 80% in identical twins and 22% in dizygotic twins, suggesting high heritability of AD (Al-Shobaili et al., 2016; Bin & Leung, 2016; Morar et al., 2006).

Null (loss-of-function) mutations in the gene encoding filaggrin (FLG), which is found in the epidermal differentiation complex on chromosome 1q21.3, are the most significant genetic risk factor for AD (Løset et al., 2019). However, several other genes usually involved in epidermal differentiation or the immune system have been identified in atopic dermatitis (Table 1.2) (Bin & Leung, 2016; Løset et al., 2019). Involved genes are mainly located on chromosome 5q31-33 and encode cytokines that are involved in the regulation of IgE synthesis such as IL-4, IL-5, IL-12, IL-13 and GM-CSF. Therefore, most studies have focused on candidate genes involved in adaptive and innate immune response genes, although over the past few decades, investigators are showing interest on skin barrier dysfunction genes such as *FLG* (Bieber, 2008; McPherson, 2016).

Table 1.2. Genes involved in adaptive and innate immune response, associated with AD (Al-Shobaili et al., 2016; Boguniewicz & Leung, 2011)**.**

Antigen presentation, cell-mediated and humoral immune response pathway
CD14 (monocyte differentiation antigen)
GATA3 (GATA- binding protein 3)
NOD1 (nucleotide-binding oligomerization domain 1)
NOD2 (nucleotide-binding oligomerization domain 2)
TLR2, TLR4, TLR6 and TLR9 (Toll-like receptor 2, 4, 6 and 9)
Cell signalling and interaction, cellular movement and hematologic system development and function pathway
BCL2A1 (BCL2-related protein A1)
BDNF (brain-derived neutrophilic factor)
CSF2 (colony-stimulating factor 2)
GSTP1 (glutathione S-transferase 1)
NAT (N-acetyl transferase)
SOCS2 (suppressor of cytokine signalling 3)
SPINK5 (serine protease inhibitor Kazal-type 5)

In addition, cytokines such as IL-1α, IL-1β, IL-4, IL-5, IL-6, IL-10, IL-12β, IL-13, IL-18, TNFα, TGF-β1, IFNγ and GM-CSF; chemokines like CCL5, CCL11, CCL17, CCR3 or CCR4, and their related genes seem to be involved in the pathogenesis of AD (Al-Shobaili et al., 2016).

It seems, therefore, that AD can be due to genetic factors that lead to deficiencies in the immune system. Skin barrier dysfunction is one of the consequences of this lack in the immunity, which can affect the course and severity of the disease. Indeed, the interplay of environmental factors and genes likely drive the pathogenesis of AD, leading to a dysregulated immune response that ultimately causes disrupted skin barrier function and pruritus.

1.3.3.2 Skin Barrier disruption

It is known that there is a reduction of the barrier function in AD patients, and studies have shown down-regulated *FLG* expression in these patients (McPherson, 2016; Palmer et al., 2006). Around 30% of AD patients worldwide (~ 9% of the UK population), present a mutation in the gene that encodes for *FLG*, an important epidermal filament-aggregating protein. *FLG* is polymorphic, with common allelic variants encoding profilaggrin (Elias et al., 2017; McPherson, 2016) that is dephosphorylated and degraded into 10-12 FLG monomeric molecules during epidermal differentiation. FLG is a key marker of keratinocyte differentiation (Al-Shobaili et al., 2016), and FLG molecules condense in the keratin cytoskeleton acting as a template for the assembly of the cornified envelope. Furthermore, breakdown products of FLG are involved in the water-binding capacity of the stratum corneum and maintenance of the barrier function (Al-Shobaili et al., 2016, p.; Bieber, 2008; McPherson, 2016). FLG is therefore a protein that is responsible for the integral structural component, maintaining stratum corneum hydration, and is essential for the cornification and structure of the epidermis, being crucial in skin barrier integrity (Egawa & Weninger, 2015; Rerknimitr et al., 2017).

FLG expression is down-regulated by cytokines such as IL-4, IL-13, IL-17A, IL-22, or IL-25 in patients with AD. Environmental factors such as low ambient humidity, pruritus or skin irritants can also lead to FLG proteolysis (Al-Shobaili et al., 2016). *FLG* mutations take place principally in early-onset AD and indicate a tendency to develop asthma. Genetic mutations of *FLG* in AD can produce alterations in the epidermal barrier function by reduction (heterozygous mutation) or complete absence (homozygous mutation) of epidermal FLG and its degradation products (Bieber, 2008; McPherson, 2016). In addition, null mutations in *FLG* cause ichthyosis vulgaris, the most common inherited disorder of keratinization (McPherson, 2016).

The findings of the importance of *FLG* and epidermal integrity suggest that *FLG* mutation-induced AD is due to a primary barrier defect that results in inflammation (McPherson, 2016). Defects in *FLG* also leads to an increased skin pH, which modifies the function of kallikrein (KLK) serine proteases that are involved in corneocyte discharge, and are regulated by protease inhibitors such as *SPINK5*, a molecule

also associated with AD. When KLK are activated, they increase the production of IL-1α and TSLP, inducing inflammation (Cork et al., 2009; Egawa & Weninger, 2015; Rerknimitr et al., 2017).

AD patients with *FLG* expression defects have decreased stratum corneum hydration driving TEWL, and high pH. Consequently, there is a higher risk of developing other atopic diseases like asthma or rhinitis, and allergies. Skin barrier disruption caused by *FLG* deficiency can also induce inflammation and decreased protein expression in keratinocytes (Boguniewicz & Leung, 2011; Zaniboni et al., 2016).

1.3.3.3 Histopathology

Histologically (Figure 1.7), skin lesions from patients in the acute phase of AD show prominent epidermal intercellular edema (spongiosis). In lesional, and sometimes in non-lesional, skin of AD patients with the IgE-associated form, LCs present surface-bound IgE molecules. In addition, there is noticeable perivascular T cell and macrophage infiltration in the dermis, but also eosinophils, and rarely basophils and neutrophils. Mast cells can also be detected at different levels of degranulation. In chronic forms of AD, a hyperplastic epidermis with elongation of the rete rides, noticeable hyperkeratosis, and minor spongiosis can be observed. In the dermis, DC that present IgE molecules and macrophages are the dominant cell types. Also, mast cells and eosinophiles numbers are increased compared to the acute lesions (Bieber, 2010).

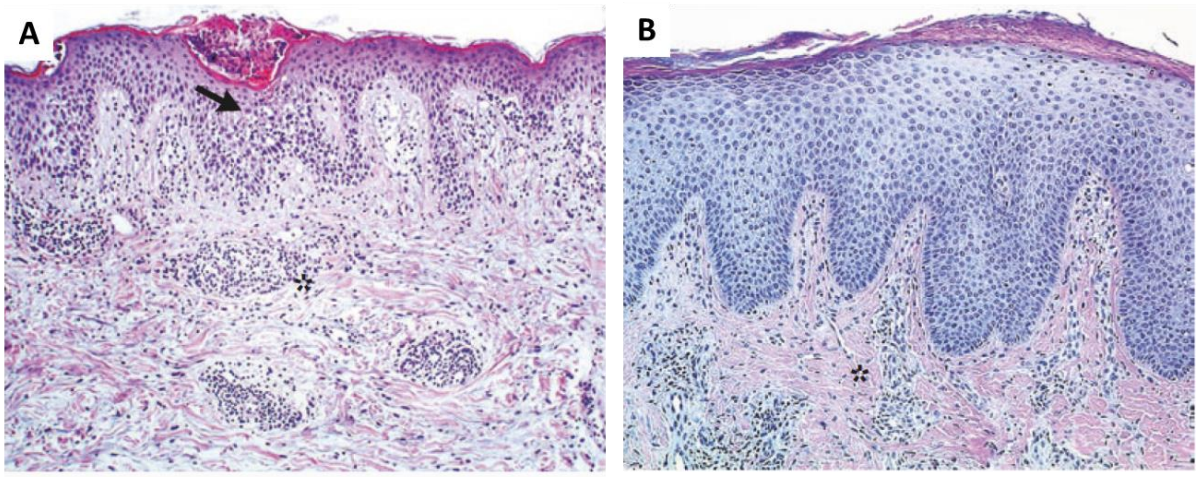

Figure 1.7. Histopathology of AD.
Haematoxylin and eosin (H&E) shows an acute lesion (A) with spongiosis within the epidermis (arrow) and high perivascular infiltration (asterisk), and a chronic lesion (B) with thicker epidermis and increase perivascular infiltration (asterisk). Image reproduced with permission from (Bieber, 2008), Copyright Massachusetts Medical Society.

1.3.3.4 Immunopathogenesis

Both innate and adaptive immune systems are involved in the development of AD; therefore, the immunopathogenesis of AD is a complex process. Keratinocytes, innate immune cells, mast cells, dendritic cells and T cells, among others, are involved in skin inflammation. In AD, all these cells interact with each other, although there is a tendency towards T_H2 responses (Figure 1.8) (Egawa & Weninger, 2015).

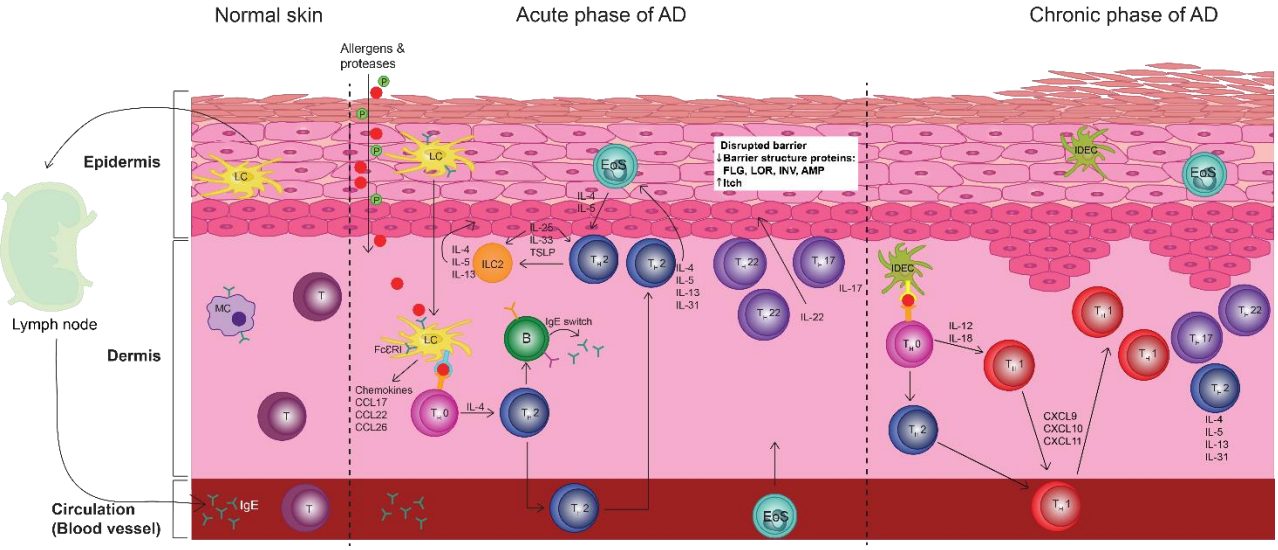

Figure 1.8 Schematic diagram illustrating the key pathological events during the acute and chronic phases of AD.

In healthy skin, Langerhans cells (LC) are present in the epidermis, while other immune cells such as T cells and mast cells (MC) are found in the dermis or in circulation. During the acute phase of AD, allergens and proteases penetrate the skin, and these are taken up by LC, which express high levels of the IgE receptor (FcεRI) on their surface, that migrate from the epidermis to the dermis. LC present the antigen to naïve T cells and stimulate these to differentiate into a T_H2 phenotype by secreting cytokines, like IL-31 that produces a characteristic itch. These cytokines stimulate eosinophils (EoS) in the epidermis, that secret cytokines that stimulate T_H2 cells. Trough the release of IL-4 and IL-13, T_H2 cells suppress the skin barrier function increasing skin permeability to further allergens and proteases, driving keratinocyte release of pro-allergic mediators such as TSLP, which stimulate innate lymphoid cells-group 2 (ILC2), that release more cytokines into the epidermis. In addition, CD4+ T cells, upon activation, develop into T_H17 and T_H22 cells secrete IL-17 and IL-22, that activate keratinocyte innate immune defences. During the chronic phase of AD, there is an increased of inflammatory dendritic epidermal cells (IDEC) and EoS, that contribute to inflammation producing IL-12, which leads to stimulation of T_H1 cells and the secretion of chemokines. This induces keratinocyte apoptosis, producing the spongiotic process observed in acute atopic dermatitis and that is mediated by IFNγ.

Allergens and proteases entering the skin are taken up by epidermal DCs. Two different types of DCs can be found in AD lesions: LCs and inflammatory dendritic epidermal cells (IDECs). Both cell types express high levels of FcεRI on their surface that capture and process the allergens. In addition, bacteria such as *Staphylococcus aureus* is recognised by TLR, a group of PRR involved in activation of

EoS and dermal fibroblasts in allergy or by cytosolic PRR nucleotide binding oligomerization domain like receptors (D. Li & Wu, 2021). Cross linking of FcεRI upon binding allergen leads to secretion of IL-6 and chemokines such as CCL22, CCL17 and CCL2. After recognising the antigen in the skin, dermal DCs migrate to skin lymphoid nodes to present the antigen to naïve T cells and stimulate these to differentiate into a T_H2 phenotype, as previously described in section 1.2.2.1 (Egawa & Weninger, 2015; Honda et al., 2019; Novak et al., 2003; Rerknimitr et al., 2017). CCR4 and CCR10 allow T cells to migrate through endothelia in the skin when binding with CCL17, CCL22 and CCL27. Once T_H2 cells are in the skin, their activation leads to cytokine secretion (Biedermann et al., 2015). T_H2 cells secrete cytokines such as IL-4, IL-5, IL-13, and IL-31 that produce a characteristic itch or pruritus, which is one of the symptoms that identifies AD. IL-31 expression in T_H2 cells depends on IL-4 and IL-33 levels, as these two cytokines stimulate IL-31 production. On the contrary, TGF-β downregulates IL-31 secretion. IL-31 activates its receptor heterodimer IL-31 receptor A (IL31RA)/Oncostatin M receptor β (OSMRβ)-expressing dorsal root ganglia (DRG) neurons and keratinocytes, relating immune cells to epithelium and the neural system. This is because stimulation of TLR2 by bacteria or "atopic" cytokines increase IL-31 receptor, which induces CCL2 secretion from keratinocytes. In addition, IL-31 stimulates DCs, that secrete pro-inflammatory cytokines such as TNFα and IL-6, but also chemokines like CCL2 and CCL22, increasing the inflammation (Datsi et al., 2021). Recently, researches have shown that hyperinnervation of the epidermis and increase of several itch mediators (histamine, some proteases, IL-31 and TSLP among other factors) are responsible for the pruritus that these patients suffer (Rerknimitr et al., 2017).

Innate lymphoid cells (ILC), that are involved in skin immunity and that do not carry an antigen receptor, are present in AD patients. Specifically, there is a marked increase in group 2 ILCs (ILC2) that produce IL-4, IL-5 and IL-13. ILC2 function is regulated by keratinocyte-derived cytokines such as IL-25, IL-33, and TSLP that also stimulate LCs (Egawa & Weninger, 2015; Rerknimitr et al., 2017). High levels of IL-5, but also IL-3 and GM-CSF, induce EoS recruitment to the inflamed tissue. EoS secrete cytokines and chemokines, such as IL-6, IL-12 and IL-13, playing a key role in immunoregulation (Liu et al., 2011).

Therefore, the interplay between keratinocytes, DCs and T cells is crucial in driving an escalating cycle of inflammation. AD patients exhibit enhanced sensitivity to allergens and an inflammatory response dominated by T_H2 cells during acute phase. Through the release of IL-4 and IL-13, T_H2 cells supress the skin barrier function increasing skin permeability to further allergens and proteases, driving keratinocyte release of pro-allergic mediators, such as TSLP, which is known to induce AD-like phenotype, IL-25, IL-33 and GM-CSF.

In addition, CD4+ T cells, upon activation, differentiate into T_H17 and T_H22 cells that secrete IL-17 and IL-22 and activate keratinocyte innate immune defences. T_H17 cells seem to be increased in most severe AD patients, and they secrete both IL-17 and IL-22, whereas, T_H22 cells secrete IL-22 and other cytokines such as IL-13, and TNFα, but not IL-17, IFNγ or IL-4. Secretion of IL-17 is enhanced by *S. aureus*, however, IL-22 is dominant in AD skin compared to IL-17, which is more frequently found in psoriatic skin (Jiang et al., 2021; Sugaya, 2020).

Development of AD is also influenced by environmental factors, such as diet, microbial exposure or climate. AD skin is preconditioned to host pathogenic microorganisms. For example, *S. aureus* can produce superantigens that are resistant to heat and proteolysis, and that can be linked to MHC-II and T cells with the TCR. *S. aureus* also induces keratinocytes to secrete cytokines such as IL-1α and IL-36α, via the induction of IL-17, and release proteases and cytolytic toxins that can injure cells, and interact with PRRs increasing inflammation (Rerknimitr et al., 2017). Patients with high-density colonization with this bacteria is associated with severe AD, while colonization with *Staphylococcus epidermidis* is associated with milder symptoms (Pothmann et al., 2019). Furthermore, airborne allergens derived from HDM lead to AD, as they disrupt skin barrier function in these patients, which exacerbate penetration of allergens into the epidermis and aggravate AD symptoms. There are different species of mites, however, the most common ones are *Dermatophagoides pteronyssinus* (Der p), *Dermatophagoides pteronyssinus* (Der f) and *Euroglyphus maynei* (Eur m). Mite extracts induce secretion of pro-T_H2 cells cytokines such as IL-25 and IL-33 (Bumbacea et al., 2020). In addition, UV exposure and climate factors such as temperature or humidity seem to induce eczema. All these factors lead to increased levels of T_H2 cells and consequently, higher levels of cytokines, producing skin inflammation and skin barrier disruption (Egawa & Weninger, 2015; Rerknimitr et al., 2017).

Several factors can therefore contribute the development of AD and/or worsen the symptoms and features of this disease in patients (**Table 1.3**).

Table 1.3. Factors involved in the development of AD

Causes of atopic dermatitis
Allergens
Antibiotic exposure
Dysfunction in the immune system
Dysfunction in the skin barrier
Excessive use of soaps and detergents
Genetic mutations
Low bacterial exposure
Low microbial diversity
Pollution
Stress
Tobacco
Urban environment
Weather, UV light
Western diet

1.3.4 Current treatment

There is not a complete cure for AD as its pathophysiology is genetically determined, and most of the treatments focus on symptom relief. To treat AD symptoms, topical corticosteroids (TCS) together with emollients are applied (Zuberbier et al., 2006). Emollients have been demonstrated to decrease the incidence of AD and show a similar effectiveness to topical application of low potency corticosteroids. These include petrolatum, which modulates the antimicrobial and epidermal barrier function, physiological lipid mixtures, and ceramide-dominant triple-physiologic lipid, composed by ceramides, cholesterol and free fatty acids, that improve the skin barrier function and decrease bacterial colonization by stimulating the amount of these three components in the lipid membrane of the stratum corneum (B. E. Kim & Leung, 2018; Kircik et al., 2011). In the UK, current treatment includes emollients to protect the skin barrier and/or TCSs, and topical calcineurin inhibitors (TCIs) to reduce the inflammation, although their long-term use can cause side effects. For children under 12 years, these medications have been adapted to the severity of the disease (Cork et al., 2020).

The use of baths with diluted bleach have been shown to improve AD symptoms, however, bathing can also produce dryness when a harsh detergent is used (Cork et al., 2020; B. E. Kim & Leung, 2018).

Some new targeted therapies have been developed that may improve the effective and safe management of patients that present with the more severe forms of AD. These include phosphodiesterase inhibitors and JAK-STAT inhibitors, such as baricitinib (Bieber, 2022; Hajar et al., 2018). There are over 90 patented JAK inhibitors (JAKi), and many are still in clinical development. These drugs can be divided into three groups: non-selective (pan-)JAKi, dual inhibitors, and selective JAK1 inhibitors. However, the low number of AD patients in clinical trials for these drugs and the fact that most of the data collected on long-term drug exposure correspond to patients with rheumatoid arthritis, make these drugs unavailable for AD patients. Another strategy to target inflammation is the inhibition of the tropomyosin receptor kinases (TRKs); however, these inhibitors are still in clinical trials and results are not currently available (Bieber, 2022).

In addition, targeted therapies have been developed to target different cytokines and chemokines involved in the immunopathogenesis of AD. These therapies include Tezepelumab, which is an anti-TSLP antibody, the anti-IL-33 antibodies etokimab and astegolimab, and bermekimab, an anti-IL-1α antibody originally developed for cancer that has shown a reduction in itching in AD patients. Researchers have also investigated potential drugs targeting the adaptive immune response. Some studies have used antibodies against OX40, a costimulatory molecule member of the TNF receptor family, or its ligand. Dupilumab, an approved drug in many countries, binds to IL-4Rα targeting IL-4 and IL-13; while tralokinumab and lebrikizumab target specifically IL-13. Attempts have been also made to target IL-5 and IL-22, however, these drugs were not efficient enough to significantly decrease the pruritus scoring. Some ongoing studies are also testing potential drugs that target IL-31 (nemolizumab), IgE synthesis, histamine receptor and S1PR, among others (Bieber, 2022).

Besides these recent advances, and some available treatments approved by the FDA, the available treatment remains very restricted. FDA approved drugs include tralokinumab, which is an IL-13 antagonist given to treat moderate to severe AD in adults when topical treatment is not advisable; abrocitinib, a JAK inhibitor recently approved to treat patients over 12 years of age with moderate to severe AD when other drugs are not recommended; dupilumab, an IL-4Rα antagonist to treat AD patients over 6 years with moderate to severe AD when topical treatment cannot be used; upadacitinib to treat severe AD in patients over 12 years of age; and ointments and creams such as Elidel, crisaborole, desonide, ruxolitinib or tacrolimus (D'Ippolito & Pisano, 2018; Guttman-Yassky et al., 2023; Perche et al., 2023; Wollenberg et al., 2021).

Therefore, a better understanding of the mechanisms involved in the development of AD and new treatments to improve the long-term control of the disease are necessary. To accomplish this, new pre-clinical models are required to support drug development and testing. Since murine experimental

models that replicate aspects of AD can show markedly different responses to drug treatments, the best approach would be the use of tissue engineered skin models.

1.4 Tissue-engineered models

Two-dimensional (2D) culture, in which cells are grown as a monolayer, has been used for many years as it is a simple and economic culture. However, they have many disadvantages, as they do not mimic the intrinsic features of tissues. In skin, for example, many functions, such as skin barrier, immune function or stratification, cannot be mimicked by 2D monolayer cultures (Klicks et al., 2017). The morphology and structure of the cells in 2D are changed as they grow; cells deform and flatten forming a monolayer where part of the cell is in contact with the plastic. In addition, change of phenotype and morphology can affect cells functionality, cell signalling, secretion, and organisation of the organelles within the cell. This changes can also alter gene expression and biochemistry of the cell (Kapałczyńska et al., 2018).

On the other hand, three-dimensional (3D) models representing human tissue can model how different cell types interact and can mimic skin barrier functions, allowing for a better comprehension of the cell-to-cell and cell-to-extracellular matrix interactions. In addition, tissue-engineered human models reduce the need for animal models (Holmes et al., 2009; Yu et al., 2019). Regarding AD, murine experimental models that replicate aspects of AD pathophysiology are available (Gupta et al., 2004), and these can be categorised in three groups: inbred strains of mice that generate AD-like phenotypes; genetically engineered models with either removal or over expression of a gene; and AD-like phenotypes induced by external agents. The first type of model mimics the development of human AD with sensitization to allergens, however, no genetic information can be obtained from most of these strains. Genetically engineered mice models are useful to study gene-related functions, however these are very expensive and time consuming models that can show adverse consequences from unexpected gene expression. The last group of murine models are suitable for different strains of mice, nonetheless doses and durations are very variable within experiments and it is time consuming (D. Kim et al., 2019). Although murine models can mimic some features of AD, these mice often display markedly different responses to drug treatments, contributing to high failure rates in drug development (A. Tanaka et al., 2012).

Therefore, new pre-clinical models are required to aid the development and identification of new drugs and treatments. New models are not only necessary in the biomedical and pharmacological research, but also in the cosmetic industries, due to ethical and legal requirements to exclude animal testing (Mathes et al., 2014; Mertsching et al., 2008).

1.4.1 Tissue-engineered skin models

Tissue-engineered skin equivalents are usually constructed by seeding dermal fibroblasts into a biodegradable matrix or hydrogel scaffold. Epidermal keratinocytes are then seeded on top and encouraged to proliferate and differentiate, resulting in the formation of the desired 3D tissue (Langer & Vacanti, 1993; Reijnders et al., 2015). These approaches are shared by regenerative medicine, which, however, encourages the use of patients' cells. Human primary keratinocytes (Mieremet et al., 2019) and human immortalised keratinocytes cell lines (N/TERT and HaCaT cells) (Dickson et al., 2000; Weinmuellner et al., 2018) have been therefore used to develop tissue-engineered human skin equivalents (HSE). Although primary human cells are of particular relevance as they are more representative of *in vivo* tissues structures and functions, a large amount of these cells are necessary to construct HSE. Furthermore, there are not many skin donors and more replicates would be needed when using these cells as there is high patient-to-patient variations. To overcome this limitation, immortalised keratinocyte cell lines are being used. Immortalised cell lines have the advantage of being cost effective, easy to culture, expand and can be used for a number of passages. They also bypass ethical concerns relating to the use of human tissue. In addition, they histologically mimic the human skin when in a 3D microenvironment, frequently showing a normally differentiating epidermis, although some immortalised cells can form a thicker epidermis with denser basal cells and more layers of spinous cells compared to primary keratinocytes (Dickson et al., 2000). However, being immortalised, they may not properly represent primary cells and tissue functions, and they can be cross-contaminated with other cell lines and mycoplasma. In fact, when generating HSE with HaCaT cells, no stratum corneum is formed and expression of cornified envelope-associated proteins such as loricrin, involucrin and filaggrin is atypical compared to primary cells (Smits et al., 2017).

Several scaffolds that mimic connective tissue have been previously used for tissue-engineered models. These include de-cellularised dermis (Figure 1.9), natural macromolecules that form hydrogels such as type I collagen, fibrinogen and chitosan or synthetic polymers and polymers synthetized from natural materials, spheroids, organ-on-a-chip, or 3D bioprinting (Boyce & Lalley, 2018; O'Brien, 2011; Z. Zhang & Michniak-Kohn, 2012).

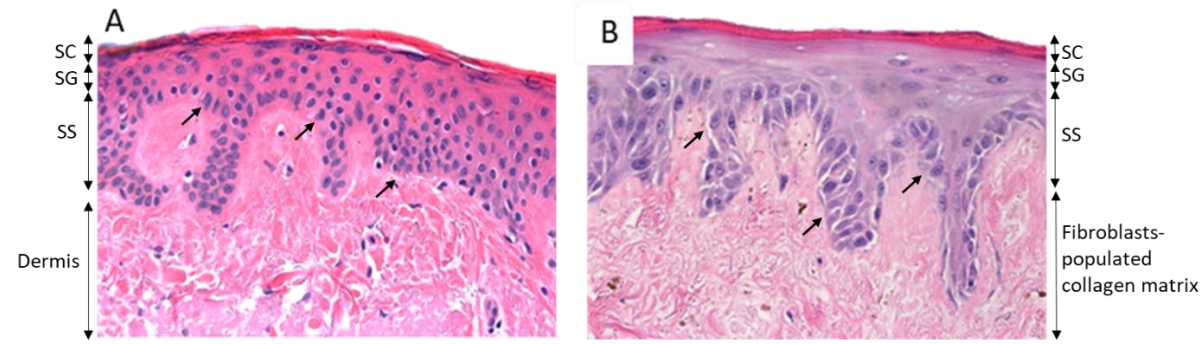

Figure 1.9 Histological sections.
(A) Image of a histological section of native human skin showing epidermal rete processes protruding into the dermis, where the dermis, basal cells (arrows) from the stratum basale, stratum spinosum (SS), stratum granulosum (SG) and stratum corneum (SC) can be observed; (B) Histological section of our "in-house" tissue-engineered skin using human-derived dermal tissue and primary cultured keratinocytes and dermal fibroblasts, which shows the fibroblast-populated collagen matrix mimicking the dermis, basal cells (arrows) from the stratum basale, SS, SG and SC.

Natural polymers such as collagen, fibronectin, fibrin, alginate or chitosan are the main candidates for *in vitro* skin models as they are usually non-cytotoxic, rarely induce inflammatory response, and are extracted from natural sources. Collagen type I is the main component of dermal extracellular matrix and is the most commonly used natural polymer in HSE (Eckl et al., 2011; Randall et al., 2018). Specifically, collagen isolated from bovine or rat-tails is commonly used as the dermal component in HSE as it contains a large amount of collagen fibrils (Walters & Stegemann, 2014). It is an exceptional material for scaffolding due to its capacity to support cell attachment, migration, proliferation and differentiation (Somuncu et al., 2018). It is also cost effective, and easy to extract and purify. However, type I collagen has fragile mechanical properties and therefore can undergo contraction when fibroblasts are embedded in the collagen matrix and can be degraded by enzymatic degradation such as collagenase treatment. In addition, due to its animal source, it can lead to foreign antigens and contaminants. In spite of this, collagen-based *in vitro* tissue-engineered models are the most commonly used for normal and disease models (Randall et al., 2018). In fact, collagen type I have been also used for the study of tumours (Katt et al., 2016), wound healing (Rossi et al., 2015) and in tissue-engineered oral mucosa (Colley et al., 2018; Jennings et al., 2016; Ollington et al., 2021). Fibroblasts can produce their own extracellular matrix if cultured long enough, therefore, there is no need of an artificial dermis. However, these models take longer to culture (Franco-Barraza et al., 2016).

To overcome the problem with the contraction, combination of different hydrogels, such as combination of collagen with silk or recombinant spider silk protein have been successfully used, however, this requires more processing. Electrospinning and 3D bioprinting have also been used;

nevertheless, *in vitro* skin models generated with some of these scaffolds do not present a stratified epidermis. Synthetic polymers including polyesters such as poly (ε-caprolactone) (PCL), polyethers such as polyethylene glycol (PEG) or polystyrene such as the Alvetex™ scaffold have also been developed to generate scaffolds to build 3D human skin equivalents. The Alvetex™ scaffold for example, allows cells to keep their natural shape in a 3D microenvironment forming more complex interactions, where fibroblasts form their own ECM matrix. However, these have poor cell adhesive properties, are more cytotoxic compared to natural polymers, and they are not biodegradable (Randall et al., 2018; Roger et al., 2019).

The selection of the culture medium is also very important. When culturing cells, culture medium is added to sustain the cells, and each type has specific needs regarding its function, and therefore, they require specific medium composition (Table 1.4). When co-culturing cells, choosing the right culture medium can be challenging. A combination of the culture medium used for the different cell types could be mixed, however supplements from one culture medium could interfere the other cell type's culture (Vis et al., 2020). Another approach would be the use of a base medium supplemented with factors that could help the co-culture (Jennings et al., 2016; Reijnders et al., 2015). Nevertheless, this is time consuming, as it requires optimisation. To overcome this, some companies have developed 3D culture medium suitable for the differentiation and co-culture of different cell types in a 3D microenvironment. This is usually more expensive, but it increases the validity of the initial findings (Smits et al., 2017). In addition, different nutrient combinations can affect tissue thickness, junctions, and number of epidermal layers (Lange et al., 2016). High calcium concentrations induce keratinocyte differentiation, while serum inhibits keratinocytes differentiation. However, serum is needed for the proliferation of fibroblasts, although animal serum (foetal bovine serum or foetal calf serum, commonly used in tissue culture laboratories) is an undefined mixture of different growth supplements frequently used in cell culture media; that is why low serum levels is commonly used for *in vitro* models. Additionally, culture of HSE requires the addition of other nutrients and growth factors such as hydrocortisone or insulin (Griffoni et al., 2021; Jennings et al., 2016; Reijnders et al., 2015). However, when generating immune-competent HSE, the addition of these nutrients and growth factors have to be tested or omitted, as hydrocortisone, for example, is well-known due to its anti-inflammatory activity (Coutinho & Chapman, 2011; Ehrchen et al., 2019).

Table 1.4 Examples of culture medium used to support HSE.

Fibroblasts	Keratinocytes	After air-to-liquid interface exposure	Reference
DMEM/Ham's F12 (3:1), 50µg/mL gentamycin, 2% UG, 5µg/mL insulin, 50µg/mL ascorbic acid, 5ng/mL EGF	DMEM/Ham's F12 (3:1), 50µg/mL gentamycin, 1µM hydrocortisone, 1µM isoproterenol, 0.1µM insulin, 1% UG, 2ng/mL KGF	DMEM/Ham's F12 (3:1), 50µg/mL gentamycin, 1µM hydrocortisone, 1µM isoproterenol, 0.1µM insulin, 0.2% UG, 10mM L-serine, 10µM L-carnitine, 1M DL-α-tocopherol acetate, 25µM palmitic acid, 15µM linoleic acid, 7µM arachidonic acid, 24µM BSA.	(Reijnders et al., 2015) (Ouwehand et al., 2011)
DMEM, 10% foetal calf serum (FCS)	Keratinocytes growth medium (KGM), 5% FCS	KGM with descending FCS concentration (5%, 2%, 0%)	(Rossi et al., 2015)
DMEM, 10% foetal bovine serum (FBS), 1% penicillin-streptomycin (P/S), 1% L-glutamine.	DMEM/Ham's F12 (3:1), 5% FCS, 1% P/S, 1µM hydrocortisone, 1µM isoproterenol, 0.1µM insulin, 2ng/mL KGF or CnT-prime airlift medium.	DMEM/Ham's F12 (3:1), 1.25% FCS, 1% P/S, 1µM hydrocortisone, 1µM isoproterenol, 0.1µM insulin, 2ng/mL KGF, 0.01M L-serine, 0.1µM L-carnitine, 50µg/mL ascorbic acid or CnT-prime airlift medium.	(Griffoni et al., 2021)

Following specific culture conditions, HSE mimic many human skin features. Human skin equivalents are used for the study of normal and diseased skin, including wound healing or infection (Reijnders et al., 2015), but also in the pharmaceutical and cosmetic industries for drug permeability testing and toxicity screening (Harding et al., 2021; Z. Zhang & Michniak-Kohn, 2012). Tissue-engineered models can also be used in clinical and research areas of skin contraction, reconstructive surgery, skin irritation studies, analysis of penetration of agents into the skin, and melanoma (Colley et al., 2011). HSE are

formed by human skin cells (usually keratinocytes and fibroblasts), and components of the ECM (mainly collagen), cultured at an air-to-liquid interface to induce the formation of a stratified epidermis (Z. Zhang & Michniak-Kohn, 2012). They can be constructed as epidermal-only models or full-thickness models (both epidermis and dermis) (Savoji et al., 2018). Full-thickness models, in comparison to epidermal models, have the advantage of representing a more *in vivo*-like morphology where basement membrane attachment of the epidermis to the dermis is present as well as keratin production and cell junctions (Hutter et al., 2018). Other researchers have cultured skin explants to generate full-thickness models; however, after 7 days the cells become less viable compared to HSE that can last in culture for up to several weeks (De Wever et al., 2015).

The majority of current *in vitro* HSE lack an inflammatory system, vasculature, and other features of native skin. Several models of skin diseases including atopic dermatitis, psoriasis, and squamous cell carcinoma, among others, have been developed. However, most of these are based on primary keratinocytes isolated from patients with the disease, cultured as epidermal only models, or together with fibroblasts. This represents a good model to study the difference between both healthy and diseased keratinocytes, but keratinocytes do not play a main role in many immunologic skin disorders. For example, atopic dermatitis is associated with increased of T cells and DCs and altered level of cytokines. Therefore, more complex models involving immune components are necessary to better understand the immune skin responses and immune skin disorders.

1.4.2 Immunocompetent human skin equivalents

Development of immunocompetent (IC)-HSE would allow the development of new treatments for infectious diseases, inflammation, and delivery agents (Pupovac et al., 2018). To generate IC-HSE, fibroblasts are usually embedded in a collagen matrix (dermal layer), keratinocytes (epidermal layer) are seeded on top of the dermal layer, and recently data have shown incorporation of immune cells isolated from blood or as cell lines. This includes DCs, LCs, macrophages and T cells. DCs and LCs have been mainly co-seeded with keratinocytes (Kosten et al., 2015; Ouwehand et al., 2011, 2012), while macrophages (Limandjaja et al., 2019; Linde et al., 2012) have been embedded in the collagen matrix together with fibroblasts. T cells have been either placed underneath in inserts or seeded with the fibroblasts. Studies previously incorporating immune cells into HSE are shown in Table 1.5.

Table 1.5 Currently available IC-HSE.

Model	Components	Limitations	Reference
Full thickness skin models containing DCs and/or LCs	Mo-DC MUTZ-LC	Other immune cells missing	(Chau et al., 2013) (Ouwehand et al., 2011)
Skin and epidermal equivalents	CD45RO+ T cells	Other immune cells missing	(Engelhart et al., 2005)
Full thickness skin models containing T cells	CD4+ T cells or PBMCs	Other immune cells missing	(Van Den Bogaard et al., 2014) (Kühbacher et al., 2017) (Lorthois et al., 2019) (Shin et al., 2020)
Dermal equivalent	MDM	Other immune cells missing	(Linde et al., 2012)

In 2005, Engelhart *et al*. generated a HSE using HaCaT keratinocytes and CD45RO+ T cells activated with anti-CD3, anti-CD2 and anti-CD28 12 hours before being added to the model, and measured the expression of inflammatory cytokines and chemokines, allowing the study of anti-inflammatory drugs. Van den Bogaard *et al*. (2014) were the first to develop a human inflammatory skin equivalent including different T cells populations on a decellularized de-epidermised dermis, by lifting the HSE and placing the T cells underneath the connective tissue layer. This allowed the study of immune cell migration and cytokine secretion in a model of psoriasis. However, keratinocyte hyperproliferation was not observed and cytokine levels were lower compared to the *in vivo* situation. This suggests that crucial mediators and relevant cell types such as dendritic cells are still missing to create a more complete model of psoriasis.

In 2017, Kühbacher *et al*. used immortalised human dermal fibroblasts to generate a full-thickness immunocompetent skin model where naïve CD4+ T cells, previously isolated from peripheral blood mononuclear cells (PBMCs), were embedded in collagen and placed underneath the tissue model. This model was used to study the response of keratinocytes and fibroblasts to *Candida albicans* invasion and the role of some cytokines in dermal protection in the presence of CD4+ T cells. However, key cell types present in skin, such as DC were missing in their model.

In addition, some researchers have used T cells to develop disease models. Lorthois *et al.* (2019) and Shin *et al*. (2020) recently constructed an immunocompetent human psoriatic skin model. Lorthois *et al*. (2019) used T cells isolated from PBMCs of human healthy donors that were then added to the

dermal layers of lesional reconstructed skin models, while Shin *et al*. (2020) used T cells isolated from both healthy and psoriasis patients, creating a separated matrix including fibroblasts and keratinocytes that was added on top of the T cells-populated matrix. These models allowed the study of the role of activated T cells in the proliferation process and the secretion of proinflammatory factors in psoriasis. Nevertheless, addition of other immune components or polarised T cells would be important to mimic the immunopathology of this disease.

On the other hand, some researchers have included Langerhans cells or dendritic cells in their human skin models. Ouwehand *et al*. (2011) and Kosten *et al.* (2016) differentiated the cell line MUTZ-3 into Langerhans cells by adding GM-CSF, TGF-β and TNFα. Kosten *et al.* (2016) co-seeded MUTZ-LC with keratinocytes onto a fibroblast-populated dermal matrix, generating an immunocompetent human full-thickness HSE. This allowed the study of LC activation and migration from the epidermis to the dermis. However, inclusion of other immune cells is necessary to create a more complete model.

In 2013, Chau *et al*. generated a 3D human skin model by incorporating Mo-DC isolated from PBMCs in an agarose-fibronectin gel, which was assembled between a bottom fibroblast-populated matrix and a top scaffold containing keratinocytes. This model was used to monitor cell activation and migration. However, histological analysis did not show a well-formed epithelium, suggesting that further characterization of the model, (e.g., transepithelial electrical resistance (TEER) analysis) to test barrier function, and inclusion of other immune cells is necessary.

Other immunocompetent human skin models that have been generated contain macrophages. Bechetoille *et al*. (2011) developed a dermal equivalent comprising MDMs and fibroblasts. Although macrophages were functional in their model, addition of other cell types such as keratinocytes and other immune cells is fundamental for dermatological and drug research. In 2012, Linde *et al.* constructed a dermal equivalent including MDMs, previously isolated from PBMCs. MDMs were embedded together with dermal fibroblasts, in a collagen hydrogel to form the dermal layer, and squamous cell carcinoma cells were seeded on top of the dermal equivalent. This model was used to study tumour progression (Linde et al., 2012).

1.4.3 AD-like human skin equivalents

In the case of AD, *in vitro* models have been modified to mimic AD features at the epidermal level, either by addition of interleukins overexpressed in the disease or by silencing gene expression of molecules required in the skin barrier formation and structure, such as *FLG*. Cells derived from AD patients can be also included in the HSE.

Several different cytokine cocktails have been used to mimic AD pathology in HSE. In fact, AD skin equivalents have been generated by incubating healthy skin equivalents with IL-4 and IL-13 when HSE were lifted to air-to-liquid interface (ALI). Cytokine treatment not only induced spongiosis, expression of AD-associated genes, and keratinocytes apoptosis (Kamsteeg et al., 2011), but also epidermal hyperplasia, acanthosis and a thinner stratum corneum (Clarysse et al., 2019), characteristics observed in eczematous lesions. Other researchers have developed reconstructed human epidermal (RHE)-only models instead. Bernard *et al.* (2012) added TNFα and IL-22 in addition to IL-4 and IL-13, to develop a RHE model to mimic the epidermis in patients with AD, observing a disunited tissue and orthokeratosis. A similar RHE model was developed later by Rouaud-Tinguely *et al.* (2015) by adding IL-4, IL-13, TNFα and polyinosinic-polycytidylic acid (immunostimulant), observing spongiosis and fewer compact layers in the AD-like model. IL-25 in addition to IL-4 and IL-13 has been also used to create AD-like RHE models (De Vuyst et al., 2018). However, Sriram *et al*. (2019) have recently shown that addition of IL-4 alone can generate an AD-like full thickness HSE. They observed a thicker epidermis, increased Ki67+ basal keratinocytes, hyperplasia, and impaired differentiation in their models, compared to normal human skin equivalents. None of these models contain T cells and so the cytokine repertoire that instigates AD is limited.

In AD, *FLG* expression is reduced, therefore, some studies have developed skin models containing knockdown of *FLG* in keratinocytes to study AD pathology. Full thickness HSE containing keratinocytes either non-transfected or transfected with small interfering RNA (siRNA) have been used to study gene functions in epidermal development (Mildner et al., 2006) and the role of *FLG* in keratin aggregation, lipid composition and maturation of the epidermal barrier (Küchler et al., 2011; Mildner et al., 2010). Mildner *et al.* (2010) showed loss of keratohyalin granules and impaired lamellar body formation in filaggrin-deficient models. However, keratinocyte differentiation and stratum corneum development was not influenced by filaggrin knockdown (FLG-KD). In addition, absence of a keratin aggregation defect was observed, suggesting that filaggrin is non-essential for keratin aggregation. Regarding lipid composition, no differences between normal and filaggrin-deficient model were observed. Similar results were also shown by Van Drongelen (2013), who used the transfected N/TERT keratinocyte cell line containing short hairpin RNA (shRNA) against FLG on dermal equivalents to study skin barrier properties. These findings suggest that FLG-KD alone is not sufficient to affect keratinocyte differentiation and stratum corneum lipid composition, and that other factors such as inflammation might be involved in these processes. On the other hand, Küchler *et al.* (2011) observed disturbed epidermal maturation and impaired barrier function resulting in higher susceptibility to irritants in their models, which could be due to a longer cultivation period, in comparison with Mildner's models

(2010). This was also observed by Pendaries *et al.* (2014), however, RHE were used in their experiments, suggesting that fibroblasts could partially improve keratinocyte differentiation.

In 2015, Hönzke *et al*. developed a normal and filaggrin-deficient full thickness HSE, which was supplemented with different cytokine cocktails, including IL-4 and IL-13. Spongiosis and parakeratosis were observed in the HSE supplemented with cytokines and those with the FLG-deficiency. In addition, higher proliferation rates were shown in FLG-deficient models. However, no differences in skin permeability and skin surface were observed between FLG+ and FLG- HSE, although treatment with cytokines showed a small increase in skin permeability and in skin surface pH.

Nevertheless, these studies lack immune cells in their models to further mimic AD pathology. To overcome this limitation, Wallmeyer *et al*. (2017) exposed the FLG+ and FLG- models to CD4+ T cells. Results showed an inflamed phenotype in the models with high levels of IL-6 and CXCL8 and increase in the surface pH when T cells were added. In addition, T cell migration was only observed in FLG- skin equivalents, demonstrating also that this T cell migration can be initiated by TSLP in the absence of DCs.

Some disease models have also been developed by including different combination of healthy and atopic skin cells (fibroblasts and keratinocytes) to study the role of these cells in patients with AD. AD patient-derived fibroblasts increased proliferation and contributed to the stratification of keratinocytes. The disease model that included both atopic fibroblasts and keratinocytes did not form a stratified epidermis, compared to the healthy model (Berroth et al., 2013). In addition, AD skin biopsies have been seeded onto dermal equivalents, as an explant model, to study the effect of *FLG* mutations in epidermal regeneration (van Drongelen et al., 2015).

However, to date, there are no reports of AD-like HSE with patient-derived dendritic cells and T cells that recreate the inflammatory cycle observed in acute AD in response to allergen challenge. An ideal HSE of AD should contain, at least, a dermis with human dermal fibroblasts and T cells, and an epidermis formed by keratinocytes and dendritic cells. Preferably, all these cells would be isolated from the same patient to study the interaction between these cells and the inflammatory cycle.

Therefore, new pre-clinical drug testing models of AD are necessary. To accomplish this, it is proposed the development of tissue engineered models that include T_H2 cells and dendritic cells.

1.5 Hypothesis

Monocyte-derived dendritic cells and polarised T_H2 cells are suitable cell types to be included into a human skin equivalent model and will still function properly within a model of atopic dermatitis.

1.6 Aim of the study

The main goal of this project was to develop an immunocompetent human skin equivalent model of AD for pre-clinical drug testing.

1.7 Objectives

To accomplish this, the following objectives were followed:

- Isolate naïve CD4+ T cells from mononuclear cells, polarise them into T_H2 cells and characterise them.
- Differentiate and characterise monocyte-derived macrophages, monocyte-derived dendritic cells, and monocyte-derived Langerhans cells.
- Examine keratinocytes response upon challenge stimulation.
- Generate and characterise reconstructed human epidermis-only and full thickness human skin equivalents models.
- Incorporate monocyte-derived dendritic cells within a reconstructed human epidermis-only and full thickness humans skin equivalents models.
- Construct and characterise full thickness immunocompetent human skin equivalents including T_H2 cells.
- Compare immunocompetent human skin equivalents to human skin biopsies from healthy and AD patients.

Chapter 2 - Materials and methods

2.1 Ethical approval

Human primary dermal fibroblasts used in this project were isolated and expanded from waste skin obtained by Mr S Hadad, Royal Hallamshire Hospital, Sheffield Teaching Hospitals NHS Foundation Trust with written, informed consent of donors undergoing breast surgery (ethical approval number 09/H1308/66). Histological sections of human skin were also used under the same ethical approval (09/H1308/66). Leukocyte-containing buffy coats were provided by NHS Blood and Transport Service (UREC 046856) and used in accordance with the Materials Transfer Agreement (REF: 12597). Leukocytes were isolated from whole blood taken from patients with diagnosed atopic dermatitis along with healthy controls as part of the skin pathology assessment with optical technologies clinical trial (SPOT STH20626, REC 19/YH/0367).

2.2 Materials

Table 2.1 Reagents and components

Reagents	Supplier	Catalogue Number
12-well translucent inserts	Greiner Bio-One	665640
2,4-Dinitrochlorobenzene (DNCB)	Sigma-Aldrick	237329
4-(2-hydroxyethyl)-1-piperazineethanesulfonic acid (HEPES)	Biochemicals (nzytech)	44285
Adenine	Sigma-Aldrich	A2786
Bovine serum albumin (BSA)	ThermoFisher Scientific	BP9701-100
$CaCl_2$	Sigma	C7902
CnT-Prime 3D barrier medium	CellNTec Advanced Cell Systems	Cnt-PR-3D
Collagenase Type I	ThermoFisher Scientific	17100017
Collagenase Type IV	ThermoFisher Scientific	17104019
Corning® PureCoat™ carboxyl dishes	Corning Inc.In	356784
Coverquick 2000 mounting medium	VWR International	05547531
CytoTox 96® non-radioactive cytotoxicity assay	Promega Corporation	G1780
Difco trypsin 0.1% (w/v)	Gibco	27250018
Dimethylsulfoxide (DMSO)	Sigma-Aldrich	D2650

Dulbecco´s Modified Eagle Medium (DMEM) 10X	Sigma-Aldrich	D2429
Epidermal growth factor (EGF)	Sigma-Aldrich	E9644
Ethylenediaminetetraacetic acid (EDTA)	Sigma-Aldrich	E6758
Fc block	MiltenyBiotec	130-059-901
Ficoll-Paque™	GE Healthcare	17-1440-03
Foetal bovine serum (FBS)	Sigma-Aldrich	F7524
Formalin	Sigma-Aldrick	HT501320
Fungizone	Sigma-Aldrich	A2942
Glucose	ThermoFisher Scientific	G/0500/53
Goat serum	Fisher scientific	11530526
Ham's F12	Sigma-Aldrich	N4888
Hank´s balanced salt solution (HBSS) (without Ca^{2+} or Mg^{2+})	Sigma-Aldrich	H6648
High glucose DMEM	Sigma-Aldrich	D5671
Histo-cassettes	Simport	M480
House dust mite (HDM) allergen Der p 1	Stallergenes Greer	XPB82D3A25
Human T activator CD3/CD28	Gibco	11161D
Hydrogen peroxide (H_2O_2)	Fisher scientific	H/1750/15
ImmunoCult human Th2 differentiation supplement	StemCell	10975
Insulin	Sigma-Aldrich	I9278
Interferon-γ (IFNγ)	Sigma-Aldrich	I3265-.1MG
Keratinocyte serum-free medium (K-sfm)	Gibco	17005042
L-glutamine	Sigma-Aldrich	G7513
Lipid mixture 1, chemically defined	Sigma-Aldrich	L0288
Lipopolysaccharide (LPS) from *Escherichia coli (E. coli)*	Invivogen	tlrl-peklps
Low glucose DMEM	Sigma-Aldrich	D5546
Medium 199	Gibco	11150059
Methanol	Fisher scientific	M/3950/17
Penicillin-Streptomycin	Sigma-Aldrich	P0781
Phosphate-buffered saline (PBS)	Sigma-Aldrich	P4417
ProLong™ gold antifade mountant	ThermoFisher Scientific	P10144

Recombinant granulocyte-macrophage colony-stimulating factor (GM-CSF)	Peprotech	300-03
Recombinant human IL-2	Peprotech	200-02
Recombinant human IL-4	Peprotech	200-04
Recombinant human keratinocyte growth factor (KGF)	Peprotech	100-19
Recombinant human thymic stromal lymphopoietin (TSLP)	Peprotech	300-62
Recombinant human transforming growth factor (TGF)-β1	Peprotech	100-21
Roswell Park Memorial Institute Medium (RPMI) 1640	Sigma-Aldrich	R8758
Sodium azide (NaN_3)	BDH	30111
Sodium bicarbonate ($NaHCO_3$)	Sigma-Aldrich	S5761
Sodium hydroxide (NaOH)	BDH AnalaR	104384F
Sodium pyruvate	Gibco	11360070
Tetramethylbenzidine (TMB) substrate solution	Sera care	5120-0075
Triiodothyronine (TT)	Sigma-Aldrich	T6397
Trypsin EDTA	Sigma-Aldrich	T3924
Tumour necrosis factor-alpha (TNF-α)	Sigma-Aldrich	H8916-10 µg

Table 2.2 TaqMan® Gene Expression Assays, all purchased from ThermoFisher Scientific

TaqMan® Gene Expression Assays	Details	Reference Sequences	Assay ID
Actin beta (ACTB; (β Actin)	Species: Human; Amplicon Length: 171; Dye: VIC	NM_001101.2	4326315E
Beta-2-Microglobulin (B2M)	Specie: Human; Amplicon Length: 75; Dye: VIC	NM_004048.2	4326319E
CCL17	Species: Human; Amplicon Length: 51; Location Chromosome: 16: 57396076 - 57416063; Dye: FAM	NM_002987.2	Hs00171074_m1
CCL22	Species: Human; Amplicon Length: 88; Location	NM_002990.4	Hs01574247_m1

	Chromosome: 16: 57357909 - 57366190; Dye: FAM		
CD14	Species: Human; Amplicon Length: 140; Location Chromosome: 5: 140631728-140633701; Dye: FAM	NM_000591.3 NM_001040021.2 NM_001174104.1 NM_001174105.1	Hs02621496_s1
CD1a	Species: Human; Amplicon Length: 60; Location Chromosome: 1: 158248329-158258269; Dye: FAM	NM_001320652.1 NM_001763.2	Hs00381754_g1
CD207	Species: Human; Amplicon Length: 105; Location Chromosome: 2: 70825248-70860787; Dye: FAM	NM_015717.4	Hs00210453_m1
CD80	Species: Human; Amplicon Length: 107; Location Chromosome: 3: 119523909-119559709; Dye: FAM	NM_005191.3	Hs00175478_m1
CD86	Species: Human; Amplicon Length: 104; Location Chromosome: 3: 122055362-122121143; Dye: FAM	NM_001206924.1 NM_001206925.1 NM_006889.4 NM_175862.4 NM_176892.1	Hs01567026_m1
Glyceraldehyde 3-phosphate dehydrogenase (GAPDH)	Species: Human; Amplicon Length: 122; Location Chromosome: 12: 6534405 – 6538375; Dye: VIC	NM_001289746.1 NM_002046.5	Hs99999905_m1
IL-1α	Species: Human; Amplicon Length: 69; Location Chromosome: 2: 112773915-112785398; Dye: FAM	NM_000575.4	Hs00174092_m1
IL-1β	Species: Human; Amplicon Length: 94; Location Chromosome: 2: 112829758-112836842; Dye: FAM	NM_000576.2	Hs00174097_m1
IL-4	Species: Human; Amplicon Length: 70; Location Chromosome: 5: 132673986-132682678; Dye: FAM	NM_000589.3 NM_172348.2	Hs00174122_m1
IL-5	Species: Human; Amplicon Length: 99; Location Chromosome: 5: 132539194-132556827; Dye: FAM	NM_000879.2	Hs01548712_g1
IL-6	Species: Human; Amplicon Length: 95; Location Chromosome: 7: 22725889-22732002; Dye: FAM	NM_000600.4 NM_001318095.1	Hs00174131_m1

IL-10	Species: Human; Amplicon Length: 74; Location Chromosome: 1: 206767603-206772494; Dye: FAM	NM_000572.2	Hs00961622_m1
IL-13	Species: Human; Amplicon Length: 82; Location Chromosome: 5: 132658173-132661109; Dye: FAM	NM_002188.2	Hs00174379_m1
IL-18	Species: Human; Amplicon Length: 115; Location Chromosome: 11: 112143251-112164117; Dye: FAM	NM_001243211.1 NM_001562.3	Hs01038788_m1
IL-25	Species: Human; Amplicon Length: 76; Location Chromosome: 14: 23372809-23376403; Dye: FAM	NM_022789.3 NM_172314.1	Hs0304484_m1
IL-33	Species: Human; Amplicon Length: 98; Location Chromosome: 9: 6214591-6257983; Dye: FAM	NM_001199640.1 NM_001199641.1 NM_001314044.1 NM_001314045.1 NM_001314046.1 NM_001314047.1 NM_001314048.1 NM_033439.3	Hs00369211_m1
Thymic stromal lymphopoietin (TSLP)	Species: Human; Amplicon Length: 97; Location Chromosome: 5: 111070080-111078024; Dye: FAM	NM_033035.4 NM_138551.4	Hs00263639_m1
Tumour necrosis factor-alpha (TNF-α)	Species: Human; Amplicon Length: 143; Location Chromosome: 6: 31575567-31578336; Dye: FAM	NM_000594.3	Hs01113624_g1
Ubiquitin C (UBC)	Species: Human; Amplicon Length: 97; Location Chromosome: 71: 124911645-124915041; Dye: VIC	NM_021009.6	Hs00824723_m1

*Reference controls are represented in blue

Table 2.3 Antibodies used for flow cytometry

Antibody	Dilution	Isotope	Supplier	Catalogue Number
CD1a APC	1:20	Monoclonal, recombinant human IgG1	MiltenyiBiotec	130-112-023
CD11c APC	1:20	Monoclonal, recombinant human IgG1	MiltenyiBiotec	130-113-584
CD119 FITC	1:8	Monoclonal, Mouse/IgG2a	eBioscience	MA5-28109
CD154 PE-eFluor610	1:8	Monoclonal, Mouse/IgG1	eBioscience	61-1548-42
CD193 PE	1:8	Monoclonal, Mouse/IgG2b	eBioscience	12-1939-42
CD194 APC	1:8	Monoclonal, Mouse/IgG2b	eBioscience	17-1939-42
CD25 PE	1:8	Monoclonal, Mouse/IgG1	eBioscience	12-0259-42
CD207 APC	1:20	Monoclonal, recombinant human IgG1	MiltenyiBiotec	130-112-369
CD4 APC	1:8	Monoclonal, Mouse/IgG1	eBioscience	17-0049-42
CD69 APC	1:8	Monoclonal, Mouse/IgG1	eBioscience	17-0699-42
HLA-DR APC	1:20	Monoclonal, recombinant human IgG1	MiltenyiBiotec	130-111-943
IgG APC	1:8	Monoclonal, Mouse/IgG1	abcam	Ab91358
IgG FITC	1:8	Monoclonal, Mouse/IgG1	eBioscience	11-4714-41
IgG PE	1:8	Monoclonal, Mouse/IgG1	eBioscience	12-4714-41

APC = allophycocyanin; FITC = fluorescein isothiocyanate; PE = phycoerythrin

Table 2.4 Antibodies used for immunohistochemistry

Antibody	Host species	Dilution	Supplier	Catalogue Number
CD3	Rabbit	1:100	Agilent	A0452
CD68	Mouse	1:100	Agilent	M0814
CK14	Mouse	1:800	ThermoFisher	MA5-11599
CK16	Rabbit	1:500	Abcam	ab181055
E-cadherin	Rabbit	1:500	Abcam	ab40772
Filaggrin	Mouse	1:50	Novus Biologicals	NBP2-53244
Involucrin	Mouse	1:200	Abcam	ab14504

Table 2.5 Commercial kits

Kit	Supplier	Catalogue Number
DAB Substrate Kit, Peroxidase (HRP), with Nickel, (3,3'-diaminobenzidine)	Vector Laboratories	SK-4100
High-capacity cDNA reverse transcription kit	Applied Biosystems	4368814
Monarch® total RNA miniprep kit	New England BioLabs	T2010
Naïve CD4+ T cell isolation kit II, human	MiltenyiBiotec	130-094-131
VECTASTAIN® Elite® ABC-HRP Kit (Peroxidase, Universal)	Vector Laboratories	PK-6200

Table 2.6 ELISA kits

Kit	Supplier	Catalogue Number
CCL5	R&D Systems	DY278-05
CXCL9	R&D Systems	DY392-05
CXCL10	R&D Systems	DY266-05
IL-10	R&D Systems	DY217B-05

Table 2.7 Cell types

Cell line	Cell type and derivation	Site	Source
BJ-5ta	hTERT-immortalised human dermal fibroblasts derived by transfecting the BJ foreskin fibroblast cell line with the pGRN145 hTERT-expressing plasmid (Bodnar et al., 1998)	Foreskin	ATCC (catalogue number: CRL-4001™)
CD4+ T cells	Primary CD4+ T cells derived from mononuclear cells	Buffy coats	NHS Blood and Transport, Sheffield, UK

MDM	Primary monocyte-derived macrophages	Buffy coats	NHS Blood and Transport, Sheffield, UK
Mo-DC	Primary monocyte-derived dendritic cells	Buffy coats	NHS Blood and Transport, Sheffield, UK
Mo-LC	Primary monocyte-derived Langerhans cells	Buffy coats	NHS Blood and Transport, Sheffield, UK
N/TERT-1	hTERT-immortalised human skin keratinocytes by the spontaneous loss of the pRB/p16^{INK4a} cell cycle control mechanism. It is diploid with an additional chromosome 20 (47, XY, +20) (Dickson et al., 2000)	Foreskin	James G. Rheinwald, Brigham and Women's Hospital, Harvard Medical School, Boston, USA
N/TERT-2G	hTERT-immortalised human skin keratinocytes by the spontaneous loss of the pRB/p16^{INK4a} cell cycle control mechanism. It is diploid (46, XY) (Dickson et al., 2000)	Foreskin	James G. Rheinwald, Brigham and Women's Hospital, Harvard Medical School, Boston, USA
NHDF	Normal human dermal fibroblasts	Breast skin	Dr. Helen E. Colley, School of Clinical Dentistry, University of Sheffield, Sheffield, UK
SPOT CD4+ T cells	Primary T helper cells	Human blood	Dr. Simon G. Danby, Sheffield Dermatology Research, University of Sheffield, Sheffield, UK
SPOT Mo-DC	Primary monocyte-derived dendritic cells	Human blood	Dr. Simon G. Danby, Sheffield Dermatology Research, University of Sheffield, Sheffield, UK

Table 2.8 Medium and solutions used for cell culture

Category and use	Culture medium	Final concentration
3D human skin models culture	Greens:	
	High glucose DMEM	66 % v/v
	Ham's F12	22 % v/v
	FBS	10 % v/v
	Penicillin	100 IU/mL
	Streptomycin	100 µg/mL
	L-Glutamine	2 mM
	Sodium Pyruvate	0.668 mM
	Adenine	0.18 mM
	Fungizone	0.625 µg/mL
	TT	0.2 µM
	Insulin	5 µg/mL
	EGF	10 ng/mL
Blocking solution	Blocking solution:	
	Fc block	5% v/v
	Goat serum	95% v/v
Phosphate-buffered saline (PBS)	1 tablet/200 mL dH_20	100 mM
Difco trypsin 0.1% (w/v)	PBS supplemented with:	
	Difco trypsin powder	11 mM
	Glucose	5.5 mM
	Penicillin	100 IU/mL
	Streptomycin	100 µg/mL
	Fungizone	0.625 µg/mL
Differentiation medium for 3D skin models	Differentiation medium:	
	CnT-Prime 3D barrier medium	60 % v/v
	DMEM	40 % v/v
	Penicillin	100 IU/mL
	Streptomycin	100 µg/mL
Flow cytometry (FACS) buffer	PBS supplemented with:	
	BSA	(0.1 % w/v) 0.015 mM
	NaN_3	(0.1 % w/v) 15 mM
Sucrose fixation solution for cryo-embedding samples	Phosphate buffer	(50% v/v) 200 M
	Distilled water (dH_2O)	50% v/v
	Sucrose	876 mM
Cell freezing medium	FBS	90 % v/v
	DMSO	10 % v/v
BJ-5ta immortalised fibroblasts growth medium	DMEM high glucose	70 % v/v
	Medium 199	20 % v/v
	FBS	10 % v/v
	Penicillin	100 IU/mL
	Streptomycin	100 µg/mL
	L-Glutamine	1.44 mM

N/TERT immortalised keratinocyte growth medium	Keratinocyte serum-free medium (K-sfm) supplemented with	
	Bovine pituitary extract	25 µg/mL
	Penicillin	100 IU/mL
	Streptomycin	100 µg/mL
	EGF	0.2 ng/mL
	Calcium chloride ($CaCl_2$)	0.3 mM
Leukocyte growth medium	RPMI-1640 supplemented with:	90 % v/v
	FBS	10 % v/v
	L-Glutamine	2 mM
	Penicillin	100 IU/mL
	Streptomycin	100 µg/mL
Primary dermal fibroblasts growth medium	Low glucose DMEM	90 % v/v
	FBS	10 % v/v
	L-Glutamine	2 mM
	Penicillin	100 IU/mL
	Streptomycin	100 µg/mL
Tissue transportation medium	DMEM supplemented with:	
	Penicillin	100 IU/mL
	Streptomycin	100 µg/mL
	Fungizone	0.625 µg/mL

2.3 Methods

2.3.1 Cell culture

2.3.1.1 Isolation of human primary skin fibroblasts

Human skin was collected from the Royal Hallamshire Hospital, Sheffield Teaching Hospitals NHS Foundation Trust, Sheffield, and transported to the cell culture laboratory at The School of Clinical Dentistry in transportation medium. The tissue was cut in small pieces and incubated in Difco trypsin at 4^{o}C overnight. The dermis was then cut into smaller pieces and incubated in 10 mL 0.5% collagenase A for 3-5 hours at 37^{o}C, 5% CO_2, and 95% relative humidity to degrade the collagen. Following collagenase treatment, cells were centrifuged at 200 g for 10 minutes and the cell pellet resuspended in 10% DMEM. Cells were seeded in T75 cm^2 flasks with supplemented DMEM for the isolation and culture of dermal fibroblasts at 37^{o}C, 5% CO_2. Medium was changed once cells had adhered to the flask and every week thereafter. Cells were cultured and used between passage 3 and 8.

2.3.1.2 Removal from liquid nitrogen and sub-culture of cells

Cells were removed from the liquid nitrogen dewar, thawed at 37^{o}C, added to 9 mL specific growth medium and centrifuged at 200 g for 5 minutes to remove the DMSO. The cell pellets were

resuspended in cell-specific growth medium, cells mixed carefully, added to tissue culture flasks at the required density and incubated at 37°C, 5% CO_2 level and 95% relative humidity. When keratinocytes and fibroblasts were confluent, the medium was removed, cells washed twice with 10 mL PBS, 2 mL trypsin/EDTA added and cells incubated until completely detached from tissue culture plastic. Eight mL of FCS supplemented DMEM were added to inactivate the trypsin activity (steps skipped for T cells, as they are cells in suspension) and 10 µL cell suspension removed and counted using a haemocytometer. Cells were centrifuged for 5 minutes at 200 g, supernatant then discarded, and the cell pellet resuspended in its respective medium. Cells were seeded at the desired density and incubated at 37°C, 5% CO_2, and 95% relative humidity.

2.3.1.3 Freezing cells

Fibroblasts, keratinocytes and immune cells were removed from tissue culture flasks and pelleted by centrifugation (see section 2.3.1.2) Cells were resuspended in freezing medium at 2 x 10^6 cells/mL, 1 mL dispensed into cryovials and these incubated in a Mr Frosty overnight at -80°C. The following day, vials were transferred to liquid nitrogen for long-term storage.

2.3.1.4 Isolation of monocytes from buffy coats

Blood from leukocyte-enriched buffy coats were mixed 1:1 with HBSS and 30 mL of this mixture overlaid slowly onto 20 mL of Ficoll-Paque™ before centrifugation for 40 minutes at 400 g without deceleration (Figure 2.1). The mononuclear leukocyte layer was removed between the upper serum and lower Ficoll layers with a sterile plastic Pasteur pipette and transferred to a fresh tube. HBSS was added to the monocytes and lymphocytes to make up to 50 mL and centrifuged for 15 minutes at 400 g to pellet the cells. The supernatant was discarded; the pellet washed again with 50 ml HBSS and centrifuged for 10 minutes at 400 g. The supernatant was discarded; pelleted cells re-suspended with 30 mL of HBSS and counted using a haemocytometer. Cells were once again centrifuged and re-suspended at the desired concentration in supplemented RPMI medium.

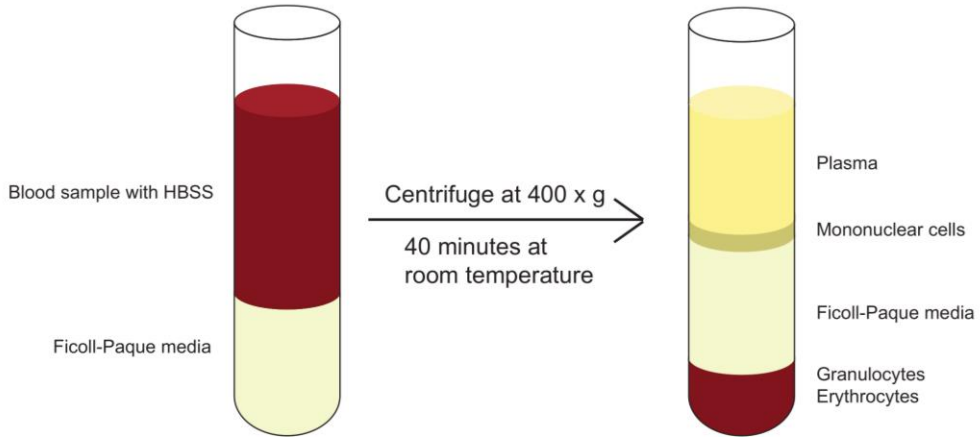

Figure 2.1 Isolation of mononuclear cells from buffy coats using Ficoll-Paque

2.3.1.5 Differentiation of monocytes into monocyte-derived macrophages

Isolated monocytes were seeded in a 10 cm Petri dish (20 x 10^6 cells/mL) in complete RPMI, and incubated at 37°C, 5% CO_2, and 95% relative humidity incubator. The following day, monocytes were purified by plastic adherence and washed with HBSS three times before adding fresh complete RPMI. Monocytes were cultured and differentiated into MDM during 7 days (Figure 2.2) (Nielsen et al., 2020), which were then used as control for future experiments.

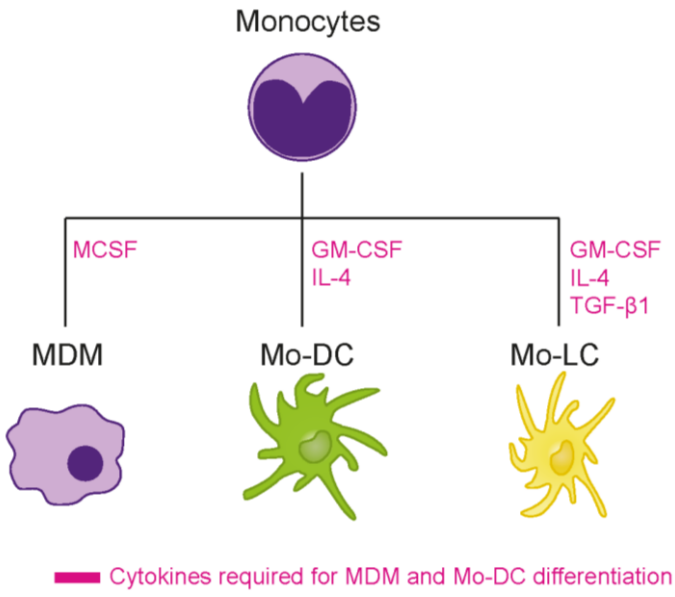

Figure 2.2 Differentiation of monocytes into dendritic cells.

2.3.1.6 Differentiation of monocytes into monocyte-derived dendritic cells

To differentiate monocytes into Mo-DC, isolated monocytes were seeded in Corning® PureCoat™ dishes at a density of 20 x 10^6 cells/mL for 24 hours in a 37°C, 5% CO_2, and 95% relative humidity incubator. Cells were then carefully washed with HBSS to remove any non-adherent or non-viable cells

and GM-CSF and IL-4 (Colic et al., 2003; Guironnet et al., 2001) added to a final concentration of 25 ng/mL and 20 ng/mL, respectively, to drive differentiation (Figure 2.2). Cytokines were added to the cells every other day for 7 days and then analysed for differentiation status using TaqMan qPCR (see section 2.3.6) and flow cytometry (see section 2.3.8).

2.3.1.7 Differentiation of monocytes into monocyte-derived Langerhans cells

To differentiate monocytes into MoLC, previously isolated monocytes were seeded in Corning® PureCoat™ dishes at a density of 20 x 10^6 cells/mL. After 24 hours cells were washed with HBSS and further cultured with medium supplemented with GM-CSF (25 ng/mL), IL-4 (20 ng/mL) and TGF-β1 (10 ng/mL) to drive differentiation (Figure 2.2) (Geissmann et al., 1998). Cytokines were added to the cells every other day and TGF-β1 was added every day. After 7 days, cells were analysed for differentiation status by TaqMan qPCR (see section 2.3.6) and flow cytometry (see section 2.3.8).

2.3.1.8 Isolation of naïve CD4+ T cells using negative selection

Naïve CD4+ T cells were isolated using the naïve $CD4^+$ T cell negative selection isolation kit II protocol according to the manufacturer's instructions. Isolated monocytes from buffy coats were counted and 10^7 cells used per large size (LS) column to isolate naïve CD4+ T cells. For magnetic bead isolation, cells were resuspended in 40 µL of isolation buffer (PBS with 0.5% BSA and 2 mM EDTA, pH 7.2) per 10^7 cells; 10 µL of naïve $CD4^+$ T cell biotin-antibody cocktail II were added, mixed well, and incubated for 5 minutes at 4°C. This antibody mixture binds to all leukocytes present in the mononuclear cell preparation apart from naïve $CD4^+$ T cells. After incubation, 30 µL of buffer was added, followed by addition of 20 µL of naïve $CD4^+$ T cell microbead cocktail II, the solutions mixed and incubated for 10 minutes at 4°C.

Magnetic field cell separation was used to separate iron-microbead labelled cells from non-labelled naïve $CD4^+$ T cells (Figure 2.3). An LS column was placed in the magnetic field of a MACS separator and washed with 3 mL of buffer. The cell suspension was applied onto the column and the flow-through containing unlabelled cells representing the enriched naïve $CD4^+$ T cell population was collected. The column was washed with 3 mL of buffer and the unlabelled cells that passed through were collected and combined with the previously obtained naïve $CD4^+$ T cells. The LS column was removed from the magnet, and the remaining iron bead-labelled mixed cell suspension was flushed from the column with a syringe using 3 mL buffer.

This allowed the collection of over 70% naïve CD4+ T cells, from which about 87% were viable.

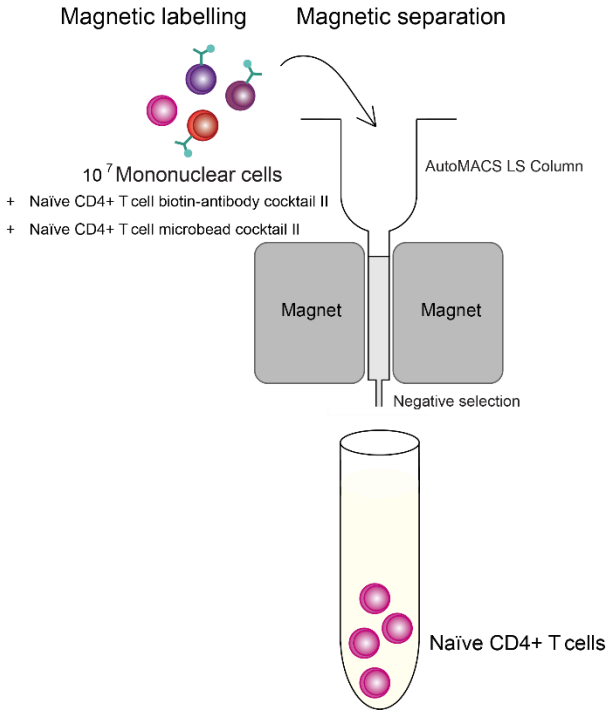

Figure 2.3 Magnetic cell separation.

2.3.1.9 Activation of CD4+ T cells

Naïve CD4+ T cells are activated when CD3 and CD28 on their cell surface bind their respective ligands, but only when done so at the same time. To achieve this, CD3/CD28 activating antibodies bound to iron beads were used. Naïve CD4+ T cells were counted to calculate how many Dynabeads Human T-Activator CD3/CD28 were needed to get a 1:1 ratio of cells to Dynabeads, knowing that 0.4 mL contains 1 x 10^5 Dynabeads. The Dynabeads were vortex for 30 seconds in the vial and the desired volume was transferred to a tube and mixed by vortex for 5 seconds with 1 mL of buffer (PBS with 0.1% BSA and 2 mM EDTA, pH 7.4) to wash the beads. A magnet was placed on the tube for 1 minute to collect the Dynabeads and the supernatant collected and discarded. The magnet was removed and the Dynabeads were re-suspended in the same volume of culture medium (RPMI) as the initial volume of Dynabeads taken from the vial. One µL of Dynabeads per 1 x 10^5 cells was added to obtain a bead-to-cell ratio of 1:1. Once the cells were activated, IL-2 was added (final concentration = 0.45 ng/mL) and incubated at 37°C, 5% CO_2 and 95% relative humidity to drive T cell proliferation. After 7 days in culture the CD4+ T cells were activated again using the same procedure.

2.3.1.10 Polarisation of CD4+ T cells into T_H2 cells

CD4+ T cells were polarised into T_H2 cells either on the first day of their isolation and CD3/CD28 activation, or after 7 days following isolation and activation, by adding 1 mL of T_H2 differentiation

supplement, which contained recombinant human IL-4 and mouse anti-human IFN-γ into 49 mL of RPMI medium and adding this to 1 x 10^6 cells. Cells were incubated at 37°C, 5% CO_2 and 95% relative humidity and were used after 14 days culture.

2.3.1.11 Allergen challenge

To study Mo-DC and N/TERT-2G functionality, Mo-DC were isolated and differentiated as described in section 2.3.1.6, and cultured for 7 days, while N/TERT-2G were cultured until 80% confluency was reached. N/TERT-2G and Mo-DC were stimulated with different allergens including 100 ng/mL of LPS from *E. coli*, increasing concentrations of DNCB (from 0.001 µM to 10 mM) and increasing concentrations of Derp1 (from 0.01 µM to 0.1 mM). After stimulation for 4 or 24 hours, cells were analysed by qPCR (see section 2.3.6) and LDH assay (see section 2.3.3), respectively.

In addition, Mo-DC were stimulated with 15 ng/mL TSLP for 48 hours. The culture conditioned medium was collected for cytokine content via ELISA analysis (see section 2.3.7) and an aliquot of cells analysed for cell surface marker expression by flow cytometry (see section 2.3.8). Mo-DC were then washed twice and co-cultured with 1 x 10^5 naïve CD4+ T cells for 6 days and re-stimulated with CD3/CD24 for 24 hours. Conditioned medium was collected for cytokine content by ELISA analysis (see section 2.3.7) and to be used as condition medium in HSE stimulation experiments. The cell pellet was analysed by flow cytometry (see section 2.3.8) and qPCR (see section 2.3.6).

2.3.2 3D human skin equivalents (HSE)

2.3.2.1 Rat tail collagen extraction

Type I collagen was isolated from rat tails donated by Dr Emma Bird, (School of Clinical Dentistry, University of Sheffield), and stored at -20°C until required. Rat tails were thawed at 4°C overnight. To expose the tendons, the tail skin was broken, and the collagen sheaths extracted from the tail and washed in PBS. The collagen fibres were dissolved by addition of 0.1 M acetic acid for 3 weeks at 4°C with stirring. This solution was freeze-dried for 3-4 days, and the collagen weighted and stored at -20°C until required, at which point it was dissolved in 0.1 M acetic acid to a stock concentration of 7.5 mg/mL and stored at 4°C for use. Stability of collagen and its solidification were tested before proceeding to the generation of 3D human skin equivalents, as batch-to-batch variation was observed after the freeze-drying process.

2.3.2.2 Construction of 3D human reconstituted epidermal-only skin equivalents

Human reconstituted epidermal (RHE)-only skin equivalents were generated by following the protocol described in Smits *et al.*, (2017) (Figure 2.4). Here, 12-well plate transwell inserts were coated with 100 µg/mL rat tail collagen at 4°C for 1 hour then washed with cold PBS. Immortalised N/TERT-1 and N/TERT-2G were removed from tissue culture flasks as described in section 2.3.1.2, pelleted by centrifugation and cells resuspended in 500 µL of K-sfm. Cells were counted and resuspended with K-sfm at 10^6 cells/mL. Two mL of K-sfm were added to the well and 200 µL (2 x 10^5 cells) of the cell suspension were added in the transwell insert. The cells were cultured at 37°C, 5% CO_2 and 95% relative humidity for 3 days submerged. The culture medium in the upper transwell was changed to 2 mL of differentiation medium 48 hours after seeding the cell suspension in the. The following day, models were brought to ALI. Medium was changed every other day and models were cultured for 10 days.

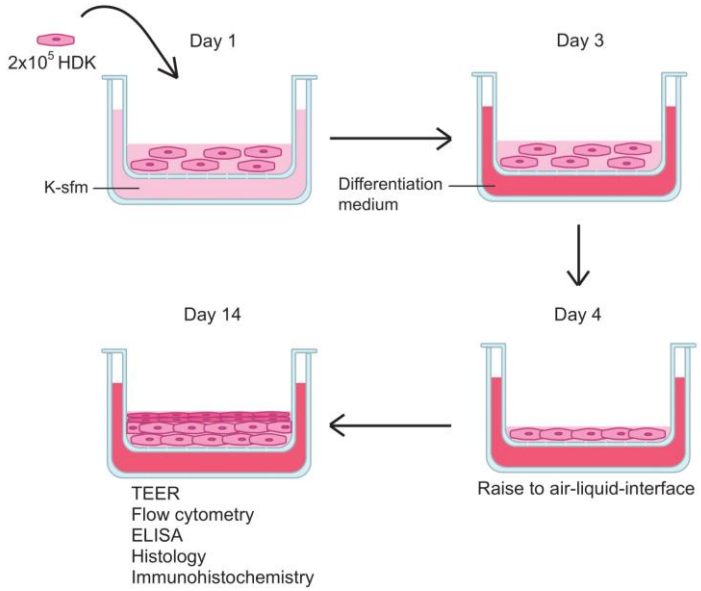

Figure 2.4 Schematic representation of the steps followed to produce tissue engineered reconstituted epidermal-only human skin equivalents.

2.3.2.3 Generation of 3D full-thickness human skin equivalents

3D full-thickness HSE were generated following the protocol described in Harding *et al.* (2021). To prepare the collagen hydrogel, components shown on Table 2.9 were combined, adding collagen last (without cells), and 2 M of NaOH was added until the solution reached pH 7.4 as determined using a pH meter. Once reconstituted, human dermal fibroblasts were detached from tissue culture plastic as described in section 2.3.1.2, centrifuged and resuspended in fresh supplemented DMEM. Dermal fibroblasts were mixed with the collagen hydrogel to obtain a cell suspension of 1.5x10^5 cells/mL (Figure 2.5).

Table 2.9 Collagen hydrogel components

Component	Final concentration	1 model (µL)/well
DMEM (10X)	1x	100
Reconstitution buffer (10X)*	1x	100
FBS	8%	80
L-Glutamine	2 mM	10
Collagen	5 mg/mL	670
Fibroblasts	$1.5x10^5$ cells/mL	40
TOTAL		1000

*Reconstitution buffer (10X): 260 mM $NaHCO_3$ + 200 mM HEPES + 59.5 mM NaOH.

One mL of fibroblast-containing gel solution was then added into transwell inserts and placed into wells of a 12 well-plate that was then incubated for 30 minutes at 37 °C. Once the collagen was set, 500 µL of supplemented DMEM were added on top of the collagen and 4.5 mL of the same medium added into the well, underneath the transwell insert. Models were then incubated for 24 hours.

After 1 day, the medium in the low well was removed and replaced with differentiation medium and 2.5 x 10^5 of N/TERT-immortalised keratinocytes in 500 µL of K-sfm added onto the surface of the fibroblast-containing collagen matrix. Models were incubated for 48 hours before bringing them to ALI, by removing the medium on top of the model and exposing the keratinocytes to air. HSE (Figure 2.5) were cultured for 14 days, and medium was changed every other day.

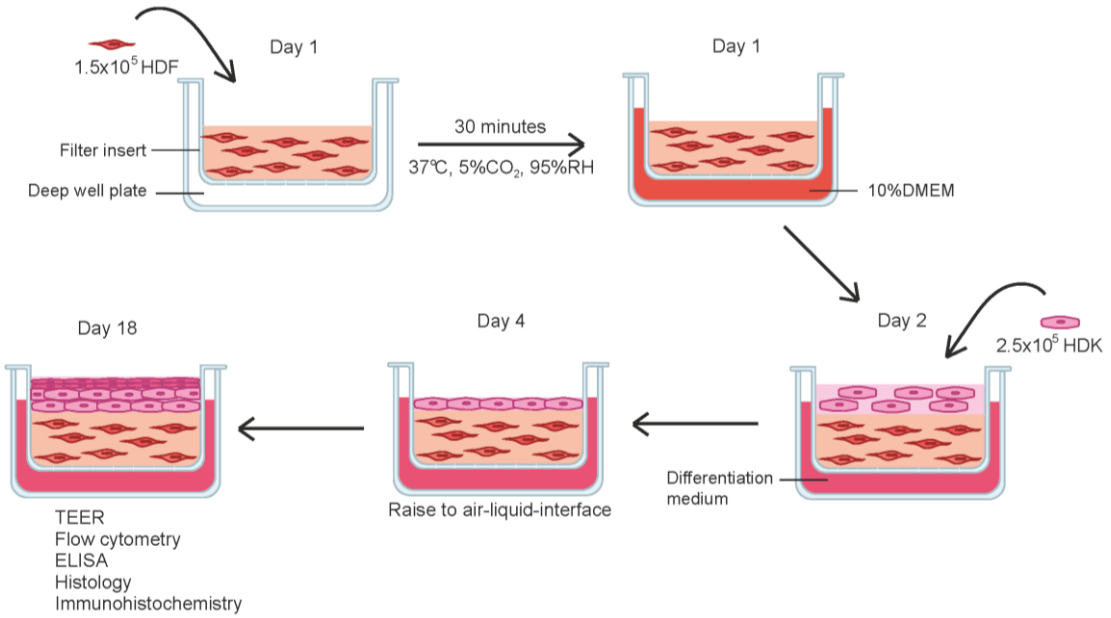

Figure 2.5 Schematic representation of the steps followed to produce tissue engineered 3D full thickness human skin equivalents.

2.3.2.4 Generation of immune-competent 3D human skin equivalents

Fibroblasts were embedded in a collagen matrix (see section 2.3.2.3.) (Figure 2.5). Once the dermal fibroblasts were mixed with the collagen hydrogel, 2 mL of the fibroblast-containing gel solution were added into each transwell inserts and placed into wells of a 6 well-plate and incubated for 30 minutes at 37 ºC. Once the collagen was set, 1 mL of supplemented DMEM was added on top of the collagen and 3-4 mL of the same medium added into the well. Models were then incubated for 48 hours.

After 2 days, the medium in the lower well was removed and replaced with differentiation medium, and 5 x 10^5 of N/TERT-immortalised keratinocytes in 1 mL of K-sfm added onto the surface of the fibroblast-containing collagen matrix. Models were incubated for 5 days before bringing them to ALI.

On the same day of the ALI, 4 x 10^6 T_H2 cells, isolated and polarised (see sections 2.3.1.8, 2.3.1.9 and 2.3.1.10), were embedded in a separated collagen matrix as described in Table 2.9, adding RPMI in the well and top of the model, in a 12-well plate.

At day 7 of ALI, 100 µL of collagen mix (Table 2.9) were added on top of the T_H2 cell-populated collagen to then attach on top the HSE containing fibroblasts and keratinocytes previously generated in parallel to create an immune-competent human skin equivalent (IC-HSE). On day 10 of ALI, medium was changed and the models were stimulated with 50 ng/mL IFNγ and 20 ng/mL TNFα. IC-HSE (Figure 2.6) were cultured for 15 days and medium was changed every other day.

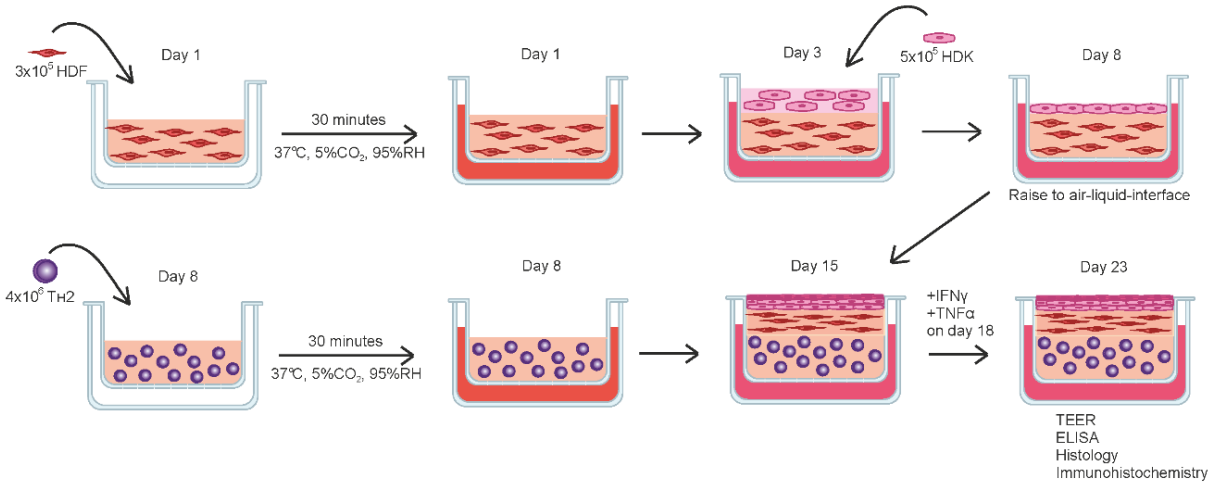

Figure 2.6 Schematic representation of the steps followed to produce tissue engineered immune-competent human skin equivalents including T_H2 cells.

2.3.2.5 Harvesting and analysis of 3D human skin equivalents

After 10-14 days in culture HSE were washed once in PBS then fixed in 10% neutral buffered formalin solution and stored at 4°C for at least 24 hours. Samples were cut in two halves, one half was designated for paraffin-embedding, and the other half for cryo-embedding.

2.3.2.5.1 PARAFFIN-EMBEDDING

Fixed samples designated for paraffin embedding were transferred into histo-cassettes and submerged in 10% formalin before dehydration and wax processing in the Shandon Citadel 2000 tissue processor that takes approximately 16 hours (Table 2.10).

Table 2.10 Program used for dehydration of samples.

Chemical	Time (hours)
10% neutral buffered formalin	Pass
70% alcohol	1
80% alcohol	1
90% alcohol	1.5
Absolute alcohol I	1.5
Absolute alcohol II	1.5
Absolute alcohol III	2
Toluene I	1.5
Toluene II	2
Xylene	Pass
Wax I (Paraplast)	2
Wax II (Paraplast)	2

Samples were then embedded in liquid paraffin by placing the sample with the straight bisected side of the HSE facing downwards. Samples were completely covered in liquid paraffin and hardened on a cooling plate (4°C) to be cut into 4 µm sections on a LEICA RM2235 microtome. Cut sections were placed in warm distilled water to facilitate the attachment to ultra-adhesive microscope slides and dried in an incubator at 60°C for 20 minutes prior to haematoxylin and eosin (H&E) staining.

2.3.2.5.2 HAEMATOXYLIN AND EOSIN STAINING

In order to evaluate the morphology of the models, H&E staining was carried out on paraffin sections. Haematoxylin is a dye that stains cellular nuclei blue, while eosin dyes cytoplasmic structures red/pink.

Microscope slides were placed into a staining rack and added into the Leica ST 4040 linear stainer, a process that takes about 20 minutes (Table 2.11). Coverslips were then mounted on the stained slides with Coverquick 2000 Mounting Media and the morphology examined using an Olympus BX51 microscope and Cell^D Software.

Table 2.11 Program used for H&E staining.

Chemical	Time (seconds)	Number of repeats
Xylene	45	3
99% IDA	45	2
70% IDA	45	1
Distilled water	45	2
Harris' haematoxylin (Shandon)	45	4
Running tap water	45	1
0.1% acid alcohol	45	1
Running tap water	45	1
Scott's Tap Water Substitute	45	1
Running tap water	45	1
Eosin Y – aqueous (Shandon)	45	3
Running tap water	45	1
99% IDA	45	3
Xylene	45	4

2.3.2.5.3 IMMUNOHISTOCHEMISTRY

In order to study specific expression of cell markers, immunohistochemistry was carried out on wax-embedded sections.

Paraffin wax-embedded sections were dewaxed with xylene, rehydrated with 99% industrial denatured alcohol (IDA), 70% IDA and then to water using an auto-stainer (Table 2.11). Following this, sections were incubated in 2% H_2O_2 in methanol for 20 minutes at room temperature to quench endogenous peroxidase activity. Samples were washed with water for 2 minutes before unmasking antigen sites with 10 mM Tris buffer, 1 mM EDTA, pH 9 using the Antigen Retriever machine. Sections were then washed with PBS and incubated with horse/rabbit serum for 20 minutes at room temperature to block non-specific antibody binding. After blotting to remove excess block sections were incubated with the primary antibody (Table 2.4) for 90 minutes at room temperature, followed by washing with PBS for 5 minutes. Sections were incubated with biotinylated secondary antibody for 30 minutes at room temperature. Sections were washed with PBS for 5 minutes and incubated with

Vectastain ABC reagent for 30 minutes at room temperature before washing them again with PBS for 5 minutes. Finally, sections were developed with 3,3'-diaminobenzidine tetrahydrochloride (DAB) peroxidase staining kit for maximum of 3 minutes, washed with water, and counter-stained with haematoxylin in the autostainer (Table 2.11) before mounting with DPX for analysis.

2.3.3 Lactate dehydrogenase assay

The cytoTox 96® non-radioactive cytotoxicity assay is a quantitative method that measures lactate dehydrogenase (LDH), a cytosolic enzyme released during cell lysis. Keratinocytes, MoDC and RHE-only HSE were cultured as previously described (see sections 2.3.1.2, 2.3.1.6, 2.3.2.2) and then challenged with different allergens to study cell lysis and pro-inflammatory response. LDH assay, was performed by incubating 50 µL of condition medium from all test and controls samples with 50 µL of the cytoTox 96® Reagent in a 96-well plate, and incubating at room temperature for 30 minutes and protected from light. After incubation, 50 µL of 1M acetic acid was added to each sample and absorbance was measured at 492 nm within 1 hour using a microplate reader (Tecan infinite M200 plate reader and Magellan software-v7.2).

2.3.4 RNA extraction

Monarch total RNA miniprep kit was used to extract RNA following the manufacturer's instructions. Cells were centrifuged to a pellet and conditioned medium removed. RNA lysis buffer (400 µL) was added directly to each cell pellet and mixed thoroughly (at this step, samples were sometimes stored at -80°C for later RNA extraction). Samples were transferred to a gDNA removal column fitted with a collection tube and centrifuged at 16000 x g for 30 seconds to remove the genomic DNA. The gDNA removal column was discarded, 400 µL of absolute ethanol were added to the flow-through and mixed by pipetting. Samples were transferred to an RNA purification column fitted with a collection tube and centrifuged at 16,000 x g for 30 seconds to bind the RNA to the column matrix. Flow-through was discarded, samples were washed with 500 µL of wash buffer and centrifuged at 16,000 x g for 30 seconds before incubating for 15 minutes at room temperature with 5 µL of DNase I added into 75 µL of DNase I reaction buffer. Following this, 500 µL of RNA priming buffer were added. Samples were centrifuged at 16,000 x g for 30 seconds and flow-through discarded. Samples were washed with 500 µL of RNA wash buffer-containing ethanol and centrifuged at 16,000 x g for 30 seconds, discarding the flow-through afterwards. Samples were washed again with 500 µL RNA wash buffer and centrifuged at 16,000 x g for 2 minutes. Columns were transferred to an RNase-free microfuge tube and

centrifuged at 16,000 for 1 minute to dry the column matrix. Fifty µL of nuclease-free water was added directly to the centre of the column matrix and centrifuged at 16,000 x g for 30 seconds. Total RNA was collected and passed again through the column to increase RNA yield. RNA quality and quantity was determined using Nanodrop 1000 (Thermo Scientific) at 240/280 nm according to the manufacturer's instructions. Samples were either placed on ice for downstream applications or stored at -80^{o}C.

2.3.5 cDNA synthesis

Total RNA (200 ng) was used to perform cDNA synthesis with the high-capacity cDNA reverse transcription kit without RNase inhibitor. Each reaction contained 2 µL of 10X RT buffer, 0.8 µL of 25X dNTP mix (100 mM), 2 µL of 10X RT random primers, 1 µL of multiScribe^{TM} reverse transcriptase, 4.2 µL of nuclease-free H_2O, and 10 µL of sample. To perform reverse transcription, the following thermal cycler conditions were used: 10 minutes at 25^{o}C, 120 minutes at 37^{o}C, and 5 minutes at 85^{o}C, following by a cooling down step in which samples were kept at 4^{o}C. cDNA was stored at -80^{o}C for future experiments.

2.3.6 TaqMan qPCR

TaqMan qPCR was performed to study gene expression. A master mix containing 5 µL of enzyme buffer, 0.5 µL of VIC-labelled housekeeping gene probe, 0.5 µL of FAM-labelled target gene probe, 3.5 µL of nuclease-free water, and 0.5 µL of cDNA was prepared on ice. The genes probes used to perform the qPCR are listed in

Table **2.2**. To perform TaqMan qPCR, the following cycles were performed using the Rotor-Gene Q Thermocycler (QIAGEN): 95oC for 10 seconds and 60oC for 45 seconds. This cycle was repeated 40 times and two channels were used: green (Source: 470 nm; Detector: 510 nm) for the test genes and yellow (Source: 530 nm; Detector: 555 nm) for the reference controls.

For data analysis, C_T values generated by the Rotor-Gene Q Thermocycler were analysed by comparative qPCR analysis. Technical repeats were used for each test and reference control reaction, so average C_T values for each reaction was calculated. ΔC_T value was calculated by subtracting C_T value of the target gene minus C_T value of the housekeeping gene. $\Delta\Delta C_T$ value was obtained by subtracting ΔC_T value of the gene minus ΔC_T value of the sample control to normalise the data. Relative gene expression ($2^{\wedge -\Delta\Delta CT}$) was used to analyse the results relative to an unstimulated control.

2.3.7 ELISA

Media was conditioned by 24-hour incubation of samples and stored at -20°C until required for analysis. Conditioned media was assessed for cytokine concentrations by ELISA kits (Table 2.6) as per manufacturer instructions. Plates were cultured overnight with 100 µL of capture antibody diluted in PBS without carrier protein. The day after, each well was aspirated and wash three times with 0.05% Tween®20 in PBS. Plates were blocked with 300 µL of 1% BSA in PBS and incubated for 1 hour at room temperature. Plates were then washed three times with 0.05% Tween®20 in PBS. One hundred µL of sample or standards diluted in 1% BSA in PBS were added to each well and incubated for 2 hours at room temperature. Plates were then washed three times with 0.05% Tween®20 in PBS, 100 µL of the Detection Antibody diluted in 1% BSA in PBS were added to each well and incubated for 2 hours at room temperature. Plates were washed three times with 0.05% Tween®20 in PBS, 100 µL of Streptavidin-HRP B were added to each well and incubated for 20 minutes at room temperature. Plates were washed three times with 0.05% Tween®20 in PBS, 100 µL of TMB substrate solution was added to each well for up to 30 minutes. Fifty µL of 2N H_2SO_4 was added to each well to stop the reaction and optical density determined using a microplate reader (Tecan infinite M200 plate reader and Magellan software-v7.2) set to 450 nm with a 570 correction.

2.3.8 Flow cytometry

Adherent immune cells cultured as monolayers were washed with HBSS and gently scraped into fresh medium and centrifuged at 200 g for 5 minutes, while suspension cells were centrifuged directly at 200 g for 5 minutes. The conditioned medium was either stored at -20°C for further analysis or discarded and cells were resuspended in 85 µL of cold FACS buffer, 10 µL of Fc Block and cells were incubated at 4°C for 15 minutes in the dark. Following this, 5 µL of fluorescent-conjugated antibody (Table 2.3) were added per test, and the cells incubated at 4°C for 20-30 minutes in the dark. Cold FACS buffer (1 mL) was added to the sample, and, after centrifugation at 1000 g for 2 minutes, the supernatant was removed and 350 µL of cold FACS buffer added to resuspend the cells. Analysis was carried out using a BD FACSCalibur or a BD LSRII flow cytometer, where 1 x 10^4 events were collected for each sample. Analysis of flow cytometry data was undertaken using FlowJo-v10.8.0. (FlowJo software) and median fluorescence intensity (MFI; which is the median fluorescence intensity of the target marker) calculated or the number of fluorescence -positive cells compared to controls.

2.3.9 Statistical analysis

All data are expressed as mean ± SD of at least three independent experiments unless otherwise stated. Statistical analysis was performed using GraphPad Prism-v9.3.1. (GraphPad Software). Pair-wise comparisons were performed with either Student's t test (paired or unpaired as appropriate). Group-wise comparisons were carried out using ANOVA. Differences were considered significant when $p<0.05$.

Chapter 3 – Isolation, differentiation/polarisation and characterisation of mononuclear-derived immune cells in monolayer or suspension culture

3.1 Introduction

In vivo, in response to inflammatory cues, peripheral blood monocytes leave the circulation by extravasation and quickly differentiate into tissue macrophages, and under specific environmental cues can form dendritic cells (Collin & Bigley, 2018; Epelman et al., 2014). CD4+ T cells also leave the circulation and enter tissues as part of the adaptive immune process, where they can be polarised, depending on the constituents of the local cytokine milieu, into a number of T cell subsets.

This process of differentiation and polarisation can be replicated *in vitro* (Cechim & Chies, 2019; Italiani & Boraschi, 2017). Due to the low availability of macrophages, dendritic cells (DCs) and Langerhans cells (LCs) in peripheral blood and availability of human tissue, as well as the technological difficulties in isolating tissue resident cells, the use of blood-derived monocytes is currently the only practical source for obtaining sufficient quantities of these primary cells for experimentation (Geissmann et al., 1998). Similarly, T cells can also be isolated from peripheral blood. To increase yield further, both monocytes and lymphocytes can be isolated from buffy coats, which are pooled leukocyte fractions from a number of individuals following extraction from whole blood following blood donation (Lozano-Ojalvo et al., 2015).

Without exogenous cytokine stimulation, monocytes can be differentiated into monocyte-derived macrophages (MDM) by adherence to tissue culture plastic (Nielsen et al., 2020). However, the presence of granulocyte-macrophage colony-stimulating factor (GM-CSF) or macrophage colony-stimulating factor (M-CSF) facilitates the differentiation process (Bender, 2004). Moreover, monocyte-derived dendritic cells (Mo-DC) can be differentiated from MDM by addition of GM-CSF and IL-4 (Colic et al., 2003; Guironnet et al., 2001), and monocyte-derived Langerhans cells (Mo-LC) by additional culture with TGF-β (Geissmann et al., 1998). Additionally, T cells can be isolated from mononuclear cells by negative selection (Schuler et al., 2011) and polarised into T_H2 cells by stimulation with anti-CD3 and anti-CD28, and in the presence of both IL-2 and IL-4 (Zhu et al., 2010). Generation of differentiated or polarised immune cells from buffy coats is often the preferred choice in experimental set ups that require a significant quantity of cells. However, it is imperative that the cells are characterised in terms of known cell-specific or differentiation/polarisation markers before use.

In this chapter, MDM, Mo-DC and Mo-LC were differentiated from mononuclear cells isolated from human buffy coats. In addition, naïve CD4+ T cells were isolated from mononuclear cells and polarised into T_H2 cells. All these immune cells were characterised for known, specific markers.

Chapter aim: To differentiate and characterise diverse immune cells from buffy coat-derived mononuclear cells.

Objectives:

- Isolate naïve CD4+ T cells from buffy coat mononuclear cells, polarise these into T_H2 cells and quantify phenotypic changes.
- Differentiate buffy coat monocytes into MDM, Mo-DC and Mo-LC and characterise.
- Examine cytokine release to confirm cell functionality.

3.2 Methods

Monocytes were isolated from human buffy coats (see section 2.3.1.4) and then differentiated into MDM (see section 2.3.1.5), Mo-DC (see section 2.3.1.6) or Mo-LC (see section 2.3.1.7). In addition, naïve CD4+ T cells were isolated from buffy coat-derived mononuclear cells using negative selection (see section 2.3.1.8), activated with anti-CD3/CD28, expanded with IL-2 (see section 2.3.1.9), and polarised into T_H2 cells using IL-4 and anti-IFNγ (see section 2.3.1.10).

Immune cell functionality was examined upon challenge with allergen (see section 2.3.1.11), LDH assay (see section 2.3.3) was carried out to measure cytotoxicity upon stimulation, RNA was extracted (see section 2.3.4), cDNA was synthesised (see section 2.3.5) followed by RT-qPCR (see section 2.3.6) that was used to determine gene expression, while ELISA (see section 2.3.7) and flow cytometry analysis (see section 2.3.8) were used to measure protein abundance.

3.3 Results

3.3.1 Isolation, activation and polarisation of T cells in suspension culture

Naïve CD4+ T cells were isolated from mononuclear cells using negative selection immunobead technology, activated with anti-CD3/CD28-conjugated beads, expanded with IL-2 and polarised into T_H2 cells using IL-4 and anti-IFNγ.

Mononuclear cells were cultured on tissue culture plastic directly following Ficoll density gradient centrifugation and compared to culture of naïve CD4+ T cells isolated from the same mononuclear cells using negative selection immunobead technology. Unselected, numerous mononuclear cells (monocytes and lymphocytes) adhered onto tissue culture plastic after 24 hours of being seeded, and were evenly spherical, dark in appearance and with few, small cell clusters (Figure 3.1A). In contrast, after 24 hours in suspension, isolated naïve CD4+ T cells were non-adherent and formed numerous cell clusters in suspension (Figure 3.1B).

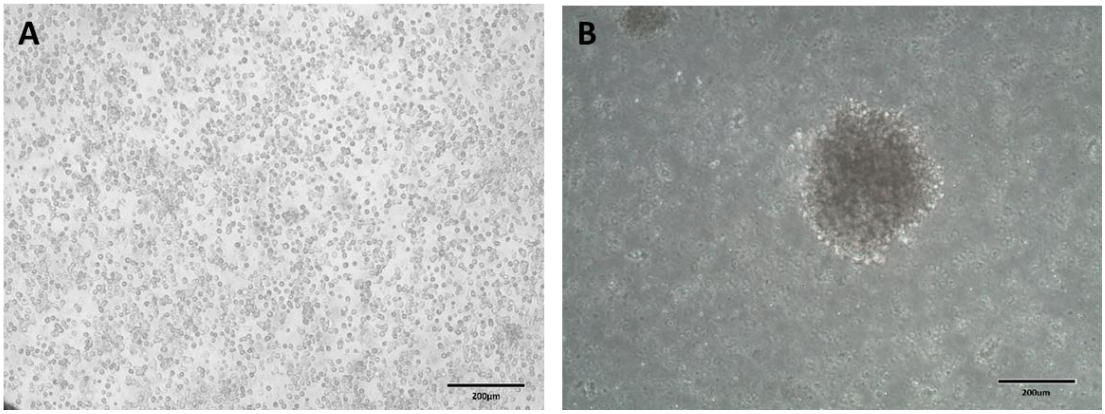

Figure 3.1 Mononuclear cells and naïve CD4+ T cells morphology.
Adherent mononuclear cells (A) 24 hours after seeding on standard tissue culture plates and naïve CD4+ T cells (B) after 24 hours in suspension. Images are representative of multiple isolations. Scale bar = 200 µm.

CD4+ T cell purity was next studied by the use of protein markers. Firstly, two different naïve CD4+ T cell isolation kits (from MiltenyiBiotec and StemCell Technologies) were compared, using CD4 as a CD4+ T cell marker and IgG as a control, to determine the percentage of positive CD4+ T cells, and from this the purity of the different kit isolation procedures. Seventy four percent of positive CD4+ T cells were obtained when using the MiltenyiBiotec kit, compared to 63% positive CD4+ T cells for the StemCell isolation kit (Figure 3.2). Consequently, the MiltenyiBiotec kit was used in subsequent

experiments. In addition, the number of viable cells following MiltenyiBiotec kit isolation was assessed by addition of propidium iodide (PI), a cell viability dye that only binds to non-viable cells. Naïve CD4+ T cells isolated with the MiltenyiBiotec isolation kit resulted in 87% viable naïve CD4+ T cells (Figure 3.3).

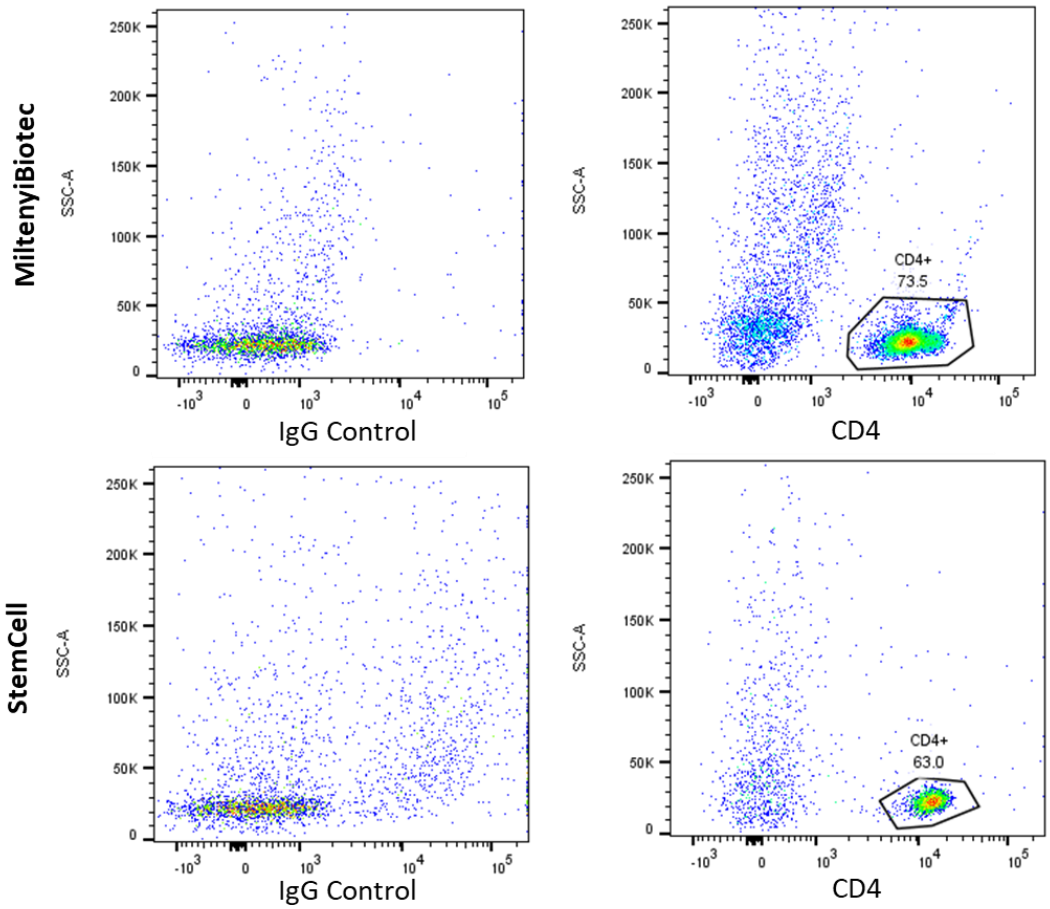

Figure 3.2 Assessment of naïve CD4+ T cell purity following negative selection isolation.
Naïve CD4+ T cells were isolated from buffy coat-derived mononuclear cells using either the MiltenyiBiotec (upper panels) or Stem Cell kit (lower panels). CD4+ purity was measured by staining for CD4 compared to IgG (control) and measured by flow cytometry. Images show representative histograms for n=3 experiments.

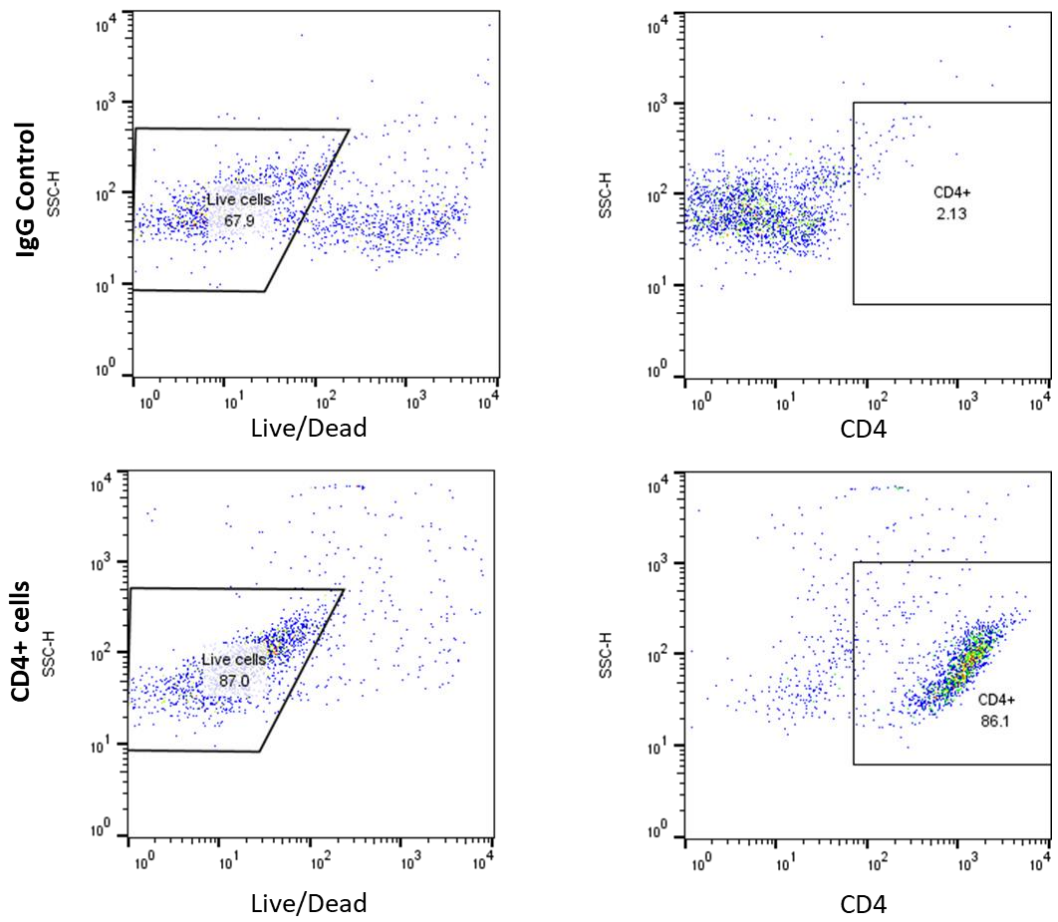

Figure 3.3 Assessment of naïve CD4+ T cell viability following negative selection isolation
Naïve CD4+ T cells were isolated from buffy coat-derived mononuclear cells using MiltenyiBiotec negative isolation kit and cell viability measured by propidium iodide exclusion (left hand panels). The viable population was gated and the number of viable CD4+ naïve T cells measured by flow cytometry (right hand panels). Images show representative histograms for n=3 experiments.

Next, naïve CD4+ T cells from a single batch each, and therefore different patient each, were activated with anti-CD3/CD28-conjugated beads which mimic T cell receptor engagement, and expanded with addition of exogenous IL-2 for 7 days. To study batch-to-batch variability, cell number was measured at increasing time points, and fresh medium was added at each time so that the cells were at a density of $0.5x10^6$ cells/mL (Figure 3.4A). The number of CD4+ T cells increased from $2.29x10^6 \pm 0.24x10^6$ at day 1 to $5.98 \times 10^6 \pm 5.78x10^6$ at day 10. Numbers then rapidly declined in all patients to $0.65x10^6 \pm 0.52x10^6$ by day 16 (F (7, 24) = 3.529, p=0.009). In addition, there was a statistically significant decrease between day 10 and day 19 (p=0.043), and between day 10 and day 22 (p=0.045). Apart from day 10 the batch-to-batch variability was low for T cell proliferation (Figure 3.4A). In addition, gene expression of cytokine markers for CD4+ T cells and T_H2 cells were examined (Figure 3.4B). *IL-4*, *IL-5*, *IL-6*, *IL-13* and *TSLP* were up-regulated upon stimulation with anti-CD3/CD28 and IL-2 but not polarised into T_H2

cells. These cells express abundant cytokines at gene level, in particular *IL-13*. Here, batch-to-batch variability was low for cytokine gene expression with the exception of transcription for *IL-13* (Figure 3.4B).

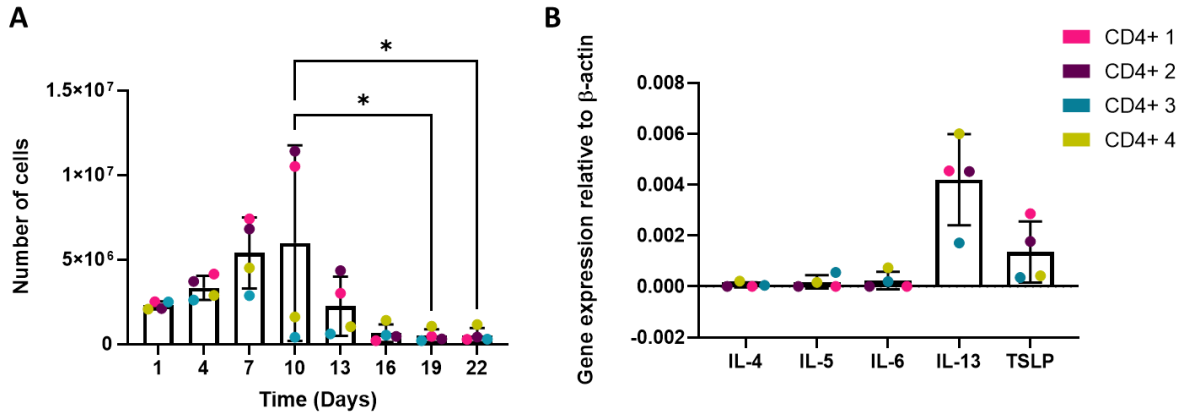

Figure 3.4 Patient-to-patient variation in activated CD4+ T cells.
Anti-CD3/CD28 activated CD4+ T cells were counted at increasing time points to measure cell proliferation (A); and gene expression of *IL-4, IL-5, IL-6, IL-13* and *TSLP* were analysed by qPCR following 7 days in culture, calculated relative to the endogenous reference gene *β-actin* (B). Data are presented as mean ± SD of n=4 independent experiments with statistically significant differences determined by one-way ANOVA followed by Tukey post hoc test; *p<0.05; and with each batch buffy coat represented by a different colour.

In order to polarise activated CD4+ T cells into T_H2 cells, two conditions were tested based on published studies (Iezzi et al., 1998; Maier et al., 2014). In the first condition, T_H2 cells were polarised at day 1 using IL-4 and anti-IFNγ, following activation with anti-CD3/CD28 and expansion with IL-2 on the first day of CD4+ T cells isolation, and then stimulated again with anti-CD3/CD28 and IL-2 on day 7-14. In the second condition, T_H2 cells were activated with anti-CD3/CD28 and expanded with IL-2 on days 1-7 following CD4+ T cell isolation, then polarised with IL-4 and anti-IFNγ, and further activated with anti-CD3/CD28 and IL-2 on day 7-14. Analysis was performed by measuring the T_H2 cell population growth rate at days 1, 7 and 14 (Figure 3.5). At day 7 both test groups had similarly increased in cell number, however, by day 14 cells polarised at day 1 had proliferated more than those polarised at day 7, although this was not found to be statistically significant.

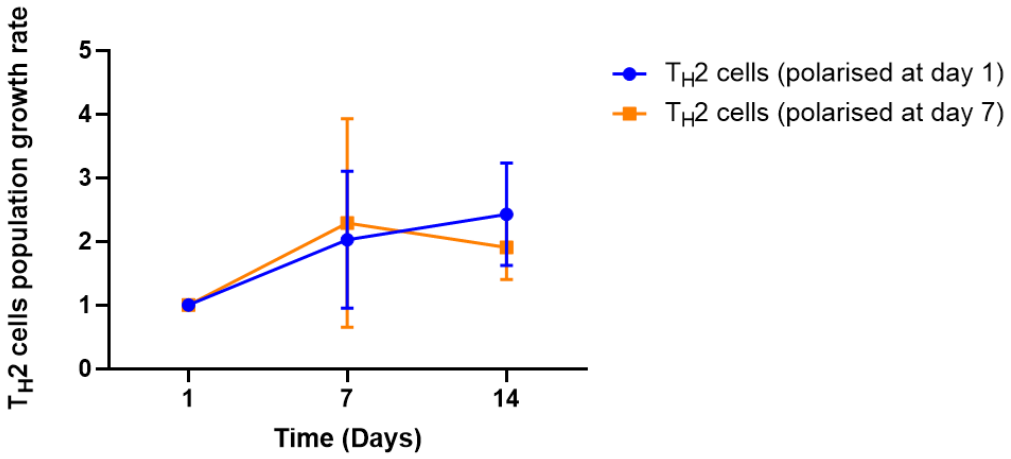

Figure 3.5 T_H2 cells population growth rate following polarisation at day 1 or day 7.
The number of T_H2 cells were measured at increasing time points for T_H2 cells polarised at day 1 (blue line) or day 7 (orange line). Data are presented as mean ± SD of n=3 independent experiments with statistically significant differences determined by two-way ANOVA.

Next, gene expression of cell polarisation markers in the T_H2 cells after being subject to the two different polarisation methods was examined. Before performing the qPCR it is important to use a reference gene whose C_T value does not vary between different polarisation conditions and controls. Therefore, the expression of different reference genes *(B2M,* β*-actin, GAPDH* and *UBC*) under T_H2 cell polarisation conditions on day 1 and day 7 was evaluated. Table 3.1 shows mean ± SD of C_T value for the reference genes. *GAPDH* and *β-actin* appear to have the more variation between the three repeats, while *B2M* and *UBC* seem to be more similar between repeats.

Table 3.1 Reference genes data.
Mean±SD of C_T value for T_H2 cells for different reference genes of n=4 independent experiments.

	B2M	***GAPDH***	***β-actin***	***UBC***
Mean±SD				
T_H2 cells (polarised at day 1)	24.825±1.92	31.58±2.89	31.95±4.30	36.47±0.40
Mean±SD				
T_H2 cells (polarised at day 7)	23.45±3.25	30.74±3.67	26.96±5.50	24.09±3.62

Having determined which reference gene to use, gene expression of *IL-4*, *IL-5*, *IL-6*, *IL-13* and *TSLP* in these two test populations was studied by RT-qPCR (Figure 3.6) at day-14 polarisation. Overall, gene expression of these 5 genes was unchanged (p>0.05) when comparing both T_H2 cell populations. However, some genes such as *IL-4* (F (2, 9) = 10.34, p=0.004) and *IL-13* (F (2, 9) = 8.792, p=0.007) were statistically significantly upregulated. *IL-4* was significantly increased (p=0.018) in T_H2 cells polarised at day 1 and in T_H2 cells polarised at day 7 (p=0.005) compared to naïve CD4+ T cells, and IL-13 was significantly increased (p=0.011) in T_H2 cells polarised at day 1 and in T_H2 cells polarised at day 7 (p=0.017) compared to naïve CD4+ T cells. There was marked batch-to-batch variation following polarisation. Similar results were observed when quantifying cell surface protein abundance (Figure 3.7) at day 14 of the polarisation, with statistically significant differences for CCR3 (F (1.376, 4.129) = 32.18, p=0.003), CD154 (F (1.557, 4.670) = 42.36, p=0.001) and CD4 (F (1.054, 3.162) = 2.388, p=0.217).

CCR3 was increased in T_H2 cells polarised at day 1 (p=0.017) and T_H2 cells polarised at day 7 (p=0.020), compared to naïve CD4+ T cells. CD154 was increased in T_H2 cells polarised at day 1 (p=0.003) and T_H2 cells polarised at day 7 (p=0.011), compared to naïve CD4+ T cells. CD4 was increased in T_H2 cells polarised at day 1 (p=0.034), compared to naïve CD4+ T cells. However, no statistically significant differences were observed for CCR4 and CD119. In addition, the percentage of positive cells in T_H2 cells polarised at day 1 was also compared to percentage of positive cells in T_H2 cells polarised at day 7 and naïve CD4+ T cells. For CCR3, 24.8% of T_H2 cells polarised at day 1 were positive compared to 5.33% at day 7 and 3.32% of naïve CD4+ T cells. For CCR4, 10.5% of T_H2 cells polarised at day 1 positive cells compared to 37.9% at day 7, and 6.73% naïve CD4+ T cells), while levels of CD119 and CD154 were similar for both polarisation protocols, and different to naïve CD4+ T cells (24.2% for CD119 and 2.81% for CD154) (Figure 3.8).

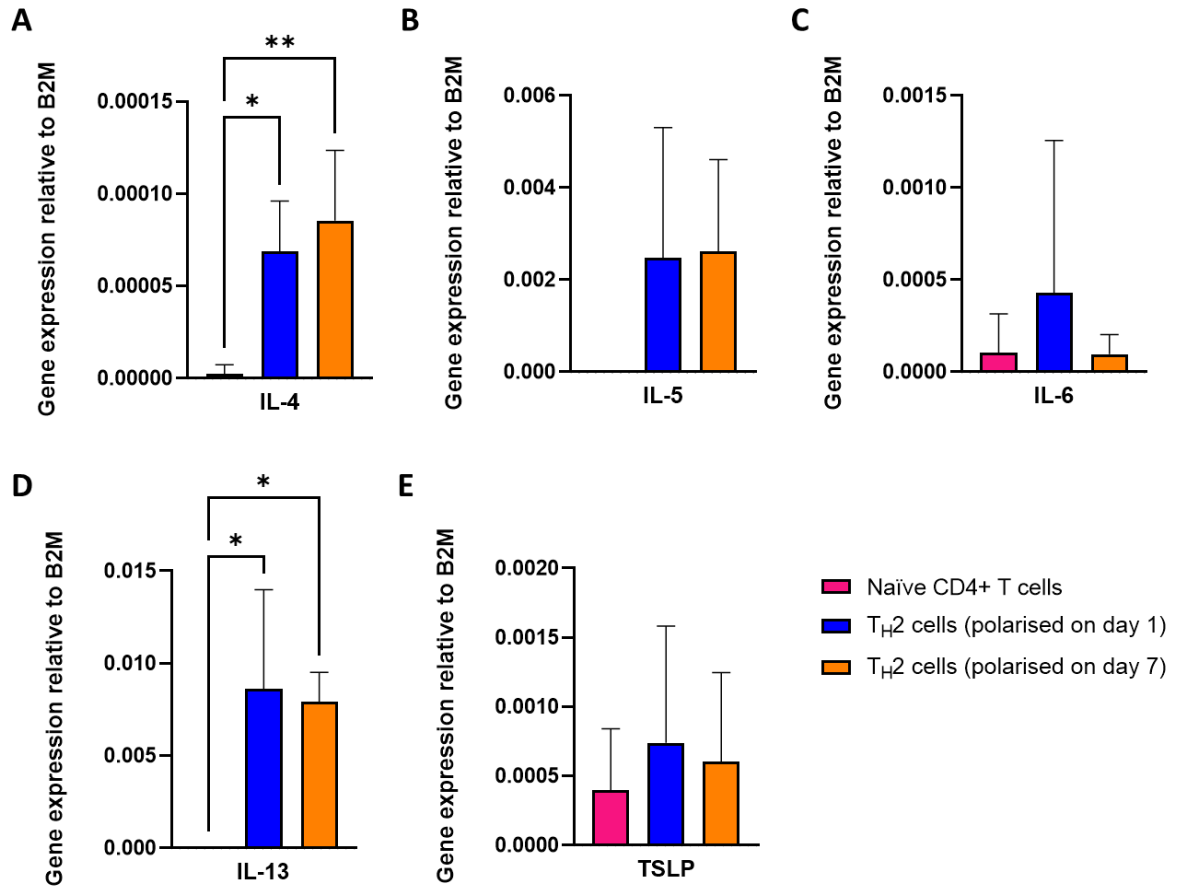

Figure 3.6 Gene expression of T_H2 cell polarisation markers in naïve CD4+ T cells, T_H2 cells polarised on day 1, and T_H2 cells polarised on day 7.

Gene expression of a panel of T_H2 genes for naïve CD4+ T cells (pink) isolated from buffy coat mononuclear cells compared to T_H2 cells polarised on day 1 (blue) and T_H2 cells polarised on day 7 (orange) following 14 days culture. Gene expression of *IL-4* (A), *IL-5* (B), *IL-6* (C), *IL-13* (D) and *TSLP* (E) were analysed by qPCR, calculated relative to the endogenous reference gene *B2M*. Data are presented as mean ± SD of n=4 independent experiments with statistically significant differences determined by one-way ANOVA followed by a Tukey post hoc test; *p<0.05, **p<0.01.

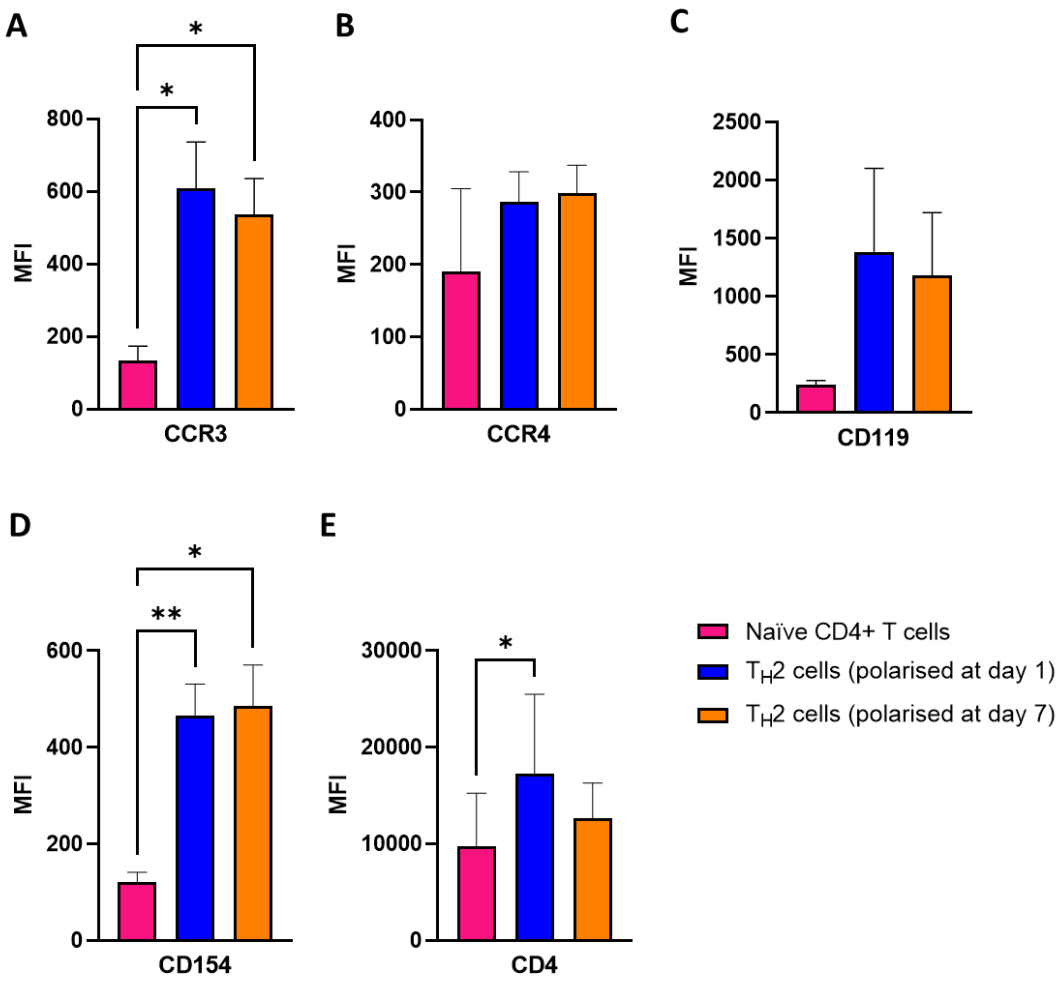

Figure 3.7 Cell surface protein abundance of T_H2 cell polarisation markers in naïve CD4+ T cells, T_H2 cells polarised at day 1, and T_H2 cells polarised at day 7.

T_H2 cells polarised at day 1 (blue) and T_H2 cells polarised at day 7 (orange) were compared to naïve CD4+ T cells following 14 days culture. Abundance of immune markers CCR3 (A), CCR4 (B), CD119 (C), CD154 (D) and CD4 (E) were measured by flow cytometry, data shown as median fluorescence index (MFI). Data are presented as mean ± SD of n=4 independent experiments with statistical significance differences determined by paired Student's t test; *p<0.05, **p<0.01. T_H2 cells showed similar protein abundance irrespective of polarisation methodology.

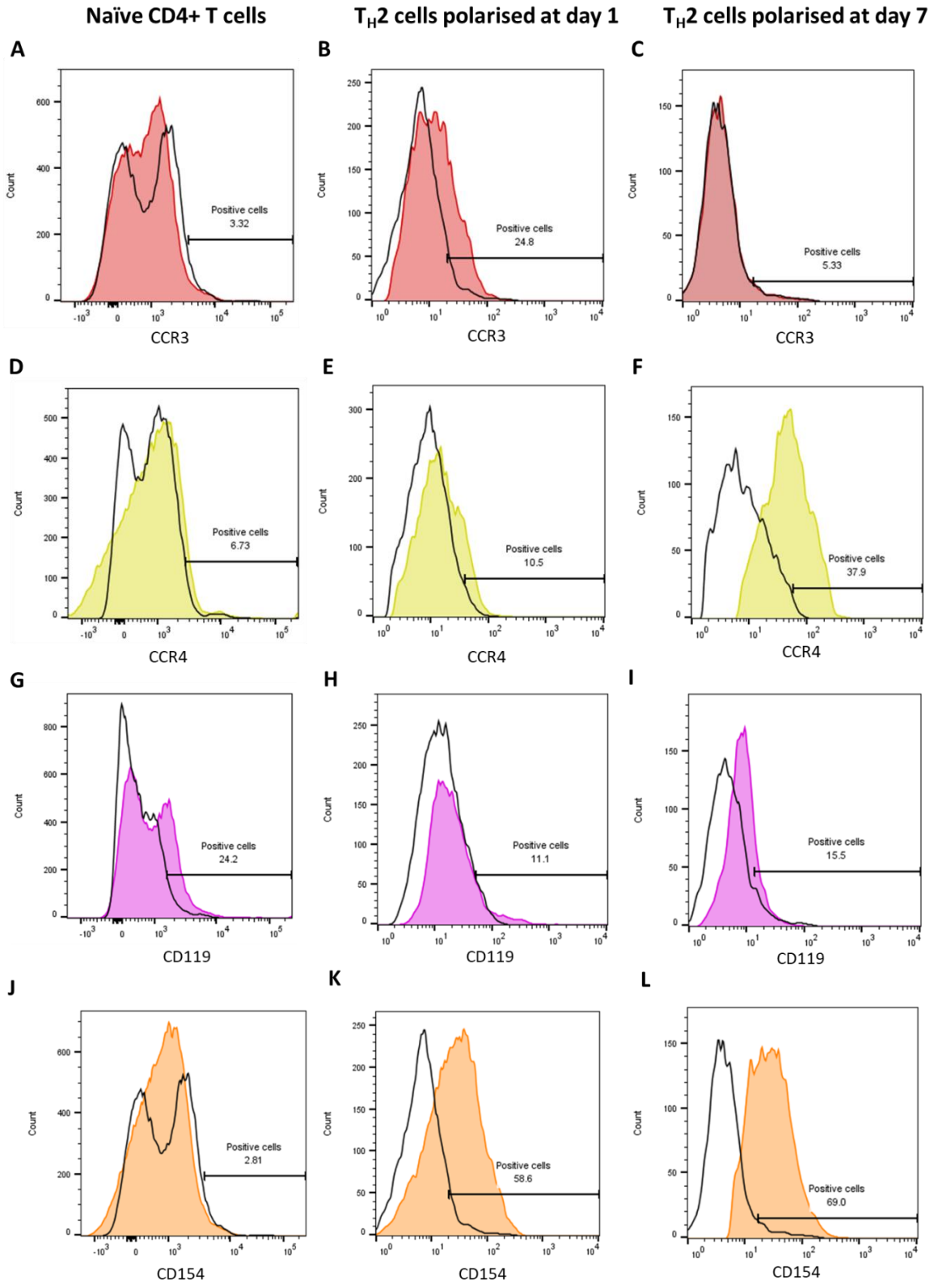

Figure 3.8 Cell surface protein abundance of T_H2 cells polarisation markers in naïve CD4+ T cells, T_H2 cells polarised at day 1, and T_H2 cells polarised at day 7.

Naïve CD4+ T cells, T_H2 cells polarised at day 1 and T_H2 cells polarised at day 7, following 14 days culture. Percentage of positive cells, compared to the IgG control (black), for immune markers CCR3 (A, B, C), CCR4 (D, E, F), CD119 (G, H, I) and CD154 (J, K, L) were measured by flow cytometry. Data is representative of 4 isolations.

Next, based on our findings to this point, T_H2 cells that were polarised at day 1 using IL-4 and anti-IFNγ were used for all subsequent experiments. Therefore, naïve CD4+ T cells were compared to T_H2 cells that were polarised at day 1 using IL-4 and anti-IFNγ, in combination with anti-CD3/CD28 activation and IL-2 expansion at day 1 of CD4+ T cell isolation. Gene expression of *IL-4*, *IL-5*, *IL-6*, *IL-13* and *TSLP* was studied by RT-qPCR (Figure 3.9). Statistically significant changes in T_H2 cells compared to naïve CD4+ T cells was observed for *IL-4* (p=0.013) and *IL-13* (p=0.048). Expression of *IL-5* and *IL-6* was markedly increased but donor variation and low experimental replicates prevented significance. Expression of *TSLP* was similar in both naïve and polarised CD4+ T cells. At the cell surface protein level, MFI (which measures surface protein levels) was similar for CCR3 for both naïve and T_H2 cells, however, a statistically significant increase in MFI was observed for T_H2 cells for CCR4 (p=0.043), CD119 (p=0.041), CD154 (p<0.001) and CD4 (p<0.001) compared to naïve CD4+ T cells (Figure 3.10). Moreover, the percentage of positive cells (i.e., the number of cells expressing high levels of cell surface protein) in naïve CD4+ T cells was compared to percentage of positive cells in T_H2 cells (Figure 3.11). CCR3 (2.80% of naïve CD4+ T cells and 5.04% of T_H2 cells positive cells), CCR4 (6.88% of naïve CD4+ T cells and 9.79% of T_H2 cells positive cells), CD119 (6.60% of naïve CD4+ T cells and 47.3% of T_H2 cells positive cells), CD154 (2.24% of naïve CD4+ T cells and 9.82% of T_H2 cells positive cells) and CD4 (4.19% of naïve CD4+ T cells and 93.1% of T_H2 cells positive cells) were increased in T_H2 cells compared to naïve CD4+ T cells.

In summary, a methodology for the production of polarised T_H2 cells was determined which included the isolation of a highly purified population of naïve CD4+ cells, their activation by CD3/CD28-conjugated beads, expansion using IL-2 and polarisation on day 1 using IL-4 and anti-IFNγ. This methodology was used in subsequent 3D tissue engineering experiments in chapter 5 of this thesis.

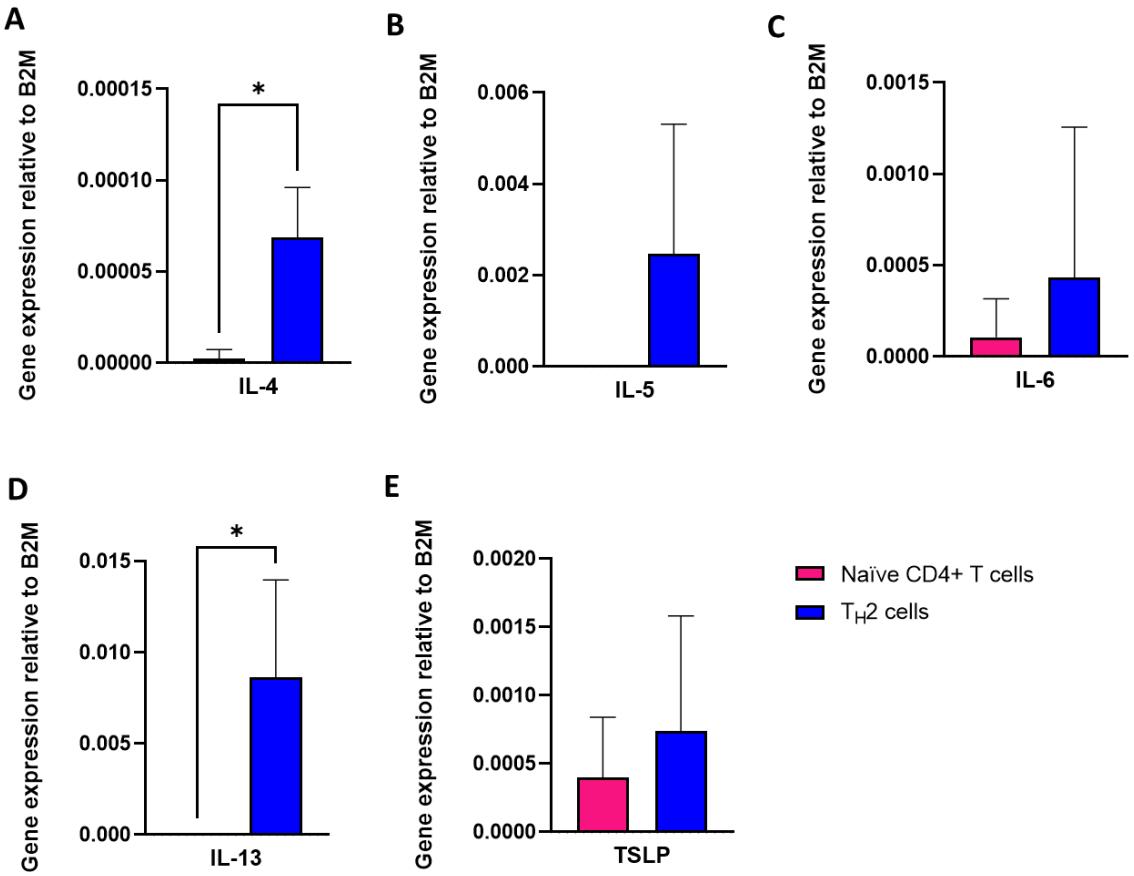

Figure 3.9 Gene expression of T_H2 cell markers in naïve CD4+ T cells and polarised T_H2 cells.
Naïve CD4+ T cells (pink) isolated from mononuclear cells from buffy coats compared to T_H2 cells (blue). Gene expression of *IL-4* (A), *IL-5* (B), *IL-6* (C), *IL-13* (D) and *TSLP* (E) were analysed by RT-qPCR, calculated relative to the endogenous reference gene *B2M*. Data are presented as mean ± SD of n=4 independent experiments with statistical significance differences determined by paired Student's t test; *p<0.05.

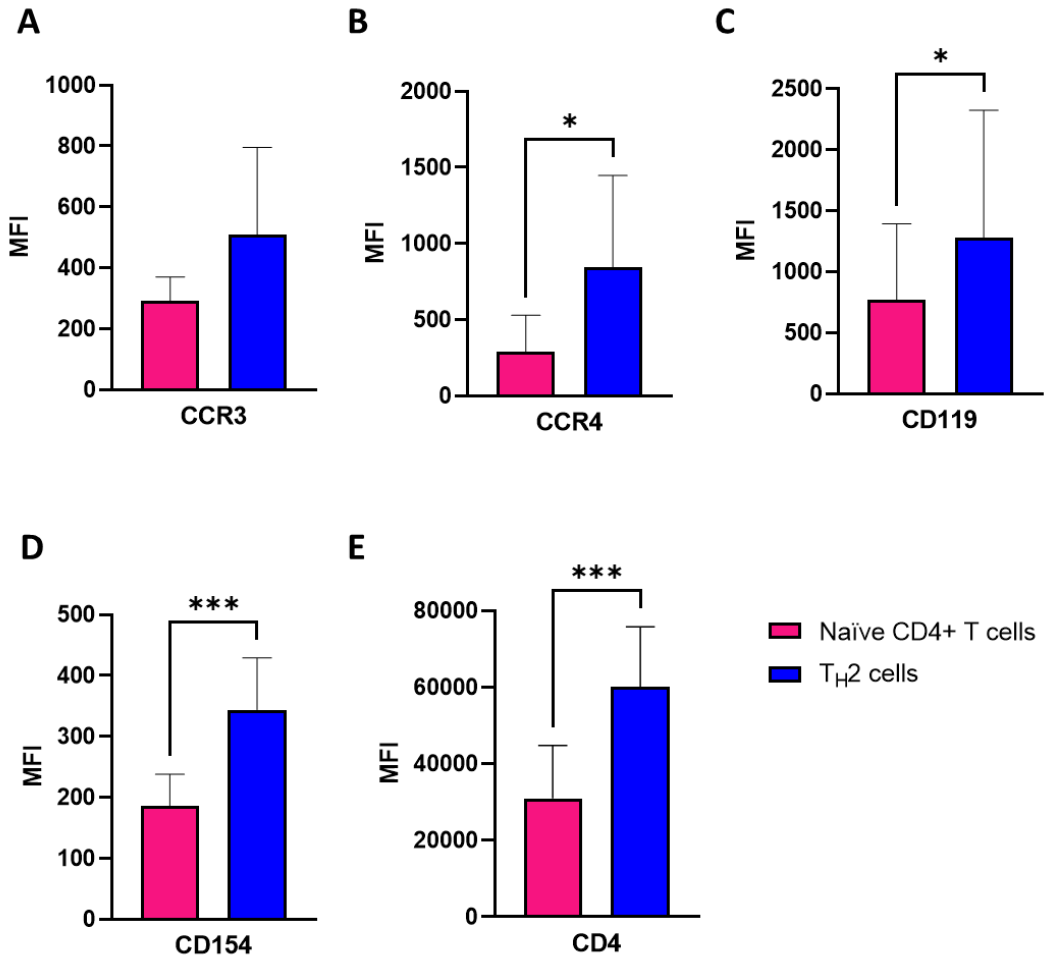

Figure 3.10 Cell surface protein abundance of T_H2 cells polarisation markers on naïve CD4+ and polarised T_H2 cells.

Naïve CD4+ T cells (pink) isolated from buffy coat mononuclear cells were compared to T_H2 cells following 7-day culture following activation and polarisation (blue). Abundance of the cell surface T_H2 immune markers CCR3 (A), CCR4 (B), CD119 (C), CD154 (D) and CD4 (E) were measured by flow cytometry. Data are presented as mean ± SD MFI of n=6 independent experiments with statistical significance differences determined by paired Student's t test; *p<0.05, ***p<0.001.

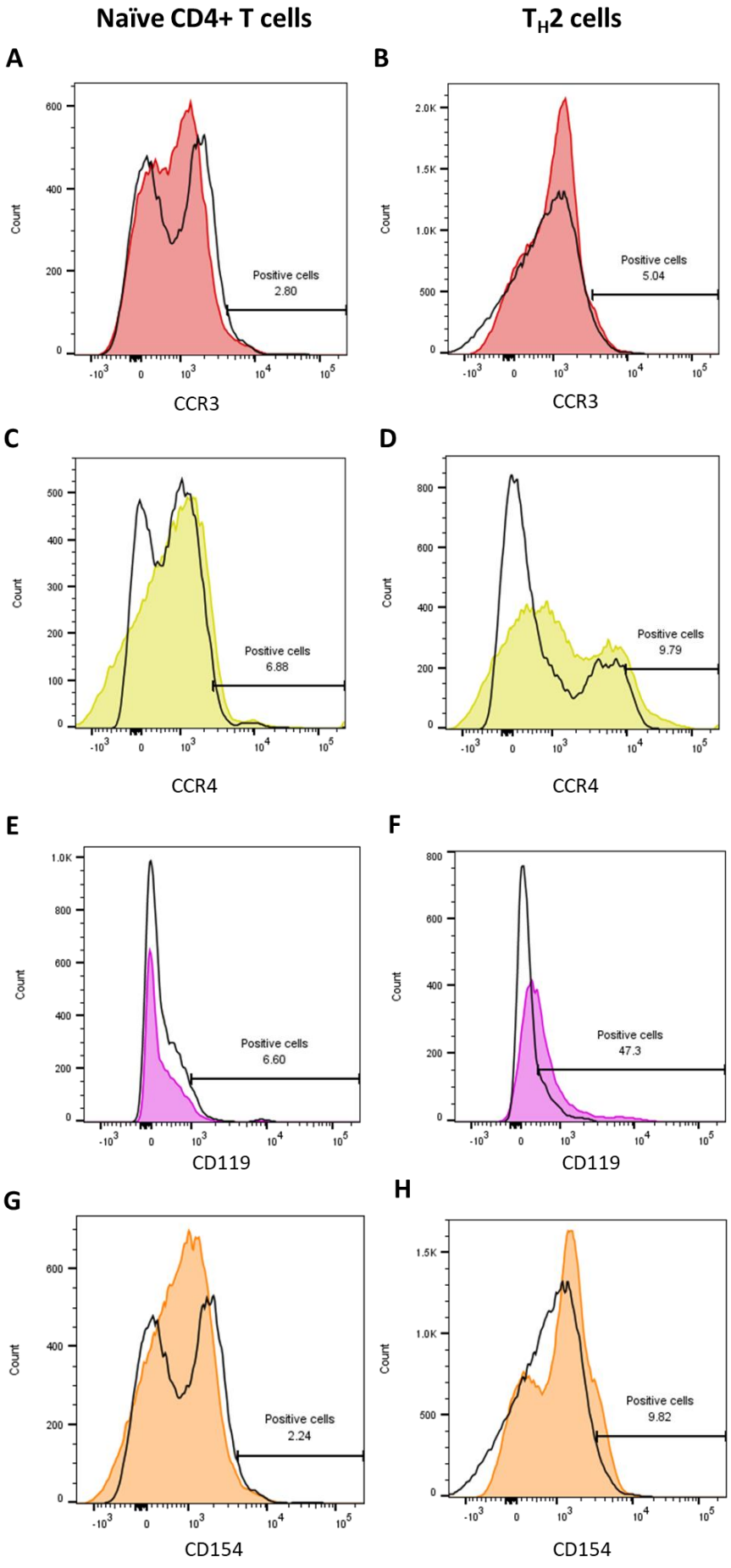
Naïve CD4+ T cells
T_H2 cells
A
B
Count
Positive cells
2.80
Positive cells
5.04
CCR3
CCR3
C
D
Positive cells
6.88
Positive cells
9.79
CCR4
CCR4
E
F
Positive cells
6.60
Positive cells
47.3
CD119
CD119
G
H
Positive cells
2.24
Positive cells
9.82
CD154
CD154

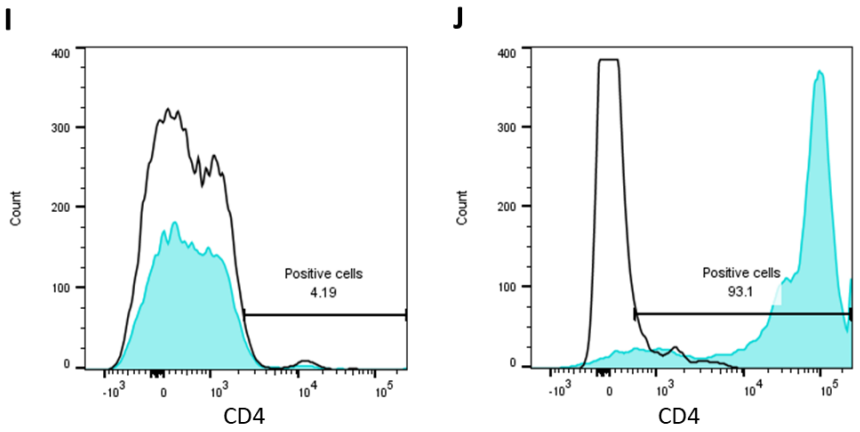

Figure 3.11 Cell surface protein abundance of T_H2 cells markers in naïve CD4+ T cells and polarised T_H2 cells.

T_H2 cells activated with anti-CD3/CD28, expanded with IL-2 and polarised at day 1 of the isolation were examined for cell surface abundance of T_H2 markers CCR3 (A, B), CCR4 (C, D), CD119 (E, F), CD154 (G, H) and CD4 (I, J) by flow cytometry, and compared to naïve CD4+ T cells. Histograms show percentage of positive cells in naïve CD4+ T cells and polarised T_H2 cells (coloured histograms) compared to the IgG control (black line). Data is representative of 6 isolations.

3.3.2 Generation of MDM, Mo-DC and Mo-LC

Mononuclear cells were isolated from human buffy coats and differentiated into MDM or Mo-DC by adding M-CSF or IL-4 and GM-CSF, respectively, for 7 days culture. LCs are predominantly found in the epidermis and research suggests that these cells display a slightly different phenotype to other dendritic cells. Geissman *et al.*, (1998) provided evidence that monocytes could be differentiated into Mo-LC via culture with GM-CSF, IL-4 and TGβ-1. Therefore, monocytes were cultured using the Geissman protocol by culturing adherent monocytes for 7 days in 40 ng/mL IL-4, 50 ng/mL GM-CSF and 10 ng/mL TGβ-1.

Firstly, the morphology of the three differentiated cell types was examined. MDM displayed a mixed phenotype with some cells containing large spherical cells with dark nuclei and light cytoplasm about 30-40 µm in diameter and displaying a classical 'fried egg' morphology, while other cells were more elongated cells of approximately 100 µm in length (Figure 3.12A). In contrast, Mo-DC differentiated cells were predominantly dendrite shaped cells of approximately 100 µm long, without any visible nuclei (Figure 3.12B). Mo-LC cells were a mixture of elongated cells similar to Mo-DC and more rounded cells with dendritic projections (Figure 3.12C).

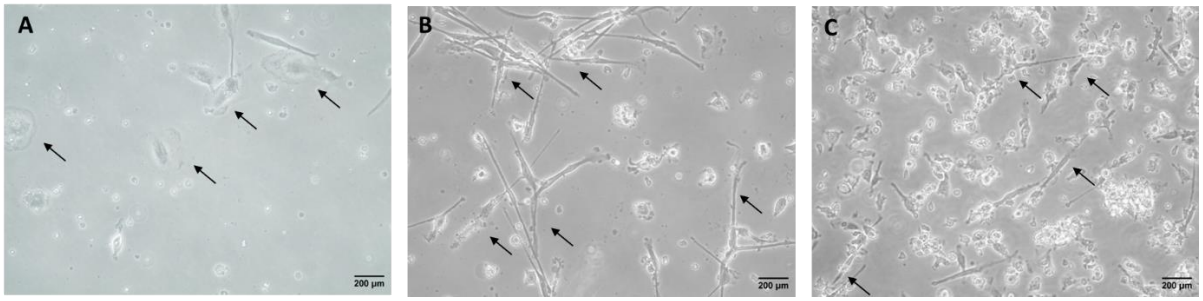

Figure 3.12 MDM, Mo-DC and Mo-LC morphology.
Micrograph images of MDM (arrows, A), Mo-DC (arrows, B) and Mo-LC (arrows, C) following 7 days of differentiation culture. MDM display the classical 'fried egg' phenotype whilst Mo-DC and Mo-LC are more dendritic in morphology. Images are representative of multiple isolations. Scale bar = 200 µm.

3.3.2.1 Defining the culture conditions of Mo-DC.

In the literature several different combinations of GM-CSF and IL-4 have been used to generate Mo-DC (Hiasa et al., 2009; Holla et al., 2014; Posch et al., 2016). So firstly, to establish which conditions were optimal, Mo-DC were differentiated for 7 days using different cytokine dose concentrations (25 ng/mL GM-CSF + 20 ng/mL IL-4, 50 ng/mL GM-CSF + 40 ng/mL IL-4, and 75 ng/mL GM-CSF + 60 ng/mL IL-4) and gene and protein markers of Mo-DC differentiation were evaluated and compared to MDM.

Although expression of some of these markers differed overall with GM-CSF and IL-4 cytokine treatment in Mo-Dc compared to MDM, none were statistically significantly different due to variation in the data, most likely due to batch-to-batch variation. For example, *CD1a*, *CD14* and *CD80* was markedly increased with the highest concentration of GM-CSF and IL-4, while a concentration of 25 ng/mL GM-CSF + 20 ng/mL IL-4 produced elevated levels of *CD207* and reduced levels of *CD86* (Figure 3.13). Similarly, cell surface protein abundance for CD1a, CD11c, CD207 and HLA-DR was not statistically significant between the two cell types at different cytokine dose concentrations due to large deviation between batch samples, although abundance of CD11c and HLA-DR were consistently increased in Mo-DC compared to MDM for all concentrations tested (Figure 3.14). Although there was little difference between the different cytokine concentrations, a cytokine dose of 25 ng/mL GM-CSF + 20 ng/mL IL-4 was chosen for future experiments because this closely resembles the Mo-DC phenotype described in the literature (Chometon et al., 2020; Colic et al., 2003).

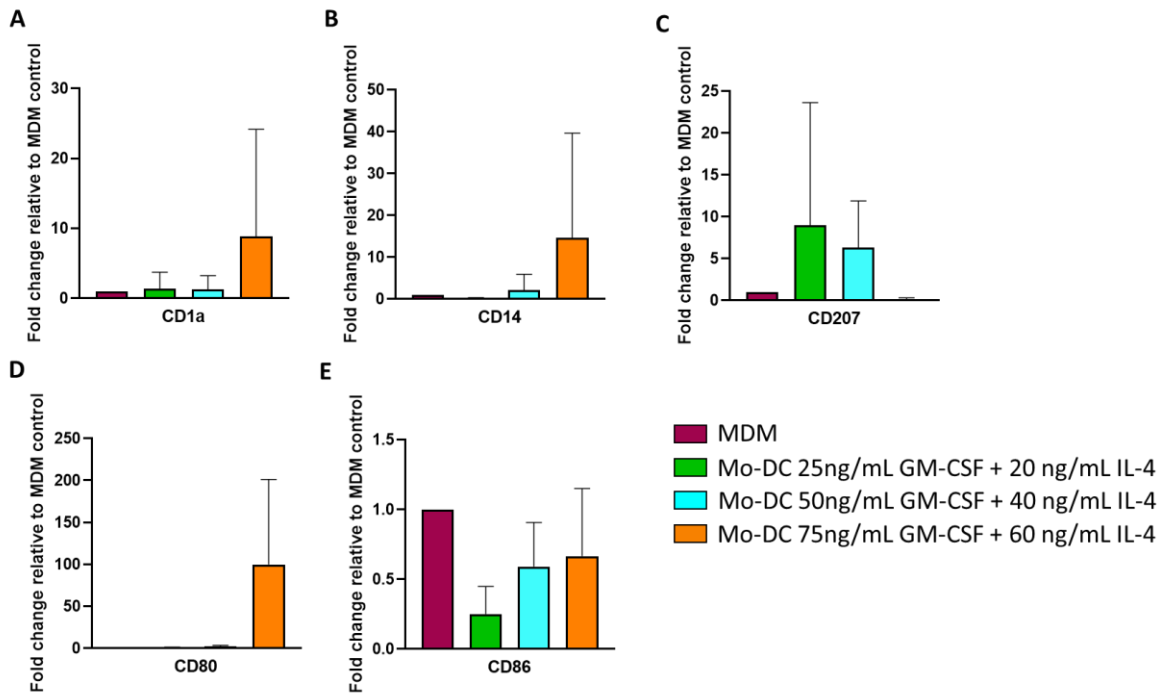

Figure 3.13 Gene expression of MDM and Mo-DC differentiation markers in response to culture with different cytokine concentrations.

Mo-DC were cultured with 25 ng/mL GM-CSF + 20 ng/mL IL-4 (green), 50 ng/mL GM-CSF + 40 ng/mL IL-4 (blue), or 75 ng/mL GM-CSF + 60 ng/mL IL-4 (orange) and gene expression of several differentiation markers compared to MDM (burgundy) following 7 days culture. Gene expression of *CD1a* (A), *CD14* (B), *CD11c* (C), *CD80* (D) and *CD86* (E) was analysed by RT-qPCR, calculated relative to the MDM. Data are presented as mean ± SD of n=3 independent experiments with statistical significance differences determined by one-way ANOVA.

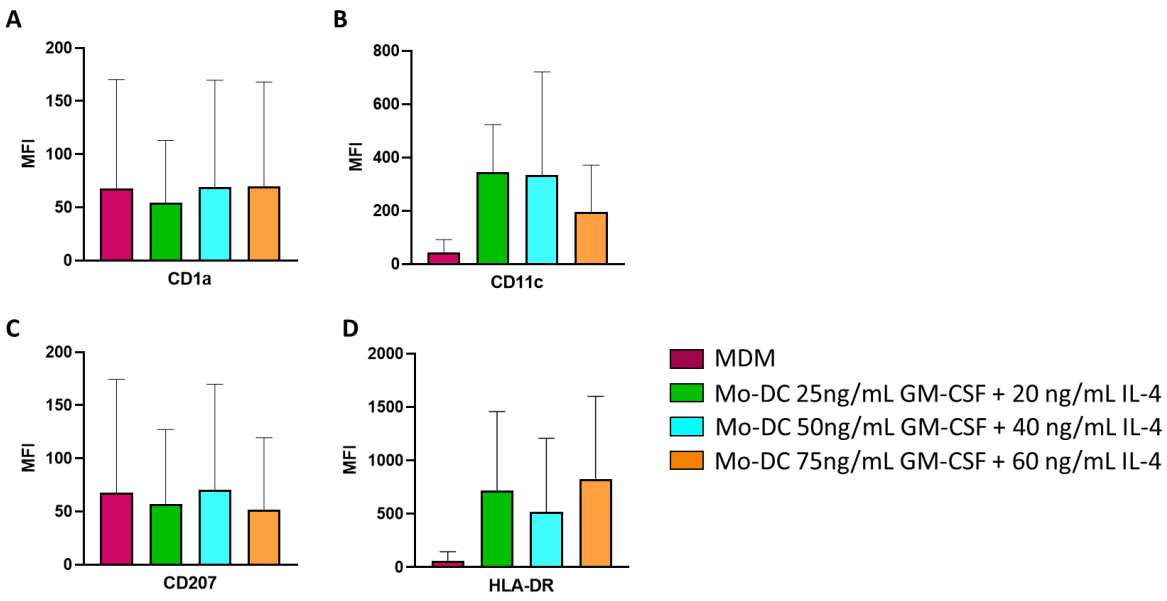

Figure 3.14 Cell surface protein abundance of MDM and Mo-DC differentiation markers in response to culture with different cytokine concentrations.
Mo-DC were cultured 25 ng/mL GM-CSF + 20 ng/mL IL-4 (green), 50 ng/mL GM-CSF + 40 ng/mL IL-4 (blue), or 75 ng/mL GM-CSF + 60 ng/mL IL-4 (orange) and cell surface differentiation marker abundance compared to MDM (burgundy) following 7 days culture. Abundance of immune markers CD1a (A), CD11c (B), CD207 (C) and HLA-DR (D) was measured by flow cytometry, data are presented as mean ± SD MFI of n=3 independent experiments with statistical significance differences determined by one-way ANOVA.

3.3.2.2 Response of MDM, Mo-DC and Mo-LC upon lipopolysaccharides stimulation

LPS is well known to stimulate Mo-DC and Mo-LC into a more mature phenotype (H. Tanaka et al., 2000), therefore, MDM, Mo-DC and Mo-LC were treated with 100 ng/mL LPS for 4 hours and 24 hours to assess response in differentiation marker expression.

In untreated samples, levels of *CD1a* gene expression increased sequentially from MDM to Mo-DC then Mo-LC. Upon stimulation with LPS, transcription levels of *CD1a* increased in Mo-DC but not in Mo-LC where levels remained similar to MDM levels (Figure 3.15A). For *CD207* untreated cells displayed similar levels for MDM and Mo-DC while Mo-LC had low levels. Once again, upon LPS stimulation, levels of *CD207* increased in Mo-DC but surprisingly not in Mo-LC (Figure 3.15B), although data variation due to donor samples was large and so no statistical significance was observed.

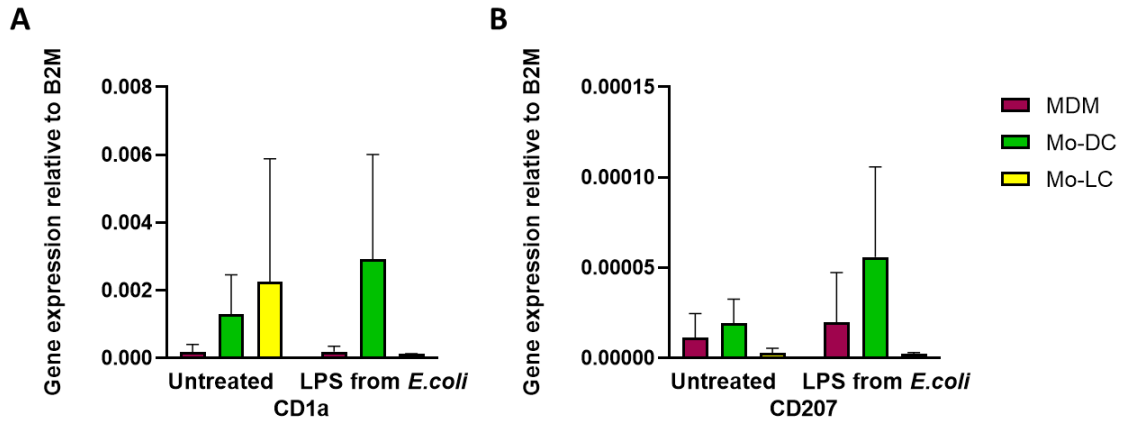

Figure 3.15 Gene expression of differentiation markers by MDM, Mo-DC and Mo-LC upon stimulation with LPS.

Mo-DC were cultured with 25 ng/mL GM-CSF + 20 ng/mL IL-4 (green) and Mo-LC cultured in 50 ng/mL GM-CSF, 40 ng/mL IL-4 and 10 ng/mL TGβ-1 (yellow) and gene expression of differentiation markers compared to MDM (burgundy) following 7 days culture alone or following treatment with 100 ng/mL LPS from E. coli for 4 hours. Gene expression of *CD1a* (A), *CD207* (B) were analysed by RT-qPCR, and expression calculated relative to the reference gene *B2M*. Data are presented as mean ± SD of n=3 independent experiments with statistical significance determined using two-way ANOVA.

For cell surface protein abundance for CD1a and CD207 was elevated in unstimulated Mo-DC and Mo-LC but levels were similar to MDM upon LPS stimulation (Figure 3.16). This could be because cells were only stimulated for 4 hours and a longer stimulation time was required. Since Mo-LC displayed reduced markers and were un-responsive to LPS compared to Mo-DC, a phenotype not characteristic of human DC or LC, these cells were excluded from all further work.

Finally, Mo-DC were compared to MDM in response to LPS with response to cytokine secretion. Statistically significances were determined by two-way ANOVA ($F(1, 8)=12.97$, $p=0.007$). IL-10 production was significantly increased in LPS-treated Mo-DC compared to MDM ($p=0.023$), and in LPS-treated Mo-DC compared to untreated MDM ($p=0.036$) (Figure 3.17). This shows that Mo-DC have functionality in response to bacterial LPS for at least one week in monolayer culture, being more responsive to LPS treatment in the context of cytokine secretion.

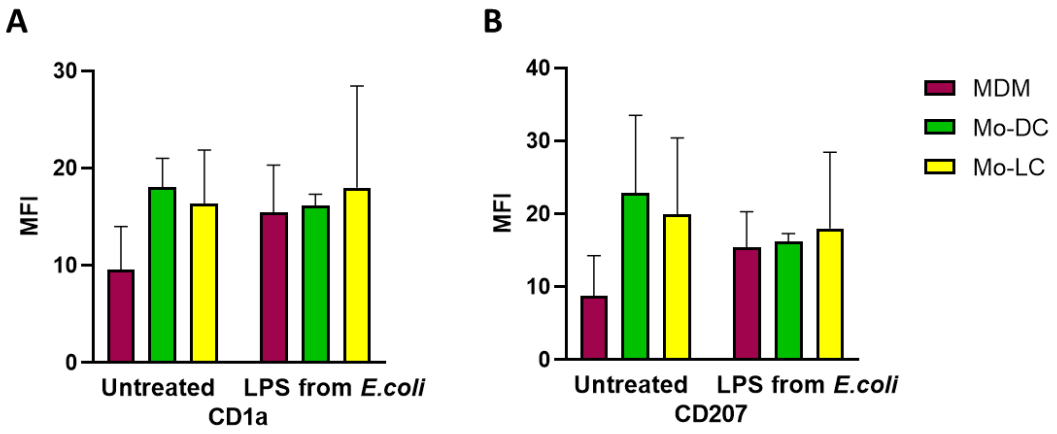

Figure 3.16 Cell surface protein abundance of MDM, Mo-DC and Mo-LC before and after stimulation with LPS.

Mo-DC were differentiated with 25 ng/mL GM-CSF and 20 ng/mL IL-4 (green), and Mo-LC differentiated with 50 ng/mL GM-CSF, 40 ng/mL IL-4 and 10 ng/mL TGβ-1 (yellow) compared to MDM (burgundy) following 7 days culture, before and after treatment with 100 ng/mL LPS from E. coli for 4 hours. Abundance of immune markers CD1a (A) and CD207 (B) were measured by flow cytometry. Data are presented as mean ± SD MFI of n=3 independent, with statistical significance determined using two-way ANOVA.

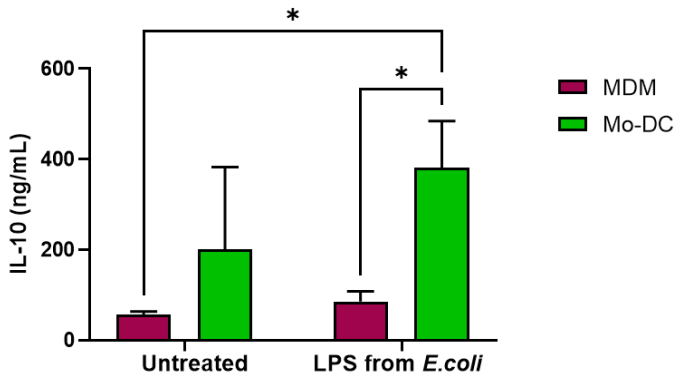

Figure 3.17 IL-10 secretion by MDM and Mo-DC before and after stimulation with LPS.

Mo-DC were cultured with 25 ng/mL GM-CSF + 20 ng/mL IL-4 (green) and compared to MDM (burgundy) following 7 days culture, before and following treatment with 100 ng/mL LPS from E. coli for 24 hours. Conditioned media was analysed for secretion of IL-10 as measured by ELISA. Data are presented as mean ± SD of n=3 independent experiments with statistical significance determined using two-way ANOVA followed by Tukey post hoc test; *p<0.05.

3.3.3 Stimulation of monocyte-derived dendritic cells with allergens

3.3.3.1 2,4-Dinitrochlorobenzene (DNCB)

DNCB is a chemical compound that is frequently used in human research of AD and induces chronic contact dermatitis (Fujii et al., 2009), and when it is topically administered to mice it produces an AD-like phenotype (Inagaki et al., 2006). It has been previously shown (Toebak et al., 2009) that stimulation of DC with sensitisers such as DNCB leads to allergen-induced DC activation. Mo-DC were activated by treatment with increasing concentrations of DNCB for 4- and 24-hours and cell viability measured. Firstly, cell morphology was assessed after 4- and 24-hours stimulation. Initially, Mo-DC were cultured in increasing concentrations of DNCB ranging from 1 μM to 10 mM DNCB but these concentrations increasingly killed the Mo-DC when examined by light microscopy and lactate dehydrogenase release for cell damage (data not shown). Consequently, a lower concentration range was examined.

Mo-DC were treated with increasing concentrations of DNCB ranging from 0.001 μM to 1 μM, for 4- and 24-hours to assess cell viability and function. Medium alone and SDS-treated cells were used as negative and positive controls, respectively. At 4-hours all cells remained viable with no marked change under light microscopy compared to SDS-treated control (Figure 3.18) although an increase in LDH was observed with the 1 μM DNCB treated cells (Figure 3.20A). By 24 hours increasing numbers of dead cells could be observed in the 1 μM DNCB treated cells by light microscopy (Figure 3.19) with increased LDH in the 0.1 and 1 μM DNCB treated cells. This was confirmed by LDH release examined in the conditioned media (Figure 3.20B). No significant increases were seen in LDH release following treatment with DNCB compared to the untreated control.

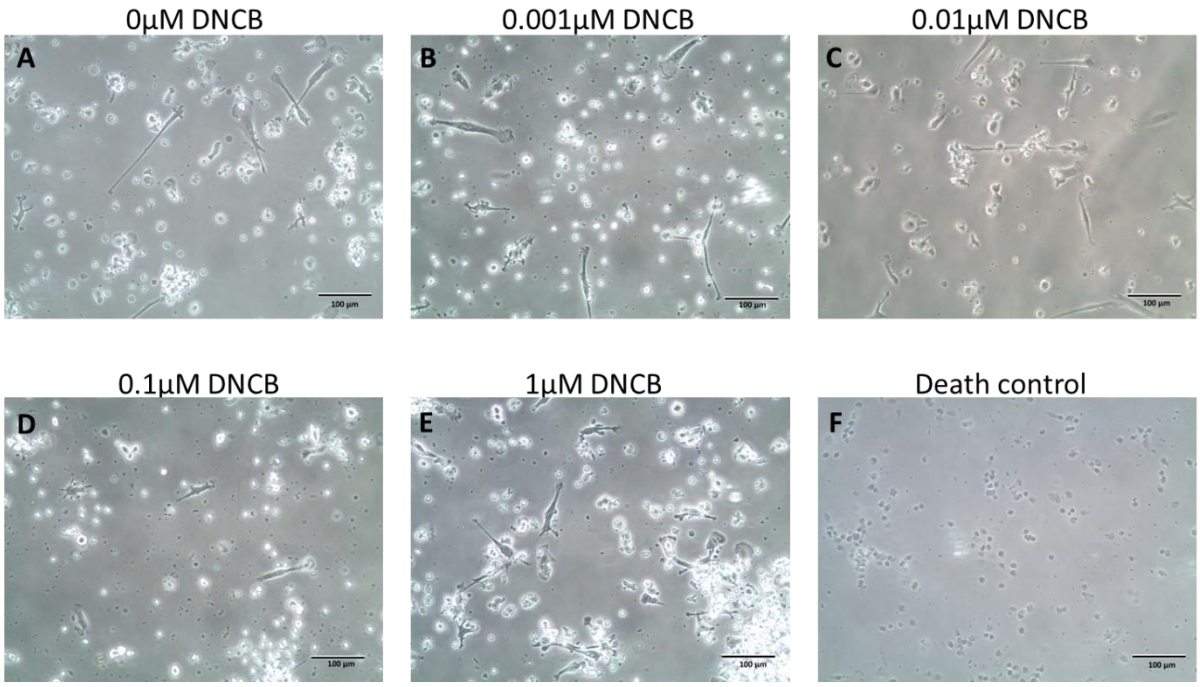

Figure 3.18 Mo-DC morphology after 4-hour stimulation with increasing concentrations of DNCB. Untreated Mo-DC (A) following 7 days of differentiation were stimulated with 0.001 µM (B), 0.01 µM (C), 0.1 µM (D), and 1 µM DNCB (E), and compared to a SDS-treated cells (death control) (F) for 4 hours. Images are representative of n=3 experiments. Scale bar = 100 µm.

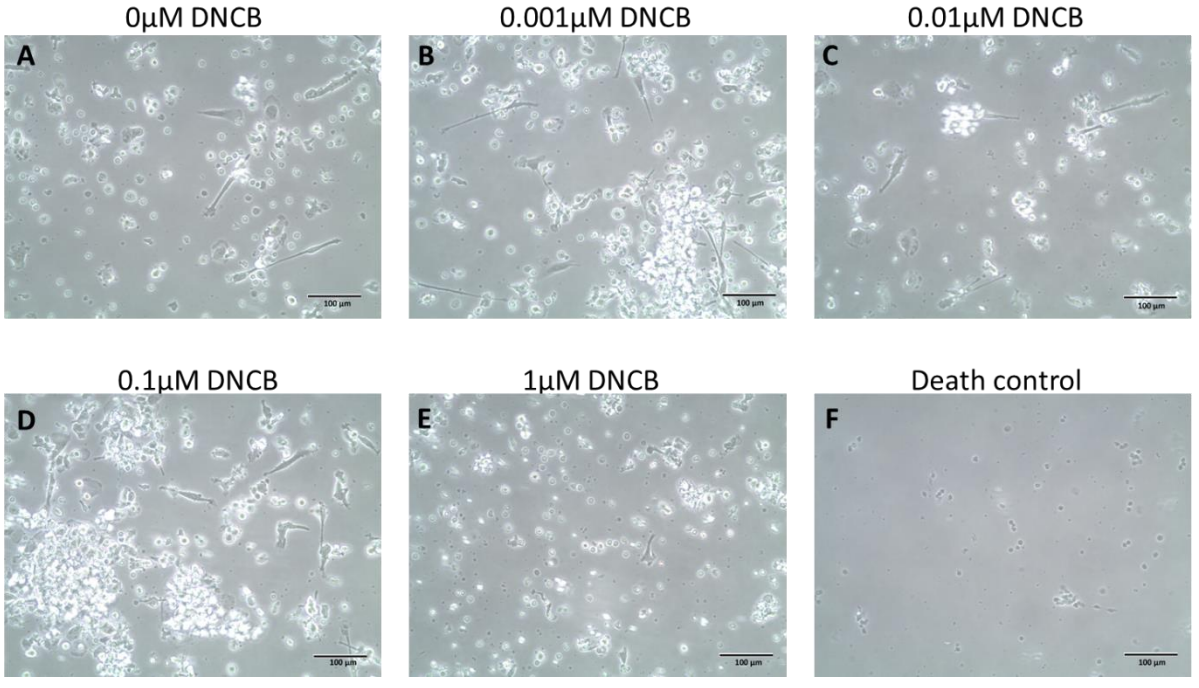

Figure 3.19 Mo-DC morphology after 24-hour stimulation with increasing concentrations of DNCB. Untreated Mo-DC (A) following 7 days of differentiation were stimulated with 0.001 µM (B), 0.01 µM (C), 0.1 µM (D), and 1 µM DNCB (E), and compared to a SDS-treated cells (death control) (F) for 24 hours. Images are representative of n=3 experiments. Scale bar = 100 µm.

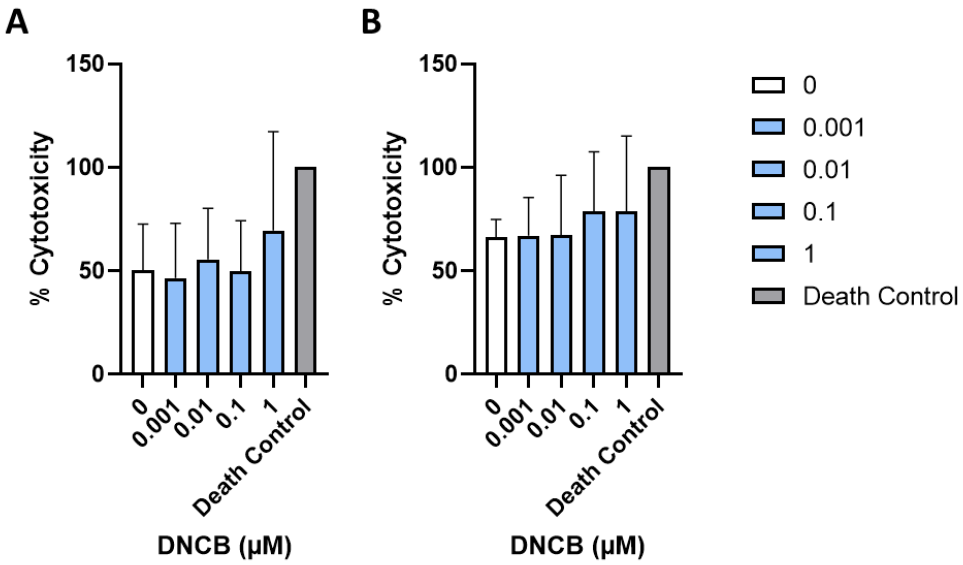

Figure 3.20 C**ytotoxicity in Mo-DC after stimulation with increasing concentrations of DNCB.**
Mo-DC (white) following 7 days of differentiation were stimulated with different concentrations of DNCB (light blue), and compared to untreated or non-viable controls (grey) for 4 hours and 24 hours. Data are presented as mean ± SD of n=3 independent experiments with statistical significance determined using one-way ANOVA.

Alterations in gene expression were measured after 4-hours treatment and compared to untreated controls. Increased gene expression was observed for *CCL17*, *IL-1*α, *IL-1*β for 0.001 µM DNCB, and although other increases were observed for other genes these were not statistically significant due to variable responses between donors (Figure 3.21).

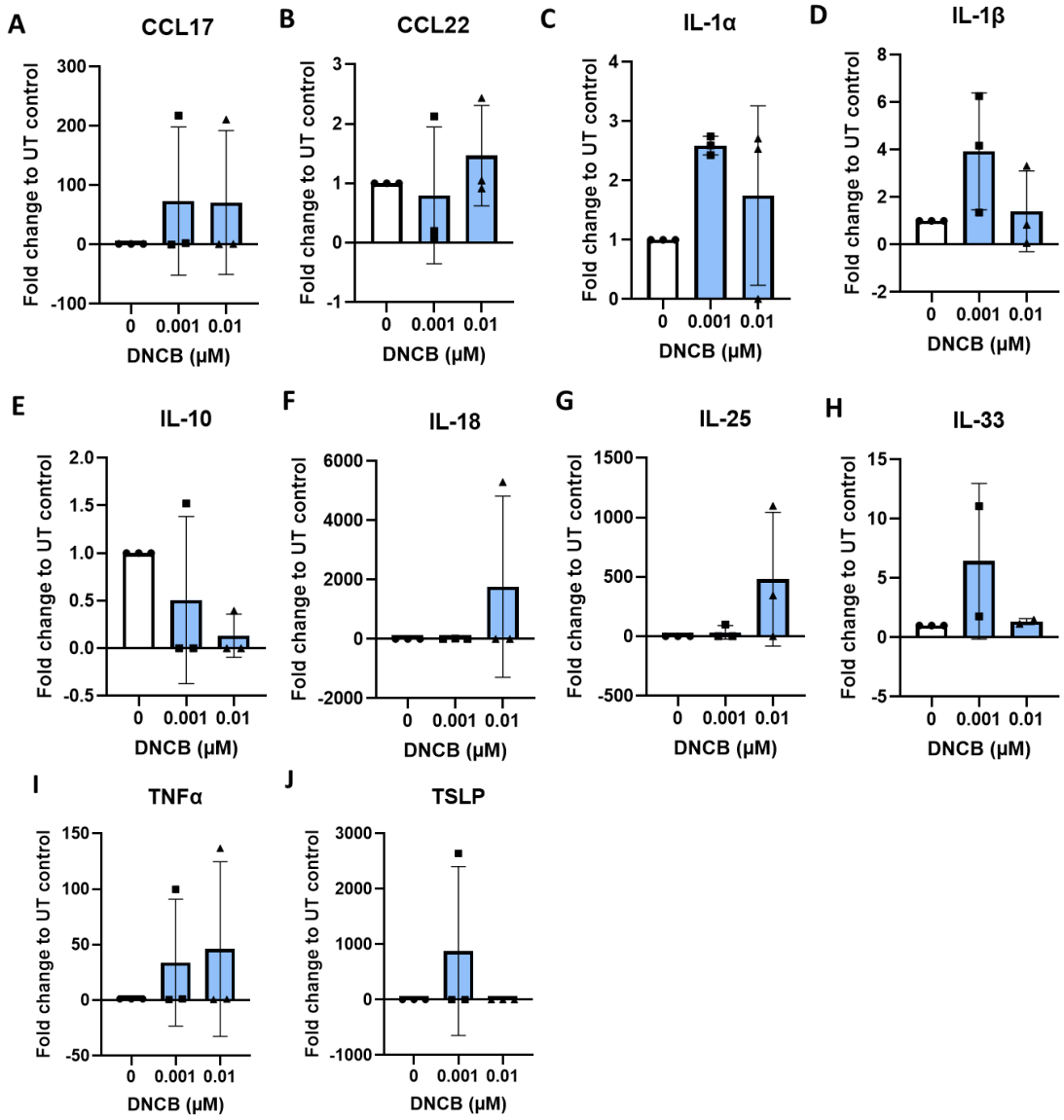

Figure 3.21 Gene expression of Mo-DC upon stimulation with DNCB for 4 hours.
Mo-DC (white) following 7 days culture and treated with 0.001 µM and 0.01 µM DNCB (light blue) for 4 hours. Gene expression of *CCL17* (A), *CCL22* (B), *IL-1α* (C), *IL-1β* (D), *IL-10* (E), *IL-18* (F), *IL-25* (G), *IL-33* (H), *TNFα* (I) and *TSLP* (J) were analysed by RT-qPCR, and expression calculated relative to the untreated control. Data are presented as mean ± SD of n=3 independent experiments with statistical significance determined using one-way ANOVA.

3.3.3.2 Dermatophagoides pteronyssinus

Derp1 and Derp2 are proteases and major allergens present in house dust mites (*Dermatophagoides pteronyssinus)* (Winton et al., 1998). Approximately 70% of allergic people with either AD and/or bronchial asthma are sensitive to house dust mite, with Derp1 sensitisation the cause in approximately 80% of these patients (de Halleux et al., 2006). As Derp1 is the most prevalent allergen found in mite faecal pellets and the most prominent stimulus of the IgE response in people with house mite allergies,

Mo-DC were treated with increasing concentrations of Derp1 for 4- and 24-hours and viability assessed. Firstly, morphology was assessed after 4- and 24-hours stimulation. After 4-hours there was no effect on cell viability as determined by light microscopy (Figure 3.22) or LDH release (Figure 3.24A). In contrast, by 24 hours concentration of 10 and 100 μM appeared to cause toxicity by light microscopy (Figure 3.23) although no increase in LDH release was observed (Figure 3.24B).

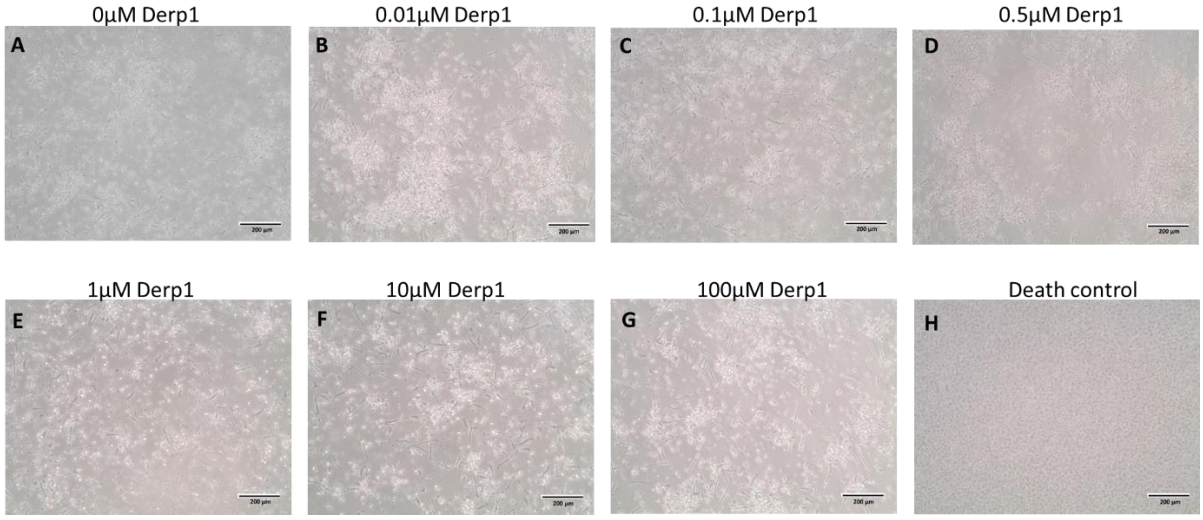

Figure 3.22 Mo-DC morphology after 4-hour stimulation with increasing concentrations of Derp1. Untreated Mo-DC (A) following 7 days of differentiation were stimulated with 0.01 μM (B), 0.1 μM (C), 0.5 μM (D), 1 μM (E), 10 μM (F), and 100 μM Derp1 (G), and compared to a non-viable control (H), for 4 hours. Images are representative of multiple isolations. Scale bar = 200 μm.

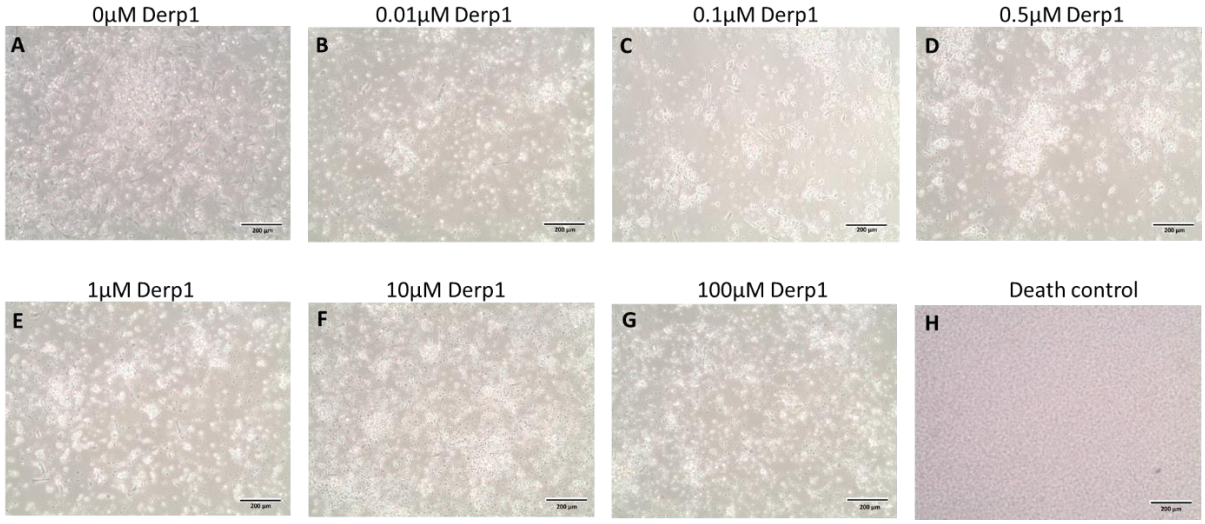

Figure 3.23 Mo-DC morphology after 24-hour stimulation with increasing concentrations of Derp1. Untreated Mo-DC (A) following 7 days of differentiation were stimulated with 0.01 μM (B), 0.1 μM (C), 0.5 μM (D), 1 μM (E), 10 μM (F), and 100 μM Derp1 (G), and compared to a non-viable control (H), for 24 hours. Images are representative of multiple isolations. Scale bar = 200 μm.

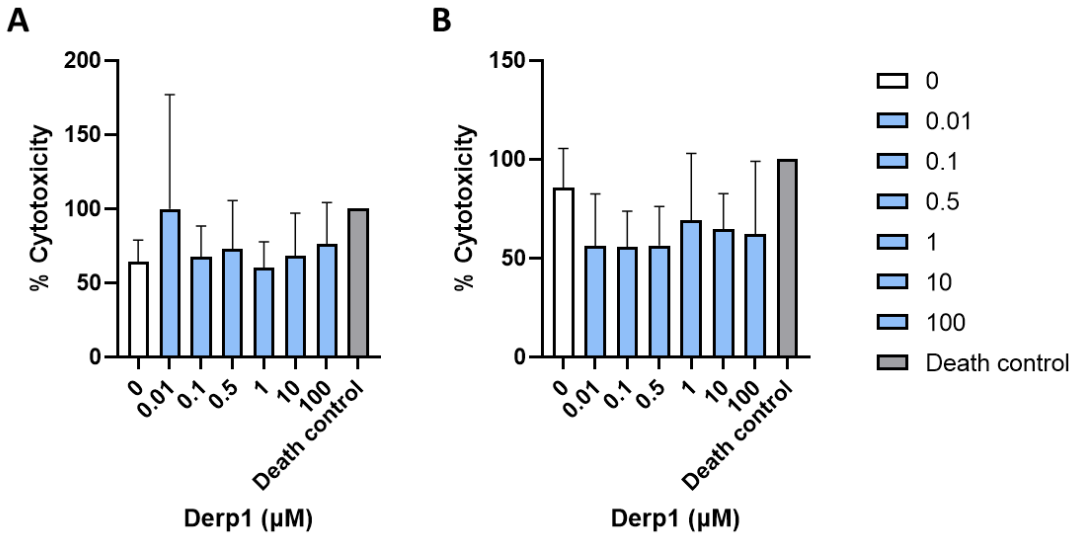

Figure 3.24 Cytotoxicity in Mo-DC after stimulation with different concentrations of Derp1.
Mo-DC (white) following 7 days of differentiation were stimulated with different concentrations of Derp1 (light blue), and compared to untreated and death controls (grey), for 4 hours and 24 hours. Data are presented as mean ± SD of n=4 independent experiments with statistical significance determined using one-way ANOVA.

Alterations in gene expression were measured after 4-hours treatment and compared to untreated controls. Increased gene expression was observed for *CCL17*, *CCL22* and *TNF*α for 0.01 μM, 0.1 μM and 1 μM Derp1, and although other increases were observed for other genes these were not statistically significant due to variable responses between donors (Figure 3.25). *IL-1*α upregulation in the untreated control was statistically significant (F (3,8) = 57.31, p<0.001). This could be because Mo-DC might not be responding to those concentrations of Derp1 or a longer exposure might be required.

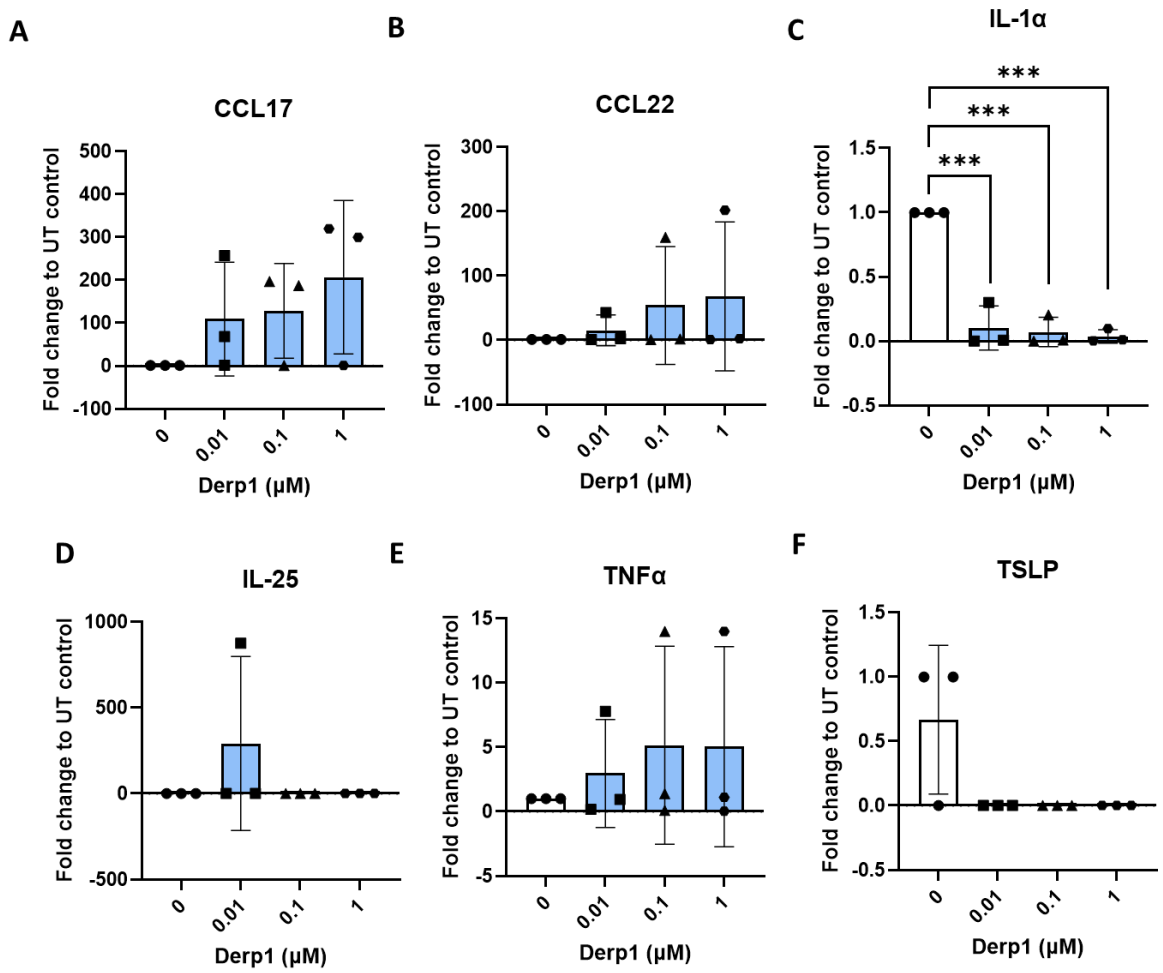

Figure 3.25 Gene expression of Mo-DC upon stimulation with Derp1 for 4 hours.
Mo-DC (white) following 7 days of differentiation were stimulated with different 0.01 μM, 0.1 μM or 1 μM of Derp1 (light blue) for 4 hours. Gene expression of *CCL17* (A), *CCL22* (B), *IL-1α* (C), *IL-25* (D), *TNFα* (E) and *TSLP* (F) were analysed by RT-qPCR, and expression calculated relative to the untreated control. Data are presented as mean ± SD of n=3 independent experiments with statistical significance determined using one-way ANOVA followed by Tukey post hoc test; ***p<0.001.

3.3.4 Interaction between Mo-DC and naïve CD4+ T cells

Naïve CD4+ T cells recognise antigens when this is presented by an APC such as DCs. During AD, naïve CD4+ T cells are stimulated upon antigen recognition to differentiate into a T_H2 phenotype by secreting cytokines such as IL-13 or IL-31. Naïve CD4+ T cells and Mo-DC were therefore cultured alone in RPMI, in a 2D monolayer, during 7 days to serve as controls. After this period, Mo-DC were either cultured in RPMI, RPMI containing 15 ng/mL of TSLP, or RPMI containing 15 ng/mL of TSLP and 0.01 μM DNCB for 48 hours. After 2 days of culture, naïve CD4+ T cells were added to the Mo-DC for 6 days and re-stimulated with CD3/CD28 for 24-hours. Firstly, morphology was assessed after 14 days of total culture. Naïve CD4+ T cells (Figure 3.26A) and Mo-DC (Figure 3.26B, C&D) alone seem to behave

similarly after stimulation with TSLP and TSLP+DNCB. When co-culturing Mo-DC with naïve CD4+ T cells (Figure 3.26E, F&G), both populations seem to be interacting when stimulating with TSLP and TSLP+DNCB as the T cells seemed to be attach to the Mo-DC.

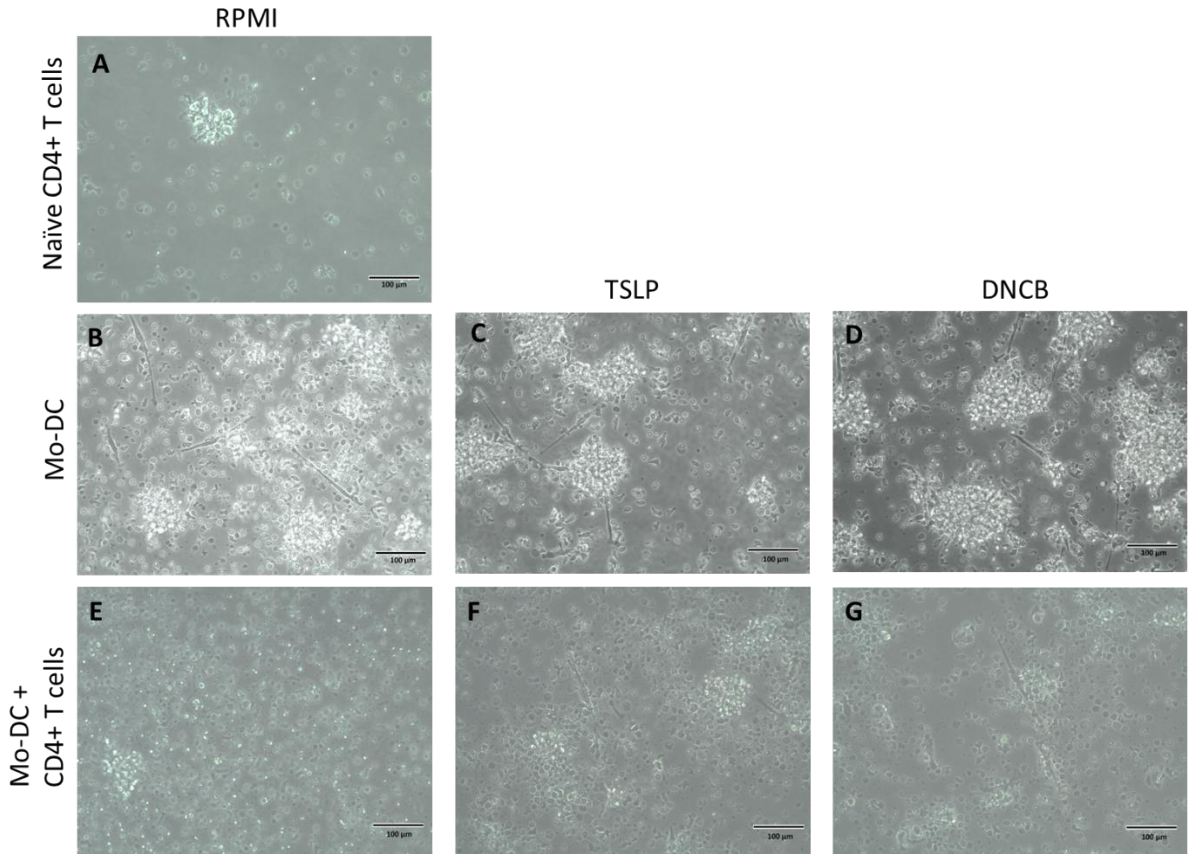

Figure 3.26 Morphology of naïve CD4+ T cells, Mo-DC and Mo-DC + CD4+ T cells co-culture.
Naïve CD4+ T cells cultured in RPMI (A); Mo-DC cultured in RPMI (B), RPMI with 15 ng/mL of TSLP (C), and RPMI with 15 ng/mL of TSLP + 0.01 μM DNCB (D); and Mo-DC co-cultured with naïve CD4+ T cells in RPMI (E), Mo-DC co-cultured with naïve CD4+ T cells with 15 ng/mL of TSLP (F), and Mo-DC co-cultured with naïve CD4+ T cells with 15 ng/mL of TSLP + 0.01 μM DNCB (G); and cultured for 14 days. Images are representative of n=3. Scale bar = 100 μm.

Alterations in gene expression (Figure 3.27) were measured after 14 days of culture for the three cell types (naïve CD4+ T cells, Mo-DC, and Mo-DC + CD4+ T cells co-culture) and the three conditions (RPMI, RPMI with 15 ng/mL of TSLP, or RPMI with 15 ng/mL of TSLP + 0.01 μM DNCB). Increased gene expression was observed for *CCL17*, *CCL22* and *IL-13* for Mo-DC and the co-culture (F (2, 18) = 4.982, p=0.019) for *IL-13* (p=0.041). On the other hand, *IL-1*α seem to be similarly expressed in all cell types, and *TNF*α is upregulated in naïve CD4+ T cells.

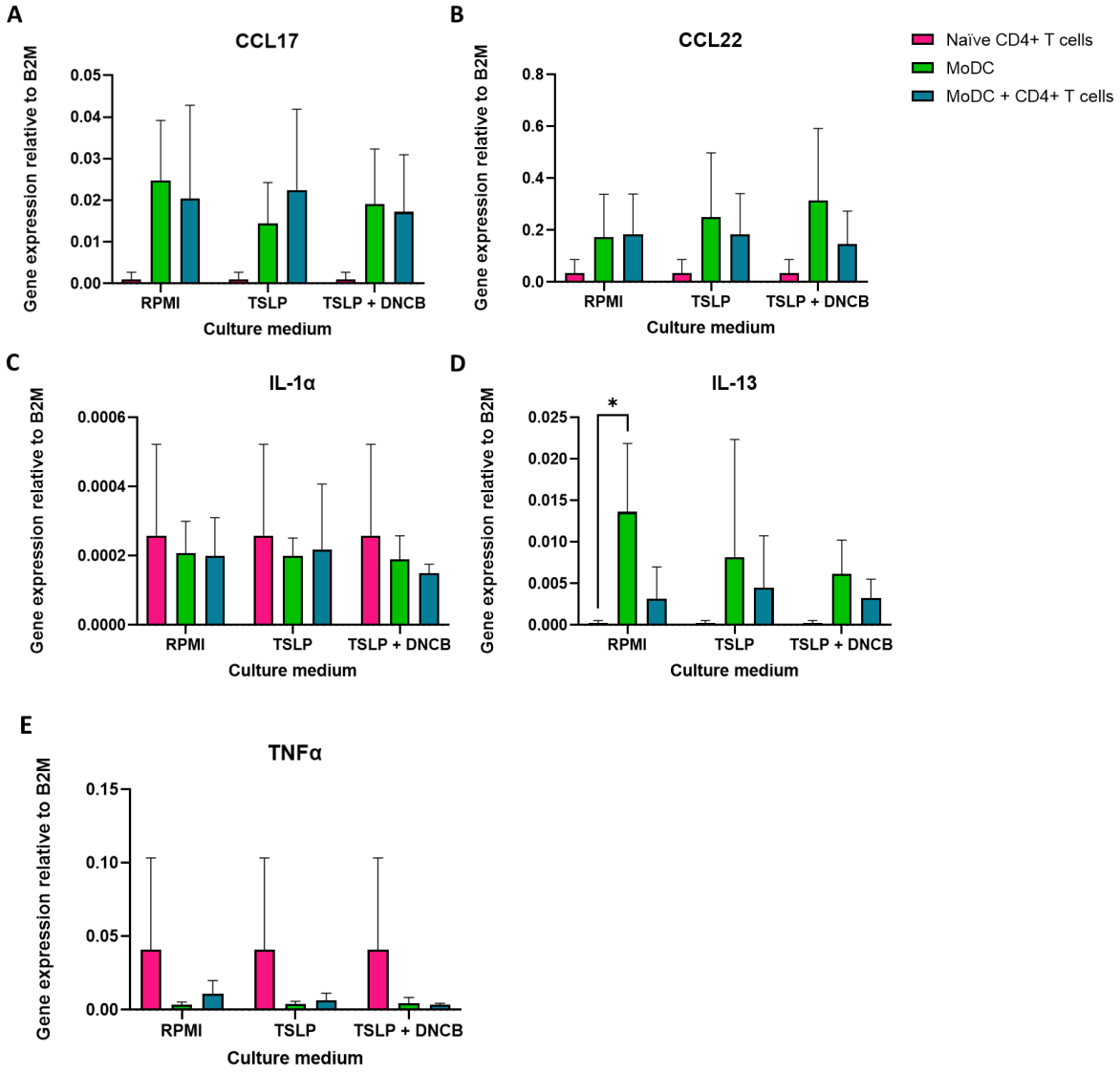

Figure 3.27 Gene expression of naïve CD4+ T cells, Mo-DC and Mo-DC + CD4+ T cells co-culture. Naïve CD4+ T cells (pink); Mo-DC (green) and Mo-DC co-cultured with naïve CD4+ T cells (blue) were cultured for 14 days in either RPMI, RPMI with 15 ng/mL of TSLP, or RPMI with 15 ng/mL of TSLP + 0.01 μM DNCB. Gene expression of *CCL17* (A), *CCL22* (B), *IL-1α* (C), *IL-13* (D), and *TNFα* (E) were analysed by RT-qPCR, and expression calculated relative to the untreated control. Data are presented as mean ± SD of n=3 independent experiments with statistical significance determined using two-way ANOVA followed by Tukey post hoc test; *p<0.05.

For cell surface protein abundance for CCR4, CD11c, CD154, CD4 and HLA-DR (Figure 3.28), no differences were observed between naïve CD4+ T cells, Mo-DC and the co-culture. This could be because when they are in 2D culture in isolation, they have already reached a very high peak of surface protein abundance expression, or that the TSLP and DNCB concentrations used in the experiment are not enough to induce an immune response and a T_H2 phenotype.

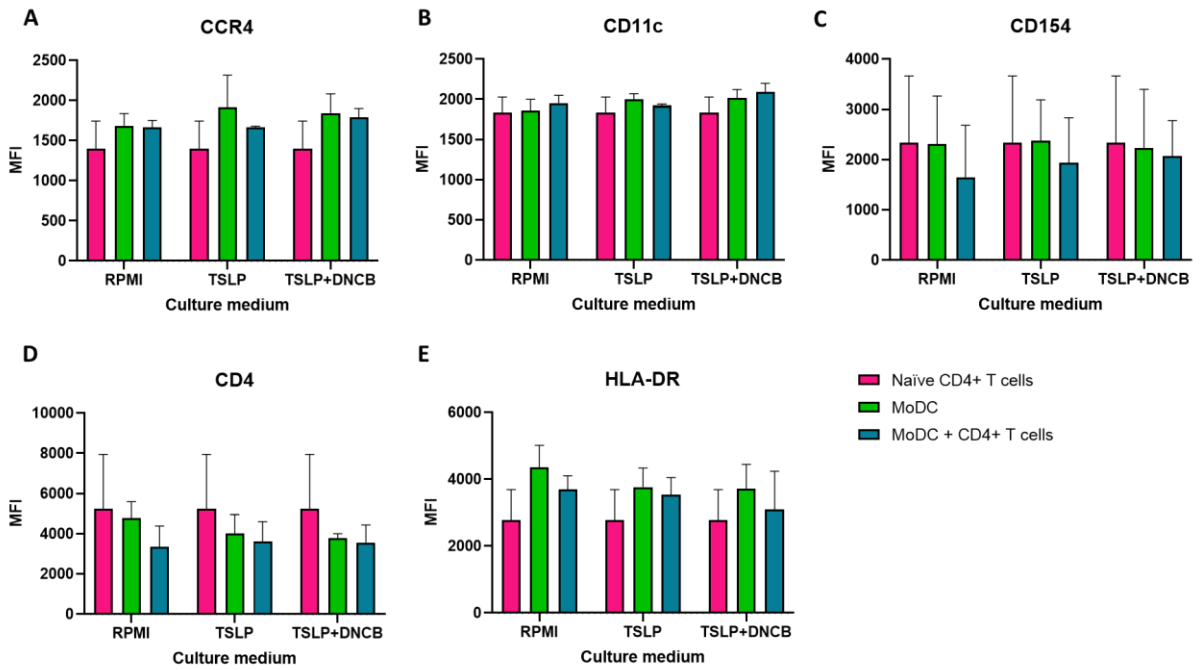

Figure 3.28 Cell surface protein abundance of naïve CD4+ T cells, Mo-DC and Mo-DC + CD4+ T cells co-culture.

Naïve CD4+ T cells (pink); Mo-DC (green) and Mo-DC co-cultured with naïve CD4+ T cells (blue) were cultured for 14 days in either RPMI, RPMI with 15 ng/mL of TSLP, or RPMI with 15 ng/mL of TSLP + 0.01 μM DNCB. Abundance of CCR4 (A), CD11c (B), CD154 (C), CD4 (D) and HLA-DR (E) were measured by flow cytometry. Data are presented as mean ± SD MFI of n=3 independent experiments with statistical significance determined using two-way ANOVA.

3.4 Discussion

3.4.1 Generating monocyte-derived immune cells

Mononuclear cells isolated from peripheral blood or buffy coats have been used for many years to generate multiple immune cell phenotypes. Monocytes isolated from buffy coats can be differentiated into macrophages and dendritic cells (Coillard & Segura, 2019) while lymphocytes can be used as a source of naïve T cells (Raulf, 2019) that can then be polarised into different subtypes, in the work presented here into T_H2 cells (Maier et al., 2014). Due to their abundance in peripheral blood, mononuclear cells are desired as an immunological source, and they can be collected in large quantities. Blood monocytes can be subdivided into three major populations: classical (CD4+CD16-), non-classical (CD14-CD16+), and intermediate (CD14+CD16+), depending on the expression of distinct surface markers and on their functions in homeostasis and disease (Kapellos et al., 2019). In this chapter, monocytes were used to generate MDM, Mo-DC, Mo-LC, *in vitro* differentiated cells that have been shown to closely mimic their *in vivo* counterparts in previous studies (Murdoch et al., 2007; Y. Otsuka et al., 2018; Tang-Huau et al., 2018).

Monocytes were differentiated into MDM by culture adhesion to tissue culture plastic (Eligini et al., 2013), which were used as controls in the experiments. Isolating DCs from human tissue is challenging and a high number of cells is needed for the development of *in vitro* models, therefore, it was decided to generate Mo-DC from monocytes. According to previous studies, culturing monocytes with GM-CSF and IL-4 cytokines generates a Mo-DC phenotype. Collin *et al.* (2018) argue that Mo-DC are only found during inflammation and that they present only an inflammatory DC phenotype. LCs constitute about 2% of cells in the oral epithelium (Bauer et al., 2001), therefore, isolating these cells from human tissue for *in vitro* experiments would be extremely challenging due to access of enough human tissue to acquire the numbers required for *in vitro* experiments. Consequently, Mo-LC were differentiated from monocytes by further addition of TGF-β to the Mo-DC culture medium (Geissmann et al., 1998; Peiser et al., 2004).

Naïve CD4+ T cells were isolated from buffy coat mononuclear cells by negative selection (Raulf, 2019) and polarised into T_H2 cells by stimulation with anti-CD3 and anti-CD28, and in the presence of IL-2 and IL-4, and anti-IFNγ (Zhu et al., 2010).

3.4.2 Characterisation of immune cell types following isolation form mononuclear cells

Mononuclear cells from buffy coats were used as a source of both CD4+ T cells and to generate MDM, Mo-DC and Mo-LC. Initially, the morphology of these immune cell types was analysed. Mononuclear cells were spherical, dark in appearance, and with no defined nuclei as described in previous publications (Pickl et al., 1996). Once isolated, naïve CD4+ T cells presented as small spherical cells that clustered in small islands after 24 hours in culture as previously described for other isolated primary CD4+ T cells (Friedman et al., 2010; Lin et al., 2015; M. J. Miller et al., 2004). In addition, naïve CD4+ T cells purity and viability was studied by flow cytometry using CD4 as naïve CD4+ T cell marker and propidium iodide as a cell viability marker, resulting in nearly 90% of live cells from which about 86% were CD4+. MDM displayed a mixed phenotype containing some elongated cells and spherical cells with dark nuclei (Lendeckel et al., 2022); Mo-DC presented visible dendrites (Grassi et al., 1998; Marzaioli et al., 2020), while Mo-LC had a similar appearance to Mo-DC but lacked dendrites (Geissmann et al., 1998). Thus, all cells isolated in this chapter displayed similar morphological characteristics to previous publications using these cells.

To further characterise these cell types, confirmation of the presence of specific marker genes or proteins must be performed by qPCR and in this case flow cytometry for cell surface markers. The combination of these techniques allows the study of a wide variety of markers at gene and protein level.

3.4.2.1 Expression of T_H2 cells markers

Previous research suggests that T_H2 cells can be identified by the specific pattern of genes they transcribe and proteins they display on their cell surface that distinguishes them from other T cell subtypes (Loyet et al., 2005). As far as gene transcription of secreted proteins are concerned, these are *IL-4*, *IL-5* and *IL-13*. *IL-4*, *IL-5* and *IL-13*, together with other interleukins form a cytokine gene cluster. *IL-4* gene encodes a pleiotropic cytokine that is secreted by activated T cells and is a ligand for IL-4 receptor, which can also bind IL-13. *IL-4* is involved in tissue repair and promotes inflammation, *IL-13* drives B cell maturation and differentiation, while *IL-5* encodes a cytokine that promotes the proliferation and differentiation of eosinophils and B cells. These 3 cytokines are important mediators of T_H2-associated inflammation such as those found in AD (Bitton et al., 2020; Dubin et al., 2021), some forms of hypersensitivity reactions (Kabesch et al., 2007) and asthma (Heeb et al., 2020; Heinzmann, 2000; Junttila, 2018). In this study, *IL-4* and *IL-13* showed marked increases in T_H2 cells compared to naïve CD4+ T cells at gene expression. *IL-4* gene transcription is induced after ligation of

the TCR of T_H2 cells (Li-Weber & Krammer, 2003). *IL-13* and *IL-5* are also expressed by T_H2 cells that are highly polarised (Bao & Reinhardt, 2015; Ikutani et al., 2012), confirming the acquisition of a T_H2 phenotype by these cells following culture.

IL-6 gene encodes a pleiotropic cytokine that is involved in the regulation of the immune system, inflammation, haematopoiesis and oncogenesis and can be expressed in T cells, B cells and macrophages amongst other cells (Wongchana & Palaga, 2012). Production by T_H2 regulates T_H17 differentiation (O'Brien, 2011). Uncontrolled levels of *IL-6* are related with autoimmunity and chronic inflammatory disorders (T. Tanaka et al., 2014). Like *IL-6*, *TSLP* (thymic stromal lymphopoietin) is also a pleiotropic cytokine that can be expressed by activated keratinocytes, fibroblasts, lung and intestinal epithelial cells, but also by DCs and mast cells. *TSLP* is involved in allergic diseases, chronic inflammation and autoimmune disorders (Corren & Ziegler, 2019; Varricchi et al., 2018). *TSLP* was not significantly increased by T_H2 cells, however, it has been shown to promote the differentiation of naïve T cells into T_H2 cells (Jang et al., 2013). This lack of expression from T_H2 cells could be due to a naïve CD4+ T cells / T_H2 cells mix population as not all the cells might have polarised into a T_H2 phenotype.

A continuous theme running through much of the data in this chapter is the variation in data. Indeed, data was markedly different between buffy coats. This is in line with the literature and is because the immune system is very different between individuals (Brodin & Davis, 2017). This is a very common problem when using primary cells compared to cell lines, which are homogeneous and therefore prone to much less experimental variation. This variation does cause issues with statistical significance testing, and to overcome this would require many more experimental repeats with additional donor batches that is often not economically possible or time permitting.

For protein characterisation, this study used the cell surface receptors CCR3, CCR4, CD119 and CD154 as these have been shown to be increased on the surface of T_H2 cells. CCR3 is the receptor for chemokines CCL11 and CCL24 (Kuse et al., 2017) that act as chemoattractant to facilitate migration of CCR3+ cells to sites of allergic disease (Beck et al., 2006). The receptor is highly expressed on T_H2 cells as well as basophiles and eosinophils (Holse et al., 2006; Oettgen & Broide, 2012). CCR4 is the receptor for CCL17 and CCL22 and is expressed in T_H2 cells, T_H17 cells, Tregs, macrophages and DCs. Specifically, in DCs, T_H2 and T_H17 cells, CCR4 and its ligands have been implicated in the pathology of allergic skin disorder such as AD (Pease, 2007; Sato et al., 2018). *CD119* (Interferon Gamma Receptor 1, IFNGR1) encodes the ligand-binding chain (alpha) of the gamma interferon receptor, and it is expressed in both T_H1 and T_H2 cells (Griffin, 2008; Tau et al., 2000). CD154 (CD40 ligand) is a type II transmembrane cytokine that belongs to the TNFα family (Fähnrich et al., 2018). It is involved in the regulation of the function of B cells by interacting with CD40 on the B cell surface during antigen presentation. CD154

is therefore a marker for antigen-specific T helper cells and it is mainly expressed by T_H1 and T_H2 cells (Kirchhoff et al., 2007). At protein level, significant increases in cell surface abundance were observed for CCR4, CD119, CD154 in T_H2 cells compared to naïve CD4+ T cells. This is in line with previous studies, where these receptors were showed to have high expression on T_H2 cells (Anderson et al., 2020; Del Zotto et al., 2021; Möller et al., 2011).

Therefore, naive CD4+ T cells can be isolated using negative selection and polarised into T_H2 cells by stimulation with anti-CD3 and anti-CD28, and in the presence of IL-2 and IL-4, and anti-IFNγ.

3.4.2.2 Expression of Mo-DC and Mo-LC markers

CD1a gene encodes for a member of the CD1 family of transmembrane glycoproteins that are related to the MHC proteins. It has an important role in antigen presentation and it is expressed on antigen presenting cells and thymocytes (Kaczmarek et al., 2017). No statistically significant differences were observed between MDM, Mo-DC and Mo-LC at gene or protein level. *CD1a* expression has been previously shown to be elevated in DC but both macrophages and DCs express gene transcripts (Al-Amodi et al., 2018; Cernadas et al., 2009), and the large variation in expression data could explain why no differences were observed.

CD11c (ITGAX) is a transmembrane protein that, together with CD18, forms the complement receptor CR4, which is involved in actin-linked functions such as migration or adhesion (Nagy-Baló et al., 2020). Although increased in DC, no significant differences were observed between MDM and Mo-DC, and the different cytokine doses used to differentiate Mo-DC, at protein level. This is likely due to the fact that this marker is expressed in both MDM and Mo-DC cell types (Lukácsi et al., 2020).

CD14 encodes a transmembrane receptor which, in association with toll-like receptors, recognises bacterial LPS and other pathogen-associated molecular patterns. *CD14* is present in cells of hematopoietic and non-hematopoietic origin (Zanoni & Granucci, 2013), including monocytes. *CD14* expression is gradually lost when culturing monocytes with GM-CSF and IL-4 as they differentiate to Mo-DC (Krakow et al., 2019), which is in line with the results obtained in this chapter.

CD207 (Langerin) is a surface receptor of the C-type lectin receptor family that is usually present on LCs from skin and oral mucosa, although is also expressed in subpopulations of dendritic cells (Idoyaga et al., 2008), where it participates in both innate and adaptive immune responses (Romani et al., 2010). Although increased at the transcription level in Mo-DC, no statistically significant changes were observed between this cell type and MDM or Mo-LC at gene or protein level. Mo-LC were first described by Geissmann (Geissmann et al., 1998), who used E-cadherin as the LC marker, as this study

was conducted before the discovery of CD207 (Valladeau et al., 2000). Surprisingly, *CD207* has not been previously used as a marker for Mo-LC even though it encodes Langerin. Indeed, *CD207* was detected at very low levels at the transcription level but cell surface abundance was similar to both MDM and Mo-DC.

CD80 and CD86 are membrane proteins that are needed to interact with CD28 and CTLA-4 for the co-stimulation of CD4+ and CD8+ T cells resulting in T cell activation, proliferation and differentiation (Halliday et al., 2020). CD80 and CD86 are expressed in multiple immune cells, including monocytes (Fleischer et al., 1996), macrophages (Foss et al., 1999) and DCs (Ke et al., 2016). No significant changes were observed between MDM and Mo-DC, and the different cytokine doses used to differentiate Mo-DC, for gene expression. Protein abundance of CD80 and CD86 has been shown to increase in immature Mo-DC compared to MDM (Ancuta et al., 2000), so it could be that this increase was not seen at gene level.

HLA-DR is MHC class II cell surface receptor and it is found on antigen-presenting cells such as DCs, LCs, monocytes and macrophages (Pinet et al., 1995). In this study, levels of MHC II were increased on Mo-DC compared to MDM at all the different cytokine doses used. Previous research has demonstrated high levels of HLA-DR between MDM and Mo-DC (Ancuta et al., 2000), and a project looking at the impact of IL-4 concentrations on HLA-DR protein abundance in Mo-DC saw a dose-dependent increment, suggesting that IL-4 regulates HLA-DR expression (te Velde et al., 1988). Such a dose-dependent increase in HLA-DR was not observed in this study. Overall, no single marker was able to sufficiently differentiate between MDM, Mo-DC and Mo-LC and this may not be entirely surprising since these cells originally descended from the same monocyte parent cell population.

In addition, MDM, Mo-DC and Mo-LC were stimulated with LPS isolated from *E. coli*. Overall, no significant changes were observed when analysing CD1a, CD207 and CD80 at gene or protein level. In agreement to this, Cernadas *et al*. (2009) did not see any effect on CD1a when stimulating DC with LPS. A previous study reported that addition of LPS and CD40 ligand to the culture of these cells caused increased expression in CD80, however, such an increase was not apparent in the absence of CD40 ligand (Sinistro et al., 2007) in either MDM or Mo-DC, which is in line with the results of this study.

In summary, although no markers were enough to differentiate between MDM, Mo-DC and Mo-LC, morphology indicates differences between these subtypes, and GM-CSF and IL-4 can therefore be used to differentiate monocytes into DC/LC phenotype.

3.4.3 Allergen challenge in Mo-DC

CCL17 and CCL22 are chemokines that bind to CCR4 and present chemotactic activity for T cells, specially T_H2 cells. CCL17 is secreted by dendritic cells and it is involved in T cell activation, while CCL22 regulates T_H2 cells circulation into allergic sites of inflammation (Hirota et al., 2011; Y. Zhang et al., 2022).

IL-1 family, which mediates the acute phase in inflammation, comprises 11 interleukins (IL). Among them, IL-1α, IL-1β, IL-18, IL-33, and IL-36 are receptor-antagonistic. IL-1α and IL-1β bind to the same IL receptors and are involved in the same processes, however, they are found in different locations within the cells. They are both secreted by DC in response to an appropriate stimulant. IL-1α is mainly membrane-associated and mainly has homeostatic actions. In contrast, IL-1β participates in inflammation (Ainscough et al., 2014; Kaneko et al., 2019; Voronov, 2013). IL-18 (IFNγ-inducing factor) regulates T_H1 response by regulating IFNγ levels and it is highly expressed by T cells, DC and endothelial cells. IL-18 induces IFNγ production by NK cells, and increased expression of *IL-18* has been seen in some autoimmune disorders such as lupus or psoriasis (Kaneko et al., 2019; Tucci et al., 2007). IL-33 can act as a nuclear factor mediating gene transcription and as a cytokine. IL-33 is involved in the stimulation of T_H2 immune response and activates the innate immune system, participating in inflammatory skin diseases such as AD (A. M. Miller, 2011).

IL-25 (IL-17E) is a member of the IL-17 family. It is present in the immune response and inflammatory disorders, being involved as a cytokine that induces the secretion of IL-4, IL-5 and IL-13 by T_H2 whilst inhibiting the differentiation of T_H17 cells (Deng et al., 2021). It is therefore high expressed in T_H2 cells and DCs (Borowczyk et al., 2021). TNFα is another multifunctional pro-inflammatory cytokine involved in cell survival, proliferation, differentiation and apoptosis (Deng et al., 2021). It is involved in autoimmune disorders, bone remodelling, and some inflammatory disorders (Bradley, 2008). It is expressed by activated monocytes and macrophages, T cells and fibroblasts, among other cells (Sedger & McDermott, 2014). In contrast, IL-10 is a cytokine that is usually involved in immunoregulation and inflammation, and down-regulates the expression of T_H1 cytokines, playing an important role in allergy and asthma (Kubo et al., 2017; Yao et al., 2013). It is expressed mainly in monocytes and lymphocytes, but it is also by DC and B cells.

Mo-DC were stimulated with increasing non-toxic doses of DNCB, a chemical reagent that is commonly used in AD research as it induces chronic contact dermatitis (Fujii et al., 2009), and when topically administered to mice it produces an AD-like phenotype (Inagaki et al., 2006). However, few studies in human primary cells have been performed. Clear changes were observed in the number of dead cells as DNCB concentrations increase during 24 hours, however, these changes were not observed at 4

hours, most probably due to a short time exposure. When analysing the LDH release data, no significant changes in % cytotoxicity were observed. This could be due to the presence of foetal calf serum, as it has extremely high background readings (Aslantürk, 2018). Therefore, although DNCB may stimulate Mo-DC, other cytotoxicity tests should carried out in order to better understand this.

At gene level, expression of *CCL17, CCL22, IL-1α, IL-1β, IL-18, IL-25, IL-33, TNFα* and *TSLP* were increased in one or more of the Mo-DC samples tested, however, there was marked donor variability making it difficult to form any conclusions. Previously, CCL17 and CCL22 were upregulated in DNCB induced mice models when compared to the untreated control (Min et al., 2022). Yao *et al*., showed that levels of IL-1β were decreased in DNCB-induced Mo-DC (Yao et al., 2013). Popov *et al*., showed higher expression of IL-10 in rat models after stimulation with DNCB for 3 days (A. Popov et al., 2011), which suggests that a longer exposure with DNCB could lead onto higher expression of this cytokine. However, studies in mice saw a decreased of IL-10 in blood of DNCB-induced mice (Cumberbatch et al., 2005; Ku et al., 2018). Increase expression of IL-33 and TSLP but no difference in IL-25 was observed in cutaneous samples of mice treated with DNCB (Jang et al., 2020). IL-18 is highly expressed in human keratinocytes after stimulation with DNCB (Galbiati et al., 2014; Toebak et al., 2009), but no studies with Mo-DC have been previously performed. *TNFα* was expressed at gene level in Mo-DC after adding 30 µM of DNCB, however this was not the case at protein level (Ohtani et al., 2009). Data suggests a possible stimulation of Mo-DC of Mo-DC after 4 hours treatment, however, no significant changes were observed. This could be due to donor variability or a long exposure time for gene expression analysis. To form any conclusion, gene expression should be also studied at shorter exposure times such as 30 minutes or 1 hour.

Mo-DC were also stimulated with increasing non-toxic doses of Derp1, a protease and allergen present in house dust mite to which patients with allergic disorders such as AD are sensitised to (J. Kim et al., 2013), and when applied directly onto the surface of mice skin, it produces an AD-like phenotype and a T_H2 immune response (Stremnitzer et al., 2014). However, a small number of studies have been done in human skin and human primary cells. At gene level, expression of *CCL17*, *CCL22*, *IL-25*, *TNFα* and *TSLP* were increased in one or more of the Mo-DC samples tested, however, there was marked donor variability making it difficult to form any conclusions. Conversely, *IL-1α* and *TSLP* expression were increased in the untreated control. Previous researches have shown high release of CCL17, IL-25 and TSLP in mice treated with Derp1, however, CCL17 release was not statistically significant when compared to the untreated control (Gregory et al., 2013; Hesse et al., 2018). In addition, increase in IL-1β and TNFα release in Mo-DC isolated from patients that are sensitised to HDM has been shown in previous research, compared to those patients who are not (Hammad et al., 2003). To further study the effect of Derp1 on immune cells, blood from healthy and allergic patients should be extracted to

isolate and stimulate Mo-DC from mononuclear cells. In this case, the lack of changes in gene expression could be due to several factors: low Derp1 dose, short exposure to the allergen, and missing a positive control for the house dust mite allergy.

In order to induce antigen presentation between Mo-DC and naïve CD4+ T cells and therefore induce differentiation of naïve CD4+ T cells into T_H2 cells, Mo-DC were co-cultured with naïve CD4+ T cells. This co-culture was stimulated with TSLP, and with TSLP together with DNCB, as TSLP has been shown as an effective factor to induce antigen presentation (Ebner et al., 2007; Soumelis et al., 2002). Very little changes between Mo-DC and the co-culture with Mo-DC and naïve CD4+ T cells were observed when stimulating with TSLP, although these changes were higher for gene expression when compared to naïve CD4+ T cells. It was expected a higher gene expression and cell surface protein abundance when co-culturing Mo-DC with naïve CD4+ T cells after stimulating with TSLP and TSLP+DNCB as they are supposed to induce differentiation of naïve CD4+ T cells into T_H2 cells, and therefore, possible induce an inflammatory response.

Taken together these data suggest DNCB, Derp1 and TSLP may stimulate Mo-DC to secrete factors that will influence T_H2 cell responses at sites of AD although additional experiments are required from many more donor samples in order to draw firm conclusions. To control this further, knowing whether the participant has any type of allergy would be useful. In addition, as cells in 2D monolayer change morphology, allergen study should be ideally done in a 3D microenvironment.

3.5 Conclusion

In this chapter, naïve CD4+ T cells were successfully isolated from mononuclear cells and polarised into T_H2 cells, while monocytes were successfully differentiated to MDM and Mo-DC but not Mo-LC phenotypes. Both T_H2 and Mo-DC were fully characterised in terms of appropriate marker expression and both T_H2 and Mo-DC produced factors that are known to be influential in the response to challenge with different allergens and in the pathogenesis of AD. Furthermore, T_H2 cells will have to be expanded and Mo-DC will have to be washed more to get a more pure population for the inclusion in human skin models. These are key factors that will be instrumental in the development of an AD-like tissue engineered skin model in the following chapters.

Chapter 4 - Development of three-dimensional human skin equivalents and response of keratinocytes to allergens.

4.1 Introduction

In the previous chapter, mononuclear leukocytes were isolated and differentiated into either monocyte-derived DC or polarised T cells. However, these are not the only cell types involved in the pathogenesis of AD. Keratinocytes are the most abundant cell type in human skin and are crucial in forming the skin's permeability barrier. Keratinocytes secrete cytokines, chemokines and growth factors, among other effector molecules, that are involved in the recruitment of inflammatory cells. Therefore, changes in keratinocyte activities as well as leukocytes are involved in the pathogenesis of AD (Chieosilapatham et al., 2021).

To further investigate the immunopathology of AD, the overall goal of incorporating these cells into a tissue engineered immunocompetent skin model was established. This chapter sought to optimise the development of HSE prior to the incorporation of immune cells.

HSE have been widely used to study the skin as two-dimensional skin cell cultures do not represent the structure and functions of the skin, such as barrier function, cell differentiation or skin immunology (Klicks et al., 2017). HSE can be in the form of a reconstructed human epidermis (RHE), where keratinocytes are seeded onto tissue culture inserts and grown to form a stratified squamous epithelium to mimic the epidermis. Several companies have developed RHE to mainly test for skin irritation and corrosion (Dijkhoff et al., 2021). RHE have been generated by multiple research groups, allowing them to compare different types and sources of keratinocytes, change of culture medium and test novel compounds or pathogens. The drawback with RHE is that they do not contain a connective tissue component and there is substantial evidence that paracrine signalling from dermal fibroblasts is important not only in the development of a stratified epidermis but also in basement membrane formation and innate immune responses. Therefore, several research groups have developed full thickness HSE that are composed of a dermal-fibroblast populated connective tissue topped by a stratified epidermis (Harding et al., 2021; van Drongelen, Danso, et al., 2014). These HSE have been used in multiple studies to investigate, amongst others, infection (L. Popov et al., 2014; Zoio et al., 2021), wound healing (Reijnders et al., 2015; Sierra-Sánchez et al., 2021), cancer (Commandeur et al., 2012; Mohapatra et al., 2007), different skin disorders (Eckl et al., 2011; Engelhart et al., 2005), for drug development and drug testing (Engelhart et al., 2005; Mohapatra et al., 2007), and in the cosmetic industry (Harding et al., 2021). Other researchers do not use exogenous ECM derivatives such as collagen or fibronectin, but they apply synthetic polymers like polyesters or polystyrene, they use 3D bioprinting, or electrospinning (Randall et al., 2018; Roger et al., 2019; Z. Zhang & Michniak-Kohn, 2012)

The HSE are most commonly made from primary human cells isolated from human tissue. However, not all laboratories have access to human skin and, moreover, primary cells, once isolated, have a short-life span and suffer from donor-to-donor variation. This has led to some investigators using immortalised skin keratinocytes as alternatives (Bertrand-Vallery et al., 2010; Robertson et al., 2012; Smits et al., 2017; van Drongelen, Danso, et al., 2014).

In this chapter, N/TERT-immortalised human skin keratinocytes cultured in 2D were stimulated with different allergens and their response examined. In addition, both RHE and full thickness HSE that included both immortalised and primary human skin fibroblasts were generated and characterised.

Chapter aim: Investigate the response of N/TERT keratinocytes towards allergens. Optimise the construction of three-dimensional RHE and HSE.

Objectives:

- Test keratinocytes response upon challenge stimulation.
- Generate epithelial models to optimise keratinocyte density.
- Optimise and generate full thickness RHE and HSE.
- Characterise full thickness HSE.

4.2 Methods

Keratinocyte responses to allergen challenge (see section 2.3.1.11) was examined by LDH assay (see section 2.3.3) to measure cytotoxicity upon stimulation, RNA was extracted (see section 2.3.4), cDNA synthesised (see section 2.3.5) and RT-qPCR performed (see section 2.3.6) to determine gene expression.

Human primary dermal fibroblasts were isolated from human skin biopsies (see section 2.3.1.1). Human primary dermal fibroblasts, immortalised human epidermal keratinocytes (N/TERT-1 and N/TERT-2G) and immortalised human fibroblasts (BJ-5ta) were cultured until confluent (see section 2.3.1.2). Type I collagen was isolated from rat tails (see section 2.3.2.1) and used to coat tissue culture inserts to generate human RHE skin equivalents (see section 2.3.2.2) and to develop full thickness HSE (see section 2.3.2.3). HSE were harvested and fixed (see sections 2.3.2.5 and 2.3.2.5.1) to analyse

morphology and different components of the skin by H&E staining (see section 2.3.2.5.2) and immunohistochemistry (see section 2.3.2.5.3).

4.3 Results

4.3.1 Stimulation of N/TERT-2G immortalised human skin keratinocytes with allergens

4.3.1.1 2,4-Dinitrochlorobenzene (DNCB)

N/TERT-2G, cultured as monolayers, were treated with increasing concentrations of DNCB ranging from 0.001 μM to 1 μM, for 4- and 24-hours to assess cell viability and function. Medium alone and SDS-treated cells were used as negative and positive controls, respectively. Firstly, cell morphology was assessed after 4- and 24-hour stimulation by light microscopy. At 4 hours there was no marked change in the morphology of cells cultured with 0.001 and 0.01 μM DNCB compared to controls, although some cells cultured at higher DNCB concentrations were refractile. In contrast, SDS-treated positive controls showed complete loss of membrane integrity (Figure 4.1). However, by 24 hours cells had begun to lose cell-to-cell contacts and display evidence of cell stress with increasing DNCB concentrations (Figure 4.2). These visual data were confirmed upon LDH analysis whereby at 4 hours LDH levels were low and similar to untreated controls, whereas the SDS positive control displayed a large and statistically significant LDH release ($F(5, 12) = 2263$, $p<0.001$), confirming complete cell lysis (Figure 4.3A). SDS positive control released large LDH levels compared to the untreated control ($p<0.001$). In contrast, at 24 hours there was an overall dose-dependent increase in LDH levels and therefore loss of cell viability due to cytotoxicity, although there were marked experimental variation (Figure 4.3B). Significant increases were seen in LDH release following treatment with SDS compared to the untreated control ($F(5, 12) = 2542$, $p=0.086$). LDH release in SDS-treated was also significantly increased compared to the untreated control ($p=0.032$).

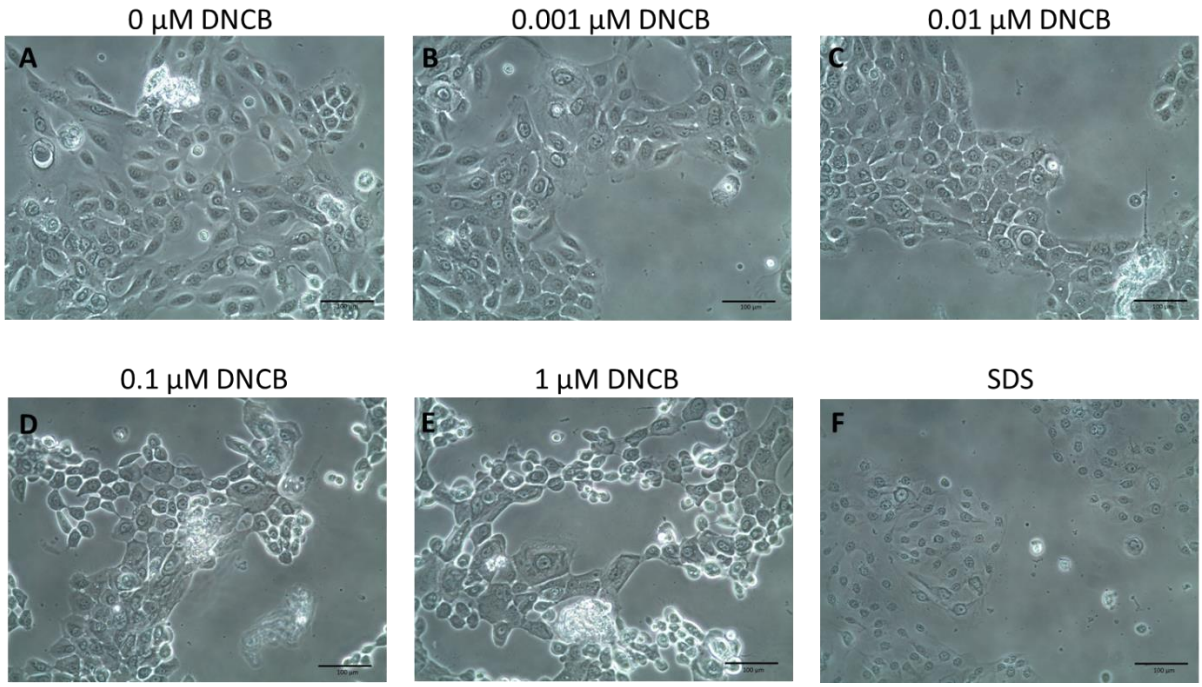

Figure 4.1 N/TERT-2G morphology after 4-hour stimulation with increasing concentrations of DNCB.
N/TERT-2G keratinocytes were cultured to 80% confluence then stimulated for 4 hours with (A) 0 (control), (B) 0.001 µM, (C) 0.01 µM, (D) 0.1 µM and (E) 1 µM DNCB, and compared to SDS-treated cells (death control) (F). Images are representative of n=3 experiments. Scale bar = 100 µm.

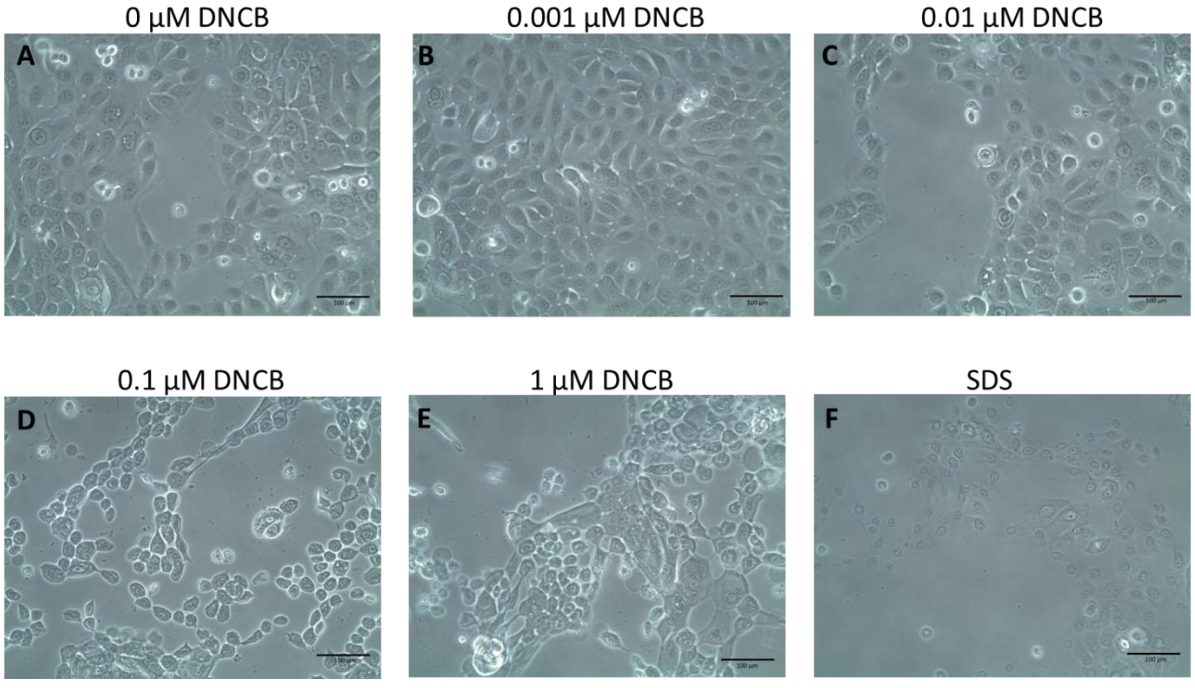

Figure 4.2 N/TERT-2G morphology after 24-hour stimulation with increasing concentrations of DNCB.
N/TERT-2G keratinocytes were cultured to 80% confluence then stimulated for 24 hours with (A) 0 (control), (B) 0.001 µM, (C) 0.01 µM, (D) 0.1 µM and (E) 1 µM DNCB, and compared to SDS-treated cells (death control) (F). Images are representative of n=3 experiments. Scale bar = 100 µm.

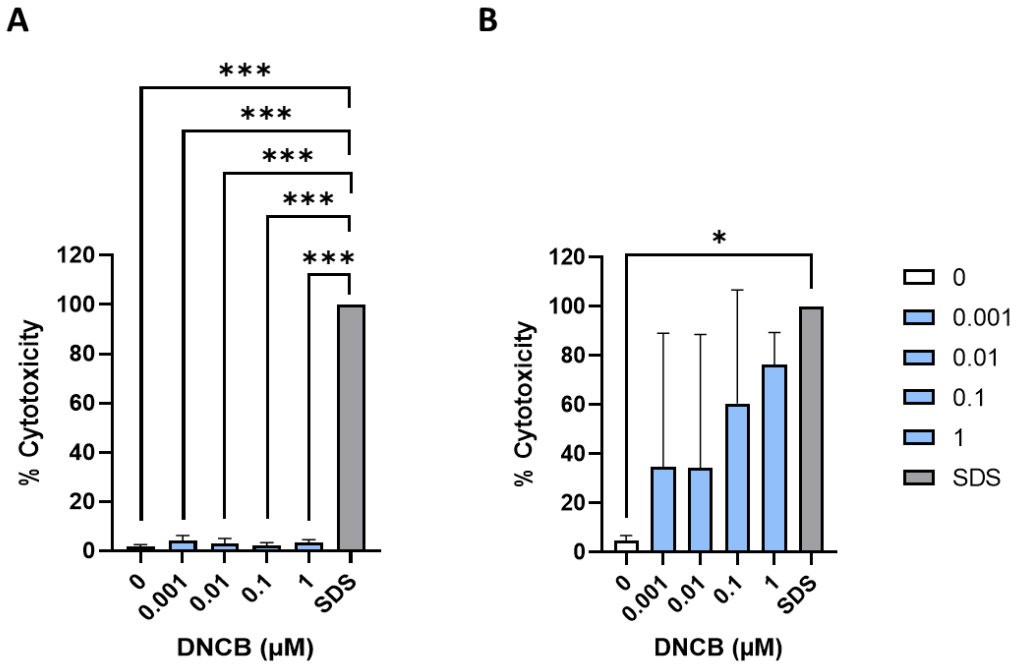

Figure 4.3 Cytotoxicity in N/TERT-2G keratinocytes after stimulation with increasing concentrations of DNCB.

N/TERT-2G keratinocytes were cultured to 80% confluence then stimulated with increasing concentrations of DNCB from 0 to 1 μM for (A) 4 hours and (B) 24 hours then levels of LDH released into the culture medium quantified. SDS-treated cells acted as positive controls. Data are presented as mean ± SD of n=3 independent experiments with statistical significance determined using one-way ANOVA followed by Dunnett's post hoc analysis; *p<0.05, ***p<0.001.

Alterations in N/TERT-2G gene expression were measured after 4 hours treatment with 0.001 and 0.01 μM DNCB (levels found to be non-toxic) and compared to untreated controls. Increased gene expression was observed for *IL-1α* and *TSLP* for 0.01 μM DNCB in one of the three experiments, so no overall significant differences were observed for these genes (Figure 4.4A-C). However, *CCL17* and *CCL22* gene expression was significantly down-regulated compared to the untreated control after 4 hours exposure to both 0.001 and 0.01 μM (Figure 4.4D&E)(F(2, 6) = 12.91, p=0.007), and for *CCL22* for 0.01 μM (p=0.005) and 0.1 μM DNCB (p=0.017) compared to untreated control.

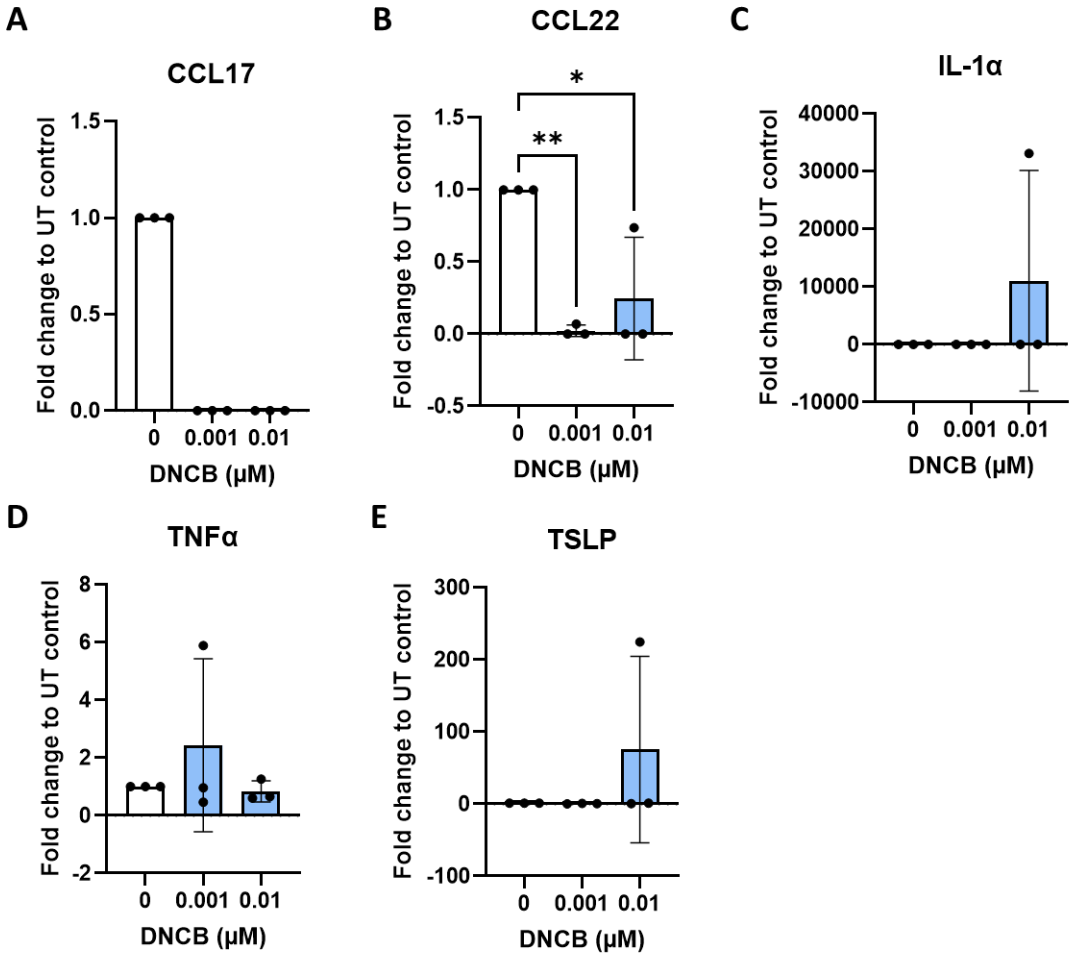

Figure 4.4 Gene expression of N/TERT-2G keratinocytes upon stimulation with DNCB for 4 hours. N/TERT-2G keratinocytes were cultured with 0 control (white), 0.001 µM or 0.01 µM DNCB (blue) for 4 hours and gene expression of *CCL17* (A), *CCL22* (B), *IL-1α* (C), *TNFα* (D) and *TSLP* (E) analysed by RT-qPCR. Gene expression was calculated relative to the untreated control. Data are presented as mean ± SD of n=3 independent experiments with statistical significance determined using one-way ANOVA followed by Dunnett's post hoc test; *p<0.05, **p<0.01.

4.3.1.2 Dermatophagoides pteronyssinus

N/TERT-2G were treated with increasing concentrations of Derp1 from *Dermatophagoides pteronyssinus* ranging from 0.01 µM to 100 µM, for 4- and 24-hours to assess cell morphology, cell viability and function. Medium alone and SDS-treated cells were used as negative and positive controls, respectively. There was no change in cell morphology at both 4 (Figure 4.5) and 24 hours (Figure 4.6) as determined by light microscopy at all concentrations tested. Similarly, cell viability, as determined by LDH assay, also showed no difference at 4 (Figure 4.7A) or 24 hours (Figure 4.7B). In contrast, significant differences were observed when cells were treated with SDS positive control (F(7, 16) = 89.07, p<0.001 at 4 hours treatment; and F(7, 16) = 173.0, p<0.001 at 24 hours). The SDS positive

control released high LDH levels compared to the untreated control (p<0.001 at all concentrations tested) at 4- and 24-hours.

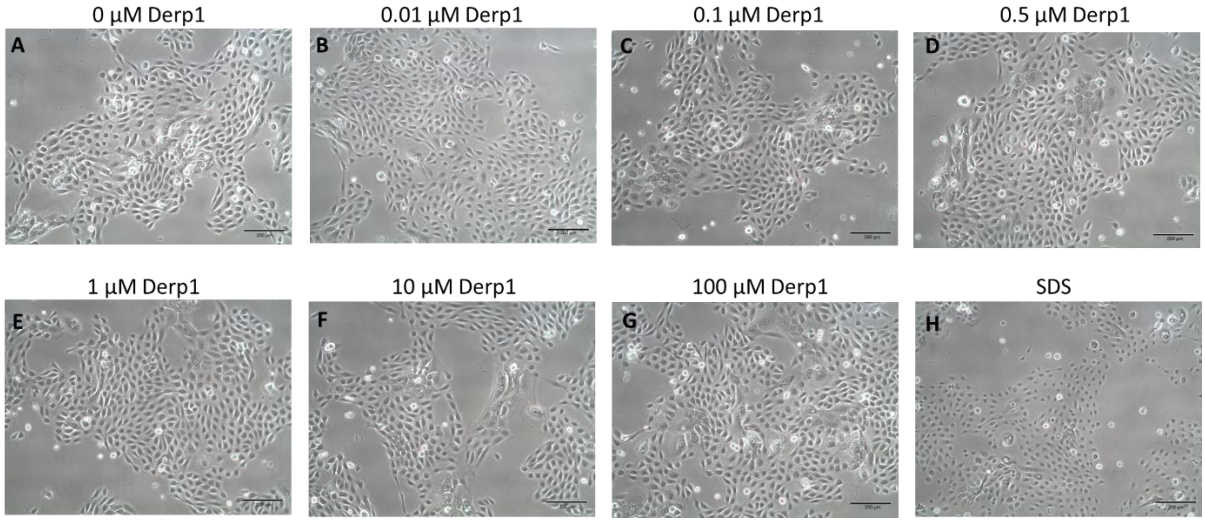

Figure 4.5 N/TERT-2G morphology after 4-hour stimulation with increasing concentrations of Derp1.
N/TERT-2G (A) were stimulated when 80% confluent with 0.01 µM (B), 0.1 µM (C), 0.5 µM (D), 1 µM (E), 10 µM (F), and 100 µM Derp1 (G). Control cells were treated with SDS (H), for 4 hours. Images are representative of n=3 independent experiments. Scale bar = 200 µm.

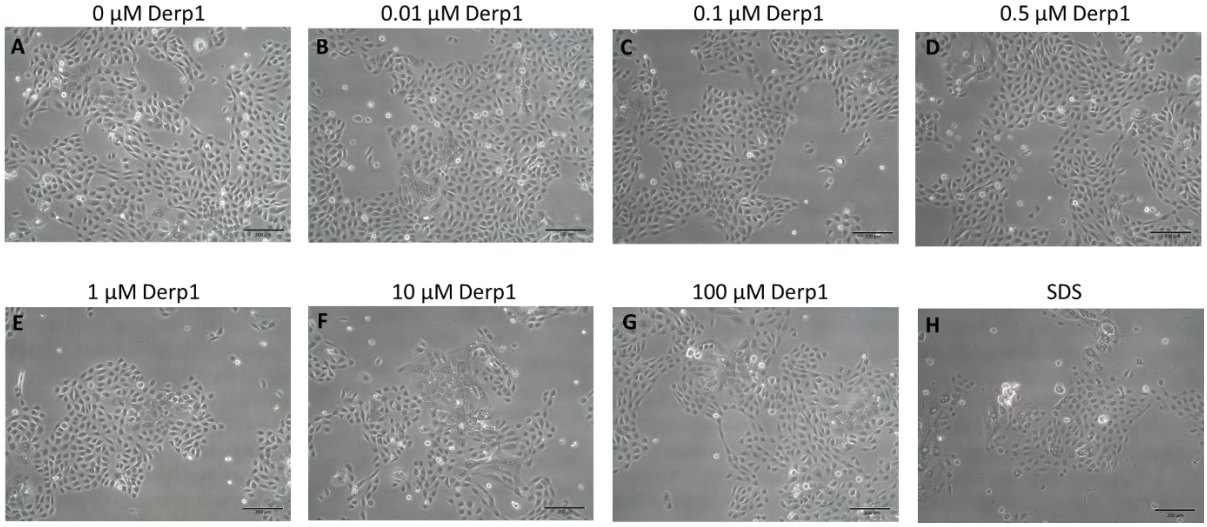

Figure 4.6 N/TERT-2G morphology after 24-hour stimulation with increasing concentrations of Derp1.
N/TERT-2G (A) were stimulated when 80% confluent with 0.01 µM (B), 0.1 µM (C), 0.5 µM (D), 1 µM (E), 10 µM (F), and 100 µM Derp1 (G). Control cells were treated with SDS (H), for 24 hours. Images are representative of n=3 independent experiments. Scale bar = 200 µm.

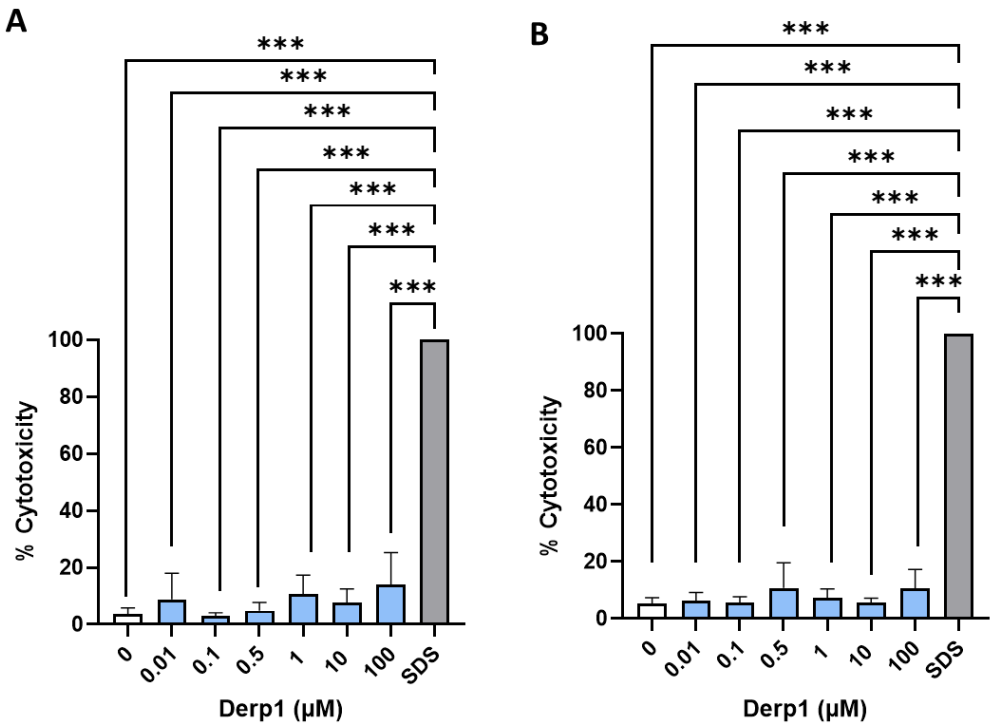

Figure 4.7 Cytotoxicity in N/TERT-2G after stimulation with increasing concentrations of Derp1. N/TERT-2G were stimulated when 80% confluent with increasing concentrations of Derp1, and compared to untreated or non-viable controls for 4 hours (A) and 24 hours (B). Data are presented as mean ± SD of n=3 independent experiments with statistical significance determined using one-way ANOVA followed by Dunnett's post hoc analysis; ***p<0.001.

Changes in gene expression were measured after 4 hours treatment and compared to untreated controls. No significant changes were observed for N/TERT-2G treated with Derp1, although data were very variable with large standard deviation between experimental repeats (Figure 4.8), and with statistically significant changes for TSLP between the untreated and 0.1 µM, (F(3, 8) = 4.011, p=0.026).

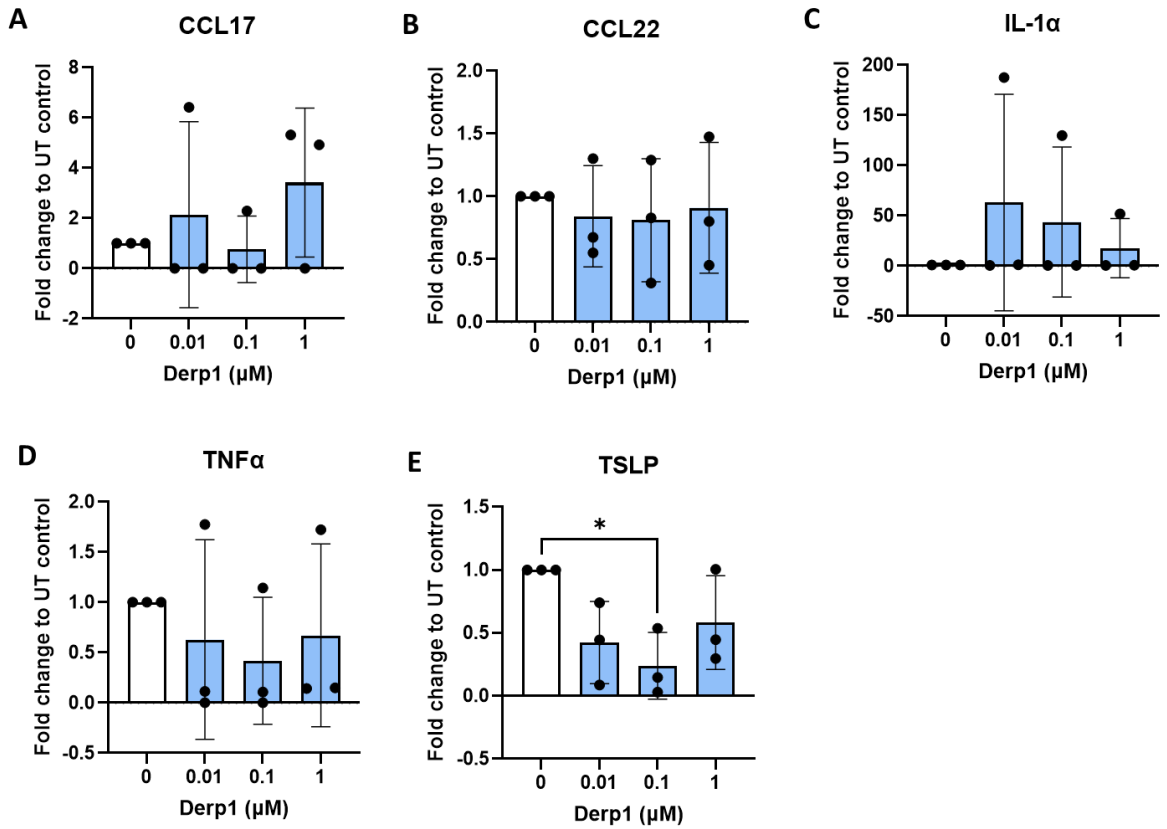

Figure 4.8 Gene expression of N/TERT-2G upon stimulation with Derp1 for 4 hours.
Untreated N/TERT-2G (white) and N/TERT-2G treated with 0.01 μM, 0.1 μM and 1 μM Derp1 (blue) for 4 hours. Gene expression of *CCL17* (A), *CCL22* (B), *IL-1α* (C), *TNFα* (D), and *TSLP* (E) were analysed by RT-qPCR, and expression calculated relative to the untreated control. Data are presented as mean ± SD of n=3 independent experiments with statistical significance determined using one-way ANOVA followed by Dunnett's post hoc test; *p<0.05.

4.3.2 Generation of human epidermal-only skin equivalents

4.3.2.1 Optimisation of human reconstituted epidermal-only skin equivalents

To mimic the human epidermis, RHE-only skin equivalents were generated using N/TERT-1 and N/TERT-2G, two human immortalised skin keratinocyte cell lines. RHE were initially cultured in a standard low volume 12-well tissue culture plate. Epidermal morphology by H&E staining was firstly examined. Both N/TERT-1 (Figure 4.9A) and N/TERT-2G (Figure 4.9B) showed a well-differentiated stratified squamous epithelium consisting of basal cells attached to the PET membrane followed by a thin layer of spinous cells that differentiate into a granular layer followed by further differentiation into a fully defined, anuclear stratum corneum.

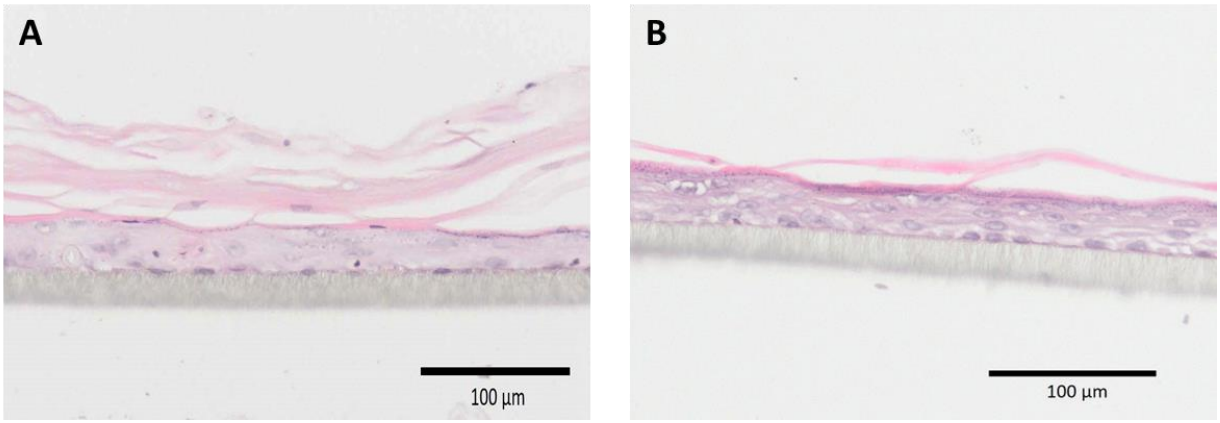

Figure 4.9 Morphology of human epidermal-only skin equivalents cultured in low volume culture medium.
N/TERT-1 (A) and N/TERT-2G (B) keratinocytes were seeded on top of a PET membrane containing tissue culture transwell insert that was previously coated with 100 µg/mL rat tail type I collagen and cultured in a standard low volume 12-well tissue culture plate. H&E staining shows the histological structure of the RHE. Images are representative of n=3 experiments. Scale bar = 100 µm.

Culture in a low volume standard 12-well plate produced RHE with a thin epithelium and disruption of keratinocytes differentiation, probably due to the low culture medium used in these models. The experiment was repeated but with culture in deep well 12-well plates to increase the volume of the culture medium to provide greater and prolonged access to culture medium and dilute waste products from cell metabolism. Culture in deep well plates produced a thicker epithelium for both N/TERT-1 (Figure 4.10A) and N/TERT-2G (Figure 4.10B) keratinocytes that also displayed a differentiated stratified squamous epithelium consisting of basal cells attached to the PET membrane followed by a stratum spinosum, a granular layer followed by an anuclear stratum corneum.

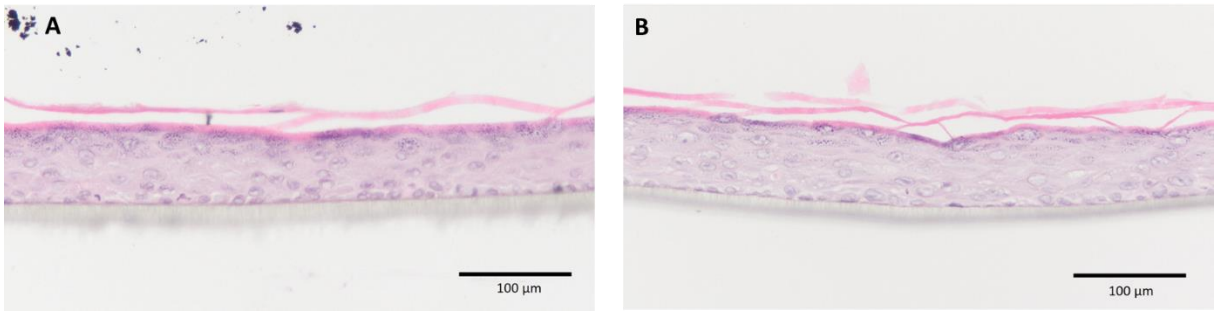

Figure 4.10 Morphology of human epidermal-only skin equivalents cultured in high volume culture medium.
N/TERT-1 (A) and N/TERT-2G (B) keratinocytes were seeded on top of a PET membrane, containing tissue culture transwell insert that was previously coated with 100 µg/mL rat tail type I collagen and cultured in deep well, large volume 12-well tissue culture plates. H&E staining shows the histological structure of the RHE. Images are representative of n=3 experiments. Scale bar = 100 µm.

4.3.2.2 Characterisation of human epidermal-only skin equivalents

Reconstituted human epidermal-only skin equivalents generated using N/TERT-1 or N/TERT-2G were characterised (Figure 4.11) with different epidermal-specific markers, such as CK14 (C, D), CK16 (E, F), E-cadherin (G, H), filaggrin (I, J) and involucrin (K, L), and compared to secondary antibody-only stained controls (A, B). CK14 was present in the basal cells in both RHE skin equivalents (C, D); CK16 was localised across all the epithelium (E, F); E-cadherin was present in the cell-cell adhesion, with higher levels in the N/TERT-1 (G) compared to the N/TERT-2G (H); filaggrin was expressed in the stratum corneum of both RHE skin equivalents, being downregulated in the N/TERT-1 (I) compared to the N/TERT-2G (J); while involucrin was present in the stratum basale, with higher expression in N/TERT-2G (L) compared to N/TERT-1 (K).

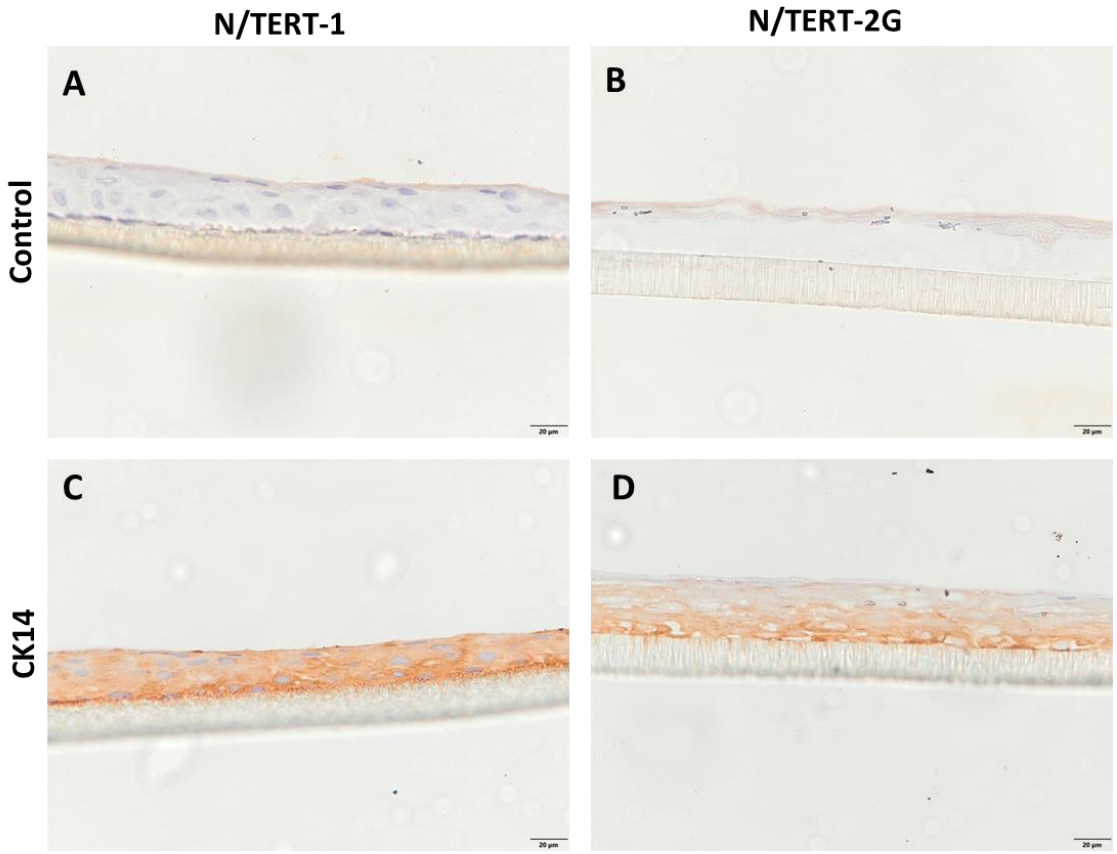

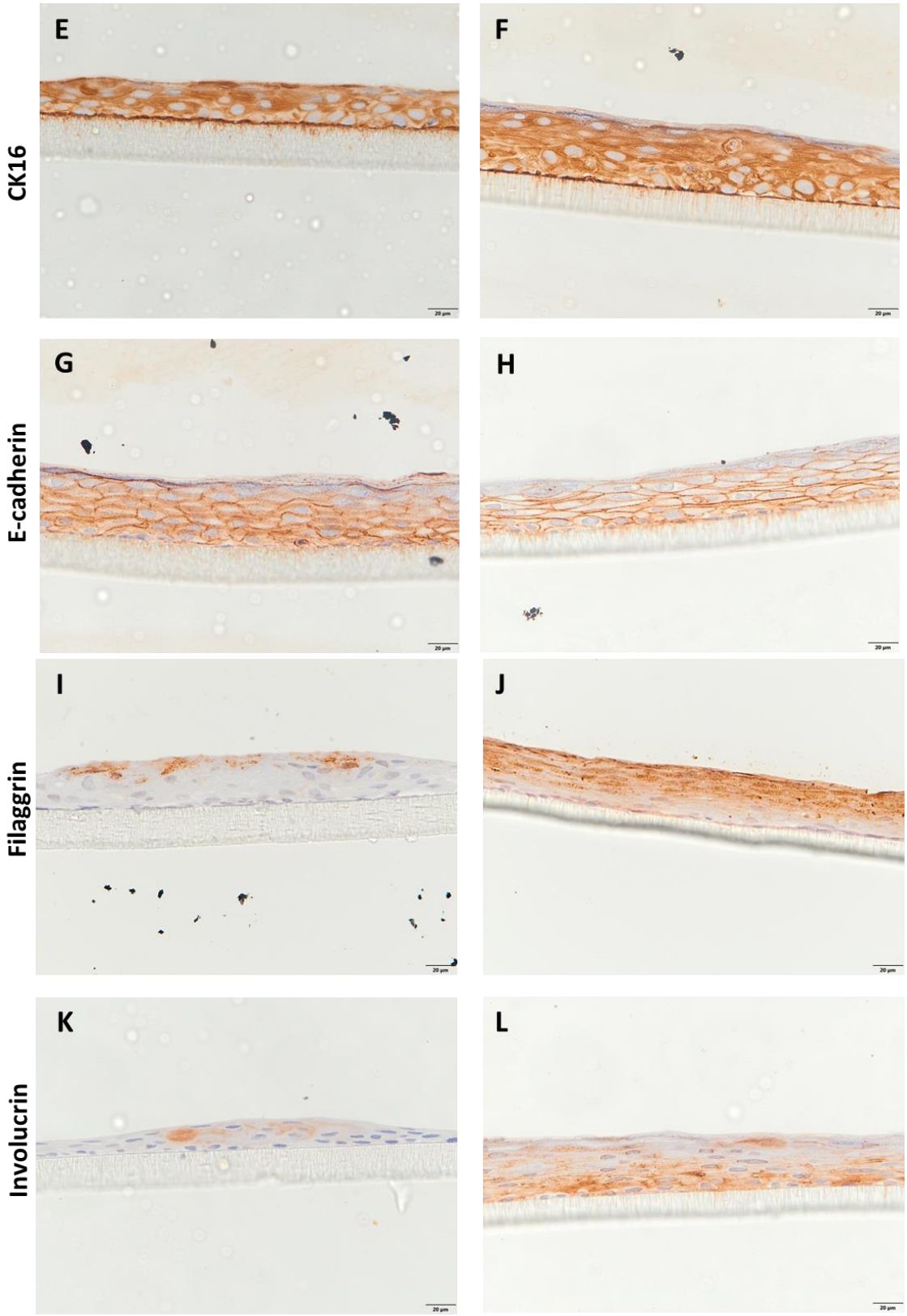

Figure 4.11 Characterisation of reconstituted human epidermal-only skin equivalents compared to human skin biopsy.

RHE skin equivalents generated using N/TERT-1 (A, C, E, G, I, K) or N/TERT-2G (B, D, F, H, J, L) were characterised and compared between each other. RHE skin equivalents were stained for CK14, CK16, E-cadherin, filaggrin, and involucrin, and compared to an unstained control. Scale bar = 20 µm.

4.3.3 Construction of full-thickness human skin equivalents

4.3.3.1 Optimisation of full-thickness human skin equivalents

To produce 3D full-thickness skin models, two combinations of cells were used: N/TERT-2G and primary normal human dermal fibroblasts (NHDF) or N/TERT-2G (immortalised epidermal keratinocytes) and BJ5ta cells (immortalised dermal fibroblasts), and full thickness HSE were constructed as described in section 2.3.2.3. Firstly, models were cultured in Green's medium for 10 days, and characterised for morphology by H&E staining. Some collagen matrix constriction was observed when adding 2.5 x 10^6 of both fibroblasts and keratinocytes (Figure 4.12 and Figure 4.13). In addition, little stratum corneum was observed in these models.

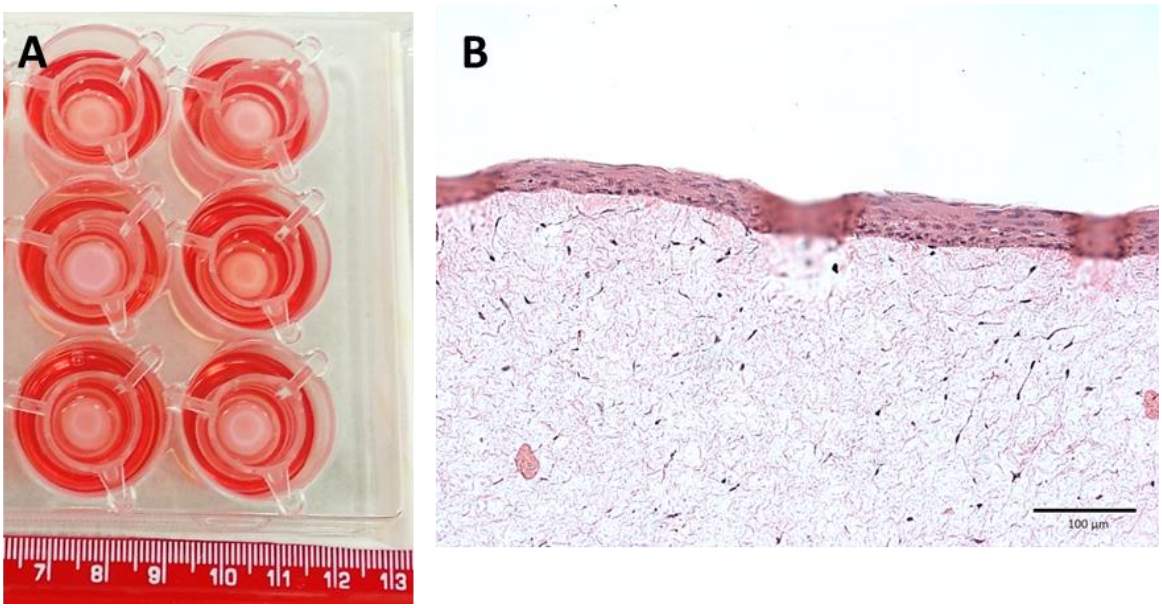

Figure 4.12 Morphology of HSE containing NHDF in a low collagen type I concentration.
2.5 x 10^6 N/TERT-2G were seeded on top of a 3.5 mg/mL collagen matrix containing 2.5 x 10^6 NHDF. HSE were cultured in Green's medium for 10 days. 12-deep well plate (A) shows HSE in culture and H&E staining (B) shows a fibroblast-populated collagen connective tissue topped by a stratified squamous epithelium with little cornification. Scale bar = 100 µm.

The same experimental conditions were used to make HSE but this time to generate fully immortalised models using TERT-immortalised BJ5ta dermal fibroblasts. Extensive collagen contraction was observed in these full-thickness models using immortalised fibroblasts (Figure 4.13) compared to HSE that contained NHDF (Figure 4.12). Moreover, histological analysis showed smaller fibroblasts in the connective tissue with an epithelium consisting of only 1-2 layers, although some cornification was evident (Figure 4.12).

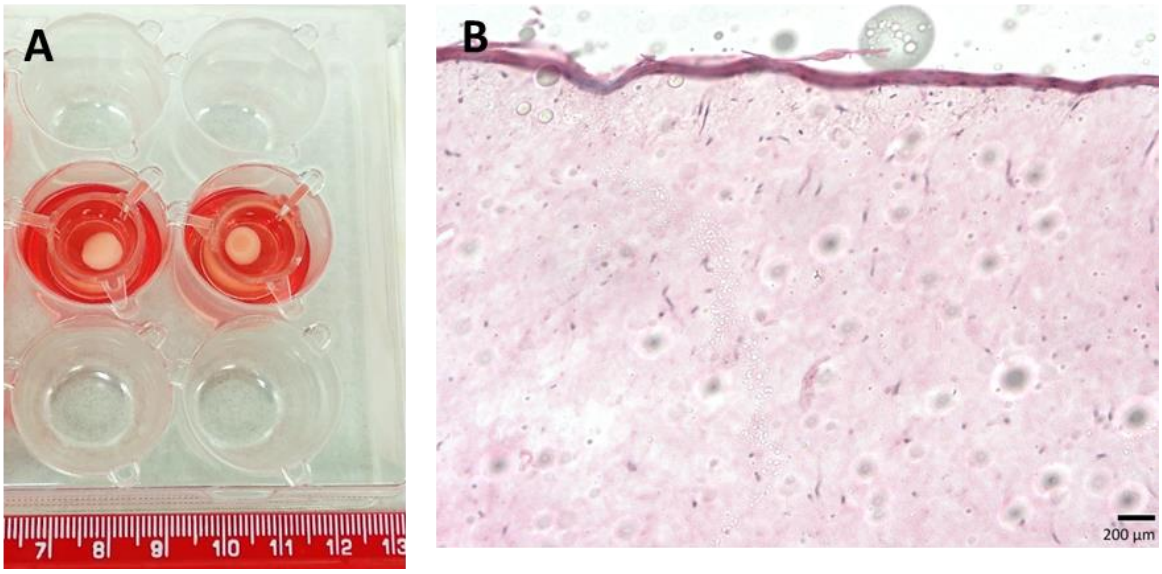

Figure 4.13 Morphology of HSE containing BJ-5ta immortalised fibroblasts in a low collagen type I concentration.
2.5 x 10^6 N/TERT-2G were seeded on top of a 3.5 mg/mL collagen matrix containing 2.5 x 10^6 BJ-5ta. HSE were cultured in Green's medium for 10 days. 12-deep well plate (A) shows HSE in culture and H&E staining (B) a fibroblast-populated collagen connective tissue topped by a stratified squamous epithelium. Scale bar = 200 µm.

To reduce collagen contraction and simultaneously induce stratum corneum formation, the number of NHDF and BJ-5ta was decreased, while the number of keratinocytes was increased. Keratinocytes were seeded on the same day as fibroblasts, and collagen concentration was increased to a final concentration equal to 5 mg/mL. HSE were cultured in Green's media for 10 days. HSE containing 3 x 10^5 N/TERT-2G appeared to form a thicker epithelium that contained large spinous cells (Figure 4.14A), whereas HSE seeded with 4 x 10^5 N/TERT-2G had a thinner epithelium with only small cells within the spinous layer (Figure 4.14B). Both models had a fibroblast-populated collagen connective tissue but both lacked a stratum corneum and the epidermis was not organised.

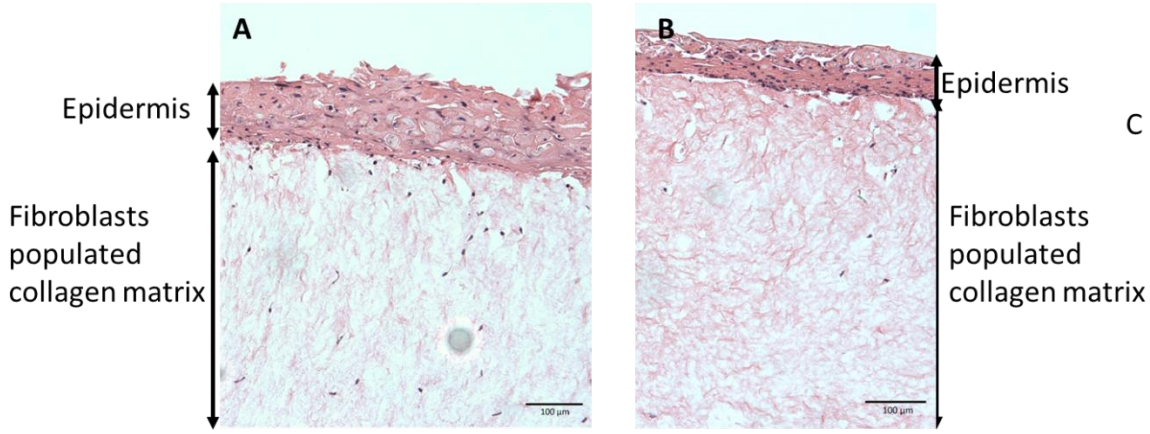

Figure 4.14 Morphology of HSE containing NHDF at different cell densities.
N/TERT-2G were seeded on top of a fibroblast-populated collagen matrix on the same day. 3 x 10^5 N/TERT-2G were seeded on top of a 5 mg/mL collagen matrix containing 1.5 x 10^5 NHDF (A); or 4 x 10^5 N/TERT-2G were seeded on top of a 5 mg/mL collagen matrix containing 2 x 10^5 NHDF (B). HSE were cultured in Green's medium for 10 days. Histology was examined by H&E staining. Scale bar = 100 µm.

For the fully immortalised models, addition of 3 x 10^5 N/TERT-2G cells produced a very thin epidermis (Figure 4.15A), while in contrast, addition of 4 x 10^5 N/TERT-2G cells produced a very thick epidermis (Figure 4.15B). Both models displayed lack of a clear spinous epithelial layer with little keratinisation. In addition, significant connective tissue contraction was observed for these cultures as was found previously. Therefore, the use of NHDF instead of BJ-5ta fibroblasts was taken forward for further experiments.

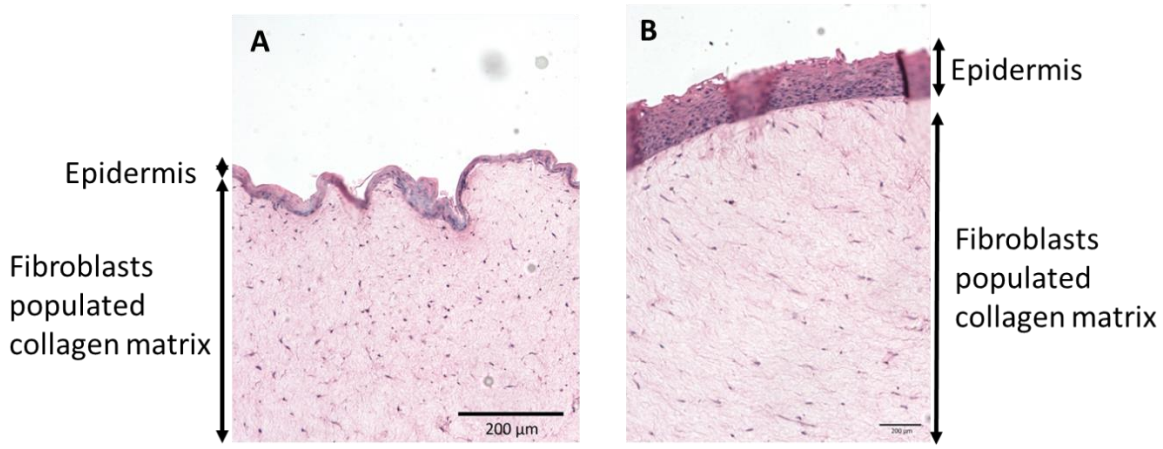

Figure 4.15. Morphology of HSE containing BJ-5ta at different cell densities.
N/TERT-2G were seeded on top of a fibroblast-populated collagen matrix on the same day. 3 x 10^5 N/TERT-2G were seeded on top of a 5 mg/mL collagen matrix containing 1.5 x 10^5 BJ-5ta (A); and 4 x 10^5 N/TERT-2G were seeded on top of a 5 mg/mL collagen matrix containing 2 x 10^5 BJ-5ta (B). HSE were cultured in Green's medium for 10 days. Histology was examined by H&E staining. Scale bar = 200 µm.

Previous studies (Harding et al., 2021, 2023; van Drongelen, Danso, et al., 2014) have added dermal fibroblasts to the connective tissue and cultured these for a number of days before the addition of keratinocytes to the apical surface. Therefore, next, a 1.5 x 10^5 NHDF populated collagen connective tissue was cultured for 48 hours prior to addition of either 3 x 10^5 or 4 x 10^5 N/TERT-2G keratinocytes. The HSE were cultured for 10 days and histology examined. Both HSE displayed a fibroblast-populated collagen with little connective tissue contraction, therefore, 1.5 x 10^5 NHDF were used for future experiments. HSE cultured with low numbers of N/TERT-2G keratinocytes produced a thin epithelium (Figure 4.16A), while those seeded with 4 x 10^5 N/TERT-2G keratinocytes produced a thicker, more defined squamous epithelium with stratification (Figure 4.16B). Neither model displayed a stratum corneum.

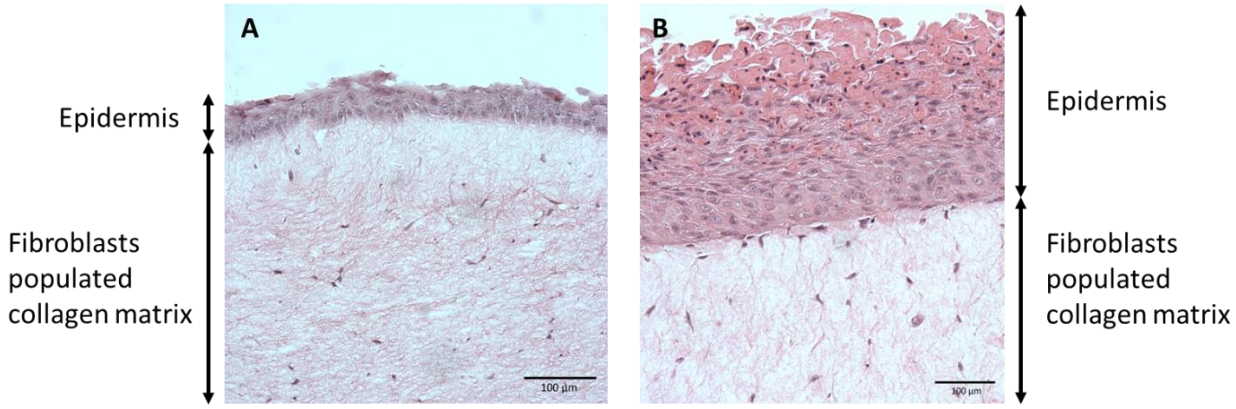

Figure 4.16 Morphology of HSE containing NHDF at different cell densities and N/TERT-2G added after 48 hours.
N/TERT-2G were seeded on top of a fibroblast-populated collagen matrix 48 hours after. 3 x 10^5 N/TERT-2G were seeded on top of a 5 mg/mL collagen matrix containing 1.5 x 10^5 NHDF (A); and 4 x 10^5 N/TERT-2G were seeded on top of a 5 mg/mL collagen matrix containing 2 x 10^5 NHDF (B). HSE were cultured in Green's medium for 10 days. Histology was examined by H&E staining. Scale bar = 100 µm.

The use of a defined differentiation medium (CnT) has been used in previous studies to culture N/TERT-2G cells. Therefore, HSE culture set-up was changed to culture the models in CnT medium. Due to the low serum content HSE were cultured for 14 rather than 10 days. Initial experiments with cell density seeding showed that a slightly reduced number (2.5 X 10^5) of N/TERT-2G cells was required. H&E staining of these HSE (Figure 4.17A) showed a well-differentiated stratified squamous epithelium consisting of basal cells attached to a fibroblast-populated matrix, followed by a thin layer of spinous cells that differentiate into a granular layer followed by further differentiation into a well-defined stratum corneum, that mimicked a human skin biopsy (Figure 4.17B).

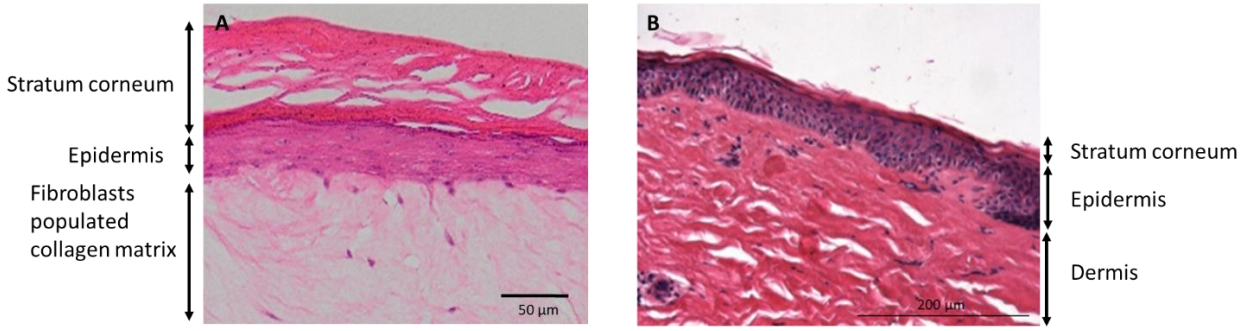

Figure 4.17 Morphology of HSE compared to human skin biopsy.
NHDF (1.5 x 10^5) were seeded in a 5 mg/mL collagen matrix and cultured for 48 hours. N/TERT-2G (2.5 x 10^5) were seeded on top of a fibroblast-populated collagen matrix and the full-thickness HSE cultured for 14 days in CnT media. HSE was examined by histological analysis. (A) H&E-stained section of N/TERT-2G HSE showing fully defined stratified squamous epithelium containing a fully developed stratum corneum compared to (B) H&E-stained section of a human skin biopsy. Scale bar = 50 µm (A) and 200 µm (B).

4.3.3.2 Characterisation of full-thickness human skin equivalents

HSE generated with N/TERT-2G were compared to HSE generated with N/TERT-1 and to a human skin biopsy (Figure 4.18) for specific skin development markers such as CK14 (D, E, F), CK16 (G, H, I), E-cadherin (J, K, L), filaggrin (M, N, O) and involucrin (P, Q, R), and compared to secondary antibody-only stained control (A, B, C).

CK14 was localised in the basal layers in the epidermis in HSE generated with N/TERT-1 (D) and N/TERT-2G (E), however, it was not present in the normal skin (F). CK16 was also present in the lower layers of the epidermis in HSE generated with N/TERT-2G (H) and in normal skin (I), however, it was expressed along the epidermis in HSE generated with N/TERT-1 (G). E-cadherin was expressed in the

cell-cell adhesions across all tissues (J, K, L). Filaggrin was expressed along the different epidermal layers in HSE (M, N), although it was expressed only in the stratum corneum of the normal skin sample (O). Involucrin was localised under the stratum corneum in HSE generated with N/TERT-2 (Q) and in normal skin (R), while it was present in the entire epidermis in HSE generated with N/TERT-1 (P).

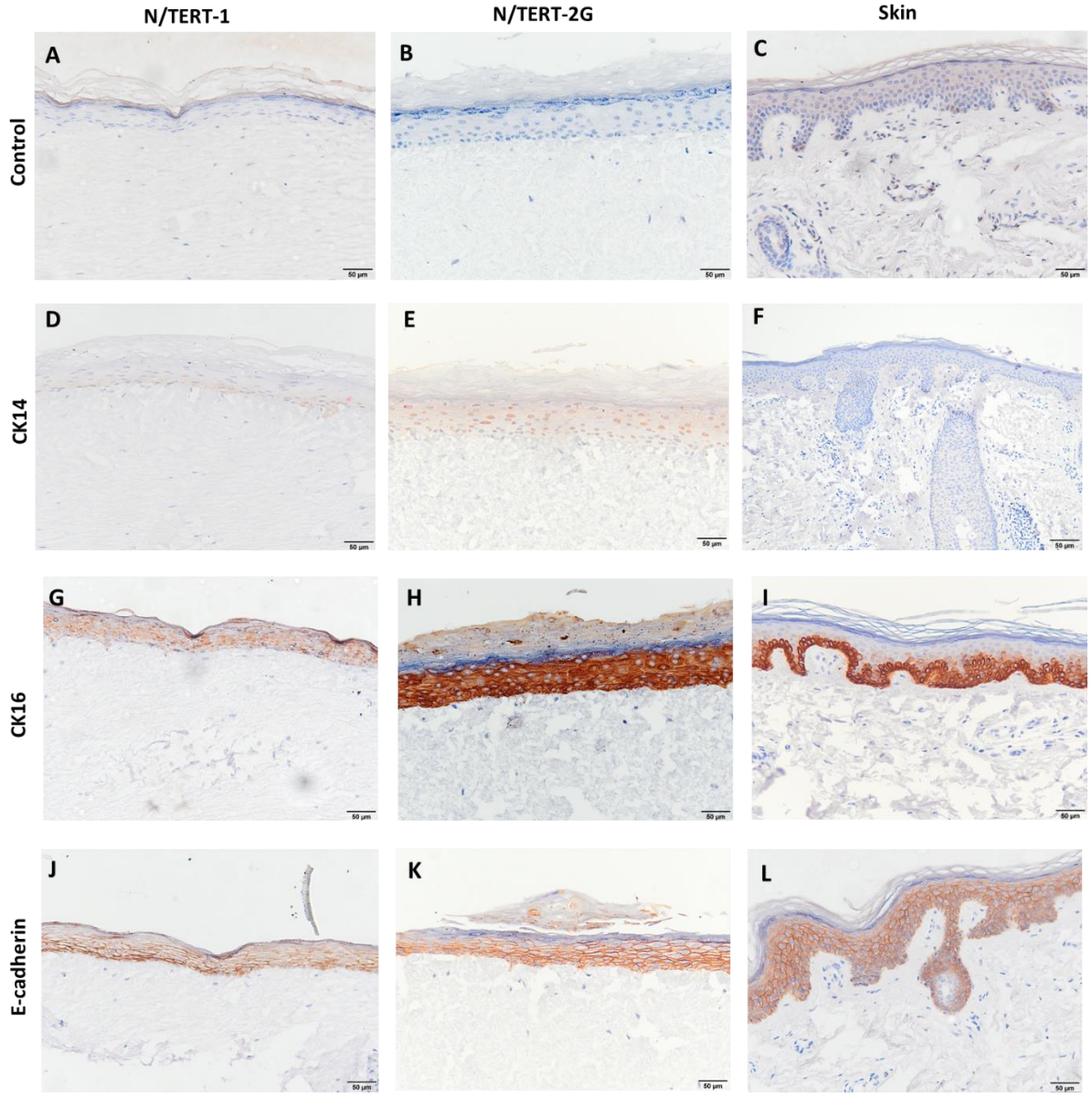

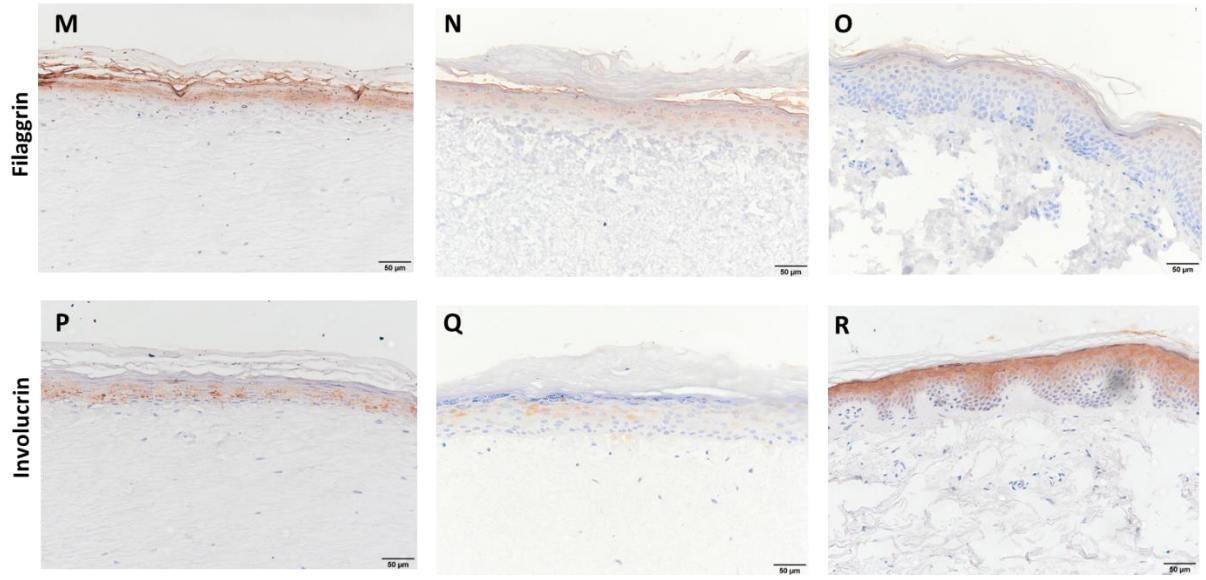

Figure 4.18 Characterisation of HSE compared to human skin biopsy.
HSE generated with N/TERT-2G (B, E, H, K, N and Q) were characterised and compared to HSE generated with N/TERT-1 (A, D, G, J, M and P) and normal human skin (C, F, I, L, O and R). HSE and normal human skin were stained for CK14, CK16, E-cadherin, filaggrin, and involucrin, and compared to an unstained control. Images are representative of a single technical repeat. Scale bar = 50 µm.

In summary, N/TERT keratinocytes have been tested in response to allergens such as DNCB and Derp1. N/TERT-1 and N/TERT-2G have been used to generate first RHE-only human skin equivalents, and then full thickness human skin equivalents. After optimising full thickness human skin equivalents conditions, and characterising both RHE-only and full thickness human skin equivalents, normal human skin primary fibroblasts and N/TERT-2G will be used for future experiments.

4.4 Discussion

4.4.1 Allergen challenge in N/TERT-2G

Keratinocytes are the most dominant cell type found in human skin and they play key roles in skin repair. Pathogenesis of chronic inflammatory skin disorders such as AD, allergic contact dermatitis and psoriasis is linked to dysregulated expression of inflammatory mediators that may be expressed by keratinocytes as well as leukocytes. For example, keratinocytes are involved in innate immune response by expressing TLRs and producing antimicrobial peptides in response to allergen penetration; and they secrete cytokines and chemokines upon proinflammatory cytokines exposure (Werfel, 2009). However, working with keratinocytes in 2D monolayer has many limitations, such as disruption of interactions between the cellular and extracellular environment, alterations in their

morphology, polarity and way in which they divide, and therefore changes in their function. In addition, keratinocytes in skin form the different layers of the epidermis, which cannot be replicated in a 2D culture.

IL-1α is found intracellularly and membrane bound in keratinocytes and in cases of injury or infection, IL-1α is secreted, leading to immune response activation (S. Yano et al., 2008). TNFα is a similar pro-inflammatory cytokine that is involved in inflammation, immune response and apoptosis. It is mainly secreted by activated macrophages, but also by other cells including keratinocytes. Although low TNFα levels are found in the upper layer of the healthy epidermis, it is mainly secreted upon injury, or in contact to sensitizers or infection (Banno et al., 2004; Udommethaporn et al., 2016). TSLP is a potential cytokine candidate to initiate and develop atopy and atopic disorders. It can be expressed by activated keratinocytes, and although it is not detected in normal skin or in non-lesional skin in patients with AD, it is highly expressed in lesions in both acute and chronic AD (Werfel, 2009). In AD, CCL17 (TARC) is expressed in lesional skin, suggesting that keratinocytes might be involved in the production of CCL17 (Tsuda et al., 2003). CCL22 (MDC) is produced by macrophages, activated B lymphocytes and DCs, but can be secreted by keratinocytes after stimulation with factors such as TNFα (C. Yano et al., 2015).

Exposure to contact allergens such as nickel or DNCB, food allergens from diet, or microbes, can induce keratinocyte activation. In this study, N/TERT-2G were stimulated with increasing non-toxic doses of DNCB. Although most studies have focussed on murine models, researchers have challenged HaCaT keratinocytes with different allergens. At the gene transcription level, *IL-1α*, *TNFα* and *TSLP* were upregulated for some DNCB doses, however these responses were variable between experiments and so were not significant. Similarly, *IL-1α* transcription was not detected in HaCaT cells response to DNCB (Summerfield, 2015), suggesting the release of pre-stored intracellular IL-1α (Coquette et al., 2003). Similar data has been observed in RHE-only models (dos Santos et al., 2011; Poumay et al., 2004), and in immunocompetent HSE (Chau et al., 2013). *IL-1α* expression is increased by other stimuli such as UV light (Kupper et al., 1987). *TNFα* is upregulated in murine models upon challenge with DNCB (Min et al., 2022; C.-C. Yang et al., 2021), although this upregulation was not seen by Ku *et al.* (Ku et al., 2018) or in HaCaT cells (Summerfield, 2015). Similar to *TNFα*, *TSLP* levels are increased in mice when they are stimulated with DNCB (C.-C. Yang et al., 2021). This could be due to a higher DNCB dose used in murine models compared to keratinocytes in 2D monolayer or release from non-keratinocyte cell sources. Expression of *CCL17* and *CCL22* appeared decreased compared upon DNCB treatment compared to untreated controls, although data was variable. Previous studies have also shown *CCL17* and *CCL22* expression in untreated HaCaT cells (Horikawa, 2002). In contrast, Vestergaard *et al*. reported secretion of *CCL17* by HaCaT cells upon stimulation only with the potent pro-inflammatory

cytokines *IFN-γ* and *TNF-α* (Vestergaard et al., 2000). Therefore, expression and production of these cytokines and chemokines might require stimulation with potent inflammatory mediators rather than with allergens that seem to give a low/varied response.

N/TERT-2G were also stimulated with increasing non-toxic doses of Derp1. No significant differences were observed in *IL-1α*, *TNFα*, *CCL17* and *CCL22* gene expression after N/TERT-2G were stimulated for 4 hours. In contrast, IL-1α secretion was significantly increased after 24 and 48 hours post-stimulation with 25 µg/ HDM extract in HaCaT cells (Lee et al., 2021). However, this increase could be due to other molecules within the extract beside Derp1. No previous studies have examined TNFα expression after stimulation with Derp1 on human epidermal keratinocytes. Maeda *et al.*, did not observe any increased *TNFα* expression upon stimulating a keratinocyte cell line derived from an adult beagle with Derf1 for 12 hours, although expression was increased after 24 hours (Maeda et al., 2009), suggesting delayed gene transcription. On the contrary, TNFα as well as TSLP was found in bronchoalveolar lavage fluid from mice following 12 hours stimulation with HDM-derived chitin (Choi et al., 2016). Secretion of these mediators may be from other cells such as alveolar macrophages and TSLP secretion has also been observed by epithelial lung cells from healthy donors (Willart et al., 2012). Maeda *et al.,* did not find an increase in *CCL17* expression after Derf1 challenge for up to 48 hours in a beagle keratinocyte cell line (Maeda et al., 2009). Similarly, CCL17 was not upregulated in HaCaT cells (Lee et al., 2021) by Derp1, which is similar to the finding of this study. No studies have examined expression of CCL22 after stimulation with Derp1 on human epidermal keratinocytes. However, Mo-DC obtained from HDM-allergic patients showed significant secretion of both CCL17 and CCL22 when incubated with Derp1 compared to the untreated control. In contrast, no increase in these chemokines was observed in healthy donors (Hammad et al., 2003). This could be due to a non-response from healthy donors, as they would not present allergy to house dust mite. Taken together, these data suggest that skin keratinocytes are mainly un-responsive to the actions of allergens such as DNCB and Derp1, and that these factors are likely to act through immune cells, or that a longer exposure might be needed for these cells to respond to allergens.

4.4.2 Construction of human reconstituted epidermal-only skin equivalents

Primary human skin keratinocytes and dermal fibroblasts have been used extensively to examine skin biology. These cells have a short life-span in culture, so a continuous supply of human skin is required for cell isolation for use in experiments, which limits their use to those laboratories able to acquire skin or afford to purchase these cells from commercial suppliers. A further problem with primary

keratinocytes is their heterogeneous nature between individuals meaning high donor-to-donor variations between experiments. Immortalised human cells have the advantage of longevity in culture meaning increased standardisation and much less intra-experiment variation. One potential drawback is that the immortalisation process may alter the keratinocyte biology and so not be representative of primary cells. Nevertheless, the use of immortalised cells, in particular, human telomerase reverse transcriptase (hTERT) immortalisation, which appears to alter the cell biology less than other forms of immortalisation (e.g., HPV E6/7), have increasingly been used to replace the need for primary cells.

N/TERT-1 and N/TERT-2G, are two immortalised keratinocytes cell lines that were developed in 2000 by the Rheinwald laboratory. These cells were generated by transduction of human primary keratinocytes with the hTERT gene by the spontaneous loss (N/TERT-1) or reduction (N/TERT-2G) of the pRB/16^{INK4a} cell cycle control mechanism (Dickson et al., 2000). N/TERT-1 is diploid with an additional chromosome 20 (47, XY, +20) and N/TERT-2G is diploid (46, XY). Studies have used these cells to generate RHE and full thickness human skin equivalents (Bertrand-Vallery et al., 2010; Dickson et al., 2000; Robertson et al., 2012; Smits et al., 2017; van Drongelen, Danso, et al., 2014).

In this study, RHE-only skin equivalents were generated by following the protocol described in Smits *et al.*, (Smits et al., 2017). Similar to the Smits study, both human RHE-only skin equivalents containing N/TERT-1 and N/TERT-2G showed a well-differentiated stratified squamous epithelium consisting of basal cells attached to the PET membrane followed by a layer of spinous cells that differentiate into a granular layer followed by further differentiation into a fully defined, anuclear stratum corneum. These models have been used for different purposes such as study of inflammation (Smits et al., 2017), UV radiation and DNA damage (Bertrand-Vallery et al., 2010), and to study the biology of the human epidermis (Robertson et al., 2012; van Drongelen, Haisma, et al., 2014).

In addition, RHE-only skin equivalents constructed with N/TERT-1 and N/TERT-2G were characterised by IHC staining with CK14, CK16, E-cadherin, filaggrin, and involucrin, and compared to a secondary-only stained control. CK14 is a type I keratin expressed in the basal cells of the epidermis; CK16 is a type I keratin upregulated in hyperproliferative keratinocytes; E-cadherin is a protein involved in cell-cell junctions; filaggrin is an important protein of the stratum corneum; and involucrin is a differentiation marker. H&E staining did not show any notable differences between N/TERT-1 and N/TERT-2G RHE-only skin equivalents, although CK14 was higher expressed in N/TERT-1, while filaggrin expression was lower than in N/TERT-2G, suggesting that the N/TERT-2G could differentiate better than the N/TERT-1. Expression of some of these key markers such as filaggrin or involucrin could potentially be increased if maintaining the RHE-only skin equivalents in culture for longer. To study this further, the use of other markers such as K10 or immunofluorescence would be favourable.

Nevertheless, RHE-only skin equivalents showed similar characteristic features as seen in previous studies (Reijnders et al., 2015; Smits et al., 2017; van Drongelen, Haisma, et al., 2014), and this closely mimics the features shown in human skin (Reijnders et al., 2015; Wagner et al., 2018).

4.4.3 Generation of full-thickness human skin equivalents

Full-thickness HSE consisting of keratinocytes and fibroblasts are highly used in dermatological research, as they better mimic human skin, when compared to 2D cultures, murine models, or even RHE-only skin equivalents. Fibroblasts in the dermal compartment secrete growth factors that aid the growth and differentiation of keratinocytes, which then synthesise basement membrane proteins such as laminin. In addition, keratinocytes secrete factors that induce fibroblasts proliferation and so paracrine signalling mechanisms enhance HSE development and are important for the formation of the basement membrane.

The construction of HSE can be a challenging process. One of the main problems has been the undesirable contraction of the dermal connective tissue. This could be due to several factors: the number, batch, age of fibroblasts (Detwiler et al., 2022) within the connective tissue (donor-to-donor variation in collagen contraction is common), the collagen batch, culture medium used, or culture time. In addition, the use of scaffolds derived from animals have some other limitations; numerous growth factors, chemokines and proteins could have several implications on cells behaviour when these are seeded in the matrix. Furthermore, the use of these scaffolds could increase the risk of immunogenic interference with human cells. Therefore, several parameters need to be determined experimentally in order to achieve a desirable fibroblast-populated connective tissue. The immortalised dermal fibroblasts that were used in this study have a fast rate of proliferation compared to primary fibroblasts. This can be a notable factor that can change the quality of the 3D skin equivalent, as generally connective tissue contraction is directly related to the number of fibroblasts seeded within the matrix. Primary fibroblasts have a long doubling time and their proliferation rate decreases when cultured in 3D compared to 2D culture, so their numbers within the collagen hydrogel do not increase over the HSE culture period. In contrast, immortalised fibroblasts have higher proliferation rates that continue in 3D meaning that increasing numbers of fibroblasts are present throughout the culture period, and explains the significant connective tissue contraction observed when using these cells. Other fibroblast factors are also important such as the levels of smooth muscle actin filaments, matrix metalloproteinases and their inhibitors, which also influence contraction. Therefore, there is a playoff between the type (primary/immortalised) and number of fibroblasts added and their ability to contract the connective tissue over-time.

After several optimisation experiments, it was decided to cease the use of the immortalised fibroblasts due to problems with excessive collagen contraction. In contrast, Reijnders *et al.*, successfully developed a fully immortalised full-thickness HSE using N/TERT-1 and BJ-5ta, although these researchers used a bovine matrix consisting of collagen I, II and V and elastic that may prevent issues with contraction (Reijnders et al., 2015). Their study does not mention issues with contraction although this does not necessarily mean contraction did not occur. This study found that 1.5×10^5 NHDF was optimal to support keratinocyte growth whilst avoiding contraction. The numbers of fibroblasts added to the collagen matrix is likely to change due to donor variation.

Recently, the levels of collagen contraction in HSE have been regulated using a combination of genipin and cytochalasin D to prevent the actions of fibroblasts within the collagen matrix. This may aid issues with contraction in future studies, although it is not known whether these factors interfere with other fibroblast activities that may have deleterious effects (Koskinen Holm & Qu, 2022).

The type of collagen that is used to generate the matrix is another important factor; a non-gelling matrix may have consequences on the structure of the model. To avoid this, Carlson *et al*., (2008) suggested keeping all reagents on ice until the gel mixture is added onto the tissue culture insert. It was also been described by Carlson *et al*. that the uppermost layers of the epithelium are thicker with a longer period of incubation time (Carlson et al., 2008).

The type of the culture medium used is also a key factor. Reijnders *et al*., (2015) and Smits *et al*., (2017), among others, previously developed full-thickness and RHE-only skin models using immortalised N/TERT-1 and N/TERT-2G keratinocytes using two different types of culture medium (Reijnders et al., 2015; Smits et al., 2017). We initially cultured the RHE and HSE in Green's medium, a medium previously used by colleagues from our group to generate oral mucosa equivalents (Jennings et al., 2016). This medium is very similar in composition to that used by Reijnders *et al.*, and so it was thought that this would successfully support 3D model growth. However, although keratinocyte stratification was observed, there were problems with keratinocyte differentiation and no stratum corneum was evident. This could also be due to the collagen shrinkage away from the edges of the well, as keratinocytes could migrate to the bottom, and therefore, there would not be enough keratinocytes differentiating and forming the stratum corneum. These HSE did not significantly improve in terms of keratinisation upon the addition of lipid supplements, as used in the Reijnders *et al.*, protocol. Therefore, following culture of the NHDF within the collagen matrix for 48 hours, the culture medium was changed to CnT-Prime 3D Barrier Medium, a highly defined commercial medium, designed to improve keratinisation and barrier formation in 3D epidermal models. This medium was previously used to generate RHE-only models using N/TERT keratinocytes (Smits et al., 2017). Upon

culture with CnT-Prime for 14 days, full-thickness N/TERT-2G HSE produced a stratified squamous epithelium where the keratinocytes had differentiated into a highly-keratinised stratum corneum that was histologically similar to native skin. These HSE were also similar to other HSE generated using immortalised N/TERT keratinocytes (Acheva et al., 2014; Dickson et al., 2000; van Drongelen, Danso, et al., 2014). These models have been used to study the development of these cell lines (Dickson et al., 2000; Rheinwald et al., 2002), skin barrier and skin biology (van Drongelen, Danso, et al., 2014), inflammation (Acheva et al., 2017), and DNA damage (Acheva et al., 2014), among others.

HSE generated with N/TERT-2G were also characterised for specific markers involved in the development of human skin, and compared to HSE generated with N/TERT-1 and to normal human skin. These markers, compared to an unstained control, included CK14, CK16, E-cadherin, filaggrin and involucrin.

CK14 was expressed in the stratum basale of HSE, however, no expression was observed in the normal skin, which was not expected, as it is usually present in basal cells of the epidermis (Strudwick et al., 2015). CK16 was also expressed in the basal cells of the epidermis in HSE generated with N/TERT-2G and in normal skin, while it was expressed across all epidermis in HSE generated with N/TERT-1. This was unexpected, as CK16 is not frequently present in normal skin (Kolesnik et al., 2018). E-cadherin, as shown in previous research (Maretzky et al., 2008; Nelson et al., 2019; Pennacchi et al., 2015), was expressed in the cell-cell junctions in all tissues. Filaggrin was observed in the epidermal layers in HSE (Niehues et al., 2017) while it was only expressed in the stratum corneum in normal skin (Wagner et al., 2018). Involucrin was expressed under the stratum corneum in HSE generated with N/TERT-2 and in normal skin (Reijnders et al., 2015), while it was present in the entire epidermis in HSE generated with N/TERT-1 (Robertson et al., 2012).

4.5 Conclusion

In conclusion, the data produced in this chapter suggests that keratinocytes are largely non-responsive in terms of cytokine and chemokine release when challenged with DNCB or Derp1 as examples of allergens. It is likely that it is the immune cells that respond to these allergens and the keratinocytes are mainly activated by the inflammatory cytokines released by stimulated immune cells. Data from this chapter also show the optimisation experiments required to generate RHE-only and full-thickness HSE. These experiments are required even though production of HSE has been demonstrated in several other laboratories due to cell donor-to-donor variation (if primary fibroblasts are used), subtle differences in medium and lab-to-lab variations in 3D culture technique. Characterisation through histology and immunohistochemistry where appropriate is highly recommended for validation. The

HSE developed in this chapter using human primary dermal fibroblasts and N/TERT-2G will be taken forward for use in generating a T cell immuno-competent HSE in the following chapter.

Chapter 5 - Development of an immunocompetent human skin equivalent of atopic dermatitis.

5.1 Introduction

In chapter three, buffy coats were used as a source of mononuclear cells from which monocytes were differentiated into monocyte derived dendritic cells (Mo-DC) and naïve CD4+ T cells were polarised into T_H2 cells. In chapter four, human skin equivalents (HSE) were generated by culturing skin keratinocytes on top of a dermal fibroblast-embedded collagen matrix.

Atopic dermatitis is a chronic inflammatory skin disorder involving multiple cell types such as dendritic cells, T cells and keratinocytes, and hypersensitivity to environmental factors. Although some disease models have been generated, these do not recreate the escalatory inflammatory cycle that occurs in patients with atopic dermatitis (AD). The experimental models that are currently available usually study FLG, as a marker of AD and these consist of filaggrin-deficient models with or without the inclusion of naïve CD4+ T cells (Hönzke et al., 2016; van Drongelen et al., 2015; Wallmeyer et al., 2017). However, no previous studies have attempted to include both dendritic cells and T_H2 cells, despite the importance of these two cell types in the immunopathology of AD.

In this chapter, experiments were performed to generate and characterise a novel immunocompetent human skin equivalent of AD that included T_H2 cells in combination with the N/TERT-2G HSE, developed in chapter four. Addition of Mo-DC within the N/TERT-2G HSE was also attempted to produce an immune-responsive epidermis.

Chapter aim: generation of an innovative immunocompetent human skin equivalent (IC-HSE) of AD including both T_H2 cells and Mo-DC for drug development and testing.

Objectives:

- Incorporate Mo-DC within a reconstituted human epidermal-only and full thickness HSE.
- Incorporate T_H2 cells with fibroblasts within a collagen matrix.
- Generate, optimise and characterise full thickness IC-HSE.
- Compare IC-HSE to human skin biopsies.

5.2 Methods

Monocytes were isolated from human buffy coats (see section 2.3.1.4) and then differentiated into Mo-DC (see section 2.3.1.6). In addition, naïve CD4+ T cells were isolated from buffy coat-derived mononuclear cells or patient blood using negative selection (see section 2.3.1.8), activated with anti-CD3/CD28, expanded with IL-2 (see section 2.3.1.9), and polarised into T_H2 cells using IL-4 and anti-IFNγ (see section 2.3.1.10).

N/TERT-2G keratinocytes and dermal fibroblasts were cultured until they were confluent (see section 2.3.1.2). Type I collagen was isolated from rat tails (section 2.3.2.1) and used to coat transwell inserts to generate RHE-only skin equivalents (see section 2.3.2.2) and to develop full thickness HSE (section 2.3.2.3) and, with the addition of immune cells, immunocompetent HSE (see section 2.3.2.4). Keratinocytes and Mo-DC response was examined upon challenge with allergen (section 2.3.1.11) in RHE and LDH assay (see section 2.3.3) was carried out to measure cytotoxicity upon stimulation. The models were harvested (see sections 2.3.2.5 and 2.3.2.5.1) to analyse morphology and different components of the skin by H&E staining (see section 2.3.2.5.2) and immunohistochemistry (see section 2.3.2.5.3).

5.3 Results

5.3.1 Human RHE-only skin equivalents

N/TERT-2 keratinocytes were seeded with Mo-DC to generate Mo-DC/RHE skin equivalents to mimic the human epidermis. Mo-DC were seeded into transwells either on the same day as N/TERT-2G or 48 hours after. Firstly, morphology of these models was compared by H&E staining. Keratinocytes-only models showed a well-differentiated stratified squamous epithelium containing basal cells attached to the PET membrane followed by a thin layer of spinous cells that differentiate into a granular layer followed by further differentiation into a fully defined, anuclear stratum corneum (Figure 5.1A). When Mo-DC were added together with the keratinocytes, a more compact epidermis was observed (Figure 5.1B). In contrast, when Mo-DC were added after 48 hours, the epidermis appeared broken on the attachment to the PET membrane (Figure 5.1C). Therefore, Mo-DC were added on the same day for future experiments.

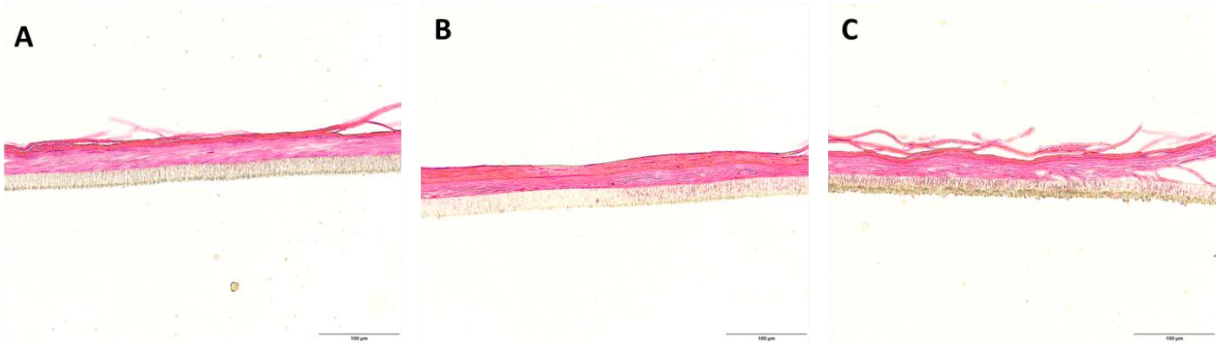

Figure 5.1 Morphology of RHE-only and Mo-DC/RHE skin equivalents
N/TERT-2 keratinocytes were seeded on top of a PET membrane, in an insert, in a normal 12-well plate, that was previously coated with 100 μg/mL rat tail type I collagen (A), with 0.5 x 10^6 Mo-DC added either on the same day (B) or 48 hours later (C) and cultured for 14 days. H&E staining shows structure of epidermal model. Images are representative of n=2. Scale bar = 100 μm.

RHE-only or Mo-DC/RHE skin equivalents were cultured for 14 days and treated with increasing concentrations of DNCB ranging from 0.001 μM to 1 μM for 4 hours to assess tissue morphology and function. Medium alone and SDS-treated cells were used as negative and positive controls, respectively. H&E staining for epidermal morphology showed that after 4 hours without stimulation the epithelium in models with and without Mo-DC were similar, each showing a stratified squamous epithelium that was keratinised (Figure 5.2A&B). Following treatment with 0.001 μM DNCB, vacuolation was observable in the RHE-only models with increased desquamation of the keratinised layer, whereas Mo-DC/RHE displayed reduced thickness with no desquamation (Figure 5.2C&D). With 0.01 μM DNCB the epithelium of RHE-only models remained thick and stratified with a defined desquamating keratinised layer, with the presence of colloid bodies within the stratum spinosum (Figure 5.2E). In comparison to RHE-only skin equivalents, Mo-DC/RHE models were much thinner, with marked number of darkly stained nuclei colloid bodies suggesting apoptosis (Figure 5.2F). Similar histological observations were seen for RHE-only and Mo-DC/RHE at both 0.1 μM (Figure 5.2G&H) and 1 μM DNCB (Figure 5.2I&J), suggesting more tissue damage was occurring in the Mo-DC/RHE than the RHE-only skin equivalents. Interesting, treatment of both models with SDS displayed significant epithelial damage (Figure 5.2K&L) but not total cellular destruction was observed for monolayer cultures of keratinocytes.

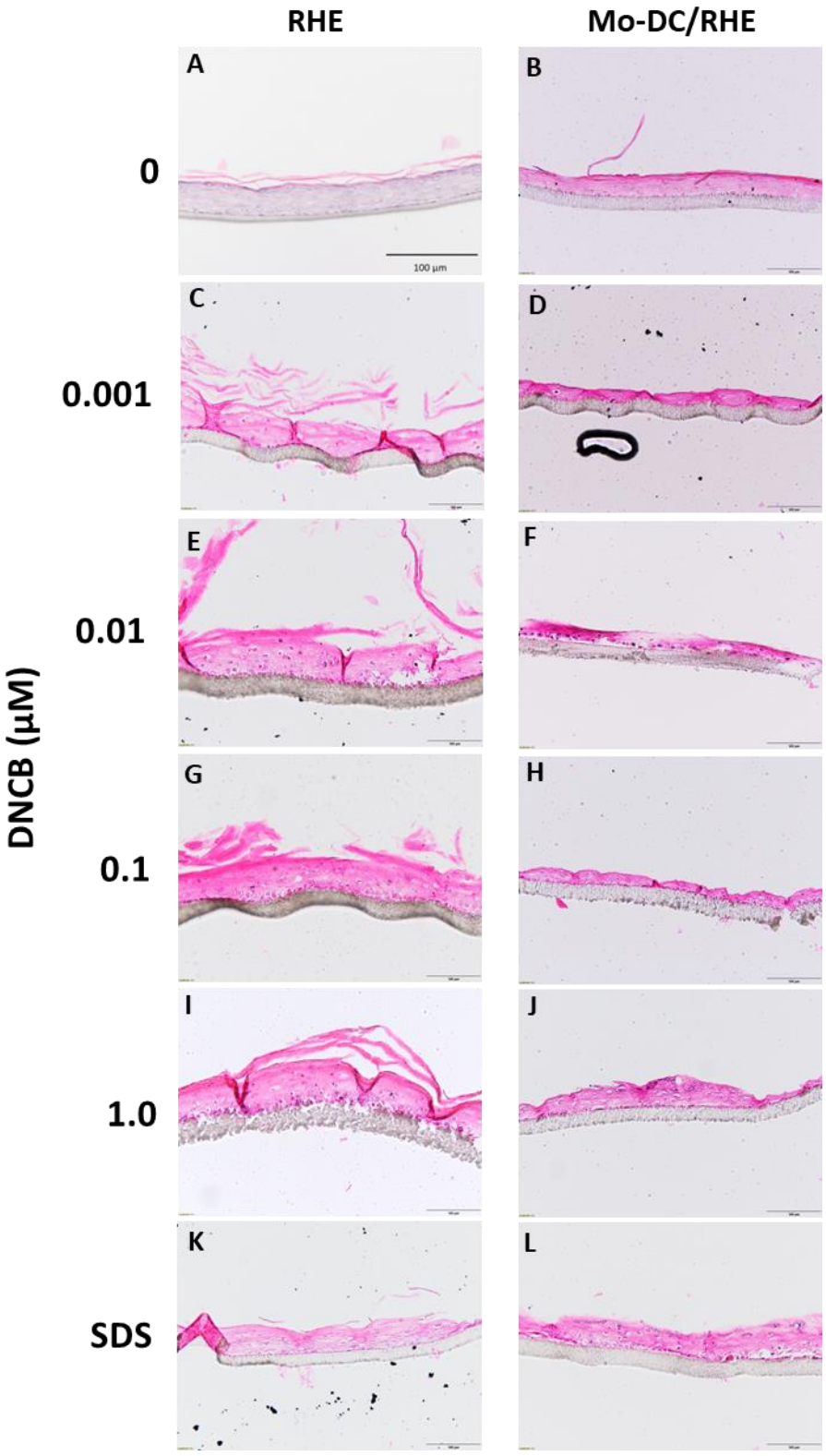

Figure 5.2 Morphology of human epidermal-only skin equivalents upon DNCB stimulation.
N/TERT-2G keratinocytes with or without Mo-DC were seeded on top of a 100 µg/mL rat tail type I collagen PET transwell membrane cultured for 14 days and stimulated with PBS as control (A&B), 0.001 µM (C&D), 0.01 µM (E&F), 0.1 µM (G&H), and 1 µM (I&J) DNCB, and compared to a SDS-treated cells (K&L) for 4 hours. H&E staining shows structure of epidermal models. Images are representative of n=1 for RHE-only and n=2 for Mo-DC/RHE. Scale bar = 100 µm.

Histological analysis was confirmed using an LDH assay to measure epithelial damage. In contrast to the histological data, LDH analysis showed that the DNCB caused more epithelial damage in RHE-only skin equivalents than the Mo-DC/RHE models with LDH levels observed higher than the SDS control, while LDH levels for Mo-DC were at 50% cytotoxicity with no significant different between untreated and DNCB-treated models (Figure 5.3).

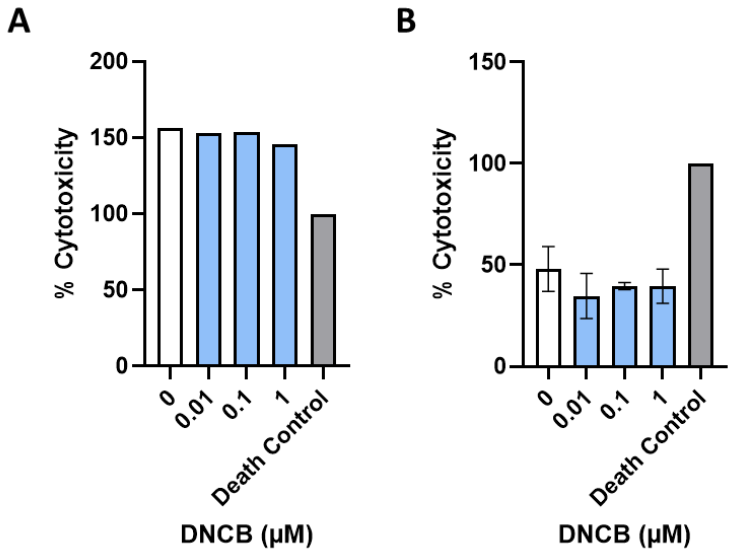

Figure 5.3 Cytotoxicity in human epidermal-only skin equivalents after stimulation with increasing concentrations of DNCB.
Human RHE-only (A) or Mo-DC/RHE (B) skin equivalents were stimulated after 14 days in culture with increasing concentrations of DNCB, and compared to untreated or non-viable controls for 4 hours. Data are presented as mean of n=1 independent experiments for RHE-only, and n=2 for Mo-DC/RHE (B).

5.3.2 Optimisation of IC-HSE

To examine if Mo-DC and T_H2 cells were compatible with a 3D collagen matrix, a fibroblast-populated collagen matrix after 48 hours and then Mo-DC were added to its apical surface. In contrast, T_H2 cells were embedded together with dermal fibroblasts within the collagen matrix. Both collagen models were cultured for 14 days and morphology then assessed by H&E staining. Models containing Mo-DC showed a fibroblasts-populated dermis with large cells attached to the apical surface that resemble the Mo-DC (Figure 5.4A). Histology of T_H2 cells within a fibroblast-populated collagen matrix showed long, spindle shaped cells corresponding to fibroblast morphology, along with small circular cells that displayed more intense nuclear haematoxylin staining, correlating to T_H2 cells (Figure 5.4B).

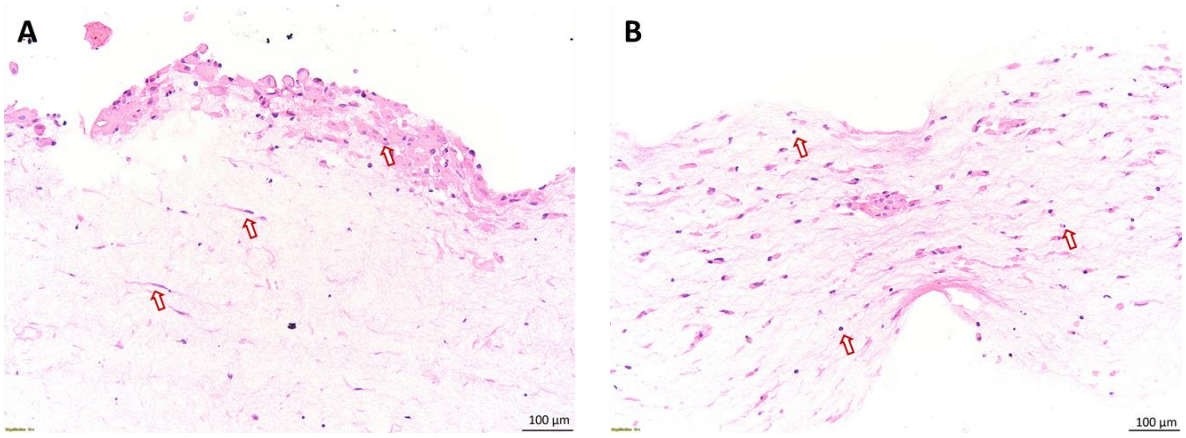

Figure 5.4 Introduction of immune cells in human skin models.
Mo-DC were seeded on top of a fibroblast-populated collagen matrix and cultured for 14 days (A); T_H2 cells were embedded together with fibroblasts in a collagen matrix and cultured for 14 days (B). Arrows in represent Mo-DC (A) and T_H2 cells (B). Images are representative of n=2. Scale bar = 100 µm.

Next, Mo-DC were mixed with N/TERT-2G keratinocytes and added to the surface of the fibroblast-populated collagen gel so that the Mo-DC were dispersed within the epidermis whilst in culture for 14 days. Skin equivalents were then fixed, wax-embedded, sectioned and immunohistochemistry performed for CD68, a myeloid cell specific marker. HSE without addition of Mo-DC displayed no staining for CD68 as expected (Figure 5.5A). In contrast, immune-positive staining for CD68 was observed for single cells in the collagen connective tissue as well as throughout the epidermis, with little evidence of keratinocytes remaining at 14 days culture (Figure 5.5B). Unfortunately, specialist low-adherence tissue culture plasticware for the culture of Mo-DC was not obtainable because of supply shortages due to the COVID pandemic. Attempts to culture Mo-DC on other treated culture flask surfaces was attempted but Mo-DC viability was low. Therefore, Mo-DC could not be cultured further and their use was discontinued at this point of the study.

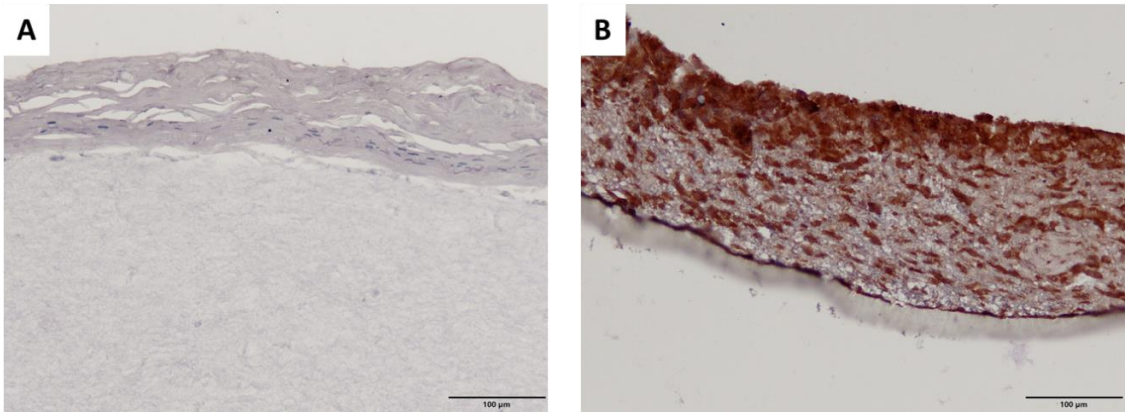

Figure 5.5 CD68+ staining is observed when Mo-DC are seeded on top of a fibroblast-populated matrix but not in HSE.
HSE (A) and 0.5 x 10^6 Mo-DC seeded with N/TERT-2G on top of a fibroblast-populated collagen matrix (B) were cultured for 14 days and stained for CD68, a protein highly expressed by cells in the monocyte lineage. Images are representative of n=1. Scale bar = 100 µm.

To make T cell containing HSE, T_H2 cells were mixed with fibroblasts and following culture, N/TERT-2G cells were added on top of the collagen. Immunohistochemistry for the T cell receptor, CD3, was performed to identify the location of T_H2 cells after culture for 14 days. In the absence of T_H2, no CD3 staining was observed (Figure 5.6A). In contrast, CD3 immuno-positive staining was observed for T_H2 cell-containing HSE. However, in these models T_H2 cells were observed at the surface of the epithelium. In addition, the epidermis was unstructured, with a loss of stratification and keratinisation and connective tissue was markedly contracted (Figure 5.6B). These data suggest that incorporation of T_H2 cells within HSE is possible but required optimisation.

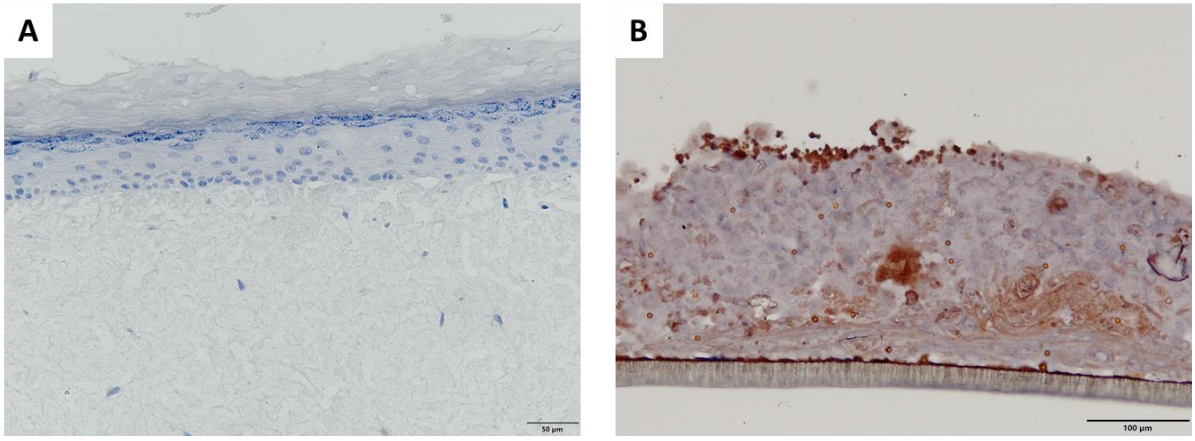

Figure 5.6 CD3+ staining was observed when T_H2 cells were embedded together with fibroblasts in a collagen matrix but not in HSE alone.
HSE without T_H2 cells (A) and T_H2 cells embedded together with fibroblasts in a collagen matrix (B) were cultured for 14 days, fixed, wax-embedded and stained for CD3, a T cell co-receptor by immunohistochemistry. Images are representative of n=1. Scale bar = 50 µm (A) and 100 µm (B).

IC-HSE were generated once again but this time a layer model was used (see section 2.3.2.4). Here, HSE was constructed and cultured at an air-to-liquid interface for 7 days. Separately, T_H2 polarised from buffy coat mononuclear cells were cultured within a collagen gel. On day 7 HSE were removed from the transwell, a small amount of collagen added to the surface of the T_H2-containing gel to act as an adhesive and the HSE placed on top to produce a three-layer model of T_H2 cells at the bottom, a fibroblast-populated collagen connective tissue in the middle and an epidermis on top (Figure 5.7A). Presence of T_H2 cells were confirmed by CD3+ staining (Figure 5.7B). It was thought this model more accurately reflects T_H2 cells being recruited to the tissue from the circulation, as migration is shown in these images.

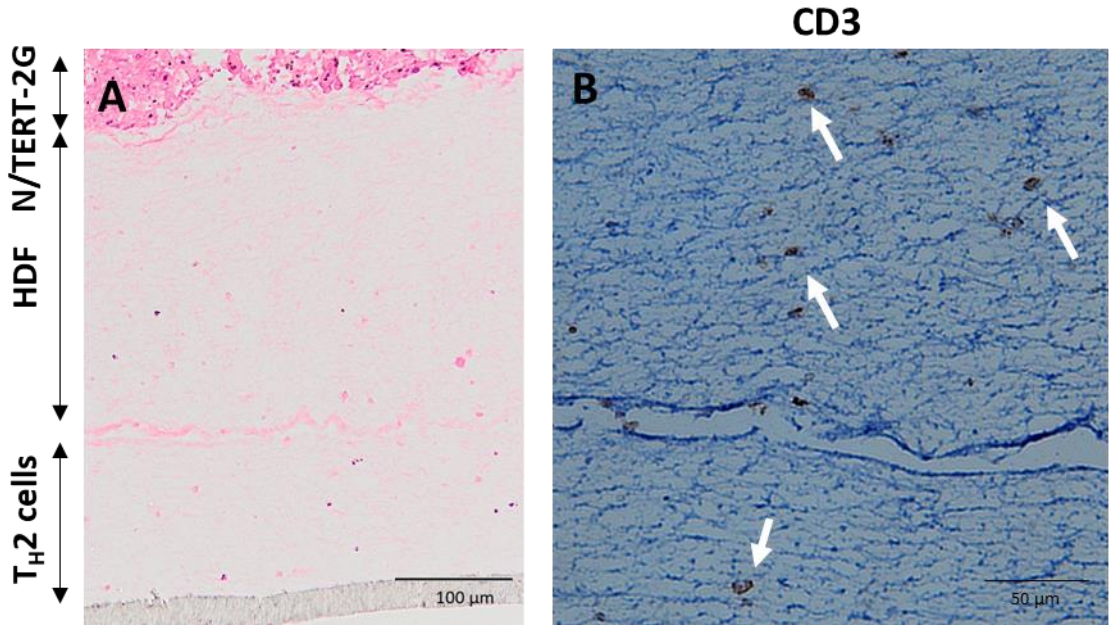

Figure 5.7 Three-layer model with T_H2 cells at the bottom.
IC-HSE consisting of a three-layer model of T_H2 cells at the bottom embedded in collagen, followed by a fibroblast-populated collagen, and N/TERT-2 mimicking the epidermis on top. H&E (A) shows structure of IC-HSE, CD3+ staining (arrows, B) shows presence of T_H2 cells. Scale bar = 100 µm (A) and 50 µm (B).

Using this layer system T_H2-containing HSE were cultured for 10, 12 and 16 days following which morphology was assessed by H&E staining. At day 10, T_H2 IC-HSE displayed a thick epithelium that displayed signs of vacuolation, epidermal damage and reduced keratinisation (Figure 5.8A). After 12 days the epithelium thickness was increased but the epithelium displayed loss of attachment to the basement membrane. Stratification was observed but displayed little keratinisation (Figure 5.8B). At day-16 the epidermis lost all structure with total loss of stratification or any recognisable histological

appearance (Figure 5.8C). This suggests that a culture time between day 10 and day 14 but not as long as 16 days are likely best for IC-HSE cultures.

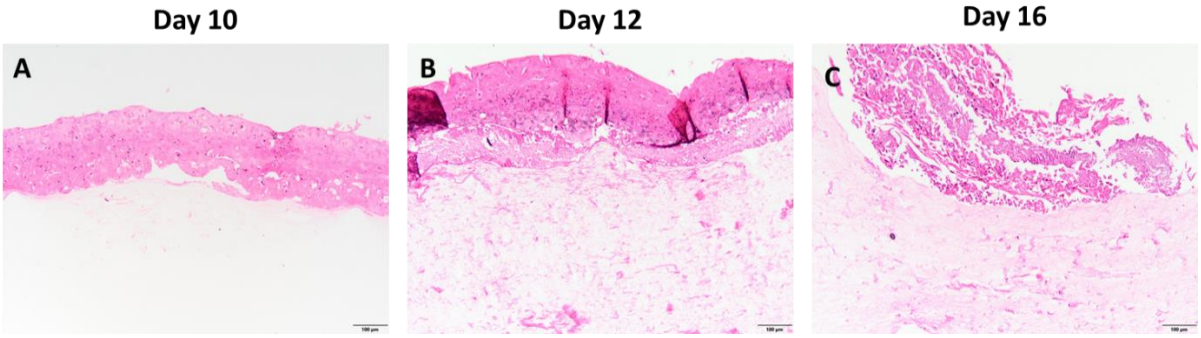

Figure 5.8 Morphology of IC-HSE containing T_H2 cells at different time points.
IC-HSE containing T_H2 cells were cultured for 10 (A), 12 (B) and 16 days (C). H&E staining shows structure of IC-HSE. Images are representative n=2 independent experiments. Scale bar = 100 µm.

5.3.3 Generation and characterisation of IC-HSE using T_H2 cells from patient samples

5.3.3.1 Assessment of IC-HSE morphology by H&E staining

So far IC-HSE were generated using T_H2 cells isolated from buffy coats obtained from the National Blood Service where leukocytes are pooled from more than one donor. To more closely mimic the in vivo situation T cells were isolated from patient whole blood from a single donor and these cells polarised to T_H2 cells using the established protocol. Blood samples along with a tissue biopsy were obtained from patients within the SPOT study. These patients were classified in the study as healthy or with mild, moderate or severe AD, based on the lesion severity. Blood and tissue samples were obtained for 43 patients, from which 13 healthy and 30 AD. Originally, the intention was to create IC-HSE using T_H2 cells derived from the whole spectrum of AD from healthy to severe and compare these to the corresponding patient tissue biopsy. However, due to no access at all and then very restricted access to the laboratory and constraints with blood sample collection because of the COVID pandemic, only a limited number of healthy and severe AD cases were eventually examined.

Using the layering technique, T_H2 cells polarised from patient T cells and incorporated into a collagen gel were added to the bottom of N/TERT-fibroblast HSE and cultured for up to 12 days. Controls were cultured in the absence of T_H2 cells.

Like previous experiments HSE on top of a collagen gel containing no T_H2 cells (control) displayed a fibroblast populated connective tissue topped with a stratified squamous epidermis containing a fully formed granular layer and a keratinised stratum corneum (Figure 5.9A). SPOT tissue 0011, 0015, 0021 and 0033 were from healthy subjects and H&E analysis of their skin tissue displayed skin structure expected of healthy skin (Figure 5.9B). Mononuclear cells isolated from these subjects were polarised to T_H2 cells and included in a collagen layer IC-HSE model with N/TERT-2G keratinocytes and dermal fibroblasts. Although all these 4 models displayed a stratified squamous epithelium, their histological structure was much different from control HSE models without T_H2 cells. These IC-HSE generally displayed a rather disorganised epidermis with epidermal separation occurring in the suprabasal layer. The spinous layer appeared disorganised with increased but inconsistent stratum corneum (Figure 5.9B), suggesting that T_H2 cells located in the model were exerting effects on the epidermis, possibly by secreted factors, causing these histological changes .

T cells isolated from patients displaying severe AD were polarised to T_H2 cells and were included in a collagen layer IC-HSE model with N/TERT-2G keratinocytes and dermal fibroblasts identical to the experimental format for healthy subjects and compared to H&E-stained tissue sections from the corresponding AD patients (SPOT0018, and SPOT0024). Histologically, AD patient H&E sections displayed a skin phenotype typical of AD with hyperproliferative epidermis, bulbous rete ridges, thinner and less organised stratum corneum (Figure 5.9C). Addition of T_H2 polarised cells into the collagen layer in IC-HSE models from severe AD patients displayed a very distinctive histology. In SPOT0018 the epidermis was disrupted but devoid of a stratum corneum, whereas for SPOT0024 the epidermis was totally absent from all sections examined (Figure 5.9C). This was a much more tissue damaged phenotype that displayed by IC-HSE constructed from polarised T_H2 isolated from healthy patients, suggesting that T_H2 cells from severe AD patients expressed additional factors that were deleterious to the epidermis.

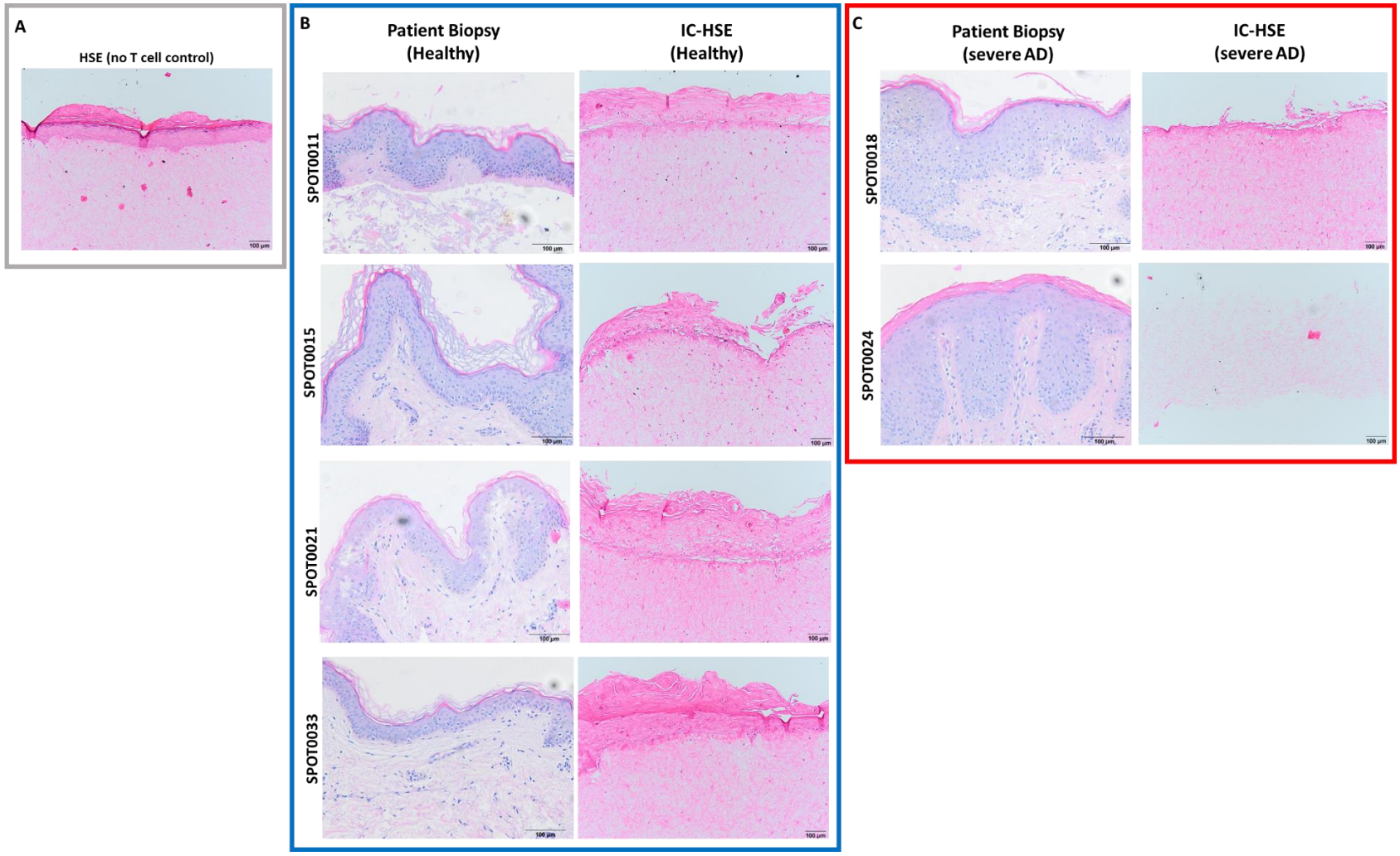

Figure 5.9 Morphology of HSE and IC-HSE containing T_H2 cells from healthy and severe AD patients.

HSE containing N/TERT-2 keratinocytes on top of a fibroblast-populated collagen matrix was cultured during 14 days at air-to-liquid interface, and used as control (Grey Boarder) (A) for IC-HSE containing T_H2 previously isolated from blood from healthy (Blue Boarder) (B) and AD patients (Red Boarder) (C). H&E staining shows structure of dermal model. Scale bar = 100 µm.

5.3.3.2 Characterisation of IC-HSE by immunohistochemistry

Two healthy patient tissue samples (SPOT0015 and SPOT0033) and one from severe AD (SPOT0018) were taken forward for immunohistochemical analysis by staining for several epidermal markers including those involved in AD (E-cadherin, CK16, CD3, filaggrin, and involucrin). In addition, IC-HSE generated from the respective subjects polarised T_H2 cells both from healthy patients and the sever AD case were also examined by immunohistochemistry. The images generated from this immunostaining are shown collated in Figure 5.10 to summarise the data. Although previous H&E staining from IC-HSE showed a more similar morphology to human skin biopsies, IHC showed a more disruptive epithelium in some cases and a fainted IHC staining, which could be due to the fact that keratinocytes are still differentiating in a IC-HSE or a problem with the antibody. The following sections provide a description of the staining observed for each protein analysed.

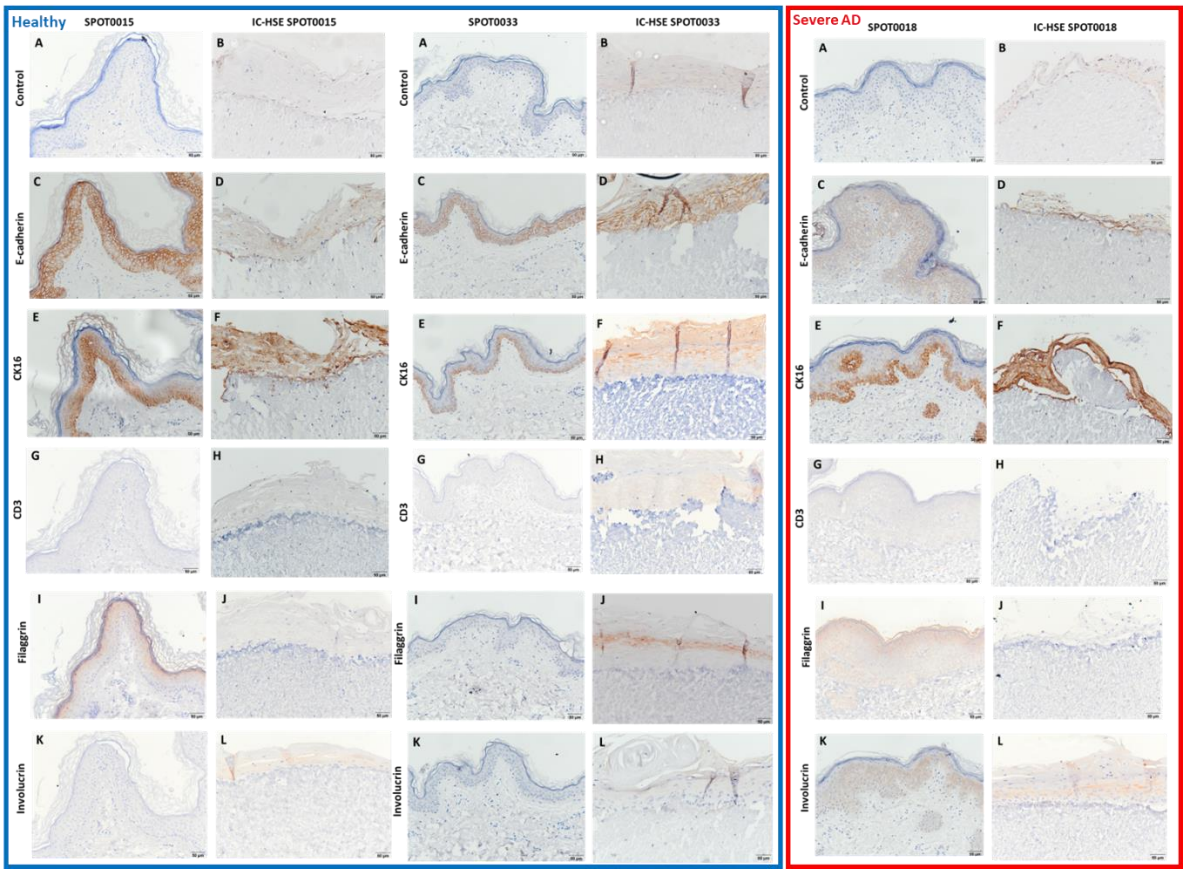

Figure 5.10 Summary of immunohistochemical staining in human skin biopsies and IC-HSE.
IC-HSE containing T_H2 cells from healthy (Blue Boarder) and AD patients (Red Boarder) were cultured for 14 days at an air-to-liquid interface and compared to their respective human skin biopsy. Image represents a summarise of the immunohistochemical staining for E-cadherin, CK16, CD3, Filaggrin and Involucrin, and compared to a control. Scale bar = 50 µm.

Control sections (i.e., those receiving secondary only antibody) displayed no specific staining; SPOT0033 showed very faint brown background staining (Figure 5.11). Immuno-positive staining of E-cadherin, a cell-cell adhesion molecule, was observed in the SPOT health subjects 0015 and 0033 at cell-to-cell contact points aligned with the plasma membrane and throughout the epidermis but not when the basal cells were in contact with the basement membrane; a staining pattern that is in line with that expected for this protein (Figure 5.12A,B,C&D). E-cadherin appeared to be less abundant in the severe AD biopsy SPOT0018 although the pattern of expression was similar to that of healthy subjects (Figure 5.12E&F). Staining for E-cadherin on IC-HSE SPOT0015 (healthy) was membrane bound but weak, whereas that for SPOT 0033 was prominent and similar to the biopsy tissue sample from this subject. The IC-HSE section from the severe AD patient was E-cadherin positive but the epidermis was largely absent. Cytokeratin 16 (CK16) immuno-positive staining was observed in the cytoplasm of the basal and suprabasal epidermal layers of both healthy and severe AD subjects (Figure 5.13). In contrast, CK16 staining in the IC-HSE models from both healthy and severe AD was prevalent throughout the entire epithelium. Indeed, SPOT0033 displayed increased CK16 in the more superficial epidermal layers and in the stratum corneum (Figure 5.13D).

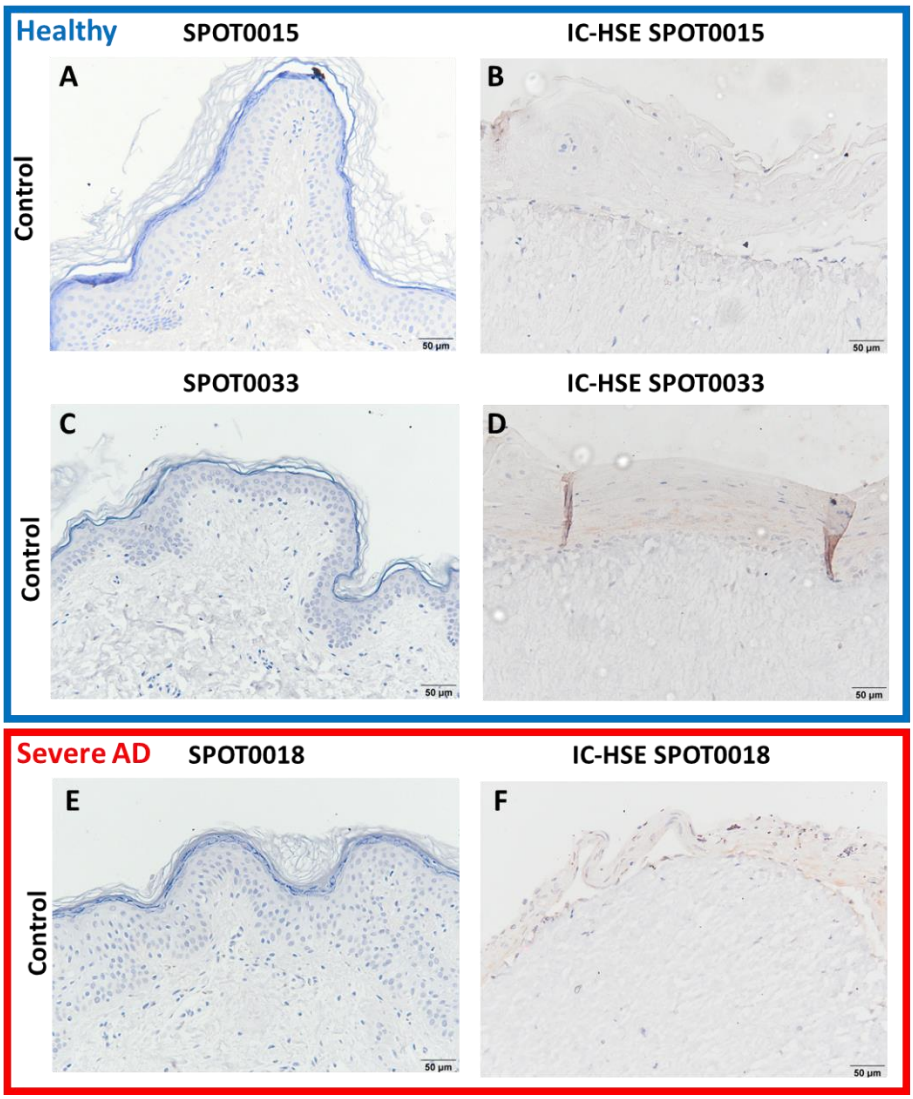

Figure 5.11 Control sections for human skin biopsies and IC-HSE.

IC-HSE containing T_H2 cells from healthy (Blue Boarder) and a severe AD patient (Red Boarder) were cultured for 14 days at an air-to-liquid interface and compared to their respective human skin biopsy. Image represents the control sections (i.e., those receiving secondary antibody only. Scale bar = 50 µm.

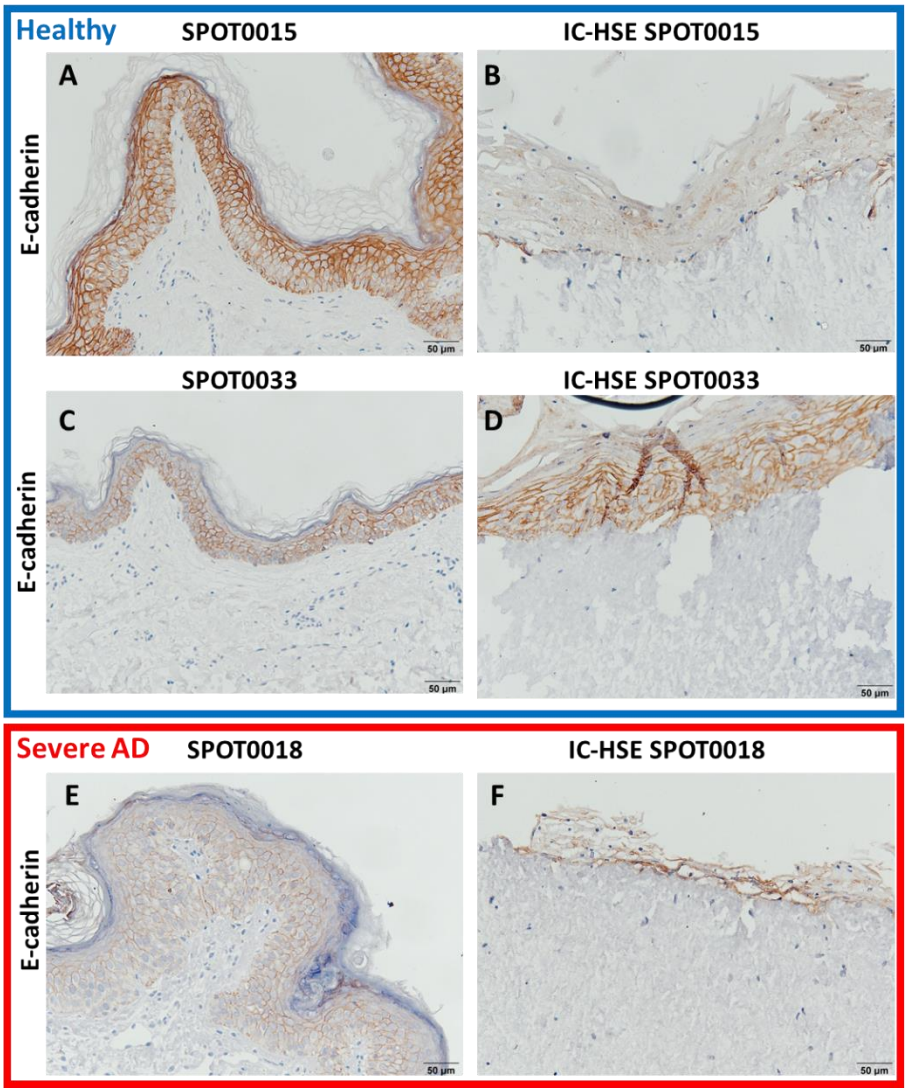

Figure 5.12 Immunohistochemical staining of E-cadherin in human skin biopsies and IC-HSE.
IC-HSE containing T_H2 cells from healthy (Blue Boarder) and a severe AD patient (Red Boarder) were cultured for 14 days at an air-to-liquid interface and compared to their respective human skin biopsy. Image represents the immunohistochemical staining for E-cadherin. Scale bar = 50 µm.

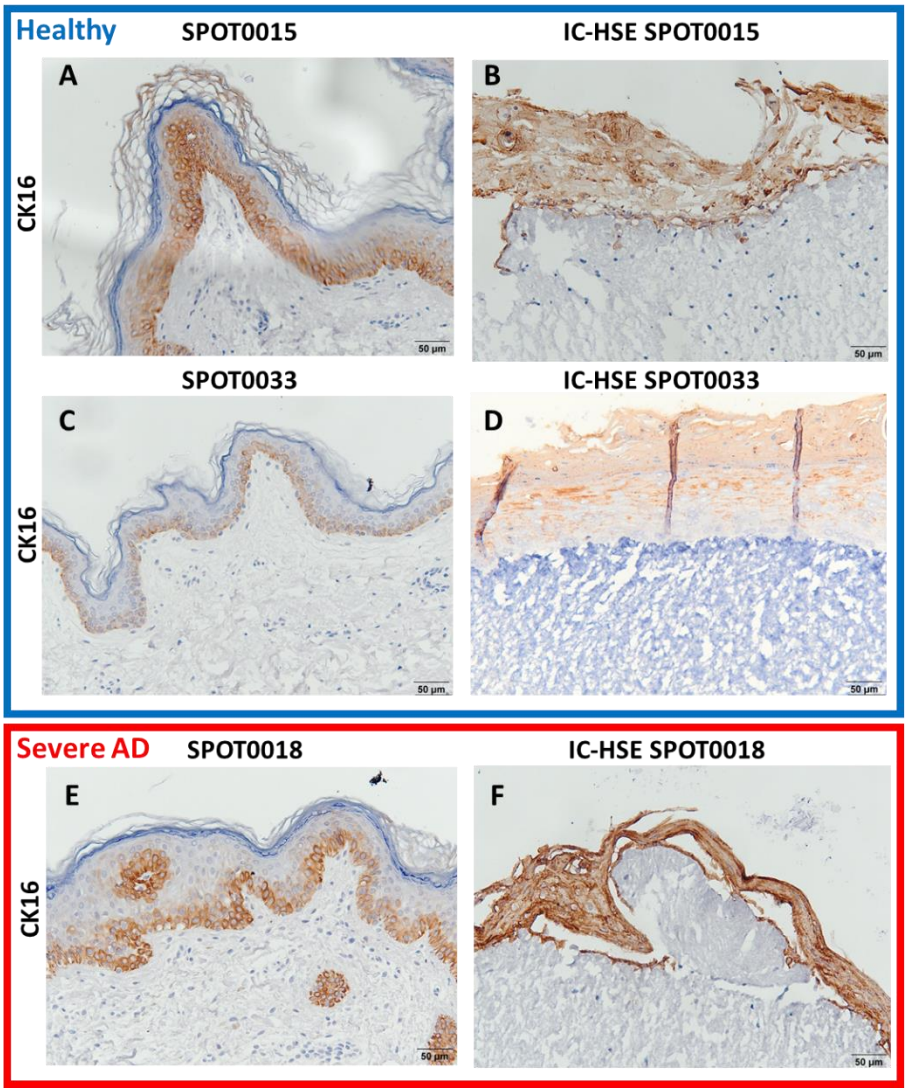

Figure 5.13 Immunohistochemical staining of CK16 in human skin biopsies and IC-HSE.
IC-HSE containing T_H2 cells from healthy (Blue Boarder) and a severe AD patient (Red Boarder) were cultured for 14 days at an air-to-liquid interface and compared to their respective human skin biopsy. Image represents the immunohistochemical staining for CK16. Scale bar = 50 µm.

Expression of CD3, the T cell receptor, was absent from all sections analysed. This was unexpected for the tissue biopsy samples as it was anticipated that T cells would be in the vicinity of the epidermis or connective tissue interface, particularly for the AD section because of known role of T cell sub-sets in the pathogenesis of AD. The staining method and antibody concentration was the same used to successfully stain T cells previously when T cells were identified in the collagen gels (Figure 5.6B). None of the IC-HSE models displayed CD3 staining, this may be due to the nature of the collagen gel layered system where the T cells would need to migrate through the collagen to reach the collagen/epidermal interface to be visible on the IHC image (Figure 5.14). Filaggrin, is a molecule that is expressed in the differentiating spinous cells with protein abundance occurring in the region of the stratum granulosum. It is known to have reduced expression in AD. Filaggrin-positive staining was observed at the expected location in healthy subject SPOT0015 but was not evident in SPOT0033. Similarly, Filaggrin-positive staining was observed around the upper spinous layers in IC-HSE SPOT0033 but not on SPOT0015 (Figure 5.15A,B,C&D). Filaggrin was largely absent and weak diffuse staining in SPOT0018, the biopsy from the severe AD patient, as might be expected, while staining was completely absent in the IC-HSE section form the same subject (Figure 5.15E&F). Staining for involucrin, another key protein expressed within the epidermis, was weak in all samples. SPOT0015 and 0033 from healthy subjects were largely involucrin negative as was IC-HSE0033, although IC-HSE0015 displayed some epidermal staining (Figure 5.16). In contrast both the biopsy from severe AD SPOT0018 and the IC-HSE0018 were weakly staining in the epidermis for involucrin. Involucrin expression was expected in the healthy skin biopsy so it is likely that sub optimal staining has occurred for staining of this protein marker.

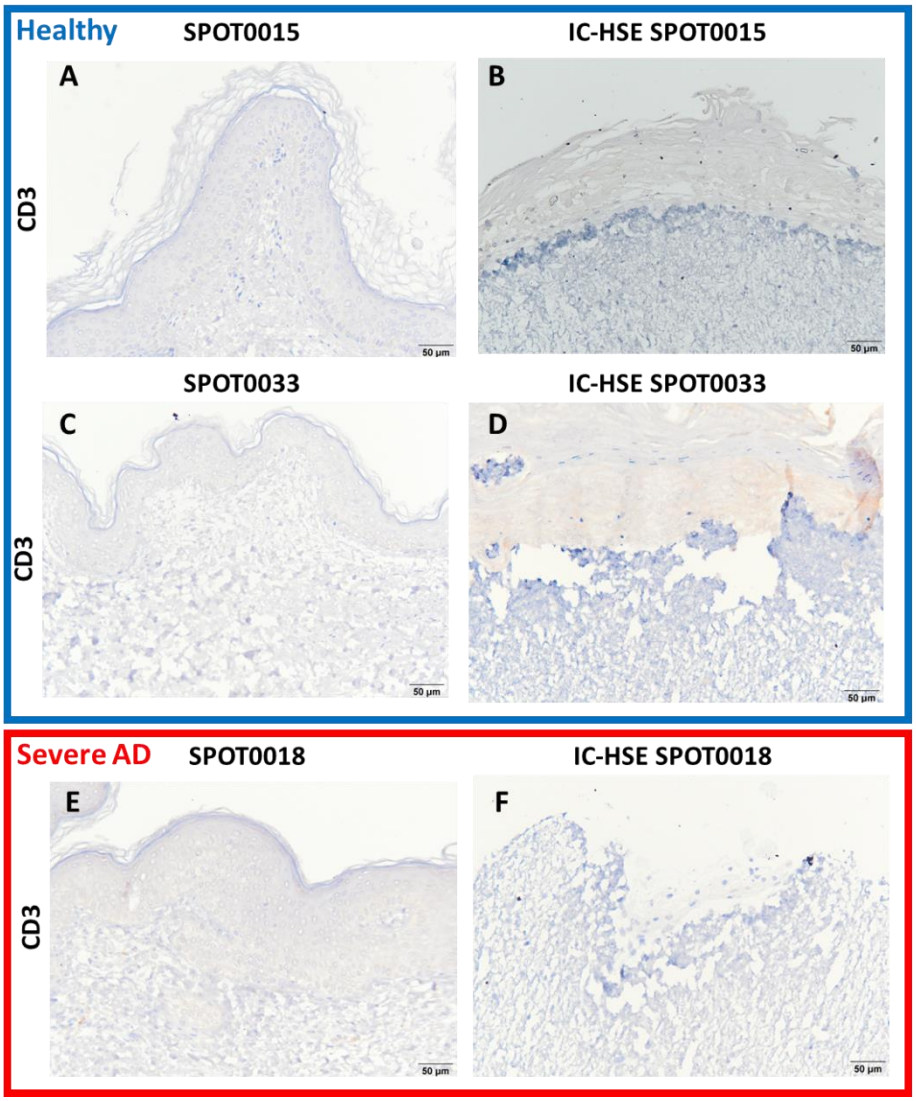

Figure 5.14 Immunohistochemical staining of CD3 in human skin biopsies and IC-HSE.
IC-HSE containing T_H2 cells from healthy (Blue Boarder) and a severe AD patient (Red Boarder) were cultured for 14 days at an air-to-liquid interface and compared to their respective human skin biopsy. Image represents the immunohistochemical staining for CD3. Scale bar = 50 µm.

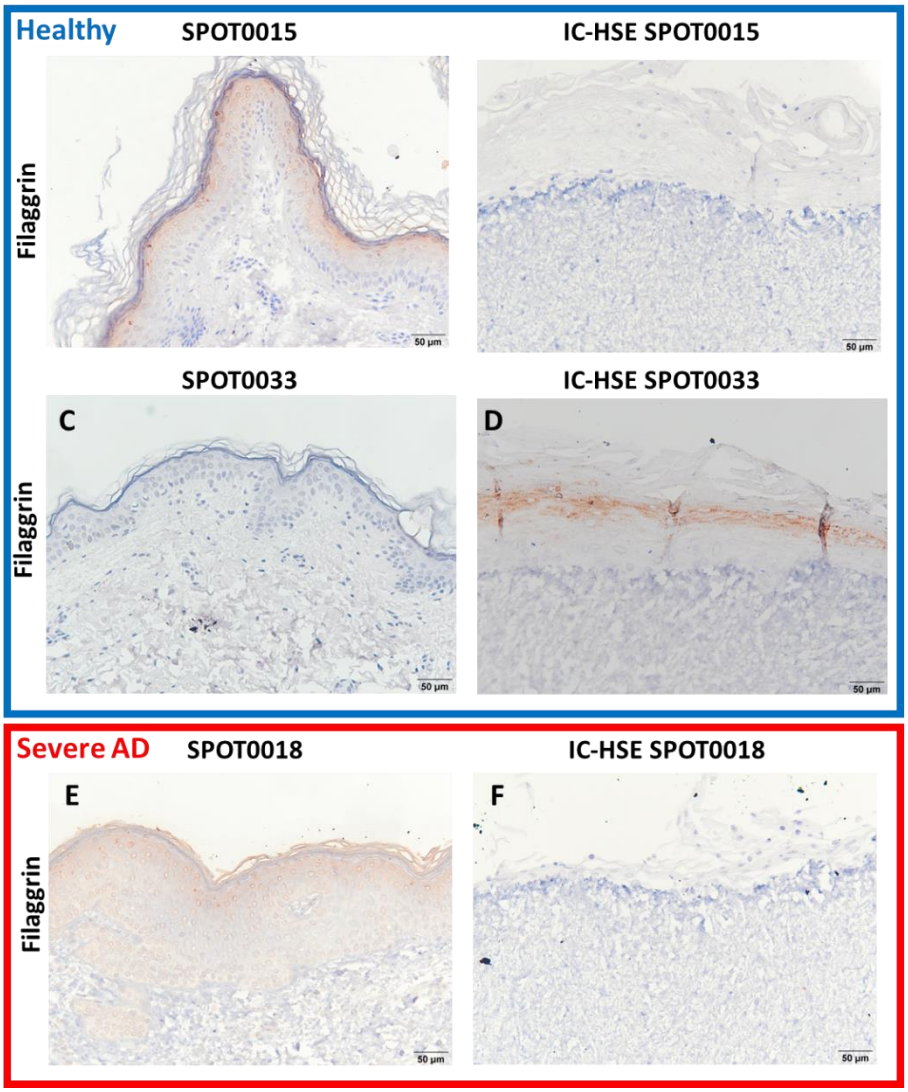

Figure 5.15 Immunohistochemical staining of Filaggrin in human skin biopsies and IC-HSE.
IC-HSE containing T_H2 cells from healthy (Blue Boarder) and a severe AD patient (Red Boarder) were cultured for 14 days at an air-to-liquid interface and compared to their respective human skin biopsy. Image represents the immunohistochemical staining for Filaggrin. Scale bar = 50 µm.

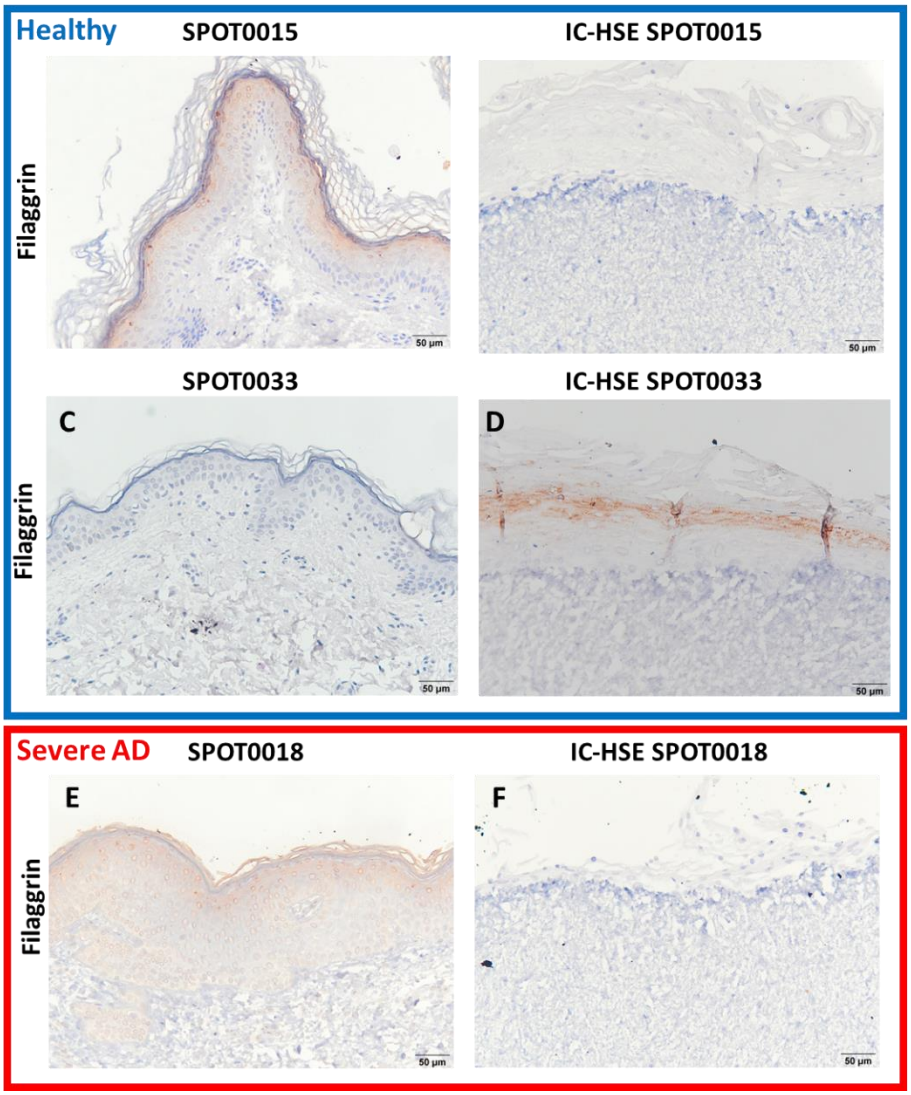

Figure 5.16 Immunohistochemical staining of Involucrin in human skin biopsies and IC-HSE.
IC-HSE containing T_H2 cells from healthy (Blue Boarder) and a severe AD patient (Red Boarder) were cultured for 14 days at an air-to-liquid interface and compared to their respective human skin biopsy. Image represents the immunohistochemical staining for Involucrin. Scale bar = 50 µm.

5.3.3.3 Characterisation of IC-HSE

Upon encounter with a foreign agent, antigen presenting cells, such as dendritic cells, will phagocytose the agent and respond by secreting inflammatory factors. Such processes occur when Langerhans cells encounter potential AD triggers, whereupon they release inflammatory factors such as TNFα as they migrate to local lymph nodes. Due to COVID-associated factors, it was not possible to add Mo-DC to the IC-HSE models and therefore exogenous cytokines were added topically to the surface of the epidermis to mimic Mo-DC release of these factors. Thus, HSE and IC-HSE containing polarised T_H2 cells from healthy patients were cultured then stimulated at day 10 with TNFα and IFNγ. The T cell specific chemokines (molecules that function to attract T cells to the lesion site) CCL5, CXCL9 and CXCL10 were measured by ELISA in the condition medium. There was an 8-fold increase in the secretion of CCL5 from IC-HSE compared to HSE that do not contain T cells (Figure 5.17A). The increased secretion of CXCL9 was more pronounced, with secretion by IC-HSE reaching nearly 3000 pg/ml compared to just 100 pg/ml for HSE only (Figure 5.17B). There was much less difference in the secretion of CXCL10 which increased from 200 pg/ml for HSE to 400 pg/ml for IC-HSE (Figure 5.17C). In all cases the secretion of T cell chemokines increased markedly in IC-HSE compared to HSE, suggesting that immune-competent HSE respond by increasing the T cell chemokine burden to recruit further T cells to the site of inflammation.

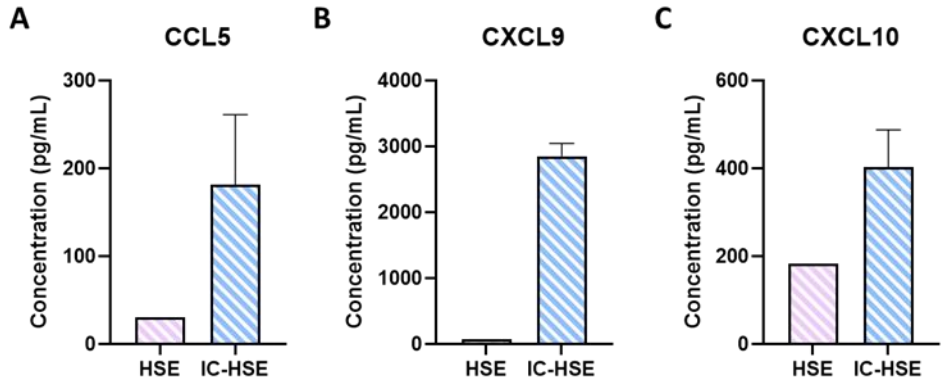

Figure 5.17 CCL5, CXCL9 and CXCL10 secretion by HSE and IC-HSE.
IC-HSE containing T_H2 cells were cultured during 14 days at air-to-liquid interface, and compared to HSE. Condition media was analysed for secretion of CCL5, CXCL9 and CXCL10 as measured by ELISA. Data are presented as mean ± SD of n=2 independent experiments for IC-HSE, and n=1 for HSE.

5.4 Discussion

5.4.1 Generation of an IC-HSE containing Mo-DC

Atopic dermatitis is a common inflammatory skin disease in which the skin becomes itchy and dry. The immunopathology of AD is a complex process as it involves an interplay between keratinocytes, dendritic cells and T cells that is crucial in increasing the cycle of inflammation.

DCs are present in the epidermis, however, during the acute phase of AD, they migrate to the dermis where they present then the antigen to naïve T cells and stimulate these to differentiate into a T_H2 phenotype by releasing cytokines such as IL-4 and IL-13.

To this date, some disease models have been constructed to mimic AD, however, they do not represent the escalatory inflammatory cycle. The current models that are available to study AD mainly focus on FLG expression, they only include naïve CD4+ T cells and/or full-thickness human skin models are generated and stimulated with cytokine cocktails that usually include IL-4 and IL-13 (Hönzke et al., 2016; Sriram et al., 2018; van Drongelen et al., 2015; Wallmeyer et al., 2017). Although, DCs have been added to HSE (Ouwehand et al., 2012), no AD-like models have been found containing DCs.

Due to the importance of DCs in AD, it was attempted to incorporate these cells into full-thickness skin models. As DCs are usually present in the epidermis of normal skin, and in order to optimise the models, Mo-DCs were incorporated into RHE-only skin equivalents, either together with N/TERT-2G or after 48 hours of generating the RHE-only skin equivalents already containing N/TERT-2G. No big differences were observed when comparing these two time points, although the epidermis seemed a bit more disrupted when adding the Mo-DC after 48 hours, therefore, Mo-DC were added together with N/TERT-2G for future experiments.

In order to study Mo-DC functionality and viability in a 3D microenvironment, RHE-only skin equivalents containing both N/TERT-2G and Mo-DC were stimulated with different DNCB concentrations ranging from 0.001 μM to 1 μM for 4 hours and 24 hours, and compared to RHE-only skin equivalents without Mo-DC. DNCB caused disruption to the stratum corneum of the RHE-only skin equivalents containing only N/TERT-2G, while the stratum corneum disappeared in those containing both N/TERT-2G and Mo-DC, compared to the untreated control. In addition, no significant increase in LDH release following treatment with DNCB was observed for both human epidermal-only skin equivalents. These data indicate that the chosen DNCB concentrations might be enough to disrupt the epithelium, even though N/TERT-2G and Mo-DC did not show response to DNCB in 2D culture. It seems that when adding Mo-DC in RHE-only skin equivalents and then stimulate them with DNCB, there could be a potential significant difference in LDH to the SDS control, nevertheless, more repeats with

other patient samples are needed. In addition, cytokine release and/or gene expression should be studied to understand if these non-toxic allergen concentrations are acting through immune cells and keratinocytes in a 3D microenvironment.

Gibbs *et al.* (2018) has previously used DNCB as a sensitizer in full-thickness human epidermis. When measuring IL-18 release, no significant differences in responses were found when compared with vehicle control. In addition, no images of the full-thickness models were included (Gibbs et al., 2018). Therefore, more experiments in this area are required to understand whether DNCB has any effect on keratinocytes and immune cells.

Human RHE-only skin equivalents lack a connective tissue and interplay with fibroblasts and so do not fully mimic human skin. Therefore, it was attempted to generate an IC-HSE containing Mo-DC in the epidermis together with N/TERT-2G, cultured on top of a fibroblast-populated collagen matrix.

Previous studies have generated IC-HSE containing the DC-like cell line MUTZ-3 and Mo-LC (Bock et al., 2018; Facy et al., 2005), but also Mo-DC (Chau et al., 2013). However, they lack other immune components and when examining the morphology of some of these models, these HSE do not seem to fully mimic the skin, appearing with a thin epidermis that is poorly stratified.

In this study, Mo-DC were added together with N/TERT-2G 48 hours after generating a collagen matrix containing fibroblasts. H&E showed Mo-DC in the epidermis, and CD68 staining showed Mo-DC throughout the collagen dermis and the epidermis, compared to the HSE with no immune cells. This suggests a possible migration of Mo-DC towards the dermis during the development. Previous studies generating HSE with LCs (Ouwehand et al., 2012) have also seen migration of these cells. Ouwehand *et al*. (2012) placed LCs underneath the dermis, and these migrated into the epidermis in about 7 days.

Unfortunately, due to the COVID-19, key reagents for the culture of Mo-DC stopped being produced. This, together with several months of lockdown and laboratory facilities closure, led to the incapability to proceed with the incorporation of Mo-DC into human skin equivalents.

5.4.2 Generation of an IC-HSE containing T_H2 cells

In AD, T cells play a crucial role in the escalatory cycle of inflammation. Naïve T cells are presented with the antigen by an APC such as DCs, which, along with other factors in the local microenvironment, polarise the naïve T cells into T_H2 cells. As mentioned above, previous HSE have included naïve CD4+ T cells or cytokine cocktails that stimulate the keratinocytes and fibroblasts into an AD phenotype, but

as yet no full-thickness models including T_H2 cells have been developed. An immunocompetent HSE containing T_H2 cells, what are considered to be the main T cell subtype in AD, was therefore developed.

To determine the optimal culture period for these IC-HSE, different culture time points were carried out. After 10 days in culture, a fully stratified epidermis was not present, and these models displayed a thin epithelium, similar to control (not shown). IC-HSE at day 10 were similar to those published previously (van Drongelen et al., 2015), in which T cells were kept in the model only for a very short amount of time (2-4 days). Therefore, the optimal culture period was around 12-14 days. Inclusion of T_H2 cells into HSE did affect the morphology of the epidermis as their morphology was different from HSE alone in terms of overall structure, stratification and cornification. This is not unexpected as presence of T_H2 cells are associated with disease phenotypes and are not usually present in disease-free skin. Indeed, it is known that the cytokines released from T_H2 cells such as IL-4 and IL-13 have a dramatic effect on the epidermis and it is likely that such cytokines are responsible for the change in epidermal phenotype in the IC-HSE models. Overexpression of T_H2 cells can also alter protein, such as FLG and involucrin, and lipid content in the skin, leading to skin barrier dysfunction. It is known that FLG is decreased in AD by upregulation of IL-4, IL-13 and IL-17A, among other cytokines. It was the intention to examine these IC-HSE models further to explore this possibility using an array of analytical techniques such as cytokine array, immunostaining and blocking antibodies, inhibitory reagents or novel compounds to see if inhibition of, for example T_H2-derived IL-4, could reverse the epidermal phenotype. It was also intended to evaluate the skin barrier function by transepidermal water loss measurement.

To take these IC-HSE models one step further, T_H2 cells were isolated from healthy and diagnosed AD subjects that participated in the SPOT study. Morphology of IC-HSE containing polarised T_H2 cells were compared to the biopsies from the same patients. HSE that did not contain T_H2 cells were similar to tissue sections from healthy subjects, whereas the addition of T_H2 cells to HSE to create IC-HSE altered the phenotype of the epidermis compared to healthy subjects. In addition, IC-HSE from healthy donors showed a thicker epithelium compared to IC-HSE from severe AD patients, in which the epithelium was absent for some of the IC-HSE. Indeed, IC-HSE from severe AD T_H2 cells appeared to cause more damage to the epithelium than IC-HSE using T_H2 cells from healthy subjects. This might be due to excessive cytokine production by these AD T_H2 cells, and impaired barrier function observed in patients with AD (Cork et al., 2009), although quantitative cytokine analysis is required to substantiate this hypothesis. Although preliminary, these data overall show that polarised T_H2 cells are able to cause damage to the epidermis. Moreover, the epidermal damage appears to increase in the presence of T_H2 cells polarised from patients with severe AD. Unfortunately, the histology of the IC-HSE was very different from that observed in the severe AD biopsy.

In addition, immunohistochemistry with several antibodies was performed to characterise IC-HSE, and compared to human skin biopsies taken from the same donor. CD3 is an important T cell co-receptor that, when together with TCR, produces the first signal necessary for the interaction with MHC peptide complex on APC, so that naïve CD4+ T cells can differentiate into T_H1 or T_H2 cells (Ariga et al., 2007). CK16 is a type I keratin usually expressed in hyperproliferative epidermal suprabasal keratinocytes and is a marker for proliferation (Kurokawa et al., 2011). E-cadherin is a key protein of cell-cell adhesions, and therefore cell junctions (Tunggal et al., 2005). Filaggrin is a protein that links keratin fibres in the stratum corneum of the epidermis (McAleer & Irvine, 2013) and involucrin is a differentiation marker usually expressed by keratinocytes in the stratum corneum (Tharakan et al., 2010).

CD3 was absent across human skin biopsies and IC-HSE from all participants. This could have been due to low exposure time to the antibody or low antibody concentration, among others (Barberis et al., 2018). CK16, E-cadherin and involucrin were present in both IC-HSE and human skin biopsies. CK16 is usually expressed in suprabasal epidermis of normal skin (Niehues et al., 2017) and its expression is increased and present in the upper epidermal layers in the skin of patients with psoriasis and inflammatory linear verrucous epidermal nevus (de Jongh et al., 2005; Kolesnik et al., 2018), therefore, it would be expected to be also upregulated in patients with AD, as CK16 is indicative of epidermal hyperplasia (Peng et al., 2017; Ungar et al., 2017). However, CK16 was expressed in both healthy and AD human skin biopsies, and across the entire epithelium in IC-HSE. E-cadherin is expressed in normal skin in cell-cell junctions in all layers of the epidermis, while it is usually localised in the plasma membrane in atopic dermatitis (Maretzky et al., 2008; Nelson et al., 2019). Indeed, E-cadherin was expressed in all layers for both healthy and AD human skin biopsies where its expression was decreased in IC-HSE. Involucrin is usually overexpressed in atopic dermatitis, compared to normal skin (Fölster-Holst et al., 2021), however the staining was faint, so no conclusions can be drawn. Filaggrin expression seems to be dependent on the presence or absent of FLG mutation in AD patients (Nemoto-Hasebe et al., 2009). Filaggrin was stained in most human skin biopsies, however it was not observed in IC-HSE. More work is required here to optimise the number of T_H2 cells added, culture conditions and the mechanisms of epidermal damage. This would also necessitate increased sample numbers and expansion of the immunohistochemistry work with additional controls to build confidence into the data obtained from this analysis.

Finally, T cell chemokine release was measured by ELISA in the condition medium, upon stimulation with TNFα and IFNγ. CCL5 is a CC chemokine that interacts with G-protein-coupled receptors such as CCR5 and CCR1. CCL5 has been shown to act via CCR5 on naïve CD4+ T cells to induce T_H2 cell polarisation (Q. Zhang et al., 2015). CXCL9 and CXCL10 are selective ligands for CXCR3 and they are mainly secreted upon stimulation with IFNγ, participating in the regulation of immune cell migration,

differentiation, and activation (Tokunaga et al., 2018). CCL5, CXCL9 and CXCL10 were highly secreted by the IC-HSE comparted to the HSE, suggesting the presence of an immune response in the IC-HSE compared to the HSE, and suggest a positive feedback mechanism whereby recruitment of T cells leads to secretion of more T cell chemokines further enhancing T cell recruitment, which may lead to disease chronicity. Further analysis and experimentation are required on this front to confirm these initial findings.

5.5 Conclusion

In this chapter, IC-HSE containing polarised T_H2 in combination with a fibroblast-populated connective tissue topped by a stratified epidermis was successfully constructed, was viable and produced a functional model whereby cells interacted with one another to cause alterations in the structure and morphology of the epidermis. Although there are shortcomings in the histological structure of the IC-HSE models compared to AD tissue, there is clear evidence that addition of T_H2 cells, in particular from AD subjects, alters the epidermal state. This is a positive step forward for the production of human AD-like *in vitro* models. Addition of DC into these IC-HSE would be a further advantage, as would be models made from the same genetic background. Further work is required to optimise and refine these models to more resemble AD *in vivo*, hopefully in a non-COVID impacted future.

Chapter 6 - Final conclusions and future work

6.1 Final conclusions

The innate immune system is the body's first line of defence against pathogens, however, it can be dysregulated in disorders such as atopic dermatitis, causing penetration of proteases and allergens through the epidermis leading to increased serum IgE levels, elevated T_H2-type cytokine secretion, and overexpression of FcεRI on Langerhans cells and inflammatory dendritic cells (Boguniewicz & Leung, 2011). In patients with AD, a down-regulation of FLG, an important marker of keratinocyte differentiation and maintenance of stratum corneum and skin barrier integrity, has been observed (McPherson, 2016; Rerknimitr et al., 2017). The pathophysiology of AD is therefore a complex process and genetically determined, making the development of a complete cure very difficult. Most of the treatments available consist of topical corticosteroids and use of emollients to relieve the symptoms (Zuberbier et al., 2006), thus new therapies are needed to improve the disease's long-term control. To identify new drugs and treatments, new models that mimic AD are required, as the mouse models available usually exhibit significantly different responses to drug treatments, resulting in high drug development failure (A. Tanaka et al., 2012). In addition, human skin models that have been generated are just often stimulated with cytokine cocktails including IL-4 and IL-13 (Rouaud-Tinguely et al., 2015) to mimic the AD inflammation cytokine release which is an over-simplification. Current HSE are used to study FLG (Mildner et al., 2006), importantly they lack some immune component (Wallmeyer et al., 2017) and so development of current models is required.

The overall aim of this ambitions study was to develop a more realistic *in vitro* model of AD by combining current skin tissue engineering knowledge and developing this using immune cells that are directly involved in AD pathogenesis. The first chapter described the generation of Mo-DC and T_H2 cells from peripheral blood monocytes. These cells were studied because they are the main immune cell types involved in the immunopathology of AD (Egawa & Weninger, 2015). Here, naïve CD4+ T cells were successfully isolated from mononuclear cells and differentiated into T_H2 cells. In addition, monocytes were successfully differentiated into MDM and Mo-DC phenotypes. Mo-DC and T_H2 cells were characterised for gene and surface protein expression. Mo-DC and skin keratinocytes were challenged with increasing non-toxic doses of allergens DNCB and Derp1, because few studies in human primary cells have been done previously. However, due to the marked donor variability, especially for Mo-DC, no conclusion could be formed. Naïve CD4+ T cells were cultured together with Mo-DC and stimulated with TSLP with or without DNCB in order to stimulate the naïve CD4+ T cells and differentiate them into T_H2 cells. As before, very little changes in gene and surface protein expression were present. DNCB, Derp1 and TSLP may stimulate Mo-DC to secrete cytokines that could potentially activate naïve CD4+ T cells causing them to differentiate into T_H2 cells. Further work is required in this area. Mo-LC could not be differentiated from monocytes. Gene and surface protein

expression showed similarities to Mo-DC data, suggesting lack of differentiation towards Mo-LC phenotype. As langerin/CD207 is not a specific marker for LCs, additional experiments such as looking at Birbeck granules (Romani et al., 2010) would be needed to confirm the possible differentiation of Mo-LC from monocytes.

The subsequent work presented in this thesis aimed to study keratinocytes response upon challenge stimulation, generation of epithelial models, and optimisation of full thickness HSE. N/TERT-2G were stimulated with increasing non-toxic doses of DNCB and Derp1, and although significant increases in LDH release were observed for the SDS control, no differences in gene expression were observed for different allergen doses, suggesting that it is the immune cells that respond to these allergens and the keratinocytes are mainly activated by the inflammatory cytokines release in the immune response.

N/TERT-2G and N/TERT-1 were used to successfully generate RHE-only HSE, which were also characterised for different epidermal development markers. IHC showed similar results to RHE and HSE previously developed with the same cells (Reijnders et al., 2015; Smits et al., 2017; van Drongelen, Danso, et al., 2014). Some differences were observed between N/TERT-1 and N/TERT-2G RHE skin equivalents. CK14 was expressed across all epithelium in N/TERT-1 RHE skin equivalents, while it was mainly present in basal cells in N/TERT-2G; and FLG and involucrin showed increased expression in N/TERT-2G RHE skin equivalents. N/TERT-2G were used to optimise the generation of full-thickness HSE. Morphology of HSE was then compared to human skin. H&E and IHC showed similar features between HSE including either N/TERT-1 or N/TERT-2G and human skin. These data support the use of Immortalised skin keratinocytes for HSE production and this data should encourage others to move toward 3D biology for skin research, making it more accessible and less reliant on access to primary human tissue.

The most challenging part of this was the development of IC-HSE using immune cells characterised in chapter 3. This was made even harder by the COIVD pandemic which stopped and then severely hampered experiments whilst also having a significant impact on morale. Mo-DC were first incorporated together with N/TERT-2G in a RHE-only skin equivalent. Although differences in morphology could be observed, no statistically significant differences between DNCB doses were found. Further work to confirm presence of immune response is required. Mo-DC were then seeded on top while T_H2 cells were included in a fibroblast-populated collagen matrix. CD68 and CD3 positive immunostaining confirmed the presence of these cells. IC-HSE containing T_H2 cells were generated using T_H2 cells isolated from healthy and AD participants, and compared to human skin biopsies from the same patients. Some positive immunohistochemical and histological data was observed giving promising proof-of-principle data but this needs much additional work and more repeat experiments

which are beyond the time-limit of this thesis. IC-HSE were stimulated with TNFα and IFNγ to generate the immune response, and functionality was successfully determined by cytokine release measurement. Mo-DC could not be further included in IC-HSE as key reagents used to generate Mo-DC were not further available after the COVID-19 pandemic. Further characterisation and inclusion of Mo-DC should be included to better understand the immunopathology of AD.

Developing a more complex immunocompetent human skin equivalent of AD is important because it provides a platform to better understand the immunopathology of AD, and for the further development and testing of therapeutic drugs and treatments. Three-dimensional *in vitro* models mimic tissues and are better representatives for drug metabolism than 2D cultures. The use of 3D *in vitro* models for drug development and testing will significantly aid the selection of drug candidates before going to clinical phases, decreasing the failure rate of drugs in clinical trials, as they can predict toxicity and efficacy. This helps reducing, and sometimes even replacing, the use of animals in research, which is in line with the "3Rs (Reduction, Refinement and Replacement)". In addition, when generating human skin equivalents, human primary cells and stem cells can be incorporated, allowing the development of patient-specific models. These models allow a more accurate study of cell interactions, stem cells, cancer and pathophysiology of many disorders (Badr-Eldin et al., 2022). The usefulness and the potential of these in vitro models cannot be underscored. They have already made a significant impact in skin research, moving researcher away from 2D monolayer experimental models to more realistic 3D tissue. Better, more advanced 3D models will become the mainstream and acceptable in vitro model in the next few years and will significantly aid drug development.

However, 3D cultures have also some limitations. Their culture can take weeks before harvesting the models, they are complex and expensive. Specifically in our model, when using primary cells, the reproducibility of these models is difficult due to patient-to-patient variability, as well as the absence of cell proliferation after differentiation. Also, isolating primary monocytes repeatedly takes time, restricting scalability for applications that require mass production. In comparison, the use of cell lines such as Jurkat or MUTZ-3 offer superior reproducibility and can be scaled, making them desirable for usage in industry, although all currently available human monocyte/dendritic cell/T cell lines are generated from cancers and many not completely simulate healthy cells. Another limitation in this study is the HLA response, as immune cells and fibroblasts were isolated from two different donors, and the keratinocytes were a cell line.

An alternative option to these limitations would be to generate and use human immortalised immune cell lines from primary cells as they would probably show better response to inflammatory stimuli. Another option would be the use of induced pluripotent humans stem cells (iPSCs), as they can be

generated from any cell type by reprogramming with a series of transcription factors. The resulting iPSCs can be used to generate different subtypes such as immune cells or keratinocytes, and therefore, all the cells present in the model would be derived from the same patient and have the same genetic background in all cells increasing immune compatibility. Although this model is still useful for looking at local inflammation and testing anti-inflammatory drugs, it does not fully mimic the pathophysiology of AD, as it lacks other immune cells.

The work presented in this thesis is the first to describe the development of an IC-HSE containing T_H2 cells from healthy and AD patients, and that these models display an altered phenotype compared to those not containing T_H2 cells. This provides a solid foundation for others interesting in tacking these tissue-engineered models forward.

6.2 Future work

Firstly, in this thesis, Mo-LC were not fully characterised, therefore, looking for the presence of Birbeck granules at the electron microscope would be the best approach to differentiate Mo-LC from Mo-DC. However, Mo-DC and T_H2 cells were isolated from mononuclear cells and characterised for specific markers, although their functionality and viability was not fully confirmed. To take this further, cytokine release studies would be carried out when cultured separately and as a co-culture. More specifically, a T_H2 cytokine array would be used, including cytokines such as IL-4, IL-5, IL-6, IL-13, TSLP, CCL17 or CCL22 among others. This would ideally be replicated in patients with AD and healthy, so differences between cells isolated from AD patients and healthy donors would be compared. To do this, cells from both AD and healthy patients would be isolated and then differentiated, cultured separately and/or as a co-culture, and condition medium would be used to study cytokine release. In addition, a bigger sample size could be used, as large patient-to-patient variability was observed. Since sensitization to allergens is a key element of AD pathophysiology, participants with known allergy to HDM and controls would be selected to stimuli the cells with different allergens.

In addition, N/TERT-2G keratinocytes functionality and viability upon stimuli challenge was not characterised, therefore, T_H2 cytokine array would be used for cytokine release study, which would be carried out to confirm whether the immune response is only produced by immune cells or whether keratinocytes are also involved.

Regarding RHE skin equivalents, HSE and IC-HSE, immune response upon allergen stimulation would be studied. As T_H2 phenotype is the main one observed in AD, a cytokine array specific for cytokines released by these cells could be used. Furthermore, Mo-DC isolated from the same donors than T_H2

cells would be included in the IC-HSE to mimic AD immunopathology. If having access to skin samples from AD and healthy patients, IC-HSE using fibroblasts, keratinocytes, Mo-DC and T_H2 cells would be developed and compared to human skin biopsies from the same patients. To generate this model, fibroblasts, keratinocytes and T_H2 cells would be added as described in chapter 5 of this thesis, and Mo-DC would be added together with the keratinocytes on top of the fibroblasts-embedded collagen matrix. Available drugs to relieve symptoms in patients with AD would be tested in our models.

6.3 COVID-19 impact statement.

The CVIS pandemic had an enormous impact on this completion of this project. When the COVID-19 started, development of IC-HSE containing Mo-DC and T_H2 cells had just begun. These cells were isolated from blood from NHS donors in order to optimise both 2D and 3D culture, although we were planning to start isolating these cells from healthy and AD patients participating in a clinical trial. In addition, volunteers with allergy to HDM had been identified to check whether cells isolated from their blood would show any response to Derp1 in the laboratory. However, with the COVID-19 outbreak, buffy coats and sample collection was halted and the clinical trial had to be postponed. Since immune cells were central to this study, work was completely inhibited. In addition, electron microscopy training, along with any other lab training, was stopped and so planned work to identify Birbeck granules present in the Langerhans cells was curtailed. Moreover, training was not available when restrictions started to be lifted. Furthermore, key consumables to carry out experiments were not in stock and some consumables, such as the coated plates used to culture the Mo-DC, stopped being produced, preventing the culture of Mo-DC and, consequently, their inclusion in IC-HSE.

Five months of total lockdown and endless months of restricted working (sometimes 10 hours per week allowed in the laboratory), along with reagent and immune cell restrictions made life as a postgraduate researcher very difficult. It takes 4 hours to isolate T cells – this constituted half the available working time in the lab for a week. Needless to state obtaining data in that latter period of this PhD was a struggle. To compound matters only three months of extension were awarded, and with half of the funding, making it more difficult to complete the project to a satisfactory conclusion. Despite these challenges I have learnt much and my enthusiasm for science has grown.

References

Abraham, J., & Mathew, S. (2019). Merkel Cells: A Collective Review of Current Concepts. *International Journal of Applied & Basic Medical Research*, *9*(1), 9–13. https://doi.org/10.4103/ijabmr.IJABMR_34_18

Acheva, A., Ghita, M., Patel, G., Prise, K. M., & Schettino, G. (2014). Mechanisms of DNA Damage Response to Targeted Irradiation in Organotypic 3D Skin Cultures. *PLoS ONE*, *9*(2), e86092. https://doi.org/10.1371/journal.pone.0086092

Acheva, A., Schettino, G., & Prise, K. M. (2017). Pro-inflammatory Signaling in a 3D Organotypic Skin Model after Low LET Irradiation—NF-κB, COX-2 Activation, and Impact on Cell Differentiation. *Frontiers in Immunology*, *8*. https://doi.org/10.3389/fimmu.2017.00082

Ahn, A. C., & Kaptchuk, T. J. (2011). Spatial anisotropy analyses of subcutaneous tissue layer: Potential insights into its biomechanical characteristics. *Journal of Anatomy*, *219*(4), 515–524. https://doi.org/10.1111/j.1469-7580.2011.01407.x

Ainscough, J. S., Frank Gerberick, G., Zahedi-Nejad, M., Lopez-Castejon, G., Brough, D., Kimber, I., & Dearman, R. J. (2014). Dendritic cell IL-1α and IL-1β are polyubiquitinated and degraded by the proteasome. *The Journal of Biological Chemistry*, *289*(51), 35582–35592. https://doi.org/10.1074/jbc.M114.595686

Al-Amodi, O., Jodeleit, H., Beigel, F., Wolf, E., Siebeck, M., & Gropp, R. (2018). CD1a-Expressing Monocytes as Mediators of Inflammation in Ulcerative Colitis. *Inflammatory Bowel Diseases*, *24*(6), 1225–1236. https://doi.org/10.1093/ibd/izy073

Al-Shobaili, H. A., Ahmed, A. A., Alnomair, N., Alobead, Z. A., & Rasheed, Z. (2016). Molecular Genetic of Atopic dermatitis: An Update. *International Journal of Health Sciences*, *10*(1), 96–120.

Amin, K. (2012). The role of mast cells in allergic inflammation. *Respiratory Medicine*, *106*(1), 9–14. https://doi.org/10.1016/j.rmed.2011.09.007

Andersen, M. H., Schrama, D., Thor Straten, P., & Becker, J. C. (2006). Cytotoxic T cells. *The Journal of Investigative Dermatology*, *126*(1), 32–41. https://doi.org/10.1038/sj.jid.5700001

Anderson, C. A., Patel, P., Viney, J. M., Phillips, R. M., Solari, R., & Pease, J. E. (2020). A degradatory fate for CCR4 suggests a primary role in Th2 inflammation. *Journal of Leukocyte Biology*, *107*(3), 455–466. https://doi.org/10.1002/JLB.2A0120-089RR

Ariga, H., Shimohakamada, Y., Nakada, M., Tokunaga, T., Kikuchi, T., Kariyone, A., Tamura, T., & Takatsu, K. (2007). Instruction of naive CD4+ T-cell fate to T-bet expression and T helper 1 development: Roles of T-cell receptor-mediated signals. *Immunology*, *122*(2), 210–221. https://doi.org/10.1111/j.1365-2567.2007.02630.x

Aslantürk, Ö. S. (2018). In Vitro Cytotoxicity and Cell Viability Assays: Principles, Advantages, and Disadvantages. In M. L. Larramendy & S. Soloneski (Eds.), *Genotoxicity—A Predictable Risk to Our Actual World*. InTech. https://doi.org/10.5772/intechopen.71923

Badr-Eldin, S. M., Aldawsari, H. M., Kotta, S., Deb, P. K., & Venugopala, K. N. (2022). Three-Dimensional In Vitro Cell Culture Models for Efficient Drug Discovery: Progress So Far and Future Prospects. *Pharmaceuticals*, *15*(8), 926. https://doi.org/10.3390/ph15080926

Balan, S., Saxena, M., & Bhardwaj, N. (2019). Dendritic cell subsets and locations. In *International Review of Cell and Molecular Biology* (Vol. 348, pp. 1–68). Elsevier. https://doi.org/10.1016/bs.ircmb.2019.07.004

Banno, T., Gazel, A., & Blumenberg, M. (2004). Effects of Tumor Necrosis Factor-α (TNFα) in Epidermal Keratinocytes Revealed Using Global Transcriptional Profiling. *Journal of Biological Chemistry*, *279*(31), 32633–32642. https://doi.org/10.1074/jbc.M400642200

Bao, K., & Reinhardt, R. L. (2015). The differential expression of IL-4 and IL-13 and its impact on type-2 immunity. *Cytokine*, *75*(1), 25–37. https://doi.org/10.1016/j.cyto.2015.05.008

Barberis, M., Helikar, T., & Verbruggen, P. (2018). Simulation of Stimulation: Cytokine Dosage and Cell Cycle Crosstalk Driving Timing-Dependent T Cell Differentiation. *Frontiers in Physiology*, *9*, 879. https://doi.org/10.3389/fphys.2018.00879

Bauer, J., Bahmer, F. A., Wörl, J., Neuhuber, W., Schuler, G., & Fartasch, M. (2001). A Strikingly Constant Ratio Exists Between Langerhans Cells and Other Epidermal Cells in Human Skin. A Stereologic Study Using the Optical Disector Method and the Confocal Laser Scanning Microscope11Presented in part at the International Investigative Dermatology 1998, Cologne, Germany 1998. *Journal of Investigative Dermatology*, *116*(2), 313–318. https://doi.org/10.1046/j.1523-1747.2001.01247.x

Beck, L. A., Tancowny, B., Brummet, M. E., Asaki, S. Y., Curry, S. L., Penno, M. B., Foster, M., Bahl, A., & Stellato, C. (2006). Functional Analysis of the Chemokine Receptor CCR3 on Airway Epithelial Cells. *The Journal of Immunology*, *177*(5), 3344–3354. https://doi.org/10.4049/jimmunol.177.5.3344

Bell, D. C., & Brown, S. J. (2017). Atopic eczema treatment now and in the future: Targeting the skin barrier and key immune mechanisms in human skin. *World Journal of Dermatology*, *6*(3), 42. https://doi.org/10.5314/wjd.v6.i3.42

Beltrani, V. S. (2002). Clinical features of atopic dermatitis. *Immunology and Allergy Clinics of North America*, *22*(1), 25–42. https://doi.org/10.1016/S0889-8561(03)00067-5

Bender, A. (2004). Differentiation of human monocytes in vitro with granulocyte–macrophage colony-stimulating factor and macrophage colony-stimulating factor produces distinct changes in cGMP phosphodiesterase expression. *Cellular Signalling*, *16*(3), 365–374. https://doi.org/10.1016/j.cellsig.2003.08.009

Benhadou, F., Mintoff, D., & del Marmol, V. (2019). Psoriasis: Keratinocytes or Immune Cells – Which Is the Trigger? *Dermatology*, *235*(2), 91–100. https://doi.org/10.1159/000495291

Berroth, A., Kühnl, J., Kurschat, N., Schwarz, A., Stäb, F., Schwarz, T., Wenck, H., Fölster-Holst, R., & Neufang, G. (2013). Role of fibroblasts in the pathogenesis of atopic dermatitis. *Journal of Allergy and Clinical Immunology*, *131*(6). https://doi.org/10.1016/j.jaci.2013.02.029

Bertrand-Vallery, V., Belot, N., Dieu, M., Delaive, E., Ninane, N., Demazy, C., Raes, M., Salmon, M., Poumay, Y., Debacq-Chainiaux, F., & Toussaint, O. (2010). Proteomic Profiling of Human Keratinocytes Undergoing UVB-Induced Alternative Differentiation Reveals TRIpartite Motif Protein 29 as a Survival Factor. *PLoS ONE*, *5*(5), e10462. https://doi.org/10.1371/journal.pone.0010462

Bhat, P., Leggatt, G., Waterhouse, N., & Frazer, I. H. (2017). Interferon-γ derived from cytotoxic lymphocytes directly enhances their motility and cytotoxicity. *Cell Death & Disease*, *8*(6), e2836. https://doi.org/10.1038/cddis.2017.67

Bieber, T. (2008). Atopic Dermatitis. *New England Journal of Medicine*, *358*(14), 1483–1494. https://doi.org/10.1056/NEJMra074081

Bieber, T. (2010). Atopic dermatitis. *Annals of Dermatology*, *22*(2), 125–137. https://doi.org/10.5021/ad.2010.22.2.125

Bieber, T. (2022). Atopic dermatitis: An expanding therapeutic pipeline for a complex disease. *Nature Reviews Drug Discovery*, *21*(1), 21–40. https://doi.org/10.1038/s41573-021-00266-6

Biedermann, T., Skabytska, Y., Kaesler, S., & Volz, T. (2015). Regulation of T Cell Immunity in Atopic Dermatitis by Microbes: The Yin and Yang of Cutaneous Inflammation. *Frontiers in Immunology*, *6*, 353. https://doi.org/10.3389/fimmu.2015.00353

Bin, L., & Leung, D. Y. M. (2016). Genetic and epigenetic studies of atopic dermatitis. *Allergy, Asthma, and Clinical Immunology: Official Journal of the Canadian Society of Allergy and Clinical Immunology*, *12*, 52. https://doi.org/10.1186/s13223-016-0158-5

Bitton, A., Avlas, S., Reichman, H., Itan, M., Karo-Atar, D., Azouz, N. P., Rozenberg, P., Diesendruck, Y., Nahary, L., Rothenberg, M. E., Benhar, I., & Munitz, A. (2020). A key role for IL-13 signaling via the type 2 IL-4 receptor in experimental atopic dermatitis. *Science Immunology*, *5*(44), eaaw2938. https://doi.org/10.1126/sciimmunol.aaw2938

Bock, S., Said, A., Müller, G., Schäfer-Korting, M., Zoschke, C., & Weindl, G. (2018). Characterization of reconstructed human skin containing Langerhans cells to monitor molecular events in skin sensitization. *Toxicology in Vitro*, *46*, 77–85. https://doi.org/10.1016/j.tiv.2017.09.019

Bodnar, A. G., Ouellette, M., Frolkis, M., Holt, S. E., Chiu, C.-P., Morin, G. B., Harley, C. B., Shay, J. W., Lichtsteiner, S., & Wright, W. E. (1998). Extension of Life-Span by Introduction of Telomerase into Normal Human Cells. *Science*, *279*(5349), 349–352. https://doi.org/10.1126/science.279.5349.349

Boer, M., Duchnik, E., Maleszka, R., & Marchlewicz, M. (2016). Structural and biophysical characteristics of human skin in maintaining proper epidermal barrier function. *Advances in Dermatology and Allergology*, *1*, 1–5. https://doi.org/10.5114/pdia.2015.48037

Boguniewicz, M., & Leung, D. Y. M. (2011). Atopic dermatitis: A disease of altered skin barrier and immune dysregulation: Immune response in atopic dermatitis. *Immunological Reviews*, *242*(1), 233–246. https://doi.org/10.1111/j.1600-065X.2011.01027.x

Borowczyk, J., Shutova, M., Brembilla, N. C., & Boehncke, W.-H. (2021). IL-25 (IL-17E) in epithelial immunology and pathophysiology. *Journal of Allergy and Clinical Immunology*, *148*(1), 40–52. https://doi.org/10.1016/j.jaci.2020.12.628

Boyce, S. T., & Lalley, A. L. (2018). Tissue engineering of skin and regenerative medicine for wound care. *Burns & Trauma*, *6*. https://doi.org/10.1186/s41038-017-0103-y

Bradley, J. (2008). TNF-mediated inflammatory disease. *The Journal of Pathology*, *214*(2), 149–160. https://doi.org/10.1002/path.2287

Brodin, P., & Davis, M. M. (2017). Human immune system variation. *Nature Reviews. Immunology*, *17*(1), 21–29. https://doi.org/10.1038/nri.2016.125

Brown, T. M., & Krishnamurthy, K. (2022). Histology, Dermis. In *StatPearls*. StatPearls Publishing. http://www.ncbi.nlm.nih.gov/books/NBK535346/

Bumbacea, R. S., Corcea, S. L., Ali, S., Dinica, L. C., Fanfaret, I. S., & Boda, D. (2020). Mite allergy and atopic dermatitis: Is there a clear link? (Review). *Experimental and Therapeutic Medicine*, *20*(4), 3554–3560. https://doi.org/10.3892/etm.2020.9120

Candi, E., Schmidt, R., & Melino, G. (2005). The cornified envelope: A model of cell death in the skin. *Nature Reviews Molecular Cell Biology*, *6*(4), 328–340. https://doi.org/10.1038/nrm1619

Carlson, M. W., Alt-Holland, A., Egles, C., & Garlick, J. A. (2008). Three-Dimensional Tissue Models of Normal and Diseased Skin. *Current Protocols in Cell Biology*, *41*(1). https://doi.org/10.1002/0471143030.cb1909s41

Cechim, G., & Chies, J. A. B. (2019). In vitro generation of human monocyte-derived dendritic cells methodological aspects in a comprehensive review. *Anais Da Academia Brasileira de Ciências*, *91*(4), e20190310. https://doi.org/10.1590/0001-3765201920190310

Celebi Sözener, Z., Cevhertas, L., Nadeau, K., Akdis, M., & Akdis, C. A. (2020). Environmental factors in epithelial barrier dysfunction. *Journal of Allergy and Clinical Immunology*, *145*(6), 1517–1528. https://doi.org/10.1016/j.jaci.2020.04.024

Cernadas, M., Lu, J., Watts, G., & Brenner, M. B. (2009). CD1a expression defines an interleukin-12 producing population of human dendritic cells. *Clinical and Experimental Immunology*, *155*(3), 523–533. https://doi.org/10.1111/j.1365-2249.2008.03853.x

Chaffey, N. (2003). Alberts, B., Johnson, A., Lewis, J., Raff, M., Roberts, K. and Walter, P. Molecular biology of the cell. 4th edn. *Annals of Botany*, *91*(3), 401–401. https://doi.org/10.1093/aob/mcg023

Chau, D. Y. S., Johnson, C., MacNeil, S., Haycock, J. W., & Ghaemmaghami, A. M. (2013). The development of a 3D immunocompetent model of human skin. *Biofabrication*, *5*(3), 035011. https://doi.org/10.1088/1758-5082/5/3/035011

Chen, L., & Flies, D. B. (2013). Molecular mechanisms of T cell co-stimulation and co-inhibition. *Nature Reviews Immunology*, *13*(4), 227–242. https://doi.org/10.1038/nri3405

Chieosilapatham, P., Kiatsurayanon, C., Umehara, Y., Trujillo-Paez, J. V., Peng, G., Yue, H., Nguyen, L. T. H., & Niyonsaba, F. (2021). Keratinocytes: Innate immune cells in atopic dermatitis. *Clinical and Experimental Immunology*, *204*(3), 296–309. https://doi.org/10.1111/cei.13575

Choi, J. P., Lee, S. M., Choi, H. I., Kim, M. H., Jeon, S. G., Jang, M. H., Jee, Y. K., Yang, S., Cho, Y. J., & Kim, Y. K. (2016). House Dust Mite-Derived Chitin Enhances Th2 Cell Response to Inhaled Allergens, Mainly via a TNF-α-Dependent Pathway. *Allergy, Asthma & Immunology Research*, *8*(4), 362–374. https://doi.org/10.4168/aair.2016.8.4.362

Chometon, T. Q., Siqueira, M. da S., Sant´anna, J. C., Almeida, M. R., Gandini, M., Martins de Almeida Nogueira, A. C., & Antas, P. R. Z. (2020). A protocol for rapid monocyte isolation and generation of singular human monocyte-derived dendritic cells. *PLOS ONE*, *15*(4), e0231132. https://doi.org/10.1371/journal.pone.0231132

Cichorek, M., Wachulska, M., Stasiewicz, A., & Tymińska, A. (2013). Skin melanocytes: Biology and development. *Advances in Dermatology and Allergology*, *1*, 30–41. https://doi.org/10.5114/pdia.2013.33376

Clark, R. A. (2010). Skin-resident T cells: The ups and downs of on site immunity. *The Journal of Investigative Dermatology*, *130*(2), 362–370. https://doi.org/10.1038/jid.2009.247

Clarysse, K., Pfaff, C. M., Marquardt, Y., Huth, L., Kortekaas Krohn, I., Kluwig, D., Lüscher, B., Gutermuth, J., & Baron, J. (2019). JAK1/3 inhibition preserves epidermal morphology in full-thickness 3D skin models of atopic dermatitis and psoriasis. *Journal of the European Academy of Dermatology and Venereology*, *33*(2), 367–375. https://doi.org/10.1111/jdv.15301

Clayton, K., Vallejo, A. F., Davies, J., Sirvent, S., & Polak, M. E. (2017). Langerhans Cells—Programmed by the Epidermis. *Frontiers in Immunology*, *8*, 1676. https://doi.org/10.3389/fimmu.2017.01676

Coillard, A., & Segura, E. (2019). In vivo Differentiation of Human Monocytes. *Frontiers in Immunology*, *10*, 1907. https://doi.org/10.3389/fimmu.2019.01907

Colic, M., Jandric, D., Stojic-Vukanic, Z., Antic-Stankovic, J., Popovic, P., Vasilijic, S., Milosavljevic, P., & Balint, B. (2003). Differentiation of human dendritic cells from monocytes in vitro using

granulocyte-macrophage colony stimulating factor and low concentration of interleukin-4. *Vojnosanitetski Pregled*, *60*(5), 531–538. https://doi.org/10.2298/VSP0305531C

Colley, H. E., Hearnden, V., Jones, A. V., Weinreb, P. H., Violette, S. M., MacNeil, S., Thornhill, M. H., & Murdoch, C. (2011). Development of tissue-engineered models of oral dysplasia and early invasive oral squamous cell carcinoma. *British Journal of Cancer*. https://doi.org/10.1038/bjc.2011.403

Colley, H. E., Said, Z., Santocildes-Romero, M. E., Baker, S. R., D'Apice, K., Hansen, J., Madsen, L. S., Thornhill, M. H., Hatton, P. V., & Murdoch, C. (2018). Pre-clinical evaluation of novel mucoadhesive bilayer patches for local delivery of clobetasol-17-propionate to the oral mucosa. *Biomaterials*, *178*, 134–146. https://doi.org/10.1016/j.biomaterials.2018.06.009

Collin, M., & Bigley, V. (2018). Human dendritic cell subsets: An update. *Immunology*, *154*(1), 3–20. https://doi.org/10.1111/imm.12888

Collin, M., McGovern, N., & Haniffa, M. (2013). Human dendritic cell subsets. *Immunology*, *140*(1), 22–30. https://doi.org/10.1111/imm.12117

Commandeur, S., van Drongelen, V., de Gruijl, F. R., & El Ghalbzouri, A. (2012). Epidermal growth factor receptor activation and inhibition in 3D *in vitro* models of normal skin and human cutaneous squamous cell carcinoma. *Cancer Science*, *103*(12), 2120–2126. https://doi.org/10.1111/cas.12026

Coquette, A., Berna, N., Vandenbosch, A., Rosdy, M., De Wever, B., & Poumay, Y. (2003). Analysis of interleukin-1α (IL-1α) and interleukin-8 (IL-8) expression and release in in vitro reconstructed human epidermis for the prediction of in vivo skin irritation and/or sensitization. *Toxicology in Vitro*, *17*(3), 311–321. https://doi.org/10.1016/S0887-2333(03)00019-5

Cork, M. J., Danby, S. G., & Ogg, G. S. (2020). Atopic dermatitis epidemiology and unmet need in the United Kingdom. *Journal of Dermatological Treatment*, *31*(8), 801–809. https://doi.org/10.1080/09546634.2019.1655137

Cork, M. J., Danby, S. G., Vasilopoulos, Y., Hadgraft, J., Lane, M. E., Moustafa, M., Guy, R. H., MacGowan, A. L., Tazi-Ahnini, R., & Ward, S. J. (2009). Epidermal Barrier Dysfunction in Atopic Dermatitis. *Journal of Investigative Dermatology*, *129*(8), 1892–1908. https://doi.org/10.1038/jid.2009.133

Cork, M. J., Robinson, D. A., Vasilopoulos, Y., Ferguson, A., Moustafa, M., MacGowan, A., Duff, G. W., Ward, S. J., & Tazi-Ahnini, R. (2006). New perspectives on epidermal barrier dysfunction in atopic dermatitis: Gene–environment interactions. *Journal of Allergy and Clinical Immunology*, *118*(1), 3–21. https://doi.org/10.1016/j.jaci.2006.04.042

Corren, J., & Ziegler, S. F. (2019). TSLP: From allergy to cancer. *Nature Immunology*, *20*(12), 1603–1609. https://doi.org/10.1038/s41590-019-0524-9

Couper, K. N., Blount, D. G., & Riley, E. M. (2008). IL-10: The master regulator of immunity to infection. *Journal of Immunology (Baltimore, Md.: 1950)*, *180*(9), 5771–5777. https://doi.org/10.4049/jimmunol.180.9.5771

Coutinho, A. E., & Chapman, K. E. (2011). The anti-inflammatory and immunosuppressive effects of glucocorticoids, recent developments and mechanistic insights. *Molecular and Cellular Endocrinology*, *335*(1), 2–13. https://doi.org/10.1016/j.mce.2010.04.005

Cumberbatch, M., Clelland, K., Dearman, R. J., & Kimber, I. (2005). Impact of Cutaneous IL-10 on Resident Epidermal Langerhans' Cells and the Development of Polarized Immune Responses. *The Journal of Immunology*, *175*(1), 43–50. https://doi.org/10.4049/jimmunol.175.1.43

Curtiss, M. L., Gorman, J. V., Businga, T. R., Traver, G., Singh, M., Meyerholz, D. K., Kline, J. N., Murphy, A. J., Valenzuela, D. M., Colgan, J. D., Rothman, P. B., & Cassel, S. L. (2012). Tim-1 regulates Th2 responses in an airway hypersensitivity model. *European Journal of Immunology*, *42*(3), 651–661. https://doi.org/10.1002/eji.201141581

da Silva, E. Z. M., Jamur, M. C., & Oliver, C. (2014). Mast cell function: A new vision of an old cell. *The Journal of Histochemistry and Cytochemistry: Official Journal of the Histochemistry Society*, *62*(10), 698–738. https://doi.org/10.1369/0022155414545334

Dąbrowska, A. K., Spano, F., Derler, S., Adlhart, C., Spencer, N. D., & Rossi, R. M. (2018). The relationship between skin function, barrier properties, and body-dependent factors. *Skin Research and Technology*, *24*(2), 165–174. https://doi.org/10.1111/srt.12424

Dasgupta, A., & Saxena, R. (2012). Regulatory T cells: A review. *The National Medical Journal of India*, *25*(6), 341–351.

Datsi, A., Steinhoff, M., Ahmad, F., Alam, M., & Buddenkotte, J. (2021). Interleukin-31: The "itchy" cytokine in inflammation and therapy. *Allergy*, *76*(10), 2982–2997. https://doi.org/10.1111/all.14791

de Halleux, S., Stura, E., VanderElst, L., Carlier, V., Jacquemin, M., & Saint-Remy, J.-M. (2006). Three-dimensional structure and IgE-binding properties of mature fully active Der p 1, a clinically relevant major allergen. *Journal of Allergy and Clinical Immunology*, *117*(3), 571–576. https://doi.org/10.1016/j.jaci.2005.11.032

de Jongh, G. J., Zeeuwen, P. L. J. M., Kucharekova, M., Pfundt, R., van der Valk, P. G., Blokx, W., Dogan, A., Hiemstra, P. S., van de Kerkhof, P. C., & Schalkwijk, J. (2005). High Expression Levels of Keratinocyte Antimicrobial Proteins in Psoriasis Compared with Atopic Dermatitis. *Journal of Investigative Dermatology*, *125*(6), 1163–1173. https://doi.org/10.1111/j.0022-202X.2005.23935.x

De Vuyst, É., Giltaire, S., Lambert de Rouvroit, C., Malaisse, J., Mound, A., Bourtembourg, M., Poumay, Y., Nikkels, A. F., Chrétien, A., & Salmon, M. (2018). Methyl-β-cyclodextrin concurs with interleukin (IL)-4, IL-13 and IL-25 to induce alterations reminiscent of atopic dermatitis in reconstructed human epidermis. *Experimental Dermatology*, *27*(4), 435–437. https://doi.org/10.1111/exd.13113

De Wever, B., Kurdykowski, S., & Descargues, P. (2015). Human Skin Models for Research Applications in Pharmacology and Toxicology: Introducing NativeSkin ® , the "Missing Link" Bridging Cell Culture and/or Reconstructed Skin Models and Human Clinical Testing . *Applied In Vitro Toxicology*, *1*(1), 26–32. https://doi.org/10.1089/aivt.2014.0010

Deckers, J., Hammad, H., & Hoste, E. (2018). Langerhans Cells: Sensing the Environment in Health and Disease. *Frontiers in Immunology*, *9*, 93. https://doi.org/10.3389/fimmu.2018.00093

Del Zotto, G., Principi, E., Antonini, F., Baratto, S., Panicucci, C., Bruno, C., & Raffaghello, L. (2021). Comprehensive Phenotyping of Peripheral Blood T Lymphocytes in Healthy Mice. *Cytometry Part A*, *99*(3), 243–250. https://doi.org/10.1002/cyto.a.24246

Deng, C., Peng, N., Tang, Y., Yu, N., Wang, C., Cai, X., Zhang, L., Hu, D., Ciccia, F., & Lu, L. (2021). Roles of IL-25 in Type 2 Inflammation and Autoimmune Pathogenesis. *Frontiers in Immunology*, *12*, 691559. https://doi.org/10.3389/fimmu.2021.691559

Detwiler, A., Polkoff, K., Gaffney, L., Freytes, D. O., & Piedrahita, J. A. (2022). Donor Age and Time in Culture Affect Dermal Fibroblast Contraction in an *In Vitro* Hydrogel Model. *Tissue Engineering Part A*, ten.tea.2021.0217. https://doi.org/10.1089/ten.tea.2021.0217

Dickson, M. A., Hahn, W. C., Ino, Y., Ronfard, V., Wu, J. Y., Weinberg, R. A., Louis, D. N., Li, F. P., & Rheinwald, J. G. (2000). Human Keratinocytes That Express hTERT and Also Bypass a p16 ^{INK4a} -Enforced Mechanism That Limits Life Span Become Immortal yet Retain Normal Growth and Differentiation Characteristics. *Molecular and Cellular Biology*, *20*(4), 1436–1447. https://doi.org/10.1128/MCB.20.4.1436-1447.2000

Dijkhoff, I. M., Petracca, B., Prieux, R., Valacchi, G., Rothen-Rutishauser, B., & Eeman, M. (2021). Cultivating a Three-dimensional Reconstructed Human Epidermis at a Large Scale. *Journal of Visualized Experiments*, *171*, 61802. https://doi.org/10.3791/61802

D'Ippolito, D., & Pisano, M. (2018). Dupilumab (Dupixent): An Interleukin-4 Receptor Antagonist for Atopic Dermatitis. *P & T: A Peer-Reviewed Journal for Formulary Management*, *43*(9), 532–535.

dos Santos, G. G., Spiekstra, S. W., Sampat-Sardjoepersad, S. C., Reinders, J., Scheper, R. J., & Gibbs, S. (2011). A potential in vitro epidermal equivalent assay to determine sensitizer potency. *Toxicology in Vitro*, *25*(1), 347–357. https://doi.org/10.1016/j.tiv.2010.10.008

Dubin, C., Del Duca, E., & Guttman-Yassky, E. (2021). The IL-4, IL-13 and IL-31 pathways in atopic dermatitis. *Expert Review of Clinical Immunology*, *17*(8), 835–852. https://doi.org/10.1080/1744666X.2021.1940962

Ebner, S., Nguyen, V. A., Forstner, M., Wang, Y.-H., Wolfram, D., Liu, Y.-J., & Romani, N. (2007). Thymic stromal lymphopoietin converts human epidermal Langerhans cells into antigen-presenting cells that induce proallergic T cells. *Journal of Allergy and Clinical Immunology*, *119*(4), 982–990. https://doi.org/10.1016/j.jaci.2007.01.003

Eckl, K. M., Alef, T., Torres, S., & Hennies, H. C. (2011). Full-thickness human skin models for congenital ichthyosis and related keratinization disorders. *Journal of Investigative Dermatology*, *131*(9), 1938–1942. https://doi.org/10.1038/jid.2011.126

Egawa, G., & Weninger, W. (2015). Pathogenesis of atopic dermatitis: A short review. *Cogent Biology*, *1*(1), 1103459. https://doi.org/10.1080/23312025.2015.1103459

Ehrchen, J. M., Roth, J., & Barczyk-Kahlert, K. (2019). More Than Suppression: Glucocorticoid Action on Monocytes and Macrophages. *Frontiers in Immunology*, *10*, 2028. https://doi.org/10.3389/fimmu.2019.02028

Elias, M. S., Long, H. A., Newman, C. F., Wilson, P. A., West, A., McGill, P. J., Wu, K. C., Donaldson, M. J., & Reynolds, N. J. (2017). Proteomic analysis of filaggrin deficiency identifies molecular signatures characteristic of atopic eczema. *Journal of Allergy and Clinical Immunology*, *140*(5), 1299–1309. https://doi.org/10.1016/j.jaci.2017.01.039

Eligini, S., Crisci, M., Bono, E., Songia, P., Tremoli, E., Colombo, G. I., & Colli, S. (2013). Human monocyte-derived macrophages spontaneously differentiated in vitro show distinct phenotypes. *Journal of Cellular Physiology*, *228*(7), 1464–1472. https://doi.org/10.1002/jcp.24301

Engelhart, K., El Hindi, T., Biesalski, H. K., & Pfitzner, I. (2005). In vitro reproduction of clinical hallmarks of eczematous dermatitis in organotypic skin models. *Archives of Dermatological Research*. https://doi.org/10.1007/s00403-005-0575-7

Epelman, S., Lavine, K. J., Beaudin, A. E., Sojka, D. K., Carrero, J. A., Calderon, B., Brija, T., Gautier, E. L., Ivanov, S., Satpathy, A. T., Schilling, J. D., Schwendener, R., Sergin, I., Razani, B., Forsberg, E. C., Yokoyama, W. M., Unanue, E. R., Colonna, M., Randolph, G. J., & Mann, D. L. (2014). Embryonic and Adult-Derived Resident Cardiac Macrophages Are Maintained through

Distinct Mechanisms at Steady State and during Inflammation. *Immunity*, *40*(1), 91–104. https://doi.org/10.1016/j.immuni.2013.11.019

Eyerich, S., Eyerich, K., Traidl-Hoffmann, C., & Biedermann, T. (2018). Cutaneous Barriers and Skin Immunity: Differentiating A Connected Network. *Trends in Immunology*, *39*(4), 315–327. https://doi.org/10.1016/j.it.2018.02.004

Facy, V., Flouret, V., Régnier, M., & Schmidt, R. (2005). Reactivity of Langerhans cells in human reconstructed epidermis to known allergens and UV radiation. *Toxicology in Vitro*, *19*(6), 787–795. https://doi.org/10.1016/j.tiv.2005.03.018

Fähnrich, A., Klein, S., Sergé, A., Nyhoegen, C., Kombrink, S., Möller, S., Keller, K., Westermann, J., & Kalies, K. (2018). CD154 Costimulation Shifts the Local T-Cell Receptor Repertoire Not Only During Thymic Selection but Also During Peripheral T-Dependent Humoral Immune Responses. *Frontiers in Immunology*, *9*, 1019. https://doi.org/10.3389/fimmu.2018.01019

Farber, D. L., Yudanin, N. A., & Restifo, N. P. (2014). Human memory T cells: Generation, compartmentalization and homeostasis. *Nature Reviews Immunology*, *14*(1), 24–35. https://doi.org/10.1038/nri3567

Farley, A., McLafferty, E., & Hendry, C. (2012). The anatomy and physiology of the locomotor system. *Nursing Standard*, *27*(7), 35–43. https://doi.org/10.7748/ns2012.10.27.7.35.c9358

Fishbein, A. B., Silverberg, J. I., Wilson, E. J., & Ong, P. Y. (2020). Update on Atopic Dermatitis: Diagnosis, Severity Assessment, and Treatment Selection. *The Journal of Allergy and Clinical Immunology: In Practice*, *8*(1), 91–101. https://doi.org/10.1016/j.jaip.2019.06.044

Fleischer, J., Soeth, E., Reiling, N., Grage-Griebenow, E., Flad, H. -D., & Ernst, M. (1996). **Differential expression and function of CD80 (B7-1) and CD86 (B7-2) on human peripheral blood monocytes**. *Immunology*, *89*(4), 592–598. https://doi.org/10.1046/j.1365-2567.1996.d01-785.x

Fölster-Holst, R., Reimer, R., Neumann, C., Proksch, E., Rodriguez, E., Weidinger, S., Goldust, M., Hanisch, E., Dähnhardt-Pfeiffer, S., & Freitag-Wolf, S. (2021). Comparison of Epidermal Barrier Integrity in Adults with Classic Atopic Dermatitis, Atopic Prurigo and Non-Atopic Prurigo Nodularis. *Biology*, *10*(10), 1008. https://doi.org/10.3390/biology10101008

Fort, M. M., Cheung, J., Yen, D., Li, J., Zurawski, S. M., Lo, S., Menon, S., Clifford, T., Hunte, B., Lesley, R., Muchamuel, T., Hurst, S. D., Zurawski, G., Leach, M. W., Gorman, D. M., & Rennick, D. M. (2001). IL-25 induces IL-4, IL-5, and IL-13 and Th2-associated pathologies in vivo. *Immunity*, *15*(6), 985–995. https://doi.org/10.1016/s1074-7613(01)00243-6

Foss, D. L., Zilliox, M. J., & Murtaugh, M. P. (1999). Differential Regulation of Macrophage Interleukin-1 (IL-1), IL-12, and CD80-CD86 by Two Bacterial Toxins. *Infection and Immunity*, *67*(10), 5275–5281. https://doi.org/10.1128/IAI.67.10.5275-5281.1999

Franco-Barraza, J., Beacham, D. A., Amatangelo, M. D., & Cukierman, E. (2016). Preparation of Extracellular Matrices Produced by Cultured and Primary Fibroblasts. *Current Protocols in Cell Biology*, *71*(1). https://doi.org/10.1002/cpcb.2

Friedman, R. S., Beemiller, P., Sorensen, C. M., Jacobelli, J., & Krummel, M. F. (2010). Real-time analysis of T cell receptors in naive cells in vitro and in vivo reveals flexibility in synapse and signaling dynamics. *Journal of Experimental Medicine*, *207*(12), 2733–2749. https://doi.org/10.1084/jem.20091201

Fujii, Y., Takeuchi, H., Sakuma, S., Sengoku, T., & Takakura, S. (2009). Characterization of a 2,4-Dinitrochlorobenzene-Induced Chronic Dermatitis Model in Rats. *Skin Pharmacology and Physiology*, *22*(5), 240–247. https://doi.org/10.1159/000235551

Galbiati, V., Papale, A., Galli, C. L., Marinovich, M., & Corsini, E. (2014). Role of ROS and HMGB1 in Contact Allergen–Induced IL-18 Production in Human Keratinocytes. *Journal of Investigative Dermatology*, *134*(11), 2719–2727. https://doi.org/10.1038/jid.2014.203

Geissmann, F., Prost, C., Monnet, J.-P., Dy, M., Brousse, N., & Hermine, O. (1998). Transforming Growth Factor β1, in the Presence of Granulocyte/Macrophage Colony-stimulating Factor and Interleukin 4, Induces Differentiation of Human Peripheral Blood Monocytes into Dendritic Langerhans Cells. *Journal of Experimental Medicine*, *187*(6), 961–966. https://doi.org/10.1084/jem.187.6.961

Gibbs, S., Kosten, I., Veldhuizen, R., Spiekstra, S., Corsini, E., Roggen, E., Rustemeyer, T., Feilzer, A. J., & Kleverlaan, C. J. (2018). Assessment of metal sensitizer potency with the reconstructed human epidermis IL-18 assay. *Toxicology*, *393*, 62–72. https://doi.org/10.1016/j.tox.2017.10.014

Glimcher, L. H., & Murphy, K. M. (2000). Lineage commitment in the immune system: The T helper lymphocyte grows up. *Genes & Development*, *14*(14), 1693–1711.

Grassi, F., Dezutter-Dambuyant, C., McIlroy, D., Jacquet, C., Yoneda, K., Imamura, S., Boumsell, L., Schmitt, D., Autran, B., Debre, P., & Hosmalin, A. (1998). Monocyte-derived dendritic cells have a phenotype comparable to that of dermal dendritic cells and display ultrastructural granules distinct from Birbeck granules. *Journal of Leukocyte Biology*, *64*(4), 484–493. https://doi.org/10.1002/jlb.64.4.484

Gregory, L. G., Jones, C. P., Walker, S. A., Sawant, D., Gowers, K. H. C., Campbell, G. A., McKenzie, A. N. J., & Lloyd, C. M. (2013). IL-25 drives remodelling in allergic airways disease induced by house dust mite. *Thorax*, *68*(1), 82–90. https://doi.org/10.1136/thoraxjnl-2012-202003

Griffin, D. E. (2008). Cytokines and Chemokines. In *Encyclopedia of Virology* (pp. 620–624). Elsevier. https://doi.org/10.1016/B978-012374410-4.00374-5

Griffoni, C., Neidhart, B., Yang, K., Groeber-Becker, F., Maniura-Weber, K., Dandekar, T., Walles, H., & Rottmar, M. (2021). In vitro skin culture media influence the viability and inflammatory response of primary macrophages. *Scientific Reports*, *11*(1), 7070. https://doi.org/10.1038/s41598-021-86486-7

Groom, J. R., & Luster, A. D. (2011). CXCR3 in T cell function. *Experimental Cell Research*, *317*(5), 620–631. https://doi.org/10.1016/j.yexcr.2010.12.017

Guilliams, M., Mildner, A., & Yona, S. (2018). Developmental and Functional Heterogeneity of Monocytes. *Immunity*, *49*(4), 595–613. https://doi.org/10.1016/j.immuni.2018.10.005

Guironnet, G., Dezutter-Dambuyant, C., Gaudillère, A., Maréchal, S., Schmitt, D., & Péguet-Navarro, J. (2001). Phenotypic and Functional Outcome of Human Monocytes or Monocyte-Derived Dendritic Cells in a Dermal Equivalent. *Journal of Investigative Dermatology*, *116*(6), 933–939. https://doi.org/10.1046/j.1523-1747.2001.01355.x

Gupta, R., Sheikh, A., Strachan, D. P., & Anderson, H. R. (2004). Burden of allergic disease in the UK: Secondary analyses of national databases. *Clinical and Experimental Allergy*, *34*(4), 520–526. https://doi.org/10.1111/j.1365-2222.2004.1935.x

Guttman-Yassky, E., & Krueger, J. G. (2017). Atopic dermatitis and psoriasis: Two different immune diseases or one spectrum? *Current Opinion in Immunology*, *48*, 68–73. https://doi.org/10.1016/j.coi.2017.08.008

Guttman-Yassky, E., Thyssen, J. P., Silverberg, J. I., Papp, K. A., Paller, A. S., Weidinger, S., Chih-ho Hong, H., Hendrickson, B., Dilley, D., Tenorio, A. R., Ladizinski, B., Chu, A. D., Liu, J., & Irvine, A. D. (2023). Safety of upadacitinib in moderate-to-severe atopic dermatitis: An integrated

analysis of phase 3 studies. *Journal of Allergy and Clinical Immunology*, *151*(1), 172–181. https://doi.org/10.1016/j.jaci.2022.09.023

Hadi, H. A., Tarmizi, A. I., Khalid, K. A., Gajdács, M., Aslam, A., & Jamshed, S. (2021). The Epidemiology and Global Burden of Atopic Dermatitis: A Narrative Review. *Life (Basel, Switzerland)*, *11*(9), 936. https://doi.org/10.3390/life11090936

Hajar, T., Gontijo, J. R. V., & Hanifin, J. M. (2018). New and developing therapies for atopic dermatitis. *Anais Brasileiros De Dermatologia*, *93*(1), 104–107. https://doi.org/10.1590/abd1806-4841.20187682

Halliday, N., Williams, C., Kennedy, A., Waters, E., Pesenacker, A. M., Soskic, B., Hinze, C., Hou, T. Z., Rowshanravan, B., Janman, D., Walker, L. S. K., & Sansom, D. M. (2020). CD86 Is a Selective CD28 Ligand Supporting FoxP3+ Regulatory T Cell Homeostasis in the Presence of High Levels of CTLA-4. *Frontiers in Immunology*, *11*, 600000. https://doi.org/10.3389/fimmu.2020.600000

Hammad, H., Smits, H. H., Ratajczak, C., Nithiananthan, A., Wierenga, E. A., Stewart, G. A., Jacquet, A., Tonnel, A.-B., & Pestel, J. (2003). Monocyte-derived dendritic cells exposed to Der p 1 allergen enhance the recruitment of Th2 cells: Major involvement of the chemokines TARC/CCL17 and MDC/CCL22. *European Cytokine Network*, *14*(4), 219–228.

Haniffa, M., Gunawan, M., & Jardine, L. (2015). Human skin dendritic cells in health and disease. *Journal of Dermatological Science*, *77*(2), 85–92. https://doi.org/10.1016/j.jdermsci.2014.08.012

Hanifin, J. M., & Rajka, G. (1980). Diagnostic features of atopic dermatitis. *Acta Derm Venereol*, *92*(0), 44–47.

Harding, A. L., Colley, H. E., Vazquez, I. B., Danby, S., Hasan, M. Z., Nakanishi, H., Furuno, T., & Murdoch, C. (2023). C-SRC activation as a potential marker of chemical-induced skin irritation using tissue-engineered skin equivalents. *Experimental Dermatology*, *32*(2), 220–225. https://doi.org/10.1111/exd.14719

Harding, A. L., Murdoch, C., Danby, S., Hasan, M. Z., Nakanishi, H., Furuno, T., Hadad, S., Turner, R., & Colley, H. E. (2021). Determination of Chemical Irritation Potential Using a Defined Gene Signature Set on Tissue-Engineered Human Skin Equivalents. *JID Innovations*, *1*(2), 100011. https://doi.org/10.1016/j.xjidi.2021.100011

Hastings, W. D., Anderson, D. E., Kassam, N., Koguchi, K., Greenfield, E. A., Kent, S. C., Zheng, X. X., Strom, T. B., Hafler, D. A., & Kuchroo, V. K. (2009). TIM-3 is expressed on activated human CD4+ T cells and regulates Th1 and Th17 cytokines. *European Journal of Immunology*, *39*(9), 2492–2501. https://doi.org/10.1002/eji.200939274

Heeb, L. E. M., Egholm, C., & Boyman, O. (2020). Evolution and function of interleukin-4 receptor signaling in adaptive immunity and neutrophils. *Genes & Immunity*, *21*(3), 143–149. https://doi.org/10.1038/s41435-020-0095-7

Heinzmann, A. (2000). Genetic variants of IL-13 signalling and human asthma and atopy. *Human Molecular Genetics*, *9*(4), 549–559. https://doi.org/10.1093/hmg/9.4.549

Hesse, L., van Ieperen, N., Habraken, C., Petersen, A. H., Korn, S., Smilda, T., Goedewaagen, B., Ruiters, M. H., van der Graaf, A. C., & Nawijn, M. C. (2018). Subcutaneous immunotherapy with purified Der p1 and 2 suppresses type 2 immunity in a murine asthma model. *Allergy*, *73*(4), 862–874. https://doi.org/10.1111/all.13382

Hiasa, M., Abe, M., Nakano, A., Oda, A., Amou, H., Kido, S., Takeuchi, K., Kagawa, K., Yata, K., Hashimoto, T., Ozaki, S., Asaoka, K., Tanaka, E., Moriyama, K., & Matsumoto, T. (2009). GM-

CSF and IL-4 induce dendritic cell differentiation and disrupt osteoclastogenesis through M-CSF receptor shedding by up-regulation of TNF-α converting enzyme (TACE). *Blood*, *114*(20), 4517–4526. https://doi.org/10.1182/blood-2009-04-215020

Hirahara, K., & Nakayama, T. (2016). CD4+ T-cell subsets in inflammatory diseases: Beyond the Th1/Th2 paradigm. *International Immunology*, *28*(4), 163–171. https://doi.org/10.1093/intimm/dxw006

Hirayama, D., Iida, T., & Nakase, H. (2017). The Phagocytic Function of Macrophage-Enforcing Innate Immunity and Tissue Homeostasis. *International Journal of Molecular Sciences*, *19*(1), E92. https://doi.org/10.3390/ijms19010092

Hirobe, T. (2014). Keratinocytes regulate the function of melanocytes. *Dermatologica Sinica*, *32*(4), 200–204. https://doi.org/10.1016/j.dsi.2014.05.002

Hirota, T., Saeki, H., Tomita, K., Tanaka, S., Ebe, K., Sakashita, M., Yamada, T., Fujieda, S., Miyatake, A., Doi, S., Enomoto, T., Hizawa, N., Sakamoto, T., Masuko, H., Sasaki, T., Ebihara, T., Amagai, M., Esaki, H., Takeuchi, S., … Tamari, M. (2011). Variants of C-C motif chemokine 22 (CCL22) are associated with susceptibility to atopic dermatitis: Case-control studies. *PloS One*, *6*(11), e26987. https://doi.org/10.1371/journal.pone.0026987

Holla, S., Sharma, M., Vani, J., Kaveri, S. V., Balaji, K. N., & Bayry, J. (2014). GM-CSF along with IL-4 but not alone is indispensable for the differentiation of human dendritic cells from monocytes. *Journal of Allergy and Clinical Immunology*, *133*(5), 1500-1502.e1. https://doi.org/10.1016/j.jaci.2014.02.021

Holmes, A., Brown, R., & Shakesheff, K. (2009). Engineering tissue alternatives to animals: Applying tissue engineering to basic research and safety testing. *Regenerative Medicine*, *4*(4), 579–592. https://doi.org/10.2217/rme.09.26

Holse, M., Assing, K., & Poulsen, L. K. (2006). CCR3, CCR5, CCR8 and CXCR3 expression in memory T helper cells from allergic rhinitis patients, asymptomatically sensitized and healthy individuals. *Clinical and Molecular Allergy: CMA*, *4*, 6. https://doi.org/10.1186/1476-7961-4-6

Honda, T., Egawa, G., & Kabashima, K. (2019). Antigen presentation and adaptive immune responses in skin. *International Immunology*, *31*(7), 423–429. https://doi.org/10.1093/intimm/dxz005

Hönzke, S., Wallmeyer, L., Ostrowski, A., Radbruch, M., Mundhenk, L., Schäfer-Korting, M., & Hedtrich, S. (2016). Influence of Th2 Cytokines on the Cornified Envelope, Tight Junction Proteins, and β-Defensins in Filaggrin-Deficient Skin Equivalents. *Journal of Investigative Dermatology*, *136*(3), 631–639. https://doi.org/10.1016/j.jid.2015.11.007

Horikawa, T. (2002). IFN-gamma-inducible expression of thymus and activation-regulated chemokine/CCL17 and macrophage-derived chemokine/CCL22 in epidermal keratinocytes and their roles in atopic dermatitis. *International Immunology*, *14*(7), 767–773. https://doi.org/10.1093/intimm/dxf044

Hurbain, I., Romao, M., Sextius, P., Bourreau, E., Marchal, C., Bernerd, F., Duval, C., & Raposo, G. (2018). Melanosome Distribution in Keratinocytes in Different Skin Types: Melanosome Clusters Are Not Degradative Organelles. *Journal of Investigative Dermatology*, *138*(3), 647–656. https://doi.org/10.1016/j.jid.2017.09.039

Hutter, V., Kirton, S. B., & Chau, D. Y. S. (2018). Immunocompetent human in vitro skin models. In *Skin Tissue Models*. Elsevier Inc. https://doi.org/10.1016/B978-0-12-810545-0.00015-2

Hwang, E. S., Hong, J.-H., & Glimcher, L. H. (2005). IL-2 production in developing Th1 cells is regulated by heterodimerization of RelA and T-bet and requires T-bet serine residue 508.

The Journal of Experimental Medicine, *202*(9), 1289–1300. https://doi.org/10.1084/jem.20051044

Idoyaga, J., Cheong, C., Suda, K., Suda, N., Kim, J. Y., Lee, H., Park, C. G., & Steinman, R. M. (2008). Cutting Edge: Langerin/CD207 Receptor on Dendritic Cells Mediates Efficient Antigen Presentation on MHC I and II Products In Vivo. *The Journal of Immunology*, *180*(6), 3647–3650. https://doi.org/10.4049/jimmunol.180.6.3647

Iezzi, G., Karjalainen, K., & Lanzavecchia, A. (1998). The Duration of Antigenic Stimulation Determines the Fate of Naive and Effector T Cells. *Immunity*, *8*(1), 89–95. https://doi.org/10.1016/S1074-7613(00)80461-6

Ikutani, M., Yanagibashi, T., Ogasawara, M., Tsuneyama, K., Yamamoto, S., Hattori, Y., Kouro, T., Itakura, A., Nagai, Y., Takaki, S., & Takatsu, K. (2012). Identification of Innate IL-5–Producing Cells and Their Role in Lung Eosinophil Regulation and Antitumor Immunity. *The Journal of Immunology*, *188*(2), 703–713. https://doi.org/10.4049/jimmunol.1101270

Inagaki, N., Shiraishi, N., Igeta, K., Itoh, T., Chikumoto, T., Nagao, M., Kim, J. F., & Nagai, H. (2006). Inhibition of scratching behavior associated with allergic dermatitis in mice by tacrolimus, but not by dexamethasone. *European Journal of Pharmacology*, *546*(1–3), 189–196. https://doi.org/10.1016/j.ejphar.2006.07.019

Italiani, P., & Boraschi, D. (2017). Development and Functional Differentiation of Tissue-Resident Versus Monocyte-Derived Macrophages in Inflammatory Reactions. In M. Kloc (Ed.), *Macrophages* (Vol. 62, pp. 23–43). Springer International Publishing. https://doi.org/10.1007/978-3-319-54090-0_2

Ito, H., & Seishima, M. (2010). Regulation of the Induction and Function of Cytotoxic T Lymphocytes by Natural Killer T Cell. *Journal of Biomedicine and Biotechnology*, *2010*, 1–8. https://doi.org/10.1155/2010/641757

Jakubzick, C. V., Randolph, G. J., & Henson, P. M. (2017). Monocyte differentiation and antigen-presenting functions. *Nature Reviews Immunology*, *17*(6), 349–362. https://doi.org/10.1038/nri.2017.28

Jang, S., Morris, S., & Lukacs, N. W. (2013). TSLP Promotes Induction of Th2 Differentiation but Is Not Necessary during Established Allergen-Induced Pulmonary Disease. *PLoS ONE*, *8*(2), e56433. https://doi.org/10.1371/journal.pone.0056433

Jang, S., Ohn, J., Kim, J. W., Kang, S. M., Jeon, D., Heo, C. Y., Lee, Y.-S., Kwon, O., & Kim, K. H. (2020). Caffeoyl–Pro–His amide relieve DNCB-Induced Atopic Dermatitis-Like phenotypes in BALB/c mice. *Scientific Reports*, *10*(1), 8417. https://doi.org/10.1038/s41598-020-65502-2

Jansen van Rensburg, S., Franken, A., & Du Plessis, J. L. (2019). Measurement of transepidermal water loss, stratum corneum hydration and skin surface pH in occupational settings: A review. *Skin Research and Technology*, *25*(5), 595–605. https://doi.org/10.1111/srt.12711

Jennings, L. R., Colley, H. E., Ong, J., Panagakos, F., Masters, J. G., Trivedi, H. M., Murdoch, C., & Whawell, S. (2016). Development and Characterization of *In Vitro* Human Oral Mucosal Equivalents Derived from Immortalized Oral Keratinocytes. *Tissue Engineering Part C: Methods*, *22*(12), 1108–1117. https://doi.org/10.1089/ten.tec.2016.0310

Jiang, Q., Yang, G., Xiao, F., Xie, J., Wang, S., Lu, L., & Cui, D. (2021). Role of Th22 Cells in the Pathogenesis of Autoimmune Diseases. *Frontiers in Immunology*, *12*, 688066. https://doi.org/10.3389/fimmu.2021.688066

Junttila, I. S. (2018). Tuning the Cytokine Responses: An Update on Interleukin (IL)-4 and IL-13 Receptor Complexes. *Frontiers in Immunology*, *9*, 888. https://doi.org/10.3389/fimmu.2018.00888

Kabashima, K., Honda, T., Ginhoux, F., & Egawa, G. (2019). The immunological anatomy of the skin. *Nature Reviews Immunology*, *19*(1), 19–30. https://doi.org/10.1038/s41577-018-0084-5

Kabesch, M., Depner, M., Dahmen, I., Weiland, S. K., Vogelberg, C., Niggemann, B., Lau, S., Illig, T., Klopp, N., Wahn, U., Reinhardt, D., Von Mutius, E., & Nickel, R. (2007). Original article: Polymorphisms in eosinophil pathway genes, asthma and atopy: Polymorphisms in eosinophil pathway genes, asthma and atopy. *Allergy*, *62*(4), 423–428. https://doi.org/10.1111/j.1398-9995.2006.01300.x

Kaczmarek, R., Pasciak, M., Szymczak-Kulus, K., & Czerwinski, M. (2017). CD1: A Singed Cat of the Three Antigen Presentation Systems. *Archivum Immunologiae Et Therapiae Experimentalis*, *65*(3), 201–214. https://doi.org/10.1007/s00005-017-0461-y

Kamsteeg, M., Bergers, M., De Boer, R., Zeeuwen, P. L. J. M., Hato, S. V., Schalkwijk, J., & Tjabringa, G. S. (2011). Type 2 helper T-cell cytokines induce morphologic and molecular characteristics of atopic dermatitis in human skin equivalent. *American Journal of Pathology*, *178*(5), 2091–2099. https://doi.org/10.1016/j.ajpath.2011.01.037

Kaneko, N., Kurata, M., Yamamoto, T., Morikawa, S., & Masumoto, J. (2019). The role of interleukin-1 in general pathology. *Inflammation and Regeneration*, *39*(1), 12. https://doi.org/10.1186/s41232-019-0101-5

Kapałczyńska, M., Kolenda, T., Przybyła, W., Zajączkowska, M., Teresiak, A., Filas, V., Ibbs, M., Bliźniak, R., Łuczewski, Ł., & Lamperska, K. (2018). 2D and 3D cell cultures—A comparison of different types of cancer cell cultures. *Archives of Medical Science: AMS*, *14*(4), 910–919. https://doi.org/10.5114/aoms.2016.63743

Kapellos, T. S., Bonaguro, L., Gemünd, I., Reusch, N., Saglam, A., Hinkley, E. R., & Schultze, J. L. (2019). Human Monocyte Subsets and Phenotypes in Major Chronic Inflammatory Diseases. *Frontiers in Immunology*, *10*, 2035. https://doi.org/10.3389/fimmu.2019.02035

Kapur, S., Watson, W., & Carr, S. (2018). Atopic dermatitis. *Allergy, Asthma & Clinical Immunology*, *14*(S2), 52. https://doi.org/10.1186/s13223-018-0281-6

Katt, M. E., Placone, A. L., Wong, A. D., Xu, Z. S., & Searson, P. C. (2016). In Vitro Tumor Models: Advantages, Disadvantages, Variables, and Selecting the Right Platform. *Frontiers in Bioengineering and Biotechnology*, *4*. https://doi.org/10.3389/fbioe.2016.00012

Ke, N., Su, A., Huang, W., Szatmary, P., & Zhang, Z. (2016). Regulating the expression of CD80/CD86 on dendritic cells to induce immune tolerance after xeno-islet transplantation. *Immunobiology*, *221*(7), 803–812. https://doi.org/10.1016/j.imbio.2016.02.002

Khammissa, R. A. G., Fourie, J., Motswaledi, M. H., Ballyram, R., Lemmer, J., & Feller, L. (2018). The Biological Activities of Vitamin D and Its Receptor in Relation to Calcium and Bone Homeostasis, Cancer, Immune and Cardiovascular Systems, Skin Biology, and Oral Health. *BioMed Research International*, *2018*, 1–9. https://doi.org/10.1155/2018/9276380

Kim, B. E., & Leung, D. Y. M. (2018). Significance of Skin Barrier Dysfunction in Atopic Dermatitis. *Allergy, Asthma & Immunology Research*, *10*(3), 207–215. https://doi.org/10.4168/aair.2018.10.3.207

Kim, D., Kobayashi, T., & Nagao, K. (2019). Research Techniques Made Simple: Mouse Models of Atopic Dermatitis. *Journal of Investigative Dermatology*, *139*(5), 984-990.e1. https://doi.org/10.1016/j.jid.2019.02.014

Kim, J., Lee, S., Woo, S., Han, Y., Lee, J. H., Lee, I.-Y., Lim, I.-S., Choi, E.-S., Choi, B.-W., Cheong, H.-K., Lee, S.-I., & Ahn, K. (2013). The indoor level of house dust mite allergen is associated with severity of atopic dermatitis in children. *Journal of Korean Medical Science*, *28*(1), 74–79. https://doi.org/10.3346/jkms.2013.28.1.74

Kirchhoff, D., Frentsch, M., Leclerk, P., Bumann, D., Rausch, S., Hartmann, S., Thiel, A., & Scheffold, A. (2007). Identification and isolation of murine antigen-reactive T cells according to CD154 expression. *European Journal of Immunology*, *37*(9), 2370–2377. https://doi.org/10.1002/eji.200737322

Kircik, L. H., Del Rosso, J. Q., & Aversa, D. (2011). Evaluating Clinical Use of a Ceramide-dominant, Physiologic Lipid-based Topical Emulsion for Atopic Dermatitis. *The Journal of Clinical and Aesthetic Dermatology*, *4*(3), 34–40.

Klicks, J., von Molitor, E., Ertongur-Fauth, T., Rudolf, R., & Hafner, M. (2017). In vitro skin three-dimensional models and their applications. *Journal of Cellular Biotechnology*. https://doi.org/10.3233/JCB-179004

Kolarsick, P. A. J., Kolarsick, M. A., & Goodwin, C. (2011). Anatomy and Physiology of the Skin: *Journal of the Dermatology Nurses' Association*, *3*(4), 203–213. https://doi.org/10.1097/JDN.0b013e3182274a98

Kolesnik, M., Franke, I., Lux, A., Quist, S., & Gollnick, H. (2018). Eczema in Psoriatico: An Important Differential Diagnosis Between Chronic Allergic Contact Dermatitis and Psoriasis in Palmoplantar Localization. *Acta Dermato Venereologica*, *98*(1), 50–58. https://doi.org/10.2340/00015555-2779

Koskinen Holm, C., & Qu, C. (2022). Engineering a 3D In Vitro Model of Human Gingival Tissue Equivalent with Genipin/Cytochalasin D. *International Journal of Molecular Sciences*, *23*(13), 7401. https://doi.org/10.3390/ijms23137401

Kosten, I. J., Spiekstra, S. W., de Gruijl, T. D., & Gibbs, S. (2015). MUTZ-3 derived Langerhans cells in human skin equivalents show differential migration and phenotypic plasticity after allergen or irritant exposure. *Toxicology and Applied Pharmacology*, *287*(1), 35–42. https://doi.org/10.1016/j.taap.2015.05.017

Koster, M. I. (2009). Making an epidermis. *Annals of the New York Academy of Sciences*, *1170*, 7–10. https://doi.org/10.1111/j.1749-6632.2009.04363.x

Krakow, S., Crescimone, M. L., Bartels, C., Wiegering, V., Eyrich, M., Schlegel, P. G., & Wölfl, M. (2019). Re-expression of CD14 in Response to a Combined IL-10/TLR Stimulus Defines Monocyte-Derived Cells With an Immunoregulatory Phenotype. *Frontiers in Immunology*, *10*, 1484. https://doi.org/10.3389/fimmu.2019.01484

Krovi, S. H., & Gapin, L. (2018). Invariant Natural Killer T Cell Subsets—More Than Just Developmental Intermediates. *Frontiers in Immunology*, *9*, 1393. https://doi.org/10.3389/fimmu.2018.01393

Ku, J. M., Hong, S. H., Kim, S. R., Choi, H.-S., Kim, H. I., Kim, D. U., Oh, S. M., Seo, H. S., Kim, T. Y., Shin, Y. C., Cheon, C., & Ko, S.-G. (2018). The prevention of 2,4-dinitrochlorobenzene-induced inflammation in atopic dermatitis-like skin lesions in BALB/c mice by Jawoongo. *BMC Complementary and Alternative Medicine*, *18*(1), 215. https://doi.org/10.1186/s12906-018-2280-z

Kubo, T., Morita, H., Sugita, K., & Akdis, C. A. (2017). Introduction to Mechanisms of Allergic Diseases. In *Middleton's Allergy Essentials* (pp. 1–27). Elsevier. https://doi.org/10.1016/B978-0-323-37579-5.00001-5

Küchler, S., Henkes, D., Eckl, K. M., Ackermann, K., Plendl, J., Korting, H. C., Hennies, H. C., & Schäfer-Korting, M. (2011). Hallmarks of atopic skin mimicked in vitro by means of a skin disease model based on FLG knock-down. *ATLA Alternatives to Laboratory Animals*, *39*(5), 471–480. https://doi.org/10.1177/026119291103900508

Kühbacher, A., Henkel, H., Stevens, P., Grumaz, C., Finkelmeier, D., Burger-Kentischer, A., Sohn, K., & Rupp, S. (2017). Central role for dermal fibroblasts in skin model protection against candida albicans. *Journal of Infectious Diseases*. https://doi.org/10.1093/infdis/jix153

Kumar, B. V., Connors, T. J., & Farber, D. L. (2018). Human T Cell Development, Localization, and Function throughout Life. *Immunity*, *48*(2), 202–213. https://doi.org/10.1016/j.immuni.2018.01.007

Kupper, T. S., Chua, A. O., Flood, P., McGuire, J., & Gubler, U. (1987). Interleukin 1 gene expression in cultured human keratinocytes is augmented by ultraviolet irradiation. *Journal of Clinical Investigation*, *80*(2), 430–436. https://doi.org/10.1172/JCI113090

Kurokawa, I., Takahashi, K., Moll, I., & Moll, R. (2011). Expression of keratins in cutaneous epithelial tumors and related disorders - distribution and clinical significance: Keratin expression in cutaneous epithelial tumors. *Experimental Dermatology*, *20*(3), 217–228. https://doi.org/10.1111/j.1600-0625.2009.01006.x

Kuse, Y., Tsuruma, K., Kanno, Y., Shimazawa, M., & Hara, H. (2017). CCR3 Is Associated with the Death of a Photoreceptor Cell-line Induced by Light Exposure. *Frontiers in Pharmacology*, *8*. https://doi.org/10.3389/fphar.2017.00207

Kushwah, R., & Hu, J. (2011). Complexity of dendritic cell subsets and their function in the host immune system: DC subsets and classification. *Immunology*, *133*(4), 409–419. https://doi.org/10.1111/j.1365-2567.2011.03457.x

Lai-Cheong, J. E., & McGrath, J. A. (2017). Structure and function of skin, hair and nails. *Medicine*, *45*(6), 347–351. https://doi.org/10.1016/j.mpmed.2017.03.004

Lambert, M. W., Maddukuri, S., Karanfilian, K. M., Elias, M. L., & Lambert, W. C. (2019). The physiology of melanin deposition in health and disease. *Clinics in Dermatology*, *37*(5), 402–417. https://doi.org/10.1016/j.clindermatol.2019.07.013

Lange, J., Weil, F., Riegler, C., Groeber, F., Rebhan, S., Kurdyn, S., Alb, M., Kneitz, H., Gelbrich, G., Walles, H., & Mielke, S. (2016). Interactions of donor sources and media influence the histo-morphological quality of full-thickness skin models. *Biotechnology Journal*, *11*(10), 1352–1361. https://doi.org/10.1002/biot.201600360

Langer, R., & Vacanti, J. P. (1993). Tissue Engineering. *Science*, *260*(5110), 920–926. https://doi.org/10.1126/science.8493529

Lee, D., Kim, Y., Jo, H., Go, C., Jeong, Y., Jang, Y., Kang, D., Park, K., Kim, Y.-S., & Kang, J. S. (2021). The Anti-Inflammatory Effect of Aptamin C on House Dust Mite Extract-Induced Inflammation in Keratinocytes via Regulation of IL-22 and GDNF Production. *Antioxidants*, *10*(6), 945. https://doi.org/10.3390/antiox10060945

Lendeckel, U., Venz, S., & Wolke, C. (2022). Macrophages: Shapes and functions. *ChemTexts*, *8*(2), 12. https://doi.org/10.1007/s40828-022-00163-4

Li, D., & Wu, M. (2021). Pattern recognition receptors in health and diseases. *Signal Transduction and Targeted Therapy*, *6*(1), 291. https://doi.org/10.1038/s41392-021-00687-0

Li, J., Chen, S., Xiao, X., Zhao, Y., Ding, W., & Li, X. C. (2017). IL-9 and Th9 cells in health and diseases-From tolerance to immunopathology. *Cytokine & Growth Factor Reviews*, *37*, 47–55. https://doi.org/10.1016/j.cytogfr.2017.07.004

Liew, P. X., & Kubes, P. (2019). The Neutrophil's Role During Health and Disease. *Physiological Reviews*, *99*(2), 1223–1248. https://doi.org/10.1152/physrev.00012.2018

Limandjaja, G. C., Waaijman, T., Roffel, S., Niessen, F. B., & Gibbs, S. (2019). Monocytes co-cultured with reconstructed keloid and normal skin models skew towards M2 macrophage phenotype. *Archives of Dermatological Research*, *311*(8), 615–627. https://doi.org/10.1007/s00403-019-01942-9

Lin, W., Suo, Y., Deng, Y., Fan, Z., Zheng, Y., Wei, X., & Chu, Y. (2015). Morphological change of CD4(+) T cell during contact with DC modulates T-cell activation by accumulation of F-actin in the immunology synapse. *BMC Immunology*, *16*, 49. https://doi.org/10.1186/s12865-015-0108-x

Linde, N., Gutschalk, C. M., Hoffmann, C., Yilmaz, D., & Mueller, M. M. (2012). Integrating Macrophages into Organotypic Co-Cultures: A 3D In Vitro Model to Study Tumor-Associated Macrophages. *PLoS ONE*, *7*(7), e40058. https://doi.org/10.1371/journal.pone.0040058

Liu, F.-T., Goodarzi, H., & Chen, H.-Y. (2011). IgE, Mast Cells, and Eosinophils in Atopic Dermatitis. *Clinical Reviews in Allergy & Immunology*, *41*(3), 298–310. https://doi.org/10.1007/s12016-011-8252-4

Li-Weber, M., & Krammer, P. H. (2003). Regulation of IL4 gene expression by T cells and therapeutic perspectives. *Nature Reviews Immunology*, *3*(7), 534–543. https://doi.org/10.1038/nri1128

Lopez-Ojeda, W., Pandey, A., Alhajj, M., & Oakley, A. M. (2021). Anatomy, Skin (Integument). In *StatPearls*. StatPearls Publishing. http://www.ncbi.nlm.nih.gov/books/NBK441980/

Lorthois, I., Simard, M., Morin, S., & Pouliot, R. (2019). Infiltration of T cells into a three-dimensional psoriatic skin model mimics pathological key features. *International Journal of Molecular Sciences*, *20*(7). https://doi.org/10.3390/ijms20071670

Løset, M., Brown, S. J., Saunes, M., & Hveem, K. (2019). Genetics of Atopic Dermatitis: From DNA Sequence to Clinical Relevance. *Dermatology*, *235*(5), 355–364. https://doi.org/10.1159/000500402

Loyet, K. M., Ouyang, W., Eaton, D. L., & Stults, J. T. (2005). Proteomic Profiling of Surface Proteins on Th1 and Th2 Cells. *Journal of Proteome Research*, *4*(2), 400–409. https://doi.org/10.1021/pr049810q

Lozano-Ojalvo, D., López-Fandiño, R., & López-Expósito, I. (2015). PBMC-Derived T Cells. In K. Verhoeckx, P. Cotter, I. López-Expósito, C. Kleiveland, T. Lea, A. Mackie, T. Requena, D. Swiatecka, & H. Wichers (Eds.), *The Impact of Food Bioactives on Health* (pp. 169–180). Springer International Publishing. https://doi.org/10.1007/978-3-319-16104-4_16

Luckheeram, R. V., Zhou, R., Verma, A. D., & Xia, B. (2012). $CD4^+$T cells: Differentiation and functions. *Clinical & Developmental Immunology*, *2012*, 925135. https://doi.org/10.1155/2012/925135

Lukácsi, S., Gerecsei, T., Balázs, K., Francz, B., Szabó, B., Erdei, A., & Bajtay, Z. (2020). The differential role of CR3 (CD11b/CD18) and CR4 (CD11c/CD18) in the adherence, migration and podosome formation of human macrophages and dendritic cells under inflammatory conditions. *PloS One*, *15*(5), e0232432. https://doi.org/10.1371/journal.pone.0232432

Lynch, E. A., Heijens, C. A. W., Horst, N. F., Center, D. M., & Cruikshank, W. W. (2003). Cutting edge: IL-16/CD4 preferentially induces Th1 cell migration: requirement of CCR5. *Journal of Immunology (Baltimore, Md.: 1950)*, *171*(10), 4965–4968. https://doi.org/10.4049/jimmunol.171.10.4965

Ma, W.-T., Gao, F., Gu, K., & Chen, D.-K. (2019). The Role of Monocytes and Macrophages in Autoimmune Diseases: A Comprehensive Review. *Frontiers in Immunology*, *10*, 1140. https://doi.org/10.3389/fimmu.2019.01140

Macri, C., Pang, E. S., Patton, T., & O'Keeffe, M. (2018). Dendritic cell subsets. *Seminars in Cell & Developmental Biology*, *84*, 11–21. https://doi.org/10.1016/j.semcdb.2017.12.009

Maeda, S., Maeda, S., Shibata, S., Chimura, N., & Fukata, T. (2009). House dust mite major allergen Der f 1 enhances proinflammatory cytokine and chemokine gene expression in a cell line of canine epidermal keratinocytes. *Veterinary Immunology and Immunopathology*, *131*(3–4), 298–302. https://doi.org/10.1016/j.vetimm.2009.04.012

Maier, E., Werner, D., Duschl, A., Bohle, B., & Horejs-Hoeck, J. (2014). Human Th2 but Not Th9 Cells Release IL-31 in a STAT6/NF-κB–Dependent Way. *The Journal of Immunology*, *193*(2), 645–654. https://doi.org/10.4049/jimmunol.1301836

Maretzky, T., Scholz, F., Köten, B., Proksch, E., Saftig, P., & Reiss, K. (2008). ADAM10-Mediated E-Cadherin Release Is Regulated by Proinflammatory Cytokines and Modulates Keratinocyte Cohesion in Eczematous Dermatitis. *Journal of Investigative Dermatology*, *128*(7), 1737–1746. https://doi.org/10.1038/sj.jid.5701242

Marshall, J. S., Warrington, R., Watson, W., & Kim, H. L. (2018). An introduction to immunology and immunopathology. *Allergy, Asthma & Clinical Immunology*, *14*(S2), 49. https://doi.org/10.1186/s13223-018-0278-1

Marzaioli, V., Canavan, M., Floudas, A., Wade, S. C., Low, C., Veale, D. J., & Fearon, U. (2020). Monocyte-Derived Dendritic Cell Differentiation in Inflammatory Arthritis Is Regulated by the JAK/STAT Axis via NADPH Oxidase Regulation. *Frontiers in Immunology*, *11*, 1406. https://doi.org/10.3389/fimmu.2020.01406

Mathes, S. H., Ruffner, H., & Graf-Hausner, U. (2014). The use of skin models in drug development. *Advanced Drug Delivery Reviews*, *69–70*, 81–102. https://doi.org/10.1016/j.addr.2013.12.006

Mayadas, T. N., Cullere, X., & Lowell, C. A. (2014). The multifaceted functions of neutrophils. *Annual Review of Pathology*, *9*, 181–218. https://doi.org/10.1146/annurev-pathol-020712-164023

McAleer, M. A., & Irvine, A. D. (2013). The multifunctional role of filaggrin in allergic skin disease. *Journal of Allergy and Clinical Immunology*, *131*(2), 280–291. https://doi.org/10.1016/j.jaci.2012.12.668

McAnulty, R. J. (2007). Fibroblasts and myofibroblasts: Their source, function and role in disease. *The International Journal of Biochemistry & Cell Biology*, *39*(4), 666–671. https://doi.org/10.1016/j.biocel.2006.11.005

McPherson, T. (2016). Current Understanding in Pathogenesis of Atopic Dermatitis. *Indian Journal of Dermatology*, *61*(6), 649–655. https://doi.org/10.4103/0019-5154.193674

Mehta, A. K., Gracias, D. T., & Croft, M. (2018). TNF activity and T cells. *Cytokine*, *101*, 14–18. https://doi.org/10.1016/j.cyto.2016.08.003

Mertsching, H., Weimer, M., Kersen, S., & Brunner, H. (2008). Human skin equivalent as an alternative to animal testing. *GMS Krankenhaushygiene Interdisziplinar*, *3*(1), Doc11.

Meyers, J. H., Ryu, A., Monney, L., Nguyen, K., Greenfield, E. A., Freeman, G. J., & Kuchroo, V. K. (2002). Cutting Edge: CD94/NKG2 Is Expressed on Th1 But Not Th2 Cells and Costimulates Th1 Effector Functions. *The Journal of Immunology*, *169*(10), 5382–5386. https://doi.org/10.4049/jimmunol.169.10.5382

Mieremet, A., Vázquez García, A., Boiten, W., van Dijk, R., Gooris, G., Bouwstra, J. A., & El Ghalbzouri, A. (2019). Human skin equivalents cultured under hypoxia display enhanced epidermal morphogenesis and lipid barrier formation. *Scientific Reports*, *9*(1), 7811. https://doi.org/10.1038/s41598-019-44204-4

Mildner, M., Ballaun, C., Stichenwirth, M., Bauer, R., Gmeiner, R., Buchberger, M., Mlitz, V., & Tschachler, E. (2006). Gene silencing in a human organotypic skin model. *Biochemical and Biophysical Research Communications*, *348*(1), 76–82. https://doi.org/10.1016/j.bbrc.2006.07.035

Mildner, M., Jin, J., Eckhart, L., Kezic, S., Gruber, F., Barresi, C., Stremnitzer, C., Buchberger, M., Mlitz, V., Ballaun, C., Sterniczky, B., Födinger, D., & Tschachler, E. (2010). Knockdown of filaggrin impairs diffusion barrier function and increases UV sensitivity in a human skin model. *Journal of Investigative Dermatology*, *130*(9), 2286–2294. https://doi.org/10.1038/jid.2010.115

Miller, A. M. (2011). Role of IL-33 in inflammation and disease. *Journal of Inflammation*, *8*(1), 22. https://doi.org/10.1186/1476-9255-8-22

Miller, M. J., Safrina, O., Parker, I., & Cahalan, M. D. (2004). Imaging the Single Cell Dynamics of CD4+ T Cell Activation by Dendritic Cells in Lymph Nodes. *Journal of Experimental Medicine*, *200*(7), 847–856. https://doi.org/10.1084/jem.20041236

Min, G.-Y., Kim, T. I., Kim, J.-H., Cho, W.-K., Yang, J.-H., & Ma, J.-Y. (2022). Inhibitory effect of Isatis tinctoria L. water extract on DNCB-induced atopic dermatitis in BALB/c mice and HaCaT cells. *Chinese Medicine*, *17*(1), 66. https://doi.org/10.1186/s13020-022-00624-5

Mizumoto, N., & Takashima, A. (2004). CD1a and langerin: Acting as more than Langerhans cell markers. *The Journal of Clinical Investigation*, *113*(5), 658–660. https://doi.org/10.1172/JCI21140

Mohapatra, S., Coppola, D., Riker, A. I., & Pledger, W. J. (2007). Roscovitine Inhibits Differentiation and Invasion in a Three-Dimensional Skin Reconstruction Model of Metastatic Melanoma. *Molecular Cancer Research*, *5*(2), 145–151. https://doi.org/10.1158/1541-7786.MCR-06-0300

Möller, J. F., Möller, B., Wiedenmann, B., Berg, T., & Schott, E. (2011). CD154, a marker of antigen-specific stimulation of CD4 T cells, is associated with response to treatment in patients with chronic HCV infection. *Journal of Viral Hepatitis*, *18*(7). https://doi.org/10.1111/j.1365-2893.2010.01430.x

Morar, N., Willis-Owen, S. A. G., Moffatt, M. F., & Cookson, W. O. C. M. (2006). The genetics of atopic dermatitis. *Journal of Allergy and Clinical Immunology*, *118*(1), 24–34. https://doi.org/10.1016/j.jaci.2006.03.037

Mortaz, E., Alipoor, S. D., Adcock, I. M., Mumby, S., & Koenderman, L. (2018). Update on Neutrophil Function in Severe Inflammation. *Frontiers in Immunology*, *9*, 2171. https://doi.org/10.3389/fimmu.2018.02171

Mukai, K., Tsai, M., Saito, H., & Galli, S. J. (2018). Mast cells as sources of cytokines, chemokines, and growth factors. *Immunological Reviews*, *282*(1), 121–150. https://doi.org/10.1111/imr.12634

Murdoch, C., Tazzyman, S., Webster, S., & Lewis, C. E. (2007). Expression of Tie-2 by Human Monocytes and Their Responses to Angiopoietin-2. *The Journal of Immunology*, *178*(11), 7405–7411. https://doi.org/10.4049/jimmunol.178.11.7405

Murphrey, M. B., Miao, J. H., & Zito, P. M. (2021). Histology, Stratum Corneum. In *StatPearls*. StatPearls Publishing. http://www.ncbi.nlm.nih.gov/books/NBK513299/

Nadif, R., Zerimech, F., Bouzigon, E., & Matran, R. (2013). The role of eosinophils and basophils in allergic diseases considering genetic findings. *Current Opinion in Allergy & Clinical Immunology*, *13*(5), 507–513. https://doi.org/10.1097/ACI.0b013e328364e9c0

Nafisi, S., & Maibach, H. I. (2018). Skin penetration of nanoparticles. In *Emerging Nanotechnologies in Immunology* (pp. 47–88). Elsevier. https://doi.org/10.1016/B978-0-323-40016-9.00003-8

Nagao, K. (Ed.). (2019). Introduction: Special Issue—Basic and Translational Skin Immunology. *International Immunology*, *31*(7), 413–414. https://doi.org/10.1093/intimm/dxz038

Nagy-Baló, Z., Kiss, R., Menge, A., Bödör, C., Bajtay, Z., & Erdei, A. (2020). Activated Human Memory B Lymphocytes Use CR4 (CD11c/CD18) for Adhesion, Migration, and Proliferation. *Frontiers in Immunology*, *11*, 565458. https://doi.org/10.3389/fimmu.2020.565458

Nakayama, T., Hirahara, K., Onodera, A., Endo, Y., Hosokawa, H., Shinoda, K., Tumes, D. J., & Okamoto, Y. (2017). Th2 Cells in Health and Disease. *Annual Review of Immunology*, *35*, 53–84. https://doi.org/10.1146/annurev-immunol-051116-052350

Nelson, A. M., Cong, Z., Gettle, S. L., Longenecker, A. L., Kidacki, M., Kirby, J. S., Adams, D. R., Stairs, D. B., & Danby, F. W. (2019). E-cadherin and p120ctn protein expression are lost in hidradenitis suppurativa lesions. *Experimental Dermatology*, *28*(7), 867–871. https://doi.org/10.1111/exd.13973

Nemoto-Hasebe, I., Akiyama, M., Nomura, T., Sandilands, A., Irwin McLean, W. H., & Shimizu, H. (2009). Clinical Severity Correlates with Impaired Barrier in Filaggrin-Related Eczema. *Journal of Investigative Dermatology*, *129*(3), 682–689. https://doi.org/10.1038/jid.2008.280

Nguyen, A. V., & Soulika, A. M. (2019). The Dynamics of the Skin's Immune System. *International Journal of Molecular Sciences*, *20*(8), 1811. https://doi.org/10.3390/ijms20081811

Niehues, H., Schalkwijk, J., van Vlijmen-Willems, I. M. J. J., Rodijk-Olthuis, D., van Rossum, M. M., Wladykowski, E., Brandner, J. M., van den Bogaard, E. H. J., & Zeeuwen, P. L. J. M. (2017). Epidermal equivalents of filaggrin null keratinocytes do not show impaired skin barrier function. *Journal of Allergy and Clinical Immunology*, *139*(6), 1979-1981.e13. https://doi.org/10.1016/j.jaci.2016.09.016

Nielsen, M. C., Andersen, M. N., & Møller, H. J. (2020). Monocyte isolation techniques significantly impact the phenotype of both isolated monocytes and derived macrophages *in vitro*. *Immunology*, *159*(1), 63–74. https://doi.org/10.1111/imm.13125

Nilforoushzadeh, M. A., Ahmadi Ashtiani, H. R., Jaffary, F., Jahangiri, F., Nikkhah, N., Mahmoudbeyk, M., Fard, M., Ansari, Z., & Zare, S. (2017). Dermal Fibroblast Cells: Biology and Function in Skin Regeneration. *Journal of Skin and Stem Cell*, *In Press*(In Press). https://doi.org/10.5812/jssc.69080

Novak, N., Bieber, T., & Leung, D. Y. M. (2003). Immune mechanisms leading to atopic dermatitis. *The Journal of Allergy and Clinical Immunology*, *112*(6 Suppl), S128-139. https://doi.org/10.1016/j.jaci.2003.09.032

Nutten, S. (2015). Atopic Dermatitis: Global Epidemiology and Risk Factors. *Annals of Nutrition and Metabolism*, *66*(Suppl. 1), 8–16. https://doi.org/10.1159/000370220

O'Brien, F. J. (2011). Biomaterials & scaffolds for tissue engineering. *Materials Today*, *14*(3), 88–95. https://doi.org/10.1016/S1369-7021(11)70058-X

Oettgen, H., & Broide, D. H. (2012). Introduction to mechanisms of allergic disease. In *Allergy* (pp. 1–32). Elsevier. https://doi.org/10.1016/B978-0-7234-3658-4.00005-6

Ohtani, T., Mizuashi, M., Nakagawa, S., Sasaki, Y., Fujimura, T., Okuyama, R., & Aiba, S. (2009). TGF-beta1 dampens the susceptibility of dendritic cells to environmental stimulation, leading to

the requirement for danger signals for activation. *Immunology*, *126*(4), 485–499. https://doi.org/10.1111/j.1365-2567.2008.02919.x

Olivera, A., Beaven, M. A., & Metcalfe, D. D. (2018). Mast cells signal their importance in health and disease. *Journal of Allergy and Clinical Immunology*, *142*(2), 381–393. https://doi.org/10.1016/j.jaci.2018.01.034

Ollington, B., Colley, H. E., & Murdoch, C. (2021). Immunoresponsive Tissue-Engineered Oral Mucosal Equivalents Containing Macrophages. *Tissue Engineering Part C: Methods*, *27*(8), 462–471. https://doi.org/10.1089/ten.tec.2021.0124

Otsuka, M., Egawa, G., & Kabashima, K. (2018). Uncovering the Mysteries of Langerhans Cells, Inflammatory Dendritic Epidermal Cells, and Monocyte-Derived Langerhans Cell-Like Cells in the Epidermis. *Frontiers in Immunology*, *9*, 1768. https://doi.org/10.3389/fimmu.2018.01768

Otsuka, Y., Watanabe, E., Shinya, E., Okura, S., Saeki, H., Geijtenbeek, T. B. H., & Takahashi, H. (2018). Differentiation of Langerhans Cells from Monocytes and Their Specific Function in Inducing IL-22-Specific Th Cells. *Journal of Immunology (Baltimore, Md.: 1950)*, *201*(10), 3006–3016. https://doi.org/10.4049/jimmunol.1701402

Ouwehand, K., Spiekstra, S. W., Waaijman, T., Breetveld, M., Scheper, R. J., de Gruijl, T. D., & Gibbs, S. (2012). CCL5 and CCL20 mediate immigration of Langerhans cells into the epidermis of full thickness human skin equivalents. *European Journal of Cell Biology*, *91*(10), 765–773. https://doi.org/10.1016/j.ejcb.2012.06.004

Ouwehand, K., Spiekstra, S. W., Waaijman, T., Scheper, R. J., de Gruijl, T. D., & Gibbs, S. (2011). Technical Advance: Langerhans cells derived from a human cell line in a full-thickness skin equivalent undergo allergen-induced maturation and migration. *Journal of Leukocyte Biology*, *90*(5), 1027–1033. https://doi.org/10.1189/jlb.0610374

Palmer, C. N. A., Irvine, A. D., Terron-Kwiatkowski, A., Zhao, Y., Liao, H., Lee, S. P., Goudie, D. R., Sandilands, A., Campbell, L. E., Smith, F. J. D., O'Regan, G. M., Watson, R. M., Cecil, J. E., Bale, S. J., Compton, J. G., DiGiovanna, J. J., Fleckman, P., Lewis-Jones, S., Arseculeratne, G., … McLean, W. H. I. (2006). Common loss-of-function variants of the epidermal barrier protein filaggrin are a major predisposing factor for atopic dermatitis. *Nature Genetics*, *38*(4), 441–446. https://doi.org/10.1038/ng1767

Papayannopoulos, V. (2018). Neutrophil extracellular traps in immunity and disease. *Nature Reviews Immunology*, *18*(2), 134–147. https://doi.org/10.1038/nri.2017.105

Patente, T. A., Pinho, M. P., Oliveira, A. A., Evangelista, G. C. M., Bergami-Santos, P. C., & Barbuto, J. A. M. (2019). Human Dendritic Cells: Their Heterogeneity and Clinical Application Potential in Cancer Immunotherapy. *Frontiers in Immunology*, *9*, 3176. https://doi.org/10.3389/fimmu.2018.03176

Pease, J. (2007). CCR4 Chemokine Receptor. In *XPharm: The Comprehensive Pharmacology Reference* (pp. 1–8). Elsevier. https://doi.org/10.1016/B978-008055232-3.60189-8

Peiser, M., Wanner, R., & Kolde, G. (2004). Human epidermal Langerhans cells differ from monocyte-derived Langerhans cells in CD80 expression and in secretion of IL-12 after CD40 cross-linking. *Journal of Leukocyte Biology*, *76*(3), 616–622. https://doi.org/10.1189/jlb.0703327

Peng, J., Sun, S.-B., Yang, P.-P., & Fan, Y.-M. (2017). Is Ki-67, keratin 16, involucrin, and filaggrin immunostaining sufficient to diagnose inflammatory linear verrucous epidermal nevus? A report of eight cases and a comparison with psoriasis vulgaris. *Anais Brasileiros De Dermatologia*, *92*(5), 682–685. https://doi.org/10.1590/abd1806-4841.20176263

Pennacchi, P. C., de Almeida, M. E. S., Gomes, O. L. A., Faião-Flores, F., de Araújo Crepaldi, M. C., dos Santos, M. F., de Moraes Barros, S. B., & Maria-Engler, S. S. (2015). Glycated Reconstructed Human Skin as a Platform to Study the Pathogenesis of Skin Aging. *Tissue Engineering Part A*, *21*(17–18), 2417–2425. https://doi.org/10.1089/ten.tea.2015.0009

Perche, P. O., Cook, M. K., & Feldman, S. R. (2023). Abrocitinib: A New FDA-Approved Drug for Moderate-to-Severe Atopic Dermatitis. *Annals of Pharmacotherapy*, *57*(1), 86–98. https://doi.org/10.1177/10600280221096713

Pickl, W. F., Majdic, O., Kohl, P., Stöckl, J., Riedl, E., Scheinecker, C., Bello-Fernandez, C., & Knapp, W. (1996). Molecular and functional characteristics of dendritic cells generated from highly purified CD14+ peripheral blood monocytes. *The Journal of Immunology*, *157*(9), 3850.

Piipponen, M., Li, D., & Landén, N. X. (2020). The Immune Functions of Keratinocytes in Skin Wound Healing. *International Journal of Molecular Sciences*, *21*(22), 8790. https://doi.org/10.3390/ijms21228790

Pinet, V., Vergelli, M., Martini, R., Bakke, O., & Long, E. O. (1995). Antigen presentation mediated by recycling of surface HLA-DR molecules. *Nature*, *375*(6532), 603–606. https://doi.org/10.1038/375603a0

Popov, A., Mirkov, I., Miljković, D., Belij, S., Zolotarevski, L., Kataranovski, D., & Kataranovski, M. (2011). Contact allergic response to dinitrochlorobenzene (DNCB) in rats: Insight from sensitization phase. *Immunobiology*, *216*(7), 763–770. https://doi.org/10.1016/j.imbio.2010.12.007

Popov, L., Kovalski, J., Grandi, G., Bagnoli, F., & Amieva, M. R. (2014). Three-Dimensional Human Skin Models to Understand Staphylococcus aureus Skin Colonization and Infection. *Frontiers in Immunology*, *5*. https://doi.org/10.3389/fimmu.2014.00041

Posch, W., Lass-Flörl, C., & Wilflingseder, D. (2016). Generation of Human Monocyte-derived Dendritic Cells from Whole Blood. *Journal of Visualized Experiments*, *118*, 54968. https://doi.org/10.3791/54968

Pothmann, A., Illing, T., Wiegand, C., Hartmann, A. A., & Elsner, P. (2019). The Microbiome and Atopic Dermatitis: A Review. *American Journal of Clinical Dermatology*, *20*(6), 749–761. https://doi.org/10.1007/s40257-019-00467-1

Poumay, Y., Dupont, F., Marcoux, S., Leclercq-Smekens, M., H�rin, M., & Coquette, A. (2004). A simple reconstructed human epidermis: Preparation of the culture model and utilization in in vitro studies. *Archives of Dermatological Research*, *296*(5), 203–211. https://doi.org/10.1007/s00403-004-0507-y

Pupovac, A., Senturk, B., Griffoni, C., Maniura-Weber, K., Rottmar, M., & McArthur, S. L. (2018). Toward Immunocompetent 3D Skin Models. *Advanced Healthcare Materials*, *7*(12), 1701405. https://doi.org/10.1002/adhm.201701405

Randall, M. J., Jüngel, A., Rimann, M., & Wuertz-Kozak, K. (2018). Advances in the biofabrication of 3D skin in vitro: Healthy and pathological models. *Frontiers in Bioengineering and Biotechnology*, *6*(OCT). https://doi.org/10.3389/fbioe.2018.00154

Raulf, M. (2019). T Cell: Primary Culture from Peripheral Blood. In P. Lympany & M. G. Jones (Eds.), *Allergy* (Vol. 2020, pp. 17–31). Springer New York. https://doi.org/10.1007/978-1-4939-9591-2_2

Redegeld, F. A., Yu, Y., Kumari, S., Charles, N., & Blank, U. (2018). Non-IgE mediated mast cell activation. *Immunological Reviews*, *282*(1), 87–113. https://doi.org/10.1111/imr.12629

Reijnders, C. M. A., van Lier, A., Roffel, S., Kramer, D., Scheper, R. J., & Gibbs, S. (2015). Development of a Full-Thickness Human Skin Equivalent *In Vitro* Model Derived from TERT-Immortalized Keratinocytes and Fibroblasts. *Tissue Engineering Part A*, *21*(17–18), 2448–2459. https://doi.org/10.1089/ten.tea.2015.0139

Rerknimitr, P., Otsuka, A., Nakashima, C., & Kabashima, K. (2017). The etiopathogenesis of atopic dermatitis: Barrier disruption, immunological derangement, and pruritus. *Inflammation and Regeneration*, *37*(1), 14. https://doi.org/10.1186/s41232-017-0044-7

Rheinwald, J. G., Hahn, W. C., Ramsey, M. R., Wu, J. Y., Guo, Z., Tsao, H., De Luca, M., Catricalà, C., & O'Toole, K. M. (2002). A two-stage, p16(INK4A)- and p53-dependent keratinocyte senescence mechanism that limits replicative potential independent of telomere status. *Molecular and Cellular Biology*, *22*(14), 5157–5172. https://doi.org/10.1128/MCB.22.14.5157-5172.2002

Richmond, J. M., & Harris, J. E. (2014). Immunology and skin in health and disease. *Cold Spring Harbor Perspectives in Medicine*, *4*(12), a015339. https://doi.org/10.1101/cshperspect.a015339

Rippa, A. L., Kalabusheva, E. P., & Vorotelyak, E. A. (2019). Regeneration of Dermis: Scarring and Cells Involved. *Cells*, *8*(6), 607. https://doi.org/10.3390/cells8060607

Robertson, E. D., Weir, L., Romanowska, M., Leigh, I. M., & Panteleyev, A. A. (2012). ARNT controls the expression of epidermal differentiation genes through HDAC- and EGFR- dependent pathways. *Journal of Cell Science*, 13.

Roger, M., Fullard, N., Costello, L., Bradbury, S., Markiewicz, E., O'Reilly, S., Darling, N., Ritchie, P., Määttä, A., Karakesisoglou, I., Nelson, G., von Zglinicki, T., Dicolandrea, T., Isfort, R., Bascom, C., & Przyborski, S. (2019). Bioengineering the microanatomy of human skin. *Journal of Anatomy*, *234*(4), 438–455. https://doi.org/10.1111/joa.12942

Romani, N., Clausen, B. E., & Stoitzner, P. (2010). Langerhans cells and more: Langerin-expressing dendritic cell subsets in the skin. *Immunological Reviews*, *234*(1), 120–141. https://doi.org/10.1111/j.0105-2896.2009.00886.x

Romani, N., Holzmann, S., Tripp, C. H., Koch, F., & Stoitzner, P. (2003). Langerhans cells—Dendritic cells of the epidermis. *APMIS*, *111*(7–8), 725–740. https://doi.org/10.1034/j.1600-0463.2003.11107805.x

Rosales, C. (2020). Neutrophils at the crossroads of innate and adaptive immunity. *Journal of Leukocyte Biology*, *108*(1), 377–396. https://doi.org/10.1002/JLB.4MIR0220-574RR

Rossi, A., Appelt-Menzel, A., Kurdyn, S., Walles, H., & Groeber, F. (2015). Generation of a three-dimensional full thickness skin equivalent and automated wounding. *Journal of Visualized Experiments*, *96*, 1–7. https://doi.org/10.3791/52576

Rouaud-Tinguely, P., Boudier, D., Marchand, L., Barruche, V., Bordes, S., Coppin, H., Roth, M. P., & Closs, B. (2015). From the morphological to the transcriptomic characterization of a compromised three-dimensional *in vitro* model mimicking atopic dermatitis. *British Journal of Dermatology*, *173*(4), 1006–1014. https://doi.org/10.1111/bjd.14012

Rudolph, M. E., McArthur, M. A., Barnes, R. S., Magder, L. S., Chen, W. H., & Sztein, M. B. (2018). Differences Between Pediatric and Adult T Cell Responses to In Vitro Staphylococcal Enterotoxin B Stimulation. *Frontiers in Immunology*, *9*, 498. https://doi.org/10.3389/fimmu.2018.00498

Sandilands, A., Sutherland, C., Irvine, A. D., & McLean, W. H. I. (2009). Filaggrin in the frontline: Role in skin barrier function and disease. *Journal of Cell Science*, *122*(9), 1285–1294. https://doi.org/10.1242/jcs.033969

Sato, F., Omura, S., Martinez, N. E., & Tsunoda, I. (2018). Animal Models of Multiple Sclerosis. In *Neuroinflammation* (pp. 37–72). Elsevier. https://doi.org/10.1016/B978-0-12-811709-5.00003-X

Savoji, H., Godau, B., Hassani, M. S., & Akbari, M. (2018). Skin Tissue Substitutes and Biomaterial Risk Assessment and Testing. *Frontiers in Bioengineering and Biotechnology*, *6*(July), 1–18. https://doi.org/10.3389/fbioe.2018.00086

Schuler, P. J., Harasymczuk, M., Schilling, B., Lang, S., & Whiteside, T. L. (2011). Separation of human CD4+CD39+ T cells by magnetic beads reveals two phenotypically and functionally different subsets. *Journal of Immunological Methods*, *369*(1–2), 59–68. https://doi.org/10.1016/j.jim.2011.04.004

Sedger, L. M., & McDermott, M. F. (2014). TNF and TNF-receptors: From mediators of cell death and inflammation to therapeutic giants – past, present and future. *Cytokine & Growth Factor Reviews*, *25*(4), 453–472. https://doi.org/10.1016/j.cytogfr.2014.07.016

Shang, L., Deng, D., Buskermolen, J. K., Janus, M. M., Krom, B. P., Roffel, S., Waaijman, T., van Loveren, C., Crielaard, W., & Gibbs, S. (2018). Multi-species oral biofilm promotes reconstructed human gingiva epithelial barrier function. *Scientific Reports*, *8*(1), 16061. https://doi.org/10.1038/s41598-018-34390-y

Shin, J. U., Abaci, H. E., Herron, L., Guo, Z., Sallee, B., Pappalardo, A., Jackow, J., Wang, E. H. C., Doucet, Y., & Christiano, A. M. (2020). Recapitulating T cell infiltration in 3D psoriatic skin models for patient-specific drug testing. *Scientific Reports*, *10*(1), 1–12. https://doi.org/10.1038/s41598-020-60275-0

Sierra-Sánchez, Á., Kim, K. H., Blasco-Morente, G., & Arias-Santiago, S. (2021). Cellular human tissue-engineered skin substitutes investigated for deep and difficult to heal injuries. *Npj Regenerative Medicine*, *6*(1), 35. https://doi.org/10.1038/s41536-021-00144-0

Simpson, C. L., Patel, D. M., & Green, K. J. (2011). Deconstructing the skin: Cytoarchitectural determinants of epidermal morphogenesis. *Nature Reviews Molecular Cell Biology*, *12*(9), 565–580. https://doi.org/10.1038/nrm3175

Sinistro, A., Ciaprini, C., Natoli, S., Sussarello, E., Carducci, F. C., Almerighi, C., Capozzi, M., Bolacchi, F., Rocchi, G., & Bergamini, A. (2007). Lipopolysaccharide desensitizes monocytes–macrophages to CD40 ligand stimulation. *Immunology*, *122*(3), 362–370. https://doi.org/10.1111/j.1365-2567.2007.02648.x

Smits, J. P. H., Niehues, H., Rikken, G., van Vlijmen-Willems, I. M. J. J., van de Zande, G. W. H. J. F., Zeeuwen, P. L. J. M., Schalkwijk, J., & van den Bogaard, E. H. (2017). Immortalized N/TERT keratinocytes as an alternative cell source in 3D human epidermal models. *Scientific Reports*, *7*(1), 11838. https://doi.org/10.1038/s41598-017-12041-y

Somuncu, Ö. S., Karahan, C., Somuncu, S., & Şahin, F. (2018). Tissue Engineering for Skin Replacement Methods. *Stem Cells in Clinical Practice and Tissue Engineering*. https://doi.org/10.5772/intechopen.69905

Sorrell, J. M., & Caplan, A. I. (2004). Fibroblast heterogeneity: More than skin deep. *Journal of Cell Science*, *117*(5), 667–675. https://doi.org/10.1242/jcs.01005

Soumelis, V., Reche, P. A., Kanzler, H., Yuan, W., Edward, G., Homey, B., Gilliet, M., Ho, S., Antonenko, S., Lauerma, A., Smith, K., Gorman, D., Zurawski, S., Abrams, J., Menon, S.,

McClanahan, T., Waal-Malefyt, R. de, Bazan, F., Kastelein, R. A., & Liu, Y.-J. (2002). Human epithelial cells trigger dendritic cell–mediated allergic inflammation by producing TSLP. *Nature Immunology*, *3*(7), 673–680. https://doi.org/10.1038/ni805

Sriram, G., Bigliardi, P. L., & Bigliardi-Qi, M. (2015). Fibroblast heterogeneity and its implications for engineering organotypic skin models in vitro. *European Journal of Cell Biology*, *94*(11), 483–512. https://doi.org/10.1016/j.ejcb.2015.08.001

Sriram, G., Bigliardi, P. L., & Bigliardi-Qi, M. (2018). Full-Thickness Human Skin Equivalent Models of Atopic Dermatitis. In K. Turksen (Ed.), *Skin Stem Cells* (Vol. 1879, pp. 367–383). Springer New York. https://doi.org/10.1007/7651_2018_163

Stremnitzer, C., Manzano-Szalai, K., Starkl, P., Willensdorfer, A., Schrom, S., Singer, J., Reichart, U., Akira, S., & Jensen-Jarolim, E. (2014). Epicutaneously applied Der p 2 induces a strong TH 2-biased antibody response in C57BL/6 mice, independent of functional TLR4. *Allergy*, *69*(6), 741–751. https://doi.org/10.1111/all.12399

Strudwick, X. L., Lang, D. L., Smith, L. E., & Cowin, A. J. (2015). Combination of Low Calcium with Y-27632 Rock Inhibitor Increases the Proliferative Capacity, Expansion Potential and Lifespan of Primary Human Keratinocytes while Retaining Their Capacity to Differentiate into Stratified Epidermis in a 3D Skin Model. *PLOS ONE*, *10*(4), e0123651. https://doi.org/10.1371/journal.pone.0123651

Sugaya, M. (2020). The Role of Th17-Related Cytokines in Atopic Dermatitis. *International Journal of Molecular Sciences*, *21*(4), E1314. https://doi.org/10.3390/ijms21041314

Suresh, M., Singh, A., & Fischer, C. (2005). Role of tumor necrosis factor receptors in regulating CD8 T-cell responses during acute lymphocytic choriomeningitis virus infection. *Journal of Virology*, *79*(1), 202–213. https://doi.org/10.1128/JVI.79.1.202-213.2005

Tai, Y., Wang, Q., Korner, H., Zhang, L., & Wei, W. (2018). Molecular Mechanisms of T Cells Activation by Dendritic Cells in Autoimmune Diseases. *Frontiers in Pharmacology*, *9*, 642. https://doi.org/10.3389/fphar.2018.00642

Tanaka, A., Amagai, Y., Oida, K., & Matsuda, H. (2012). Recent Findings in Mouse Models for Human Atopic Dermatitis. *Experimental Animals*, *61*(2), 77–84. https://doi.org/10.1538/expanim.61.77

Tanaka, H., Demeure, C. E., Rubio, M., Delespesse, G., & Sarfati, M. (2000). Human Monocyte–Derived Dendritic Cells Induce Naive T Cell Differentiation into T Helper Cell Type 2 (Th2) or Th1/Th2 Effectors. *Journal of Experimental Medicine*, *192*(3), 405–412. https://doi.org/10.1084/jem.192.3.405

Tanaka, T., Narazaki, M., & Kishimoto, T. (2014). IL-6 in Inflammation, Immunity, and Disease. *Cold Spring Harbor Perspectives in Biology*, *6*(10), a016295–a016295. https://doi.org/10.1101/cshperspect.a016295

Tang-Huau, T.-L., Gueguen, P., Goudot, C., Durand, M., Bohec, M., Baulande, S., Pasquier, B., Amigorena, S., & Segura, E. (2018). Human in vivo-generated monocyte-derived dendritic cells and macrophages cross-present antigens through a vacuolar pathway. *Nature Communications*, *9*, 2570. https://doi.org/10.1038/s41467-018-04985-0

Tau, G. Z., von der Weid, T., Lu, B., Cowan, S., Kvatyuk, M., Pernis, A., Cattoretti, G., Braunstein, N. S., Coffman, R. L., & Rothman, P. B. (2000). Interferon γ Signaling Alters the Function of T Helper Type 1 Cells. *Journal of Experimental Medicine*, *192*(7), 977–986. https://doi.org/10.1084/jem.192.7.977

te Velde, A. A., Klomp, J. P., Yard, B. A., de Vries, J. E., & Figdor, C. G. (1988). Modulation of phenotypic and functional properties of human peripheral blood monocytes by IL-4. *Journal of Immunology (Baltimore, Md.: 1950)*, *140*(5), 1548–1554.

Tharakan, S., Pontiggia, L., Biedermann, T., Böttcher-Haberzeth, S., Schiestl, C., Reichmann, E., & Meuli, M. (2010). Transglutaminases, involucrin, and loricrin as markers of epidermal differentiation in skin substitutes derived from human sweat gland cells. *Pediatric Surgery International*, *26*(1), 71–77. https://doi.org/10.1007/s00383-009-2517-5

Thomsen, S. F. (2014). Atopic Dermatitis: Natural History, Diagnosis, and Treatment. *ISRN Allergy*, *2014*, 1–7. https://doi.org/10.1155/2014/354250

Thornton, S. M., Samararatne, V. D., Skeate, J. G., Buser, C., Lühen, K. P., Taylor, J. R., Da Silva, D. M., & Kast, W. M. (2020). The Essential Role of anxA2 in Langerhans Cell Birbeck Granules Formation. *Cells*, *9*(4), E974. https://doi.org/10.3390/cells9040974

Toebak, M. J., Gibbs, S., Bruynzeel, D. P., Scheper, R. J., & Rustemeyer, T. (2009). Dendritic cells: Biology of the skin. *Contact Dermatitis*, *60*(1), 2–20. https://doi.org/10.1111/j.1600-0536.2008.01443.x

Tokunaga, R., Zhang, W., Naseem, M., Puccini, A., Berger, M. D., Soni, S., McSkane, M., Baba, H., & Lenz, H.-J. (2018). CXCL9, CXCL10, CXCL11/CXCR3 axis for immune activation – A target for novel cancer therapy. *Cancer Treatment Reviews*, *63*, 40–47. https://doi.org/10.1016/j.ctrv.2017.11.007

Torres, T., Ferreira, E. O., Gonçalo, M., Mendes-Bastos, P., Selores, M., & Filipe, P. (2019). Update on Atopic Dermatitis. *Acta Médica Portuguesa*, *32*(9), 606. https://doi.org/10.20344/amp.11963

Tracy, L. E., Minasian, R. A., & Caterson, E. J. (2016). Extracellular Matrix and Dermal Fibroblast Function in the Healing Wound. *Advances in Wound Care*, *5*(3), 119–136. https://doi.org/10.1089/wound.2014.0561

Trinchieri, G. (2007). Interleukin-10 production by effector T cells: Th1 cells show self control. *The Journal of Experimental Medicine*, *204*(2), 239–243. https://doi.org/10.1084/jem.20070104

Tsuda, T., Tohyama, M., Yamasaki, K., Shirakata, Y., Yahata, Y., Tokumaru, S., Sayama, K., & Hashimoto, K. (2003). Lack of evidence for TARC/CCL17 production by normal human keratinocytes in vitro. *Journal of Dermatological Science*, *31*(1), 37–42. https://doi.org/10.1016/S0923-1811(02)00138-X

Tucci, M., Quatraro, C., Dammacco, F., & Silvestris, F. (2007). Increased IL-18 Production by Dendritic Cells in Active Inflammatory Myopathies. *Annals of the New York Academy of Sciences*, *1107*(1), 184–192. https://doi.org/10.1196/annals.1381.020

Tugues, S., Burkhard, S. H., Ohs, I., Vrohlings, M., Nussbaum, K., Vom Berg, J., Kulig, P., & Becher, B. (2015). New insights into IL-12-mediated tumor suppression. *Cell Death and Differentiation*, *22*(2), 237–246. https://doi.org/10.1038/cdd.2014.134

Tunggal, J. A., Helfrich, I., Schmitz, A., Schwarz, H., Günzel, D., Fromm, M., Kemler, R., Krieg, T., & Niessen, C. M. (2005). E-cadherin is essential for in vivo epidermal barrier function by regulating tight junctions. *The EMBO Journal*, *24*(6), 1146–1156. https://doi.org/10.1038/sj.emboj.7600605

Tungland, B. (2018). Role of Gut Microbiota in Immune Homeostasis. In *Human Microbiota in Health and Disease* (pp. 135–154). Elsevier. https://doi.org/10.1016/B978-0-12-814649-1.00004-1

Udommethaporn, S., Tencomnao, T., McGowan, E. M., & Boonyaratanakornkit, V. (2016). Assessment of Anti-TNF-α Activities in Keratinocytes Expressing Inducible TNF- α: A Novel

Tool for Anti-TNF-α Drug Screening. *PloS One*, *11*(7), e0159151. https://doi.org/10.1371/journal.pone.0159151

Ungar, B., Garcet, S., Gonzalez, J., Dhingra, N., Correa da Rosa, J., Shemer, A., Krueger, J. G., Suarez-Farinas, M., & Guttman-Yassky, E. (2017). An Integrated Model of Atopic Dermatitis Biomarkers Highlights the Systemic Nature of the Disease. *Journal of Investigative Dermatology*, *137*(3), 603–613. https://doi.org/10.1016/j.jid.2016.09.037

Valladeau, J., Ravel, O., Dezutter-Dambuyant, C., Moore, K., Kleijmeer, M., Liu, Y., Duvert-Frances, V., Vincent, C., Schmitt, D., Davoust, J., Caux, C., Lebecque, S., & Saeland, S. (2000). Langerin, a Novel C-Type Lectin Specific to Langerhans Cells, Is an Endocytic Receptor that Induces the Formation of Birbeck Granules. *Immunity*, *12*(1), 71–81. https://doi.org/10.1016/S1074-7613(00)80160-0

Van Den Bogaard, E. H., Tjabringa, G. S., Joosten, I., Vonk-Bergers, M., Van Rijssen, E., Tijssen, H. J., Erkens, M., Schalkwijk, J., & Koenen, H. J. P. M. (2014). Crosstalk between keratinocytes and T cells in a 3D microenvironment: A model to study inflammatory skin diseases. *Journal of Investigative Dermatology*. https://doi.org/10.1038/jid.2013.417

van Drongelen, V., Danso, M. O., Mulder, A., Mieremet, A., van Smeden, J., Bouwstra, J. A., & El Ghalbzouri, A. (2014). Barrier Properties of an N/TERT-Based Human Skin Equivalent. *Tissue Engineering Part A*, *20*(21–22), 3041–3049. https://doi.org/10.1089/ten.tea.2014.0011

van Drongelen, V., Danso, M. O., Out, J. J., Mulder, A., Lavrijsen, A. P. M., Bouwstra, J. A., & El Ghalbzouri, A. (2015). Explant cultures of atopic dermatitis biopsies maintain their epidermal characteristics in vitro. *Cell and Tissue Research*, *361*(3), 789–797. https://doi.org/10.1007/s00441-015-2162-3

van Drongelen, V., Haisma, E. M., Out-Luiting, J. J., Nibbering, P. H., & El Ghalbzouri, A. (2014). Reduced filaggrin expression is accompanied by increased Staphylococcus aureus colonization of epidermal skin models. *Clinical & Experimental Allergy*, *44*(12), 1515–1524. https://doi.org/10.1111/cea.12443

Varricchi, G., Pecoraro, A., Marone, G., Criscuolo, G., Spadaro, G., Genovese, A., & Marone, G. (2018). Thymic Stromal Lymphopoietin Isoforms, Inflammatory Disorders, and Cancer. *Frontiers in Immunology*, *9*, 1595. https://doi.org/10.3389/fimmu.2018.01595

Vestergaard, C., Bang, K., Gesser, B., Yoneyama, H., Matsushima, K., & Larsen, C. G. (2000). A Th2 Chemokine, TARC, Produced by Keratinocytes May Recruit CLA+CCR4+ Lymphocytes into Lesional Atopic Dermatitis Skin. *Journal of Investigative Dermatology*, *115*(4), 640–646. https://doi.org/10.1046/j.1523-1747.2000.00115.x

Vignali, D. A. A., Collison, L. W., & Workman, C. J. (2008). How regulatory T cells work. *Nature Reviews. Immunology*, *8*(7), 523–532. https://doi.org/10.1038/nri2343

Viola, A., Munari, F., Sánchez-Rodríguez, R., Scolaro, T., & Castegna, A. (2019). The Metabolic Signature of Macrophage Responses. *Frontiers in Immunology*, *10*, 1462. https://doi.org/10.3389/fimmu.2019.01462

Vis, M. A. M., Ito, K., & Hofmann, S. (2020). Impact of Culture Medium on Cellular Interactions in in vitro Co-culture Systems. *Frontiers in Bioengineering and Biotechnology*, *8*, 911. https://doi.org/10.3389/fbioe.2020.00911

Voronov, E. (2013). Unique versus redundant functions of IL-1α and IL-1β in the tumor microenvironment. *Frontiers in Immunology*, *4*. https://doi.org/10.3389/fimmu.2013.00177

Wagner, T., Gschwandtner, M., Strajeriu, A., Elbe-Bürger, A., Grillari, J., Grillari-Voglauer, R., Greiner, G., Golabi, B., Tschachler, E., & Mildner, M. (2018). Establishment of keratinocyte cell lines

from human hair follicles. *Scientific Reports*, *8*(1), 13434. https://doi.org/10.1038/s41598-018-31829-0

Waite, J. C., & Skokos, D. (2012). Th17 response and inflammatory autoimmune diseases. *International Journal of Inflammation*, *2012*, 819467. https://doi.org/10.1155/2012/819467

Walko, G., Castañón, M. J., & Wiche, G. (2015). Molecular architecture and function of the hemidesmosome. *Cell and Tissue Research*, *360*(3), 529–544. https://doi.org/10.1007/s00441-015-2216-6

Wallmeyer, L., Dietert, K., Sochorová, M., Gruber, A. D., Kleuser, B., Vávrová, K., & Hedtrich, S. (2017). TSLP is a direct trigger for T cell migration in filaggrin-deficient skin equivalents. *Scientific Reports*, *7*(1), 774. https://doi.org/10.1038/s41598-017-00670-2

Walters, B. D., & Stegemann, J. P. (2014). Strategies for directing the structure and function of three-dimensional collagen biomaterials across length scales. *Acta Biomaterialia*, *10*(4), 1488–1501. https://doi.org/10.1016/j.actbio.2013.08.038

Weinmuellner, R., Kryeziu, K., Zbiral, B., Tav, K., Schoenhacker-Alte, B., Groza, D., Wimmer, L., Schosserer, M., Nagelreiter, F., Rösinger, S., Mildner, M., Tschachler, E., Grusch, M., Grillari, J., & Heffeter, P. (2018). Long-term exposure of immortalized keratinocytes to arsenic induces EMT, impairs differentiation in organotypic skin models and mimics aspects of human skin derangements. *Archives of Toxicology*, *92*(1), 181–194. https://doi.org/10.1007/s00204-017-2034-6

Werfel, T. (2009). The Role of Leukocytes, Keratinocytes, and Allergen-Specific IgE in the Development of Atopic Dermatitis. *Journal of Investigative Dermatology*, *129*(8), 1878–1891. https://doi.org/10.1038/jid.2009.71

Wickett, R. R., & Visscher, M. O. (2006). Structure and function of the epidermal barrier. *American Journal of Infection Control*, *34*(10), S98–S110. https://doi.org/10.1016/j.ajic.2006.05.295

Wieczorek, M., Abualrous, E. T., Sticht, J., Álvaro-Benito, M., Stolzenberg, S., Noé, F., & Freund, C. (2017). Major Histocompatibility Complex (MHC) Class I and MHC Class II Proteins: Conformational Plasticity in Antigen Presentation. *Frontiers in Immunology*, *8*. https://doi.org/10.3389/fimmu.2017.00292

Willart, M. A. M., Deswarte, K., Pouliot, P., Braun, H., Beyaert, R., Lambrecht, B. N., & Hammad, H. (2012). Interleukin-1α controls allergic sensitization to inhaled house dust mite via the epithelial release of GM-CSF and IL-33. *The Journal of Experimental Medicine*, *209*(8), 1505–1517. https://doi.org/10.1084/jem.20112691

Winton, H. L., Wan, H., Cannell, M. B., Thompson, P. J., Garrod, D. R., Stewart, G. A., & Robinson, C. (1998). Class specific inhibition of house dust mite proteinases which cleave cell adhesion, induce cell death and which increase the permeability of lung epithelium: Inhibitors of mite proteinases. *British Journal of Pharmacology*, *124*(6), 1048–1059. https://doi.org/10.1038/sj.bjp.0701905

Wollenberg, A., Barbarot, S., Bieber, T., Christen-Zaech, S., Deleuran, M., Fink-Wagner, A., Gieler, U., Girolomoni, G., Lau, S., Muraro, A., Czarnecka-Operacz, M., Schäfer, T., Schmid-Grendelmeier, P., Simon, D., Szalai, Z., Szepietowski, J. C., Taïeb, A., Torrelo, A., Werfel, T., … the European Dermatology Forum (EDF), the European Academy of Dermatology and Venereology (EADV), the European Academy of Allergy and Clinical Immunology (EAACI), the European Task Force on Atopic Dermatitis (ETFAD), European Federation of Allergy and Airways Diseases Patients' Associations (EFA), the European Society for Dermatology and Psychiatry (ESDaP), the European Society of Pediatric Dermatology (ESPD), Global Allergy

and Asthma European Network (GA2LEN) and the European Union of Medical Specialists. (2018). Consensus-based European guidelines for treatment of atopic eczema (atopic dermatitis) in adults and children: Part I. *Journal of the European Academy of Dermatology and Venereology*, *32*(5), 657–682. https://doi.org/10.1111/jdv.14891

Wollenberg, A., Blauvelt, A., Guttman-Yassky, E., Worm, M., Lynde, C., Lacour, J. -P., Spelman, L., Katoh, N., Saeki, H., Poulin, Y., Lesiak, A., Kircik, L., Cho, S. H., Herranz, P., Cork, M. J., Peris, K., Steffensen, L. A., Bang, B., Kuznetsova, A., … the ECZTRA 1 and ECZTRA 2 study investigators. (2021). Tralokinumab for moderate-to-severe atopic dermatitis: Results from two 52-week, randomized, double-blind, multicentre, placebo-controlled phase III trials (ECZTRA 1 and ECZTRA 2)*. *British Journal of Dermatology*, *184*(3), 437–449. https://doi.org/10.1111/bjd.19574

Wong, R., Geyer, S., Weninger, W., Guimberteau, J.-C., & Wong, J. K. (2016). The dynamic anatomy and patterning of skin. *Experimental Dermatology*, *25*(2), 92–98. https://doi.org/10.1111/exd.12832

Wongchana, W., & Palaga, T. (2012). Direct regulation of interleukin-6 expression by Notch signaling in macrophages. *Cellular & Molecular Immunology*, *9*(2), 155–162. https://doi.org/10.1038/cmi.2011.36

Wright, H. L., Moots, R. J., Bucknall, R. C., & Edwards, S. W. (2010). Neutrophil function in inflammation and inflammatory diseases. *Rheumatology (Oxford, England)*, *49*(9), 1618–1631. https://doi.org/10.1093/rheumatology/keq045

Xiao, X., & Cai, J. (2017). Mucosal-Associated Invariant T Cells: New Insights into Antigen Recognition and Activation. *Frontiers in Immunology*, *8*, 1540. https://doi.org/10.3389/fimmu.2017.01540

Xie, S., Ding, L., Xiong, Z., & Zhu, S. (2012). Implications of Th1 and Th17 cells in pathogenesis of oral lichen planus. *Journal of Huazhong University of Science and Technology. Medical Sciences = Hua Zhong Ke Ji Da Xue Xue Bao. Yi Xue Ying De Wen Ban = Huazhong Keji Daxue Xuebao. Yixue Yingdewen Ban*, *32*(3), 451–457. https://doi.org/10.1007/s11596-012-0078-7

Yamamoto, J., Adachi, Y., Onoue, Y., Adachi, Y. S., Okabe, Y., Itazawa, T., Toyoda, M., Seki, T., Morohashi, M., Matsushima, K., & Miyawaki, T. (2000). Differential expression of the chemokine receptors by the Th1- and Th2-type effector populations within circulating CD4+ T cells. *Journal of Leukocyte Biology*, *68*(4), 568–574.

Yang, C.-C., Hung, Y.-L., Ko, W.-C., Tsai, Y.-J., Chang, J.-F., Liang, C.-W., Chang, D.-C., & Hung, C.-F. (2021). Effect of Neferine on DNCB-Induced Atopic Dermatitis in HaCaT Cells and BALB/c Mice. *International Journal of Molecular Sciences*, *22*(15), 8237. https://doi.org/10.3390/ijms22158237

Yang, E. J., Sekhon, S., Sanchez, I. M., Beck, K. M., & Bhutani, T. (2018). Recent Developments in Atopic Dermatitis. *Pediatrics*, *142*(4), e20181102. https://doi.org/10.1542/peds.2018-1102

Yano, C., Saeki, H., Komine, M., Kagami, S., Tsunemi, Y., Ohtsuki, M., & Nakagawa, H. (2015). Mechanism of Macrophage-Derived Chemokine/CCL22 Production by HaCaT Keratinocytes. *Annals of Dermatology*, *27*(2), 152–156. https://doi.org/10.5021/ad.2015.27.2.152

Yano, S., Banno, T., Walsh, R., & Blumenberg, M. (2008). Transcriptional responses of human epidermal keratinocytes to cytokine interleukin-1. *Journal of Cellular Physiology*, *214*(1), 1–13. https://doi.org/10.1002/jcp.21300

Yanofsky, V. R., Mitsui, H., Felsen, D., & Carucci, J. A. (2013). Understanding dendritic cells and their role in cutaneous carcinoma and cancer immunotherapy. *Clinical & Developmental Immunology*, *2013*, 624123. https://doi.org/10.1155/2013/624123

Yao, Y., Simard, A. R., Shi, F.-D., & Hao, J. (2013). IL-10-Producing Lymphocytes in Inflammatory Disease. *International Reviews of Immunology*, *32*(3), 324–336. https://doi.org/10.3109/08830185.2012.762361

Yatim, K. M., & Lakkis, F. G. (2015). A brief journey through the immune system. *Clinical Journal of the American Society of Nephrology: CJASN*, *10*(7), 1274–1281. https://doi.org/10.2215/CJN.10031014

Yu, J. R., Navarro, J., Coburn, J. C., Mahadik, B., Molnar, J., Holmes, J. H., Nam, A. J., & Fisher, J. P. (2019). Current and Future Perspectives on Skin Tissue Engineering: Key Features of Biomedical Research, Translational Assessment, and Clinical Application. *Advanced Healthcare Materials*, *8*(5), 1–19. https://doi.org/10.1002/adhm.201801471

Yunna, C., Mengru, H., Lei, W., & Weidong, C. (2020). Macrophage M1/M2 polarization. *European Journal of Pharmacology*, *877*, 173090. https://doi.org/10.1016/j.ejphar.2020.173090

Zaniboni, M. C., Samorano, L. P., Orfali, R. L., & Aoki, V. (2016). Skin barrier in atopic dermatitis: Beyond filaggrin. *Anais Brasileiros De Dermatologia*, *91*(4), 472–478. https://doi.org/10.1590/abd1806-4841.20164412

Zanoni, I., & Granucci, F. (2013). Role of CD14 in host protection against infections and in metabolism regulation. *Frontiers in Cellular and Infection Microbiology*, *3*, 32. https://doi.org/10.3389/fcimb.2013.00032

Zhang, F., Wang, H., Wang, X., Jiang, G., Liu, H., Zhang, G., Wang, H., Fang, R., Bu, X., Cai, S., & Du, J. (2016). TGF-β induces M2-like macrophage polarization via SNAIL-mediated suppression of a pro-inflammatory phenotype. *Oncotarget*, *7*(32), 52294–52306. https://doi.org/10.18632/oncotarget.10561

Zhang, Q., Qin, J., Zhong, L., Gong, L., Zhang, B., Zhang, Y., & Gao, W.-Q. (2015). CCL5-Mediated Th2 Immune Polarization Promotes Metastasis in Luminal Breast Cancer. *Cancer Research*, *75*(20), 4312–4321. https://doi.org/10.1158/0008-5472.CAN-14-3590

Zhang, Y., Ye, Y., Tang, X., Wang, H., Tanaka, T., Tian, R., Yang, X., Wang, L., Xiao, Y., Hu, X., Jin, Y., Pang, H., Du, T., Liu, H., Sun, L., Xiao, S., Dong, R., Ferrucci, L., Tian, Z., & Zhang, S. (2022). CCL17 acts as a novel therapeutic target in pathological cardiac hypertrophy and heart failure. *Journal of Experimental Medicine*, *219*(8), e20200418. https://doi.org/10.1084/jem.20200418

Zhang, Z., & Michniak-Kohn, B. B. (2012). Tissue engineered human skin equivalents. *Pharmaceutics*, *4*(1), 26–41. https://doi.org/10.3390/pharmaceutics4010026

Zhu, J., Yamane, H., & Paul, W. E. (2010). Differentiation of Effector CD4 T Cell Populations. *Annual Review of Immunology*, *28*(1), 445–489. https://doi.org/10.1146/annurev-immunol-030409-101212

Zoio, P., Ventura, S., Leite, M., & Oliva, A. (2021). Pigmented Full-Thickness Human Skin Model Based on a Fibroblast-Derived Matrix for Long-Term Studies. *Tissue Engineering Part C: Methods*, *27*(7), 433–443. https://doi.org/10.1089/ten.tec.2021.0069

Zuberbier, T., Orlow, S. J., Paller, A. S., Taïeb, A., Allen, R., Hernanz-Hermosa, J. M., Ocampo-Candiani, J., Cox, M., Langeraar, J., & Simon, J. C. (2006). Patient perspectives on the management of atopic dermatitis. *Journal of Allergy and Clinical Immunology*, *118*(1), 226–232. https://doi.org/10.1016/j.jaci.2006.02.031